DRAFT

BMI-2104
Volume III

Radionuclide Release Under Specific LWR Accident Conditions

Volume III
BWR, MARK III Design

Prepared by
J. A. Gieseke, P. Cybulskis, R. S. Denning,
M. R. Kuhlman, K. W. Lee, H. Chen

Battelle Columbus Laboratories
Columbus, Ohio 43201

July 1984

DRAFT

BMI-2104
Volume III

Radionuclide Release Under Specific LWR Accident Conditions

Volume III
BWR, MARK III Design

Prepared by
J. A. Gieseke, P. Cybulskis, R. S. Denning,
M. R. Kuhlman, K. W. Lee, H. Chen

Battelle Columbus Laboratories
Columbus, Ohio 43201

July 1984

Prepared for
Office of Nuclear Regulatory Research
U.S. Nuclear Regulatory Commission
Washington, D.C. 20555

ACKNOWLEDGMENTS

Battelle's Columbus Laboratories wishes to acknowledge and express appreciation for the computer codes made available for this program by Sandia National Laboratory, Battelle's Pacific Northwest Laboratories, and the Kernforschungszentrum Karlsruhe, and for the computations and consultation provided by Sandia and the Oak Ridge National Laboratories. Further, members of the Peer Review Group have contributed significantly to this effort by providing comments, suggestions, and information on various reactor systems design.

The support of the U.S. Nuclear Regulatory Commission is gratefully acknowledged, and is the untiring leadership of the NRC staff, particularly Mel Silberberg and Mike Jankowski.

The diligent efforts of many Battelle staff members contributed to the preparation of this report. The following list identifies those staff making major contributions:

RJ Avers
GT Brooks
EP Bryant
R Freeman-Kelly
CS Jarrett
H Jordan
RG Jung
DJ Lehmicke
MB Neher
DR Rhodes
PM Schumacher
RO Wooton.

TABLE OF CONTENTS

		Page
1.	EXECUTIVE SUMMARY	1-1
	Approach	1-2
	The Grand Gulf Plant	1-3
	Accident Sequences Chosen for Study	1-3
	Computer Codes Used in the Study	1-4
	Summary of Results	1-5
2.	INTRODUCTION	2-1
	2.1 References	2-3
3.	GENERAL APPROACH	3-1
	3.1 Plant Selection	3-1
	3.2 Selection of Accident Sequences	3-2
	3.3 Computer Codes Used in the Study	3-2
	3.3.1 Assumptions	3-3
	3.3.2 Uncertainty Considerations	3-5
	3.4 References	3-7
4.	PLANT SELECTION AND ACCIDENT SEQUENCES	4-1
	4.1 General Plant Description	4-1
	4.2 Selection Basis and General Description of Accident Sequences	4-3
	4.2.1 Sequence TC (Transient with Failure to Scram)	4-7
	4.2.2 Sequence TPI (Transient with Stuck Open Relief Valve and Loss of Decay Heat Removal)	4-9
	4.2.3 Sequence TQUV (Transient with Loss of all Makeup Water	4-9
	4.2.4 Sequence S_2E (Small Break LOCA, Failure of Emergency Core Cooling System	4-11
	4.3 References	4-14
5.	ANALYTICAL METHODS	5-1
	5.1 Thermal Hydraulic Behavior	5-1
	5.1.1 Overall System Thermal Hydraulics: MARCH 2	5-1
	5.1.2 Primary System Thermal Hydraulics: MERGE	5-5

TABLE OF CONTENTS
(Continued)

		Page
5.2	Radionuclide Release from Fuel	5-6
5.2.1	Source Within Pressure Vessel: CORSOR	5-6
5.2.2	Source from Melt-Concrete Interactions: VANESA	5-9
5.3	Radionuclide Transport and Deposition	5-11
5.3.1	Transport in Reactor Coolant System: TRAP-MELT	5-11
5.3.2	Transport in Containment: SPARC	5-16
5.3.3	Transport in Containment: NAUA 4	5-17
5.4	References	5-21
6.	BASES FOR TRANSPORT CALCULATIONS	6-1
6.1	Plant Geometry and Thermal Hydraulic Conditions	6-1
6.1.1	Sequence TC	6-1
6.1.2	Sequence TPI	6-2
6.1.3	Sequence TQUV	6-18
6.1.4	Sequence S_2E	6-31
6.2	Radionuclide Sources	6-57
6.2.1	Source Within Pressure Vessel	6-57
6.2.2	Source Within the Containment	6-60
6.3	References	6-63
7.	RESULTS AND DISCUSSION	7-1
7.1	Introduction	7-1
7.2	Transport and Deposition in Reactor Coolant System (RCS)	7-1
7.2.1	RCS Transport and Deposition for Sequence TC	7-2
7.2.2	RCS Transport and Deposition for Sequence TPI	7-10
7.2.3	RCS Transport and Deposition for Sequence TQUV	7-15
7.2.4	RCS Transport and Deposition for Sequence S_2E	7-21
7.3	Transport of Fission Products Through Containment	7-31
7.3.1	TC Sequence	7-33
7.3.2	TPI Sequence	7-36
7.3.3	TQUV Sequence	7-41
7.3.4	S_2E Sequences	7-45
7.3.5	Results for Fission Product Groups of Reactor Safety Study	7-57
7.3.6	Summary	7-57
7.4	Discussion	7-60

1. EXECUTIVE SUMMARY

This is Volume 3, dealing with the Grand Gulf nuclear power plant, of a seven-volume report of work done at Battelle's Columbus Laboratories to estimate the amount of radioactive material that could be released from light water reactor (LWR) power plants under specific, hypothetical accident conditions. To make these estimates, five power plants were selected that represent the major categories of LWRs: three pressurized water reactors (PWRs) and two boiling water reactors (BWRs). Specifications and data from these plants, along with data from laboratory experiments, were input to computer codes designed to describe various conditions prevailing inside an operating reactor. Ultimately, these computer codes provide an estimate of how much radioactive material would be able to escape to the environment if a specific series of events (an "accident sequence") took place.

Volume 3 of this report deals with the Grand Gulf Power station, a General Electric BWR, Mark III containment design. The specific accident sequences investigated for the Grand Gulf plant were selected to represent cases of high risk, severe consequences, and most importantly, a wide range of physical conditions. The computer codes used to analyze the accident sequences were the best available, including the new MARCH 2 code. Other power plants included in the study are Surry PWR (Volumes 1 and 5); Peach Bottom BWR (Volume 2); Sequoyah PWR (Volume 4); and Zion PWR (Volume 6). The seventh volume will address technical questions raised during peer review meetings sponsored by the Nuclear Regulatory Commission.

The possibility of radioactive material being released to the environment has long been the focus of considerable public concern about the safety of nuclear power plants. Since 1962, several major reports have addressed that concern by using computer codes to estimate the release of fission products (radioactive material produced during reactor operations) to the reactor containment building, and thence to the environment, during a hypothetical severe accident. Although these analyses have improved over the years, in terms of how realistically they describe what happens during a hypothetical accident, it has not previously been possible to apply the various codes consistently to follow the transport of fission products along their flow path

from the core to the environment. This limitation resulted in piecemeal, parametric estimates of release.

The research results reported here are intended to provide a systematic, sequential application of the codes as well as to present analyses performed with improved computational procedures. It is to be recognized that this report describes an analytical approach for estimating radionuclide transport and deposition which incorporates individual physical and chemical processes or mechanisms. This approach is being evaluated for use in predicting the amount fission product release (the "source term") to the environment for specific reactors and accident sequences. When verified, these prediction techniques are expected to be more specific and perhaps to supersede generic tables of release fractions provided by previous analyses.

The purpose of this report is then to:

(1) Develop updated release-from-plant fission product source terms for four types of nuclear power plants and for accident sequences giving a range of conditions. The estimated source terms are to be based on consistent step-by-step analyses using improved computational tools for predicting radionuclide release from the fuel and radionuclide transport and deposition.

(2) Determine the effects on fission product releases associated with major differences in plant design and accident sequences.

(3) Provide in-plant time- and location-dependent distributions of fission product mass for use in equipment qualification.

Approach

This study was conducted by selecting specific plants and accident sequences and then using consistent and improved analyses of fission product release from fuel and radionuclide transport and deposition to predict fission product release to the environment for these specific cases. The approach comprises a sequence of steps; in the combined analysis, the results are specific to a particular set of accident conditions, and each step is based on results from analyses of the previous step.

The Grand Gulf Plant

Grand Gulf Unit 1 was selected to characterize BWR Mark III containment designs. Typical of Mark III designs, the Grand Gulf 1 wetwell is at the periphery of the drywell, with the wetwell vapor space forming an outer containment around the drywell. The primary containment area is made of steel-lined, reinforced concrete, with an internal design pressure of 15 psig (0.1 MPa).

Grand Gulf has a Standby Gas Treatment System (SGTS) that provides for mixing between the auxiliary and enclosure buildings. However, the SGTS is not expected to affect significantly the amount of radioactive material that could be released to the environment because (1) its exhaust capacity is quite small and (2) the encloure building would be expected to fail shortly after primary containment failure.

Accident Sequences Chosen for Study

The following accident sequences were selected because they represent high-risk situations with potentially severe consequences and because they involve a considerable range in physical conditions:

TC Sequence:

- Transient, failure of control rod insertion (failure to scram).
- Emergency Core Cooling Systems operate.
- Containment failure results from imbalance in power generation and containment heat removal due to the continued high power level of the reactor.

TPI Sequence:

- Transient, stuck open relief valve, loss of containment heat removal.
- Emergency Core Cooling system supplies makeup water to reactor vessel.
- Containment fails before core melts.

- Emergency Core Cooling pumps are assumed to fail after containment failure.

TQUV Sequence:

- Transient, loss of all primary system makeup water.
- Operators depressurize primary system prior to core melting.
- Hydrogen igniters are assumed to be operable.
- Containment failure results from buildup of noncondensible gases.

S_2E Sequence:

- Small-break loss-of-coolant accident (LOCA), failure of Emergency Core Cooling injection system.
- Hydrogen igniters are operable.
- Suppression pool heat removal is available.
- Some leakage, including fission products, from the drywell to the main containment, bypassing the suppression pool is assumed.

Computer Codes Used in the Study

The current efforts build on previous computer modeling work performed at Battelle-Columbus, at Sandia, and in the Federal Republic of Germany, and on experimental and model evaluation studies performed at Oak Ridge, EG&G Idaho, Sandia, and Pacific Northwest Laboratories. In addition to the calculations performed at Battelle-Columbus, calculations of thermal-hydraulic behavior and fission product release related to molten core-concrete interactions were performed by Sandia. Research efforts specifically directed toward increasing our understanding of fission product release and transport under severe accident conditions are under way at the laboratories listed above, as well as at other research installations around the world. Over the next few years, it is expected that considerable progress will be made in this area. Therefore, this report must be considered as an expression of current knowledge, with the

expectation of future validation or modification of the calculated fission product releases.

The first step in analyzing accident sequences was to collect plant design data and perform thermal-hydraulic calculations. Thermal-hydraulic conditions in the reactor over time were estimated with the MARCH 2 code, and detailed thermal-hydraulic conditions for the reactor's primary coolant system were estimated with the MERGE code, developed specifically for this program.

The time-dependent core temperatures from the MARCH 2 code were used as input to another code developed for this program, CORSOR, which predicts time- and temperature-dependent releases of radionuclides from the fuel inside the reactor pressure vessel. Releases of radionuclides from the interaction of the melted reactor core with the concrete outside the reactor vessel were estimated by Sandia National Laboratories using their computer code, VANESA.

Using the MARCH/MERGE-predicted thermal-hydraulic conditions and the CORSOR-predicted radionuclide release rates as input, a newly developed version of the TRAP-MELT code was used to predict vapor and particulate transport in the primary coolant circuit. Transport and deposition of radionuclides in the containment were calculated using the NAUA-4 code. The attenuation of particulate fission products during flow through pressure suppression pools was calculated with the SPARC code.

The calculations performed in this study were of a "best estimate" type. Whenever possible, input was derived from experimental measurements. Data employed in these analyses include vapor deposition velocities, aerosol deposition rates, aerosol agglomeration rates, fission product release rates from fuel, particle sizes formed from vaporizing/condensing fuel materials, engineering correlations for heat and mass transfer, and physical properties of various fuel, fission product, and structural materials.

Summary of Results

The sequences TC, TQUV, and TPI were emphasized for the Mark III containment design because the transient sequences are expected to be major contributors to risk. Two variations of the S_2E sequence were included to investigate the effects of suppression pool bypass.

The fission product releases from the fuel are generally similar to those predicted for the Peach Bottom plant and those given in WASH-1400. The volatile fission products are released almost completely during core melting although between 26 and 36 percent of the tellurium is predicted to remain with the molten core materials indefinitely.

Deposition of fission products in the RCS was found to be very sequence dependent with the fraction of CsI, CsOH, and Te retained ranging from about 6 to 54 percent depending on the sequence and species. CsI is predicted to be the species least effectively retained in the RCS. In general, fission product retention in the RCS for the Mark III plant is predicted to be slightly greater but roughly the same as that for the Mark I design. Retention of fission products in the RCS, of course, was not credited in WASH-1400.

Because the suppression pool was not bypassed in sequences TC, TQUV, and TPI, major fractions of the fission products are collected there. Nearly all of the fission products not deposited in the reactor coolant system or drywell are deposited in the suppression pool. The subcooled pool in the S_2E sequence is also an effective attenuating factor for flow through the pool but the pool bypass flow has a major influence on release from the plant. The two bypass flow cases (both S_2E) considered were a nominal leakage flow and an assumed stuck-open vacuum breaker. The nominal leakage and vacuum breaker cases gave source terms of about a factor of 10 higher than the source terms predicted for the transient cases with no bypass flow. The largest release fraction predicted was 0.14 for tellurium in the case with the stuck-open vacuum breaker.

2. INTRODUCTION

The possibility of radioactive material being released to the environment from LWRs has long been the impetus for considerable concern and research. Most reactors in the United States were designed, and their sites were chosen, on the basis of research report TID-14844.(2.1) Published in 1962, TID-14844 makes certain assumptions about the release of fission products (radioactive material produced during reactor operations) to the reactor containment area during a hypothetical severe accident. Although these assumptions are representative of the state of knowledge at the time, the behavior of fission products has become better understood in the intervening years. Accordingly, the Nuclear Regulatory Commission conducted the Reactor Safety Study to reassess the accident risks in U.S. commercial nuclear power plants. The report of that study, known as WASH-1400,(2.2) was published in 1975 are provided a more comprehensive and physically accurate description of fission product behavior. The amount of fission product release (the "source term") estimated in WASH-1400 has since been used extensively in planning and evaluating reactor operations.

The WASH-1400 source term to the environment for accident sequences has had broad implications for operating LWRs--in licensing, emergency planning, safety goals, and indemnification policy. However, additional research continued to provide even better methods for estimating fission product release and transport. In 1981, the Nuclear Regulatory Commission issued the report "Technical Bases for Estimating Fission Product Behavior During LWR Accidents",(2.3) a review of the state of knowledge at the time. As part of the Technical Bases report, the assumptions, analytical procedures, and available data were evaluated, and new estimates were made. One advantage of the new estimates was that they took into account the fact that some radioactive material would be deposited inside the reactor primary system during an accident and would therefore not be available to escape to the containment and from there to the environment. On the other hand, because of the limitations of the computer codes available at that time, the new estimates could not follow the transport of fission products along their flow path from the core to the environment by applying the various codes consistently. This resulted in piecemeal, parametric estimates of release.

The research results reported here are intended to provide this systematic, sequential application of the codes as well as to present analyses performed with computational procedures improved since the "Technical Bases" report. It is to be recognized that in this study, an analytical approach was developed for estimating radionuclide transport and deposition which incorporates individual physical and chemical processes or mechanisms. This approach is being evaluated for use in predicting fission product source terms for release to the environment for specific reactors and accident sequences. When verified, predictions made with the approach used here are expected to replace the generic tabular release fractions such as those in Table 6, Appendix V of WASH-1400, where release fractions are given for broad classes of accidents.

The purpose of this report is then to:

(1) Develop analytical procedures and use them to predict updated release-from-plant fission product source terms for four types of nuclear power plants and for accident sequences giving a range of conditions. The estimated source terms are to be based on consistent step-by-step analyses using improved computational tools for predicting radionuclide release from the fuel and radionuclide transport and deposition.

(2) Determine the effects on fission product releases associated with major differences in plant design and accident sequences.

(3) Provide in-plant time- and location-dependent distributions of fission product mass for use in equipment qualification.

It is not necessarily the intent of this work to produce an all-encompassing definition of source terms, but rather to make best estimates of source terms for a range of typical plants and several risk-significant sequences covering a wide range of conditions. These analyses are to be made with the best available techniques, in a consistent manner, following along release pathways for fission products, and at a level of detail consistent with current knowledge of pertinent physical processes. Based on state-of-the-art techniques, these best-estimate analyses should provide an indication of the conservatisms inherent in current source term assumptions and guidance for the development of new source terms. The analytical methods and corresponding predictions presented here are based on currently available information and are subject to revision and improvement as better analytical procedures are developed and as a more extensive experimental base evolves.

The preparation of this report, therefore, is an evolutionary process which will be carried out over a period of time, with verification and possibly revision of the procedures continuing over several years.

2.1 References

(2.1) DiNunno, J. J., et al, "Calculation of Distance Factors for Power and Test Reactors Sites", TID-14844 (March 23, 1962).

(2.2) "Reactor Safety Study--An Assessment of Accident Risks in U.S. Commercial Nuclear Power Plants", WASH-1400, NUREG-75/014 (October, 1975).

(2.3) "Technical Bases for Estimating Fission Product Behavior During LWR Accidents", NUREG-0772 (June, 1981).

3. GENERAL APPROACH

The general philosophy behind this study is that mechanistic predictions of radionuclide release and transport are possible if proper modeling is performed to represent the physical and chemical processes occurring during LWR accidents. The study, then, represents an attempt to describe in a reasonably complete but tractable fashion the processes influencing radionuclide release to the environment for selected plants and accident conditions.

The objectives of this study originally called for a consistent analysis of radionuclide behavior by following fission product transport along flow paths, starting with release into the core region and ending with final release to the environment. To meet these objectives, numerous decisions and assumptions were required for the analyses: selection of plants and sequences for consideration; choice of analytical tools to be used or upgraded; evaluation and incorporation of experimental data; and determination of major physical effects which would be considered on a parametric variation basis to determine the sensitivity of calculations to such variations. Some of the major considerations will be reviewed and discussed in this section.

The general approach in this study was to select specific plants and accident sequences for consideration and then to use consistent and improved analyses of fission product release from fuel, transport, and deposition to predict fission product release to the environment for these specific cases. The approach consists of a series of steps performed in sequence such that in the combined analysis, the results are specific to an individual set of accident conditions, and each step is based on results from analyses of the previous step.

3.1 Plant Selection

The first major step in the process was the selection of types of nuclear power plant designs to be considered and a specific plant to represent each type. The types to be considered were: large, dry PWRs; Mark I BWRs; Mark III BWRs; and ice-condenser containment PWR designs. The specific plants chosen to represent each type, respectively, are the Surry and Zion, Peach Bottom, Grand Gulf, and Sequoyah plants. These selections were made on a

combined basis of typicality of design and availability of design details needed for analysis.

3.2 Selection of Accident Sequences

Accident sequences were chosen for each plant such that significant contributions to risk and a wide range of physical conditions were represented in the analyses. The selected plants and accident sequences are listed below:

PWR: Large Dry Containment (Surry-Volumes 1 and 5)	PWR: Large Dry Containment (Zion-Volume 6)	BWR: Mark I (Peach Bottom-Volume 2)
AB	TMLB'	TC
S_2D	S_2D	AE
V		TW
TMLB'		

BWR: Mark III (Grand Gulf-Volume 3)	PWR: Ice Condenser Containment (Sequoyah-Volume 4)
TPI	S_2HF
TQUV	TMLB'
TC	TML
S_2E	

The accident sequences for each plant are described in detail in Section 4.2 of the volume of the report dealing with that plant.

3.3 Computer Codes Used in the Study

Following the selection of plants and sequences, the required plant design data were collected and thermal-hydraulic analyses performed for each accident sequence. Overall thermal-hydraulic conditions on a time-dependent basis were estimated with the MARCH code,[3.1] and detailed thermal-hydraulic conditions for the primary system were estimated with the MERGE[3.2] code developed specifically for this program.

The time-dependent core temperatures were used as input to another code developed for this program, CORSOR[3.3], which predicts time- and

temperature-dependent mass releases of radionuclides from the fuel within the pressure vessel. Releases during core-concrete interactions of radionuclides remaining with the melt were provided by Sandia National Laboratories using their newly developed model, VANESA[3.4].

Using the MARCH/MERGE-predicted thermal-hydraulic conditions and the CORSOR-predicted radionuclide release rates as input, a newly developed version of the TRAP-MELT code (TRAP-MELT 2)[3.5] was used to predict vapor and particulate transport in the primary coolant circuit.

Retention of aerosols in suppression pools was calculated using the SPARC[3.6] code and transport and deposition of radionuclides in the containment were calculated using the NAUA-4[3.7] code.

The basic stepwise procedure described above is illustrated in Figure 3.1, which shows the relationships among the computational models. The calculations were of a "best estimate" type using input derived from experimental measurements whenever possible. Types of data employed in the analyses include vapor deposition velocities, aerosol deposition rates, aerosol agglomeration rates, fission product release rates from fuel, particle sizes formed from vaporizing/condensing fuel materials, engineering correlations for heat and mass transfer, and physical properties of various fuel, fission product and structural materials.

3.3.1 Assumptions

In preparation for performing calculations of thermal-hydraulic conditions and radionuclide transport and deposition, it was necessary to make a number of assumptions or to select conditions from among several options. Major assumptions used in this study of the Grand Gulf plant are listed below in the categories of geometry, thermal hydraulics, and mechanisms.

Geometry

(1) Surfaces within the containment building available for radionuclide deposition include only the major geometrical features of the building.

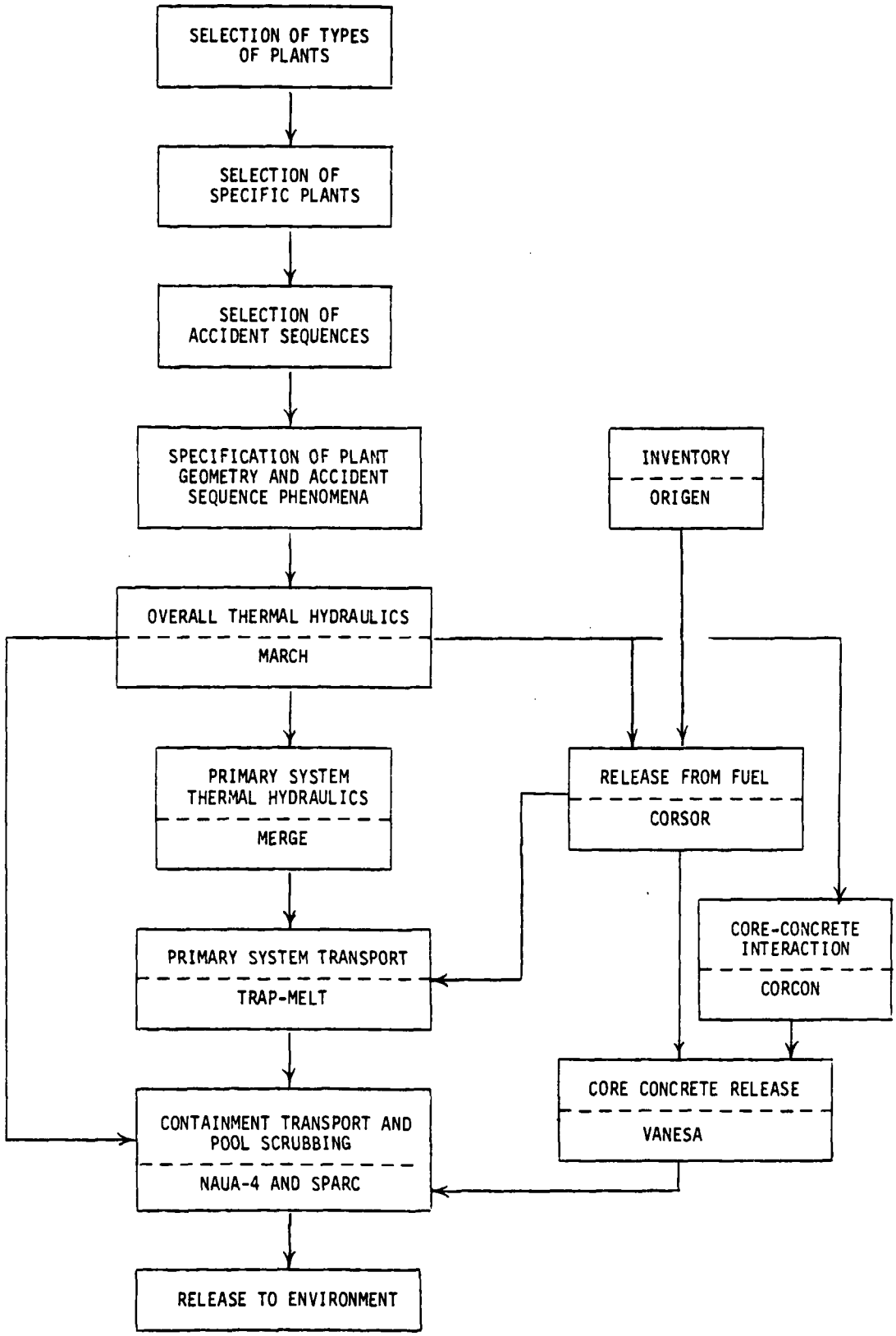

FIGURE 3.1. INFORMATION FLOW FOR RELEASE, TRANSPORT AND DEPOSITION CALCULATION

(2) There is no attenuation of radionuclides as they pass through leak paths in the containment shell.

Thermal Hydraulics

(3) Before pressure vessel failure, flow from the primary coolant system is restricted to direct leak paths.

(4) The upper plenum geometry is modeled in terms of surface areas, steel thickness, and compartment heights rather than with exact geometries.

(5) Decay heating of surfaces by deposited fission products is neglected in the calculations reported in this study.

Mechanisms

(6) Neither deposition nor resuspension of radionuclides occurs during rector coolant system depressurization at the time of pressure vessel melt-through.

(7) In the long term (after pressure vessel failure), deposited radionuclides remain in the primary system indefinitely.

(8) No change in fission product physical or chemical properties results from radioactive decay.

Some of the above assumptions have been relaxed or changed to accommodate best estimates of conditions and occurrences in specific cases. These are discussed in greater detail for each plant in Section 6.1 of the volume of the report dealing with that plant.

3.3.2 Uncertainty Considerations

The computation of radionuclide release and transport using mechanistic models is subject to many uncertainties of various magnitudes and importance. Quantitative estimates of uncertainties in individual parameters, and hence the overall importance of such uncertainties, has been outside the scope of this study. Where practical, however, qualitative (and in some cases quantitative) estimates of uncertainties have been noted.

Some of the uncertainties in the analyses and procedures can be identified that are currently considered significant. The following is a list of some uncertainties that are believed significant and warrant further evaluation through more detailed analyses:

(1) The simplified fuel melting model in MARCH (i.e., a single melting temperature) could bias the predicted release of material from overheated fuel, particularly regarding the source of inert and low volatility fission product aerosols.

(2) The rate coefficients for the release of fission products from overheated fuel are empirical, rather than mechanistically based, and rely largely on scaled, simulant experiments.

(3) The model for the release of fission products and inert materials during the attack of concrete has a very limited experimental basis.

(4) The flow patterns in the reactor coolant system are uncertain. The adequacy of the simple thermal-hydraulic models used in this study will require experimental verification.

(5) Primary system transport models used in these analyses have not been validated against integral experiments.

(6) The mode and timing of containment failure in severe accident sequences can have a major influence on fission product behavior but are subject to large uncertainty.

(7) The calculation methods for water condensation in the containment are based on limited, small-scale experiments and require verification at larger scales.

(8) Deposition velocities for vapor species used in the TRAP-MELT calculations were taken as a mid-points in order-of-magnitude ranges of experimental data. More accurate data would reduce the uncertainty in these parameters and in the resulting rates for deposition by sorption.

3.4 References

(3.1) Wooton, R. O. and Avci, H. I., "MARCH (Meltdown Accident Response Characteristics) Code Description and User's Manual", NUREG/CR-1711, BMI-2064 (October, 1980).

(3.2) Freeman-Kelly, R. G. and Jung, R. G., "A User's Guide for MERGE" (February 10, 1984).

(3.3) CORSOR Manual.

(3.4) VANESA Manual.

(3.5) TRAP-MELT 2.1 User's Manual.

(3.6) Owczarski, P. C., Postma, A. K., and Schreck, R. I., "Technical Bases and User's Manual for SPARC -- Suppression Pool Aerosol Removal Code", report to the U.S. NRC, NUREG/CR-3317 (May, 1983).

(3.7) Bunz, H., Koyro, M., and Schock, W., "A Code for Calculating Aerosol Behavior in LWR Core Melt Accidents Code Description and User's Manual".

4. PLANT SELECTION AND ACCIDENT SEQUENCES

4.1 General Plant Description

The Grand Gulf Nuclear Station Unit 1[4.1] was selected to characterize boiling water reactors with Mark III containment design. A recent U.S. design, the BWR Mark III designs include containment systems with pressure suppression pools in a different configuration than in the Mark I or Mark II designs. Some of the data used to represent the plant have been adapted from values provided in the General Electric Standard Safety Analysis Report (GESSAR)[4.2].

The Grand Gulf Nuclear Station involves two twin units in a common facility with the sharing of some facilities. Each unit has a BWR/6 boiling water reactor (251-inch diameter vessel with 800 fuel assemblies) which was designed and supplied by the General Electric Company. The thermal power output of each unit is approximately 3800 MW(t) and the net electrical output is approximately 1250 MW(e). Although the Grand Gulf reactor coolant system differs someowhat from that of Peach Bottom 2, the in-vessel meltdown behavior and transport of fission products within the reactor coolant system would be expected to be similar for the two plants for most accident sequences. A greater difference in accident behavior would result from differences in the physical layout of the plant outside the reactor coolant system.

The Mark III containment design employed in the Grand Gulf plant is illustrated in Figure 4.1. In this design, the suppression pool is located at the periphery of the containment. In the event of a loss of coolant accident, the water level in the channel internal to the weir wall would be depressed, uncovering horizontal vent pipes. Steam in the drywell would then be relieved to the suppression pool through the vents. In the Mark III design, the vapor space of the wetwell actually forms an outer containment volume surrounding the drywell. The volume of the drywell, 270,000 ft^3 (7650 m^3), is comparable to but somewhat greater than the volume of the Peach Bottom drywell. The primary containment volume, 1.4×10^6 ft^3 (4.0×10^4 m^3), is substantially larger than the wetwell vapor spaces in the Mark I and Mark II designs. The containment is a steel-lined, reinforced concrete structure.

The internal design pressures of the drywell and containment are 30 and 15 psig (0.2 and 0.1 MPa), respectively. In this study, it has been assumed

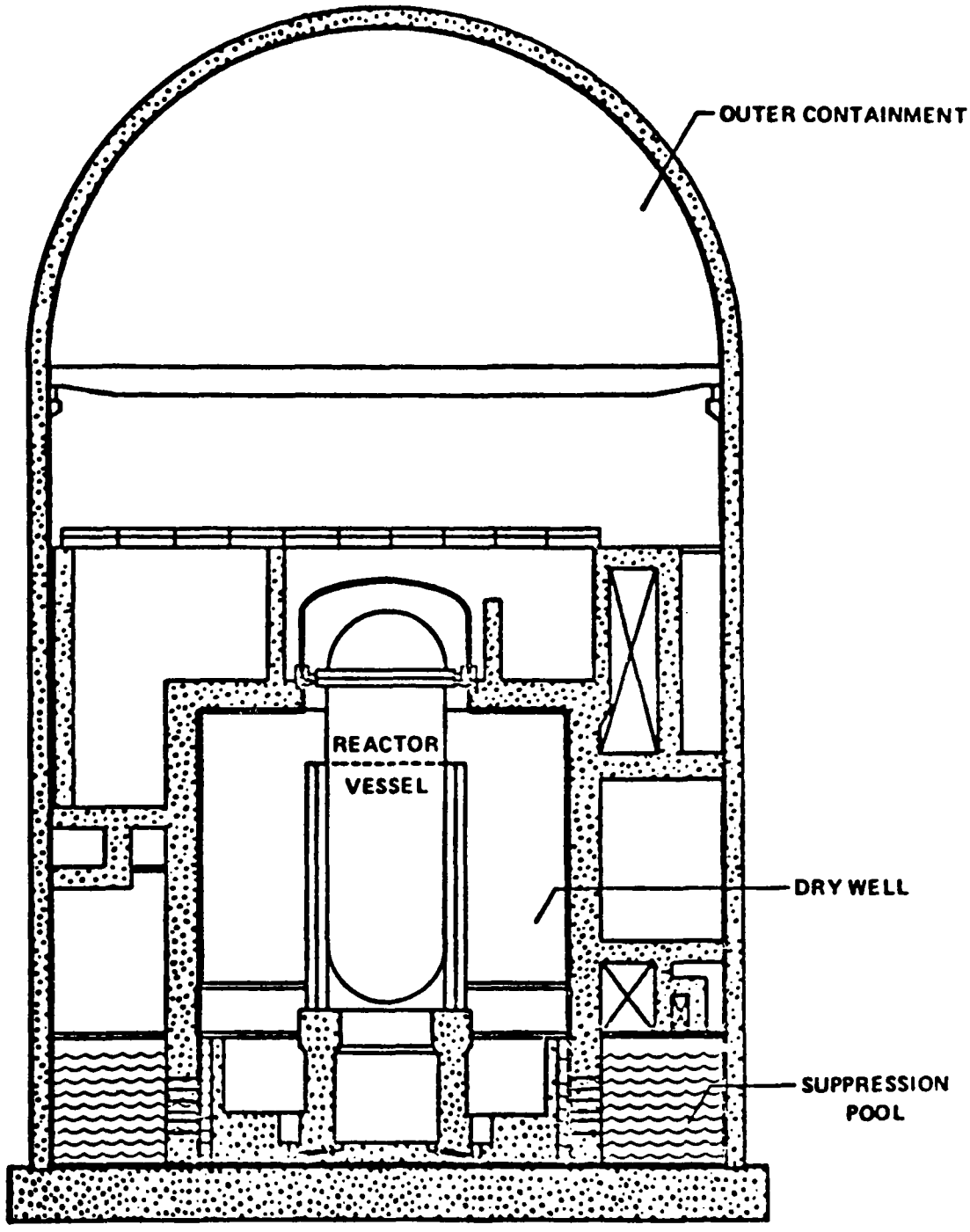

FIGURE 4.1 **BWR MARK III CONTAINMENT DESIGN**

that failure of the containment would occur at an internal pressure of 72 psia (0.5 MPa), based upon discussions with industry representives. This failure pressure is considerably higher than the 45 psia (0.3 MPa) nominal value utilized in the RSSMAP analyses of Grand Gulf[4.3] and is 3.8 times the design value. The expected location of failure is in the upper region of the containment at the junction of the cylindrical wall with the hemispherical dome.

There is little basis for predicting the leakage characteristics of the containment following failure. A large leakage was assumed to result for the purposes of this study. Since the failure location was elevated with respect to the suppression pool, it was assumed that water would remain in the pool following failure.

The Standby Gas Treatment System at Grand Gulf provides for mixing between the auxiliary and enclosure building. The capacity of the system to exhaust to the atmosphere is quite small, however: 4000 cfm (1.9×10^3 l/s). The enclosure building is expected to fail shortly after failure of the primary containment. Other plant data used in the analyses are provided in Table 4.1.

4.2 Selection Basis and General Description of Accident Sequences

Four accident sequences were selected for analysis in this plant: TC, TPI, TQUV, and S_2E. (Table 4.2 relates the letters used to describe the accident sequence with the systems that fail during the accident.) These sequences are consistent with the dominant sequences identified by the ASEP (Accident Sequence Evaluation Program).[4.4] In the transient sequences considered here, the fission products released during the in-vessel phase of the accident are released through the relief/safety valves directly to the suppression pool; after vessel failure, the release is to the drywell and then to the suppression pool. Both the ASEP and GESSAR studies indicate that pipe break accidents leading to core melt are very unlikely because many water makeup sources would be available. For pipe break sequences in which the suppression pool remains subcooled during the period of fission product release, the suppression pool would be very effective in scrubbing fission products. In order to investigate the possible effect of potential suppression pool bypass, the S_2E sequence was included in the study. In this sequence, the fission products are released to the drywell through the break in the piping and then

TABLE 4.1. MARK III DATA

Nominal Power	3,833 MW(t) 13,082 x 10^6 Btu/hr
Steam Pressure in Core	1040 psig (7.3 MPa)
Primary System Operating Temperature	555 F (290.6 C)
Primary System Total Coolant Volume	24,953 ft^3 (706.7 m^3)
Liquid Volume in Vessel	15,315 ft^3 (433.7 m^3)
Steam Volume in Vessel	8,811 ft^3 (249.5 m^3)
Steam Volume in Recirculation Loop	827 ft^3 (23.4 m^3)
Reactor Coolant System Liquid Mass	6.988 x 10^5 lbm (3.17 x 10^5 kg)
Reactor Coolant System Steam Mass	23,667 lbm (10,736 kg)
Reactor Vessel	
Inside diameter	251 inches (6.375 m)
Inside height	73 ft (22.25 m)
Design pressure	1250 psig (8.7 MPa)
Design temperature	575 F (301.7 C)
Thickness (with clad)	6.265 inches (1.91 m)
Core	
Equivalent diameter	15.96 ft (4.9 m)
Active fuel height	12.5 ft (3.8 m)
Total cross sectional area	169 ft^2 (15.7 m^2)
Flow area of core	84.3 ft^2 (7.8 m^2)
Number of fuel assemblies	800
Rods per assembly	62
Pitch	5.3 x 10^{-2} ft (0.016 m)
Assembly dimensions	5.46 inches square (0.14 m square)
Fuel rod diameter	4.025 x 10^{-2} ft (0.012 m)

TABLE 4.1. (Continued)

Fuel pellet diameter	3.417×10^{-2} ft (0.104 m)
Clad thickness of fuel rods	5.543×10^{-3} ft (0.002 m)
Total number of fuel rods	49,600
Core weight	
UO_2	366,400 lbm (166,195 kg)
Zircaloy	174,700 lbm (79,242 kg)
Miscellaneous	30,450 lbm (13,812 kg)
Total Vessel Weight	1.945×10^{6} lb (882,233 kg)
Drywell	
Free volume	270,100 ft^3 (7649 m^3)
Design temperature	330 F (165.6 C)
Internal design pressure	30 psig (0.31 MPa)
Vent Pipes	
Number	135
Internal diameter	2.33 ft (0.71 m)
Suppression Pool	
Water volume	136,000 ft^3 (3,851.5 m^3)
Design temperature	185 F (85 C)
Internal design pressure	15 psig (0.21 MPa)

TABLE 4.2 KEY TO BWR ACCIDENT SEQUENCE SYMBOLS

A - Rupture of reactor coolent boundary with an equivalent diameter of greater than six inches.

B - Failure of electric power to engineered safety features.

C - Failure of the reactor protection system.

D - Failure of vapor suppression.

E - Failure of emergency core cooling injection.

F - Failure of emergency core cooling functionability.

G - Failure of containment isolation to limit leakage to less than 100 volume percent per day.

H - Failure of core spray recirculation system.

I - Failure of low pressure recirculation system.

J - Failure of high pressure service water system.

M - Failure of safety/relief valves to open.

P - Failure of safety/relief valves to reclose after opening.

Q - Failure of normal feedwater system to provide core make-up water.

S_1 - Small pipe break with an equivalent diameter of about 2" - 6"

S_2 - Small pipe break with an equivalent diameter of about 1/2"-2".

T - Transient event.

U - Failure of high pressure coolant injection or reactor core isolation cooling system to provide core make-up water.

V - Failure of low pressure emergency core cooling system to provide core make-up water.

W - Failure to remove residual core heat.

Containment Failure Modes.

α = steam explosion in reactor vessel.

β = steam explosion in containment.

γ = containment failure due to overpressure-release through reactor building

γ' = containment failure due to overpressure-release direct to atmosphere.

δ = containment isolation failure in drywell.

ξ = containment isolation failure in wetwell.

ζ = containment leakage greater than 2400 volume percent per day.

η = reactor building isolation failure.

θ = Standby Gas Treatment System failure.

to the suppression pool by way of the horizontal vents. Some direct leakage from the drywell to the outer containment without passing through the suppression pool was included in the analysis.

4.2.1 Sequence TC (Transient with Failure to Scram)

In this transient, the control rods fail to insert and the reactor stays at elevated power, dumping heat to the suppression pool through the safety/relief valves. The emergency core cooling system supplies makeup water to the primary system, and the resulting equilibrium power level is determined by the makeup flow rates and the core reactivity coefficients. Since the equilibrium power level of the reactor (16 percent of full power) exceeds the heat removal capability for cooling the pool, the temperature of the pool rises and the pressure in the containment increases to the failure pressure. After containment failure, the containment pressure decreases, the suppression pool boils, and the makeup pumps stop delivering coolant to the vessel.

As the core heats up and melts, fission products are released from the fuel, and then flow with the gases through the steam separator (see Figure 4.2). The flow then divides, with a major fraction (85 percent) going through the steam dryers and the rest bypassing the steam dryers through an outer annular region. The flows then merge at the steam line and pass through safety/relief valves and relief lines. The flow exits the relief line into the suppression pool through a sparger. From the top of the suppression pool, gases and entrained aerosols disperse in the outer containment volume before leaking through the breach in containment. Although the containment spray system could possibly survive failure of the containment, its operation would be very difficult to demonstrate with confidence. In these analyses, it was assumed that the spray system would not operate.

The enclosure building is expected to fail at the time of containment failure. The mode of failure of the enclosure building would be sensitive to the mode of failure of the containment building. It is assumed in these analyses that major failure of the enclosure building results and that fission products leak from the containment directly to the environment.

After melt-through of the reactor vessel, the airborne fission products in the vessel flow to the drywell as the system depressurizes. Fission products released over time from reactor coolant system surfaces also enter

Phase 1. Up to Vessel Penetration (Containment failed prior to core melt).

Melt Release

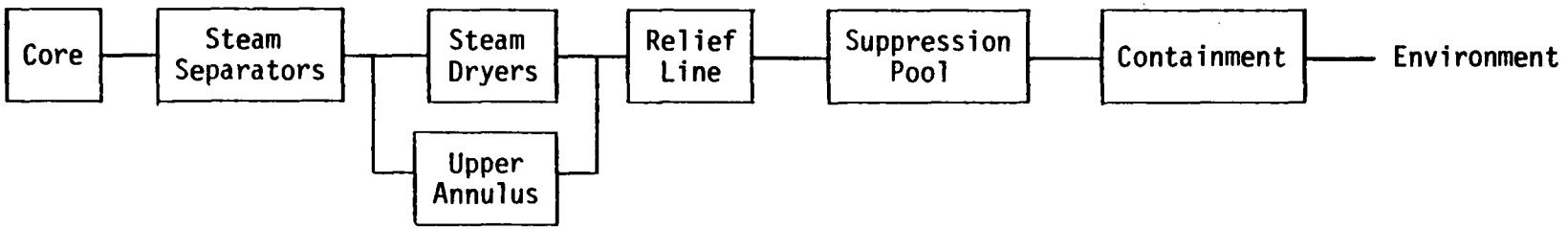

Phase 2. After Vessel Penetration

Vaporization Release and Evolution from RCS

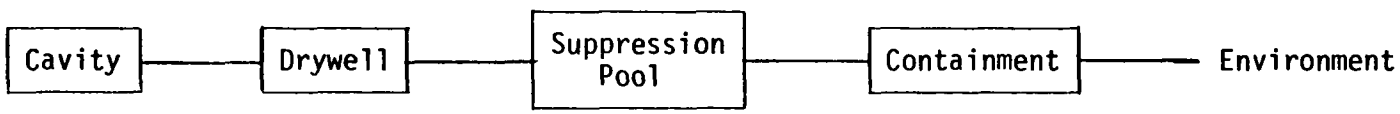

FIGURE 4.2 FLOW PATHS FOR TC AND TW SEQUENCES

the drywell, and attack of the concrete by the molten core also produces a source term to the drywell. The fission products are then carried to the suppression pool, to the outer containment volume, and through the break in containment to the environment.

4.2.2 Sequence TPI (Transient with Stuck Open Relief Valve and Loss of Decay Heat Removal)

In this sequence, a safety/relief valve sticks in the open position and the system depressurizes into the suppression pool, but the emergency core cooling system supplies makeup water to the reactor vessel. In addition, the residual heat removal system fails so that, over time, the pool heats up and the containment pressure rises. As in sequence TC, the containment fails prior to core melting, but since the core is at decay heat power level, the time to failure is substantially longer (22 hours). The emergency core cooling system pumps are assumed to fail after containment failure due to flashing of the suppression pool. This sequence is essentially the same as the TW sequence (transient with loss of decay heat removal) which was analyzed for the Peach Bottom design in Volume 2.

The flow paths to the environment are illustrated in Figure 4.2. These paths are the same as described for the TC sequence.

4.2.3 Sequence TQUV (Transient with Loss of All Makeup Water)

This is a transient sequence in which all water makeup systems to the reactor vessel fail. It is assumed, based on current BWR operating procedures, in the analysis that before depressurizing the reactor coolant system (RCS), the operators test the low pressure pumps and determine that they are unavailable. The reactor coolant system is therefore maintained at pressure until the water level in the core reaches approximately 2 feet. At this point, the RCS is depressurized. Thus the core undergoes a heatup transient which is temporarily quenched at the time of depressurization due to level swell. The core subsequently uncovers, reheats, and melts.

The flow paths for fission product transport can be divided into three time phases (see Figure 4.3). Before the vessel melts through, the path is essentially the same as for the TC and TW sequences except that the

Phase 1. Up to Vessel Penetration

Melt Release

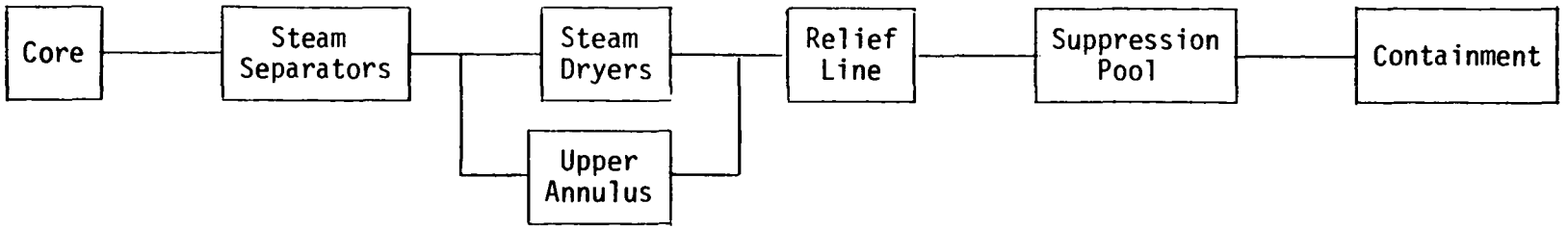

Phase 2. After Vessel Penetration to Containment Failure

Vaporization Release and Evolution from RCS

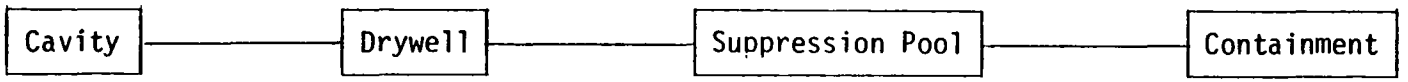

Phase 3. After Containment Failure

Vaporization Release and Evolution from RCS

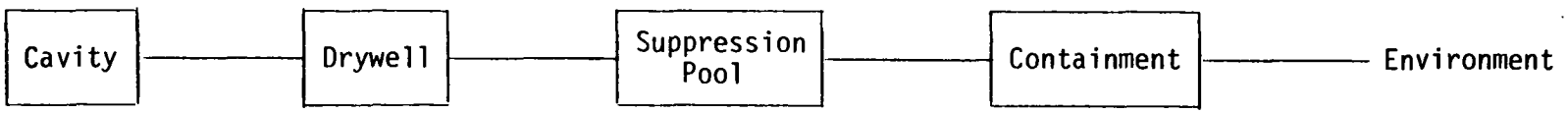

FIGURE 4.3 FLOW PATHS FOR SEQUENCE TQUV

containment is intact. After vessel penetration but before containment failure, the pathway is from the reactor cavity to the drywell, to the suppression pool, and to the containment. In this case, the suppression pool would be subcooled and potentially very effective in removing fission products. For this sequence, it is unlikely that the containment spray system would be operable considering the other systems that are failed; though the suppression pool would provide significant fission product retention. Following failure, the containment would blow down to the environment. The pathway for any subsequent release would be from the cavity to the drywell, to the suppression pool, to the containment, and to the environment.

In the analysis of the TQUV sequence it is assumed that hydrogen igniters are present and operable, and that combustion of hydrogen released to the containment through the safety/relief valves occurs. Burning of the hydrogen released during primary system depressurization is expected to result in significant pressure rises, though not sufficient to lead to containment failure for the assumed failure pressure. The pressures resulting from such hydrogen burning can be sensitive to the rates of hydrogen release, hydrogen concentrations at ignition, containment compartmentalization, etc. For the TQUV sequence as analyzed here, the peak pressures resulting from hydrogen ignition would be sensitive to the relative timing of primary system depressurization and core melting.

Assuming accommodation of hydrogen burning, the containment would then be expected to fail because of the buildup of noncondensibles, both from the reaction of the Zircaloy with steam and from the attack of the concrete by core debris. Failure due to the buildup of noncondensibles would take place late in time with respect to core melting.

4.2.4 Sequence S_2E (Small Break LOCA, Failure of Emergency Core Cooling

This accident sequence is initiated by a small break in the primary coolant system; the initiating event is accompanied by the failure of the emergency core cooling system. In the absence of coolant makeup, the primary coolant inventory would be lost through the break and lead to core uncovery and melting. The rate of coolant loss and the timing of core uncovery and subsequent melting would depend on the size and location of the break in the

primary system piping. For the purposes of this analysis, a break size equal to a 2-inch diameter opening was assumed.

In the S_2E sequence, the fission products from the core would be released to the drywell through the break in the piping and then to the suppression pool by way of the horizontal vents. In this sequence the suppression pool is expected to be subcooled and be very effective in the removal of fission products. In order to investigate the possible effect of potential suppression pool bypass, some direct leakage from the drywell to the outer containment was included in the analyses for the S_2E sequence. Two specific bypass leak rates were examined. The first corresponds to possible or nominal leakage from the drywell to the containment; the specific value used was based on measured leakage data provided by the General Electric Company. The second case considered modeled a stuck open vacuum breaker between the outer containment and the drywell. The bypass leakage rate in the second case was about a factor of 10 greater than for the nominal case. Figure 4.4 illustrates the fission product flow paths assumed for the S_2E sequence.

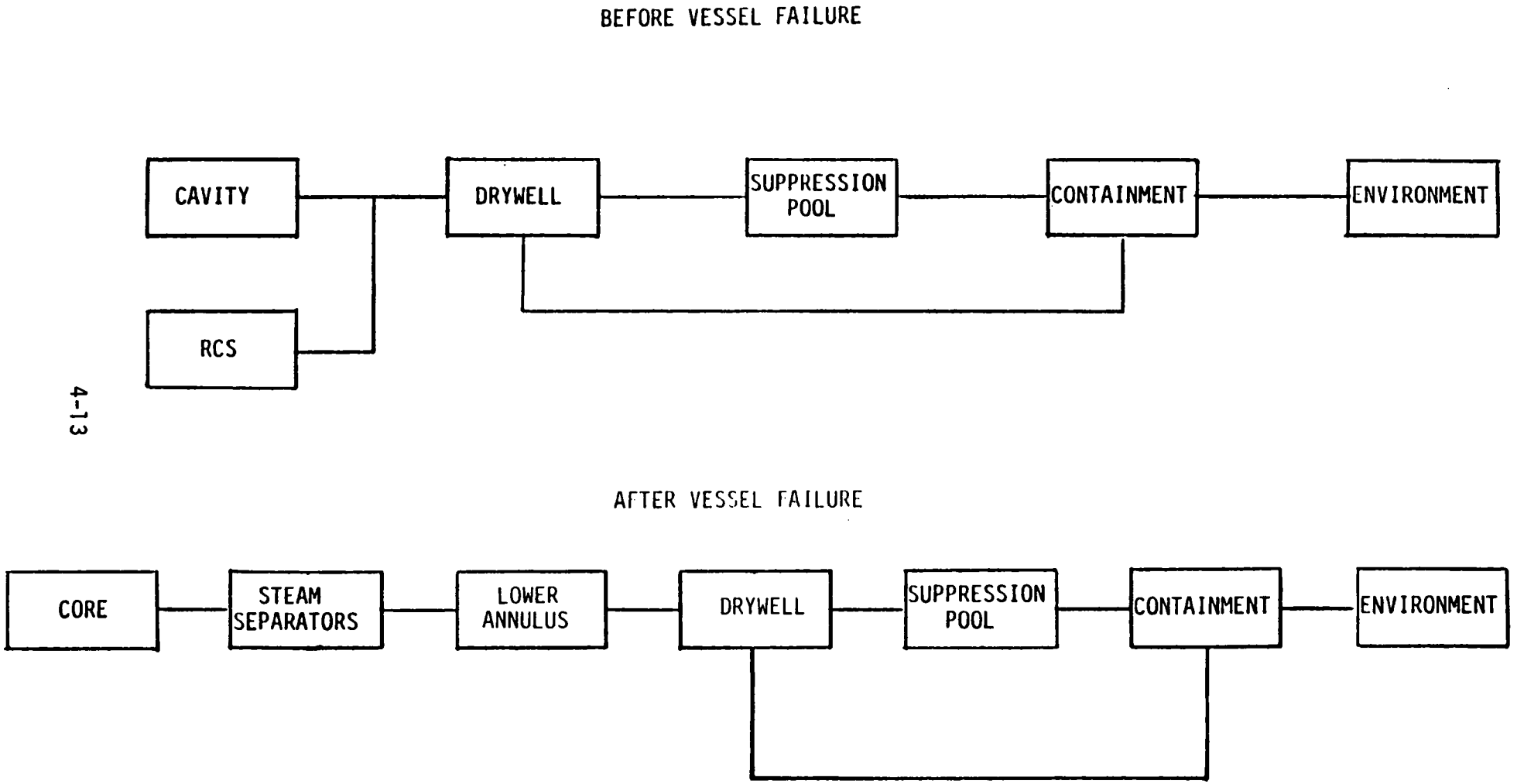

FIGURE 4.4 FLOW PATHS FOR FISSION PRODUCT TRANSPORT IN GRAND GULF - SEQUENCE S2E

References

(4.1) Grand Gulf Nuclear Station Units 1 and 2, Final Safety Analysis Report, Docket No. 50-416 (November, 1972).

(4.2) GESSAR II, 238 Nuclear Island, Appendix 15D, BWR/6 Standard Plant Probabilistic Risk Assessment, Docket No. STN50-447.

(4.3) Hatch, S. W., Cybulskis, P., and Wooton, R. O., "Reactor Safety Study Methodology Applications Program: Grand Gulf 1 BWR Power Plant", NUREG/CR-1659/4 of 4 (October, 1981).

(4.4) Kolaczkowski, A. M., et al, "Interim Report on Accident Sequence Likelihood Reassessment (Accident Sequence Evaluation Program)", Draft (February, 1983).

5. ANALYTICAL METHODS

This section describes the analytical methods used in assessing the source term to the environment for the Grand Gulf plant, a BWR Mark III design. The methods employed here differ significantly from those used to analyze the Surry plant, as described in Volume 1 of this report[5.1]. The Surry plant has been reevaluated using these revised methods; the results of the Surry reevaluation are reported in Volume 5[5.2].

The first major difference between the methods used here and those described in Volume 1 is that the MARCH 2 code is used here for the overall thermal-hydraulic calculations, replacing the MARCH 1.1 code used for Volume 1. MARCH 2 incorporates a number of improvements in the treatment of accident thermal-hydraulics over the earlier version of the code. The second major change is that in the present analysis, an accounting is made for the effect of Zircaloy cladding oxidation on the release rate for tellurium. Finally, the SPARC code is used here to predict the retention of aerosols in suppression pools.

Some other, less significant changes have been made as well. These are discussed in the text.

5.1 Thermal Hydraulic Behavior

This section describes the computer code MARCH 2, which, along with the MERGE code, was used to analyze the thermal-hydraulic response of the reactor core, the primary coolant system, and the containment system for the selected accident sequences.

5.1.1 Overall System Thermal Hydraulics: MARCH 2

The MARCH 2[5.3] (Meltdown Accident Response CHaracteristics) computer code describes the physical processes involved in severe fuel-damage accidents in light water reactors. Version 2 of the code replaces Version 1.1.[5.4] The differences between the two versions include changes in models, code structure, and programming language. The new models in MARCH 2 were developed at a

number of institutions, including Battelle, Sandia National Laboratories, Oak Ridge National Laboratories, Brookhaven National Laboratory, and the Tennessee Valley Authority. In many cases, these models are provided as options to existing models. The changes in MARCH were largely undertaken to address recognized deficiencies in the early version related to modeling approximations, time-step control, and transportability of the code to other installations.

The MARCH 2 code was developed primarily for use in probabilistic risk assessment. The uncertainties in many of the MARCH 2 models are large, and in many cases the extent to which the models have been validated against experiments is limited. More mechanistic codes are being developed by the NRC, such as SCDAP and HECTR, but they were not available for use in this program.

The MARCH 2 code examines the behavior of a large variety of accident processes including depressurization or leakage from the reactor coolant system, core uncovery, core heatup, oxidation of Zircaloy cladding, fuel melting, fuel slumping, fuel-coolant interaction in the lower vessel head, vessel head failure, fuel-coolant interaction in the reactor cavity, debris bed coolability, core-concrete interactions, production of combustible gases, gas combustion in the containment, containment heat transfer, intercompartment flows, and the effect of engineered safety features on containment thermal hydraulic behavior. Some of the principal modeling improvements in Version 2 of the MARCH code are described below.

5.1.1.1 Containment Response. The containment response modeling in MARCH 2 includes the following principal changes: provision for expanded blowdown input via subroutine INITIAL, the ability to accept two input terms from the primary system, completely revised treatment of burning of combustibles, addition of a heat sink for radiation heat transfer from the debris in the reactor cavity, and removal of a number of restrictions in the earlier code.

The expanded blowdown table input capability is intended to facilitate the interfacing of the MARCH code with more detailed thermal-hydraulic codes that may be used to describe the initial portion of the accident sequence.

The containment response subroutine, MACE, has been changed to accommodate simultaneous break and relief/safety valve flows from the primary system. The two inputs can be directed to different compartments if desired, e.g.,

break flow to the drywell and relief/safety valve flow to the suppression pool of a BWR.

5.1.1.2 Primary System Response. The MARCH 2 treatment of the primary system includes both improvements in the treatment of initial (early) primary system response and the addition of several phenomenological models to treat the processes following core collapse into the bottom head. Included are changes in the steam generator model to remove some of the restrictions and limitations of the earlier version, improved break flow models, changes in the flashing model in response to primary system pressure changes, provisions for simultaneous break and relief/safety valve flow, changes in the treatment of heat transfer to structures, and consideration of the transport of fission products within the primary system.

5.1.1.3 Water and Steam Properties. The representation of the properties of water and steam has been improved in MARCH 2. This has included expansion of the property tables and correlations incorporated in the code as well as inclusion of additional properties required by the new phenomenological models. The input parameters are based on the ASME steam tables.

5.1.1.4 Decay Heat. MARCH 2 incorporates the current American National Standard[5.5] for evaluating fission product decay heating as a function of time after shutdown and time at power, including the contributions from heavy element decay. This replaces the earlier, simplified version incorporated in MARCH 1.1. Alternatively, decay heat as a function of time may be input in tabular form; this approach would be particularly appropriate for transients with failure to scram, where the power history would be provided by more detailed system codes.

5.1.1.5 Core Heat Transfer. MARCH 2 retains the basic model of the core as developed for the earlier version, but incorporates additional models for a more detailed treatment of heat transfer processes. Heat transfer between the fuel rods and the steam-hydrogen gas mixture is now calculated using either the full Dittus-Boelter correlation[5.6] for turbulent flow or a laminar flow correlation. A subroutine has also been added to approximate axial conduction

heat transfer in the fuel rods using the Fourier law of heat conduction and the BOIL-calculated node temperatures. The effect of axial and radial thermal radiation heat transfer within the core, as well as between the core and surrounding structures and water surfaces, can now be calculated. The heatup of the core support barrel by thermal radiation is included. Additional changes include corrections in the heat transfer analysis of partially covered core nodes and improvements in the metal-water reaction model.

5.1.1.6 Core Debris. A number of phenomenological models have been added for the treatment of the core debris in the reactor vessel bottom head. These include a flat plate critical heat flux model, a fragmented debris-to-water heat transfer correlation, and several options that consider formation of debris beds within the vessel head while water is still in the vessel. The bottom head heatup model utilizes a calculated heat transfer coefficient between the molten debris and the vessel head.

A major area of concern and controversy in the analysis of core meltdown accidents has been the behavior of core and structural debris upon contact with water in the reactor cavity. The highly simplified models of MARCH 1.1 have been supplemented with a flat plate critical heat flux model, a particulate heat transfer model with more mechanistic heat transfer coefficients, and several debris bed heat transfer correlations. If desired, the switchover from one model to another can be based on calculated conditions, e.g., debris temperature. The production of hydrogen from steel-water reactions has been incorporated into these models in addition to the zirconium-water reaction previously available. Also included are the heating of the evolved gases by the debris beds and the effect of hydrogen flow on bed floodings.

A heat sink has been provided for the thermal radiation from the top of the core debris as calculated by the INTER subroutine. The decomposition of concrete due to radiated heat flux is treated by an ablation-type model with the resulting gases added to the containment atmosphere. Also, the geometry of the corium-concrete mixture is fixed following solidification of the melt.

5.1.1.7 Burning in Containment. The treatment of combustible gases now includes consideration of the burning of hydrogen and carbon monoxide if

their concentrations exceed flammability limits. Included are explicit considerations of inerting due to high steam concentrations and oxygen depletion, direction-dependent compositions for flame propagation between compartments, and burn velocities as functions of composition. Various options are available to explore the effects of assumptions about the burning of hydrogen and carbon monoxide.

5.1.2 Primary System Thermal Hydraulics: MERGE

When the MERGE[5.7] code was written, the existing computer codes describing the thermal-hydraulic behavior of a core meltdown accident were not capable of analyzing the flow and temperatures in the individual volumes of the reactor coolant system downstream of the core in the pathway for release to the containment. The report "Technical Bases for Estimating Fission Product Behavior During LWR Accidents"[5.8], published by the NRC in 1981, indicated that in at least some accident sequences, the retention of fission products in the reactor coolant system (RCS) could be significant. To support more realistic analyses of fission product retention with the TRAP-MELT code discussed in Section 5.3.1, an effort was undertaken to write a simple stand-alone code, MERGE, to predict gas temperature, surface temperature, and flow within the reactor coolant system.

MERGE calculations are based on the output of MARCH, and the output of MERGE is input to the TRAP-MELT code. The MARCH results used by MERGE are: the primary system pressure, the flow rate of hydrogen leaving the core, the flow rate of steam leaving the core, and the average temperature of gases leaving the core. The MERGE analysis accounts for conservation of energy and conservation of mass by species. It is assumed that the gases within a volume are well mixed and have the same temperature, and that the pressure differential between volumes is negligible.

In MERGE, the equations are solved with an explicit time difference scheme. At a particular time step, conditions within the first volume downstream of the core are calculated first, and the solution proceeds from each volume to the next downstream volume. Knowing the initial and inlet flow conditions for each volume, MERGE solves for the value of the outlet flow from

the volume that yields the known pressure. Heat transfer from flowing gas to structures is accounted for. Forced laminar, forced turbulent, and natural convection heat transfer coefficients are utilized as appropriate, with a radiative term added to the coefficient. In addition, the MERGE-calculated radiative heat transfer from the core to the first structure is calculated based on a MARCH-calculated radiative flux.

The MERGE code involves certain approximations and limitations. In the MERGE analysis, the flow of gases in the upper plenum is assumed to be one-dimensional; in reality, circulation patterns would more probably be established in this region due to the strong temperature gradients. Whether a more detailed analysis is required for this region must be determined by the results of sensitivity studies with the TRAP-MELT code. The need for validation experiments must also be evaluated.

5.2 Radionuclide Release from Fuel

5.2.1 Source Within Pressure Vessel: CORSOR

CORSOR[5.9] is a simple correlative code which estimates aerosol and fission product release rates from the core during the period of core melting in a light water reactor. Quantifying the aerosol and fission product release from the core region is an important first step in determining the radionuclide source term to the containment during a hypothetical severe core damage accident. The timing of the release of various materials influences their retention in the reactor coolant system because it determines which species emanating from the core will be able to interact. The timing also determines the residence time of the released materials and the temperatures in the reactor coolant system, since these are both dynamic parameters. Simplistic source terms, such as constant or linearly increasing release rates with concurrent releases for all radionuclides, may therefore lead to unrealistic estimates of radionuclide transport behavior.

For the present analysis, the core has been divided into 216 nodes, 9 radial and 24 axial, which have distinct temperatures as predicted by MARCH. The core inventory, determined from the program ORIGEN[5.10], has been divided

equally among the nodes, according to a nine region radial power distribution provided by the General Electric Company. The axial distribution of the inventory has been assumed to be homogeneous.

Temperatures at each of the nodes are obtained from the MARCH code for each of a number of time steps, beginning at the start of the accident and continuing to a user-specified time. An average temperature is computed over each time span during core heatup and melting, and if the temperature is less than 900 C for any node, no release will occur from that node. The average temperature for failure of the cladding of a fuel rod is taken to be 900 C.[5.8] The sensitivity of CORSOR release estimates to the temperature set for cladding failure was also discussed in Appendix B of Volume 1.[5.1] When any axial position in a fuel bundle achieves a temperature of 900 C, CORSOR calculates a gap release of certain volatile fission products for all fuel rods in that radial zone. This is intended to simulate the gap release accompanying the bursting of individual fuel rods. This release occurs because certain fission products accumulate in the fuel-cladding gap because of migration within the fuel. The amount of the gap release is taken to be 5 percent of the initial amount present for cesium, 1.7 percent for iodine, 3 percent for the noble fission gases, 0.01 percent for tellurium and antimony, and 0.0001 percent for barium and strontium. Since this emission is very small in comparison with the melt release, and is concurrent with the melt release, it is not treated separately in any of the transport analyses. Clearly, the gap release would require more careful analysis if less severe hypothetical accident conditions were considered.

Subsequent mass release as the nodes progress toward melting is calculated on a nodal basis as the product of the amount of each species remaining, the release rate coefficient, and the time interval of integration. The mass released is then summed over all the nodes in the core for each species to give the total mass released during the time step. It should be noted that the MARCH code predictions for core temperatures do not take into account the heat of vaporization of materials released from the core.

The computation of the fractional release rate coefficients for fission products is based on empirical correlations derived from experiments performed by Lorenz, Parker, Albrecht, and others.[5.11-5.17] The data from these experiments were graphed and curves developed for the releases. A

fractional release rate coefficient, K(T), is derived for species by fitting an equation of the form

$$K(T) = Ae^{BT}$$

to each of these curves. The resulting values of A and B for three different temperature regions of the graph are basically the same as those defined in Appendix B of the "Technical Bases Report"[5.8] but have, in many cases, been adjusted to account for updated evaluations.[5.18] It should be noted that the fractional release rate is a function of temperature and elemental species only, and any effects of pressure and specific surface area of the melt on the release rate are not considered. Additionally, details of complex phase interactions of various components within the melting core are, for the most part, not known quantitatively; hence the release rates are valid only to the extent that the experiments upon which the release rates are based adequately modeled a core meltdown situation.

The release rate coefficients used in CORSOR are the same as those used in Volume I of this report, with the following exception. Tellurium release from the fuel elements appears to be strongly dependent on the extent of oxidation of the zirconium cladding. At this time the effect of zirconium oxidation on the tellurium release rate is not well quantified, nor is it known with any certainty whether this phenomenon is exhibited in the release rates of other metals' releases. In an attempt to factor into these the inhibition of tellurium release caused by the presence of unoxidized zirconium, the following sets of release rate coefficients[5.19] were employed for calculation of the fractional release rate for tellurium according to the usual equation, $K(T) = Ae^{BT}$:

Zirconium Oxidation:	<90%		≥90%	
	A	B	A	B
T < 1600 °C	1.65 E-11	0.01061	6.50 E-10	0.01061
T ≥ 1600 °C	9.04 E-8	0.00522	3.62 E-6	0.00522

This is obviously not an ideal approach to the problem at hand, but much remains to be learned about releases from molten core materials.

Several uncertainties associated with the CORSOR predictions must be mentioned. These uncertainties most strongly impact the predicted release rates for aerosols, rather than for the more volatile materials. One difficulty in predicting aerosol release is that as core melting progresses, the temperatures increase throughout the core until, eventually, a loss of geometry would be expected to occur. In the BWR analyses, core slumping occurs in such a way as to remove radial regions from the core in an incremental fashion. Thus, the emission of fission products from the fuel rods which have fallen to the lower structures is included in the calculations of the source to the primary system. This represents a change from the PWR analysis reported in Volume 1, in which emission into the primary system was halted at the time of core slumping. A further difference between the two sets of analyses is that for the BWR sequences, significant periods of time elapse between vessel dryout and bottom head failure. Thus, during a portion of the melt period, the core is emitting fission products into an essentially stagnant volume.

The behavior of the control rods during core melting is also a source of uncertainty with respect to aerosol generation. In the sequences modeled here, the rods are fully inserted into the core, and it is assumed that these rods are at the same temperatures as the core nodes in which they reside. Thus the release of control rod materials is simulated in CORSOR by the addition of the tin and steel to the inventory of materials available for release. The burnable poison rods are not considered as a source of aerosol material though it is understood that the boron in them may play a role in aerosol formation.

5.2.2 Source from Melt-Concrete Interactions: VANESA

The release of fission products and nonradioactive aerosols during the interaction of molten core materials with concrete plays an important role in determining the risk of severe reactor accidents and is modeled with the VANESA code. Aerosol production and fission product release from core debris outside the reactor vessel can persist for many hours. The aerosols produced in this way do not usually have to traverse a convoluted pathway before they enter the reactor containment as do aerosols produced in the reactor vessel. The increased inventory of aerosols in the reactor containment brought on by

ex-vessel core-debris interactions could lead to rapid agglomeration and settling of the condensed fission products released during the in-vessel phases of an accident. If containment failure is delayed, the primary source of radioactivity released to the environment would come from ex-vessel sources. Release of fission products from core-concrete interactions can compensate for any inhibition in the release of volatile species during the in-vessel phase of an accident because gases from the thermal decomposition of concrete sparge through the melt and drive the release processes. Ex-vessel processes can also lead to the release of fission product elements that are ordinarily quite refractory. This, again, is because of the strong driving force produced by gas sparging and the unusual melt chemistry that arises during ex-vessel interactions of core debris with concrete.

Also of importance is the generation of aerosols from nonradioactive materials, such as concrete and steel, during ex-vessel interactions. The additional concentrations of suspended particulates in the containment brought on by these aerosols naturally mitigate the inventory of radioactivity released from the fuel that would then be available for release to the environment. This additional material, on the other hand, poses yet another threat to equipment in the containment whose performance is degraded by the presence of aerosols.

VANESA is a mechanistic model of fission product release and aerosol generation during core-concrete interactions. This model was based on observation from experiments involving high-temperature melts on concrete and information from analogous industrial processes. Two broad mechanisms of aerosol formation are considered in the model:vaporization of melt species accentuated by gas sparging, and mechanical formation of aerosols by violent agitation of the molten debris sparged with decomposition gases. Vaporization processes produce the most intense aerosol generation during ex-vessel core debris interactions, while mechanical processes provide a mechanism for aerosol formation that persists even when debris temperatures are so low that little vaporization of species in the debris can occur.

Input to this model includes melt temperature, concrete erosion rate, and gas generation rate predicted by the CORCON model of melt-concrete interactions. It computes the thermochemical limits of vaporization from the melt, and then compares the extent of vaporization recognizing kinetic barriers,

such as mass transport, to the approach to the thermochemical limits for vaporization. Mechanical aerosol generation is estimated by analogy to experimental data with simulant systems.

More complete descriptions of the model are provided in the users' manual[5.20] and its uncertainties are discussed further in Appendix C of Volume 1.[5.1]

5.3 Radionuclide Transport and Deposition

5.3.1 Transport in Reactor Coolant System: TRAP-MELT

The TRAP-MELT code that was used for the primary system radionuclide transport analyses of this study was developed from the published TRAP-MELT code[5.21] used for the "Technical Bases" report[5.8]. Major changes were made in the treatment of aerosol particle transport and behavior and in radionuclide condensation on and evaporation from particles. In addition, the internal data base of the code was increased to include physical property data for tellurium and cesium hydroxide. An outline of the code, highlighting these changes, is given below. A more detailed description is given in the TRAP-MELT Users' Manual[5.22].

The TRAP-MELT model is designed to treat radionuclide transport in an arbitrary flow system whose thermal-hydraulic conditions are given as functions of time. For this study, the data needed by TRAP-MELT to define the thermal-hydraulic conditions of the primary system were generated by MERGE. In addition, TRAP-MELT requires the definition of source terms for each radionuclide; these terms were developed by CORSOR.

Once the flow system is defined, it is subdivided into a series of control volumes that can, in principle, be arbitrary in number and flow connections and that are chosen on the basis of characteristic geometry, thermal-hydraulic conditions, and suspected significant radionuclide behavior such as change of phase, agglomeration, or deposition. Radionuclides in each control volume are assigned, with uniform distribution, to one of two carriers: the wall surfaces and the gas phase. Each radionuclide is allowed to reside on these carriers in either particulate (liquid or solid) or vapor form so that

by combining carrier with form in the concept of "state", the condition of a radionuclide in a given control volume is completely determined by its state. TRAP-MELT thus considers five states:

- Radionuclide vapor carried by gas
- Radionuclide particle carried by gas
- Radionuclide vapor carried on wall surface
- Radionuclide particle carried on wall surface
- Radionuclide vapor reacted with wall surface.

This list of states is not exhaustive (for instance, in two-phase flow, the carrier water must be considered) and the logic of the code has been chosen to accept an arbitrary number of states readily.

Radionuclide transport can occur among the five states of an individual control volume or between certain states of different control volumes connected by fluid flow. The former types of transport are modeled or correlated in the code itself. The latter are assumed to occur in phase with the fluid flow (as developed by codes such as MERGE) and are imposed on the system. Sources of radionuclides to the system may occur in any volume and any state, and they must be input to the code as mass rate functions of time.

At present, the intravolume transport mechanisms contained in TRAP-MELT are:

- Competitive condensation on, or evaporation from, wall surfaces and particles of cesium iodide, cesium hydroxide, and tellurium
- Irreversible reaction of molecular iodine, cesium hydroxide, and tellurium with stainless steel surfaces
- Particle deposition on surfaces due to
  - Settling
  - Diffusion from laminar and turbulent flow
  - Inertial impaction from turbulent flow
  - Thermophoresis.

Particle transport (and evaporation or condensation from or on particles) depends on particle size. TRAP-MELT takes this into account by considering a discretized particle size distribution that is subject to change, in each volume, by the deposition processes themselves, by possible particle sources, by flow of particles from other volumes, by flow of particles out of the volume

in question, and by agglomeration. The last can be due to many mechanisms. TRAP-MELT considers the following agglomeration mechanisms:

- Brownian
- Gravitational
- Turbulent (shear and inertial).

Considerations of stiffness and linearity split the system of first-order differential equations resulting from the above-listed transport mechanisms into three classes. Most of the deposition mechanisms (transfer from gas to wall surface) are taken as first order in the concentration of radionuclide species on the carrier (gas, particle, or wall) from which the transfer occurs. They constitute the first class, whose transport scheme can be written in the form:

$$\frac{dC}{dt} = S + MC, \tag{5.1}$$

where C is the concentration vector of the species in question for each state and volume, S is the source rate vector for each state and volume, and M is the transport matrix between all states and volumes. Because the deposition terms are taken as first order, M is independent of C and depends, with S, on time only. It is thus possible to solve Equation (5.1) as a set of first-order differential equations with constant coefficients by standard techniques. This is done in TRAP-MELT for the class of linear mechanisms. Condensation and evaporation, which have a much shorter time constant than the linear processes, constitute the second class and are treated outside this framework but parallel to it, as is particle agglomeration, which constitutes the third class of mechanisms in the TRAP-MELT code.

The approach to this parallel treatment is as follows: Equation (5.1) is taken as the master time-translation operation of the radionuclide system. Time steps are adjusted so that S and M change little over a time step and so that the time step does not exceed one-third of the smallest flow residence time for any control volume. The latter assures that the system does not translate excessively between couplings to the other two classes of mechanisms. In addition, the characteristic coagulation time for the aerosol

in each volume is evaluated and compared to the master time step. If the former is short compared to the latter, the master time step is appropriately reduced.

At the beginning of each time step, phase transitions of radionuclides are modeled by examining each control volume in turn and solving the molecular mass transport equations for vapor transport among the gas phase, particles, and wall surfaces. Because of the low heats of vaporization of the radionuclides in question, this transport is assumed to be isothermal. Transfer to the walls assumes the Dittus-Boelter correlation[5.6] for pipe flow and transfer to the particles occurs by diffusion based on the size distribution at the beginning of the time step. Redistribution of the vapor phase occurs in a time that is small compared to the master time step; therefore, this redistribution is essentially decoupled from the other processes considered which justifies the use of a time parallel solution treatment.

Once redistribution of the vapor phase has been effected, its effect on the existing particle size distribution (in the volume in question) is calculated by assuming that each size class gains (or loses) mass in proportion to the rate of vapor transfer to (or from) that size class. Conservation of number for each size class then dictates redistribution between, in general, two new contiguous size classes, the number in each size class being determined by mass conservation.

At the end of a time step, the particle size distribution in each volume is reevaluated over that time step to account for possible particle agglomeration, sources, and flow terms. The agglomeration algorithm has been excerpted from the QUICK aerosol behavior code[5.23], which is based on a size discretization scheme.

The approximations inherent in this parallel treatment are minimized by relegating mass redistribution and conservation to the master Equation (5.1), except for redistribution due to radionuclide phase change. Agglomeration and particle evaporation/condensation serve only to modify the particle size distribution and therefore affect particle deposition indirectly through mass-distribution-averaged deposition velocities. Thus the aerosol aspect is solved (over a master time step) completely in parallel to Equation (5.1), using all sources, flow terms, and particle removal terms evaluated for each size class considered. The resultant distribution is used to evaluate average particle deposition terms for use in the master equation only. Similarly, reevaluation

of the particle size distribution due to radionuclide phase change affects these average deposition terms only.

In addition to the time-dependent thermal-hydraulic conditions and mass input rates by species, the TRAP-MELT code requires input information on the initial particle size distribution of the source, the control volume geometry, and the physical properties of species (including deposition velocities on surface materials). The code provides output in terms of time- and location-dependent mass by species and state, as well as size distribution of suspended particulate material.

There are a number of uncertainties which affect the TRAP-MELT code predictions of primary system retention of materials. Any errors or imprecisions in the input to the code will clearly affect the quality of the results, both for the primary system thermal-hydraulics provided by MERGE and for the core release rates determined by CORSOR. The extent of interaction among the materials released from the melting core is determined largely by the timing of their releases, and this represents a less straightforward, but no less important, potential effect on the code's results due to input inaccuracies.

The experimentally determined vapor deposition velocities for Te, CsOH and I_2 on hot surfaces may not represent an accurate description of the process as it occurs in the reactor coolant system (RCS) because of the imprecision in the available data and because the experimental systems may differ from the actual RCS conditions. Nevertheless, what data are available have been incorporated, since these analyses are intended to reflect the state of the art. Additional uncertainties affecting vapor and aerosol deposition arise from possibly inadequate specifications of primary system geometry and flow patterns.

The disposition of materials suspended in the coolant system at the time of core slumping or at depressurization of the pressure vessel can have significant impact on retention calculated for some of the sequences analyzed. This is because some fission products and aerosols emitted from the core have not escaped the RCS at the time of core slumping and are still available for injection into the containment. The large burst of steam which accompanies core slumping or depressurization when the pressure vessel fails will rapidly sweep out the coolant system, and the very short transit time to the containment is expected to lead to minimal retention of these materials. Thus, in

the analyses in this document, the material suspended in the RCS at the time of core slump or pressure vessel failure is assumed to be injected into the containment as a "puff" release, with no further retention in the primary system.

The analyses in the main body of this document are subject to some uncertainties which may overpredict retention in the primary system. One mechanism not included in the current analysis is the structure heatup due to decay heat from the deposited fission products. Heatup of surfaces where species of intermediate volatility (e.g., CsI and CsOH) are deposited would lead to reevolution and transport of the previously deposited materials through the reactor coolant system to regions of lower surface temperature or to the containment. Thus, the deposition of these species may be self-limiting to some extent.

5.3.2 Transport in Containment: SPARC

Many BWR accident sequences involve a fission-product flow path which passes through a suppression pool. Although the importance of the suppression pool in removing fission products has long been recognized, comprehensive analytical models that consider all pertinent parameters (such as particle size, bubble size, pool dimensions, and pressure and temperature conditions) have not been available. The SPARC code was written specifically for the analysis reported here and was used to calculate removal of particulate matter by a suppression pool.

The SPARC code was developed by Owczarski, et al[5.24]. The model includes particulate removal due to steam condensation, gravitational settling, inertial impaction both inside the gas bubbles and in the gas injection regime, diffusion deposition, and mechanical entrainment of pool liquid at the pool surface. In addition, a mechanism which retards particle deposition due to evaporation of steam is considered. Details of the model are provided in the SPARC Users' Manual[5.24]. The bubble shape in the SPARC code is assumed as an oblate spheroid. For all calculations of pool scrubbing in this study, the ratio of minor to major axes (aspect ratio) for the bubble was taken as 1:3. The bubble diameter based on a spherical shape was taken as 0.75 cm in all cases.

Recognizing that the role of the suppression pool in removing particulates was neglected in the past, or a fixed removal efficiency or decontamination factor was arbitrarily assumed, use of the SPARC code in this program represents an improvement over previous source term analyses by accounting mechanistically for the effects of the suppression pool.

5.3.3 Transport in Containment: NAUA 4

The NAUA code was developed at the Kernforschungszentrum Karlsruhe, West Germany, for calculating aerosol behavior in LWR core melt accidents.[5.25] It is based on mechanistic modeling of aerosol agglomeration and deposition within a containment vessel where a condensing steam atmosphere may exist. The model for steam condensation on particles was validated by small-scale experimental measurements[5.26], and larger-scale validation is being planned.

The NAUA code calculates physical processes, excluding chemical changes and radioactive decay. The removal processes considered include gravitational settling and diffusional plateout. Interactive processes include Brownian and gravitational agglomeration and steam condensation. Aerosol sources and leakage are also included. Compositional changes resulting from time-dependent compositions for the input aerosol are tracked by the code.

The particle size distribution is defined by a number of monodisperse fractions. In this approach, the governing integro-differential equation is transformed into a system of coupled first-order differential equations. In effect, the particle size fractions interact and deposit according to the included mechanisms, generating a time-dependent distribution of mass among the various size fractions. Steam condensation is handled in a separate integration. Output from the code includes mass concentrations of condensed water and dry aerosol materials (airborne and on surfaces), as well as particle size distributions at various times throughout the calculation.

Since the original version of the NAUA code has no provision for engineered safeguards, calculations were made to account for removal of aerosol particles by sprays, as follows:

$$\frac{dn}{dt} = -\varepsilon\pi R^2 N\ (V_g - v_g)n, \qquad (5.2)$$

where

n is the aerosol particle concentration,

ϵ is the collision efficiency,

V_g and v_g are settling velocities of the spray drops and aerosol particles, respectively,

R is the radius of the spray drop, and

N is the water drop concentration.

Due to hydrodynamic interaction between a falling water drop and airborne particles, only a small fraction of the particles within the cross-sectional area of the water drop is removed by spraying. To account for this hydrodynamic effect, the collision mechanisms due to inertial impaction, interception, and Brownian diffusion of aerosol particles were used by defining ϵ in Equation (5.2) as:

$$\epsilon = \epsilon_I + \epsilon_R + \epsilon_D, \tag{5.3}$$

where ϵ_I, ϵ_R and ϵ_D are the collision efficiencies due to inertial impaction, interception, and Brownian diffusion, respectively. The following collision efficiency models were utilized for the three mechanisms:

$$\epsilon_I = \frac{Stk^2}{(Stk + 0.35)2} \tag{5.4}$$

$$\epsilon_R = \frac{1.5(r/R)^2}{(1+r/R)^{1/3}} \tag{5.5}$$

$$\epsilon_D = 3.5\ Pe^{-2/3}, \tag{5.6}$$

where Stk is the Stokes number for aerosol particles based on a characteristic length of water drop with radius R; r is the particle radius; and Pe is the Peclet number. The Stokes number and the Peclet number are defined as

$$Stk = \frac{2\ r^2 \rho_p V_g C}{9\mu R} \text{ and} \tag{5.7}$$

$$Pe = \frac{2V_g R}{\bar{D}} \qquad (5.8)$$

where $\bar{D}$ is the diffusion coefficient of aerosol particle
v_g is the settling velocity of water drop
C is the Cunningham slip correction factor
ρ_p is the particle density
μ is the gas viscosity.

In general, for relatively large particles, the inertial effects on the overall collision efficiency are larger than the interception term because the water drops are much larger than the aerosol particles. As particle size becomes smaller, the Brownian diffusion term will become increasingly important. It should also be mentioned that Equation (5.4) is given by Hetsroni[5.27] and Equations (5.5) and (5.6) are based on the work of Lee and Gieseke[5.28, 5.29].

Another particle deposition mechanism, diffusiophoresis, was added to the NAUA code. Diffusiophoresis results from steam condensation onto containment walls and involves two mechanisms: a net flow of gas toward the wall surface (known as Stefan flow), and a molecular weight gradient caused by the steam concentration gradient. In general, the effects of Stefan flow are much larger than those of the molecular weight gradient and result in deposition of particles on the wall surface. The condensation rate toward wall surfaces calculated by the MARCH code has been used to calculate deposition due to diffusiophoresis.

In utilizing the NAUA computer code for calculating aerosol behavior during various accident sequences, it was noted that in certain cases the code requires a long computing time to calculate the rate of condensation of water vapor onto particles. This type of problem takes place when a large amount of condensible water vapor was used as an input. It was noted that a saturation ratio of much greater than 1.0 was frequently encountered even after the condensation calculation was completed.

Some literature suggests that pure water vapor at 20 C will spontaneously form water droplets in the absence of condensation nuclei when the saturation ratio exceeds 3.5, and at 0 C a saturation ratio of 4.3 is required for homogeneous nucleation. This mechanism has been implemented in NAUA in addition

to the existing condensation calculation. As the critical supersaturation for the homogeneous nucleation, the following correlation equation given by Green and Lane[5.30] was used:

$$S = \exp(0.557 \cdot (\sigma/T)^{3/2} \cdot M),$$

where

S is the critical supersaturation

σ is surface tension

T is the temperature in °C

M is the molecular weight of water.

No nucleation or self-condensation rates are calculated in the code. Rather, if critical supersaturation is realized at a given time, the excess water vapor is assumed to form water particles of a uniform size spontaneously. Of course, these small pure water droplets are subsequently subject to NAUA's usual condensation and coagulation processes both among themselves and with other particles containing solids. Although the effects of this mechanism on the overall aerosol concentration change are insignificant, the computational time is reduced considerably by this implementation.

References

(5.1) Gieseke, J. A., et al, "Radionuclide Release Under Specific LWR Accident Conditions, Volume 1", BMI-2104 (July, 1983).

(5.2) Gieseke, J. A., et al, "Radionuclide Release Under Specific LWR Accident Conditions, Volume 5", BMI-2104 (July, 1984).

(5.3) Wooton, R. O., et al, "MARCH 2 Code Description and Users' Manual", Draft (December, 1982).

(5.4) Wooton, R. O. and Avci, H. I., "MARCH (Meltdown Accident Response Characteristics) Code Description and Users' Manual", NUREG/CR-1711, BMI-2064 (October, 1980).

(5.5) "American National Standard for Decay Heat Power in Light Water Reactors", ANSI/ANS-5.1-1979.

(5.6) Geankoplis, C. J., "Mass Transport Phenomena", Holt, Rinehart, and Winston (1972).

(5.7) Freeman-Kelly, R., "A Users' Guide for MERGE", Battelle's Columbus Laboratories, October, 1982.

(5.8) "Technical Basis for Estimating Fission Product Behavior During LWR Accidents", NUREG-0772 (June, 1981).

(5.9) CORSOR Manual.

(5.10) Bell, M. J., "ORIGEN, The ORNL Isotope Generation and Depletion Code", ORNL-4628 (1973).

(5.11) Lorenz, R. A., et al, "Fission Product Release from Highly Irradiated LWR Fuel", NUREG/CR-0722 (1980).

(5.12) Lorenz, R. A., Collins, J. L., and Malinauskas, A. P., "Fission Product Source Terms for the LWR Loss-of-Coolant Accident", NUREG/CR-1288 (1980).

(5.13) Lorenz, R. A., et al, "Fission Product Release from Highly Irradiated LWR Fuel Heated to 1300-1600 C in Steam", NUREG/CR-1386 (1980).

(5.14) Lorenz, R. A., "Fission Product Release from BWR Fuel Under LOCA Conditions", NUREG/CR-1773 (1981).

(5.15) Parker, G. W., Martin, W. J., and Creek, G. E., "Effect of Time and Gas Velocity of Distribution of Fission Products from UO_2 Melted in a Tungsten Crucible in Helium", Nuclear Safety Program Semi-Annual Report for period ending June 30, 1963, ORNL-3483, 19-20 (1967).

(5.16) Albrecht, H., Matschoss, V., and Wild, H., "Experimental Investigation of Fission and Activation Product Release from LWR Fuel Rods at Temperatures Ranging from 1500-2800 C", proceedings of the Specialists' Meeting on the Behavior of Defected Zirconium Alloy Clad Ceramic Fuel in Water Cooled Reactors, 141-146 (September, 1979).

(5.17) Albrecht, H., Matschoss, V., and Wild, H., "Release of Fission and Activation Products During Light Water Reactor Core Meltdown", Nuclear Technology, 46, 559-565 (1979).

(5.18) Niemczyk, S. J. and McDowell-Boyer, L. M., "Technical Considerations Related to Interim Source Term Assumptions for Emergency Planning and Equipment Qualification", ORNL/TM-8275 (1982).

(5.19) Lorenz, R. A., Beahm, E. C., and Wichner, R. P., "Review of Tellurium Release Rates from LWR Fuel Elements and Aerosol Formation from Silver Control Rod Materials", ORNL, letter report, February 28, 1983.

(5.20) VANESA Manual.

(5.21) Jordan, H., Gieseke, J. A., and Baybutt, P., "TRAP-MELT Users' Manual", NUREG/CR-0632, BMI-2017 (February, 1979).

(5.22) TRAP-MELT 2.1 User's Manual.

(5.23) Jordan, H., Schumacher, P. M., and Gieseke, J. A., "QUICK Users' Manual", NUREG/CR-2105, BMI-2082 (April, 1981).

(5.24) Owczarski, P. C., Postma, A. K., and Schreck, R. I., "Technical Bases and Users' Manual for SPARC -- Suppression Pool Aerosol Removal Code", report to the U.S. NRC, NUREG/CR-3317 (May, 1983).

(5.25) Bunz, H., Koyro, M., and Schock, W., "A Code for Calculating Aerosol Behavior in LWR Core Melt Accidents Code Description and Users' Manual".

(5.26) Schock, W., Bunz, H., and Koyro, M., "Messungen der Wasserdampfkondensation an Aerosolen unter LWR-un-falltypischen Bedingungen", KfK 3153 (August, 1981).

(5.27) Hetsroni, G., "Handbook of Multiphase Systems", McGraw Hill Book Company and Hemisphere Pub. Co. (1982).

(5.28) Lee, K. W. and Gieseke, J. A., J. Aerosol Science, 11, 335 (1980).

(5.29) Lee, K. W. and Gieseke, J. A., Environ. Sci. & Technol., 13, 446 (1979).

(5.30) Green, H. L. and Lane, W. R., Particulate Clouds: Dust, Smokes and Mists, D. Van Nostrand Co., Princeton, New Jersey (1957).

6. BASES FOR TRANSPORT CALCULATIONS

6.1 Plant Geometry and Thermal Hydraulic Conditions

The MARCH 2 and MERGE codes were used to predict the thermal hydraulic behavior of the four accident sequences evaluated. A summary of important reactor characteristics, containment parameters, and MARCH options is presented in Table 6.1.* The detailed parameters used to describe the reactor coolant system such as the masses, surface areas, volumes, etc., were primarily obtained from the General Electric Company. These results are not presented because of their proprietary nature.

6.1.1 Sequence TC

In the transient accident sequence TC, the reactor fails to shut down, the emergency core cooling systems operate, and the reactor power level stabilizes at approximately 16 percent of full power after isolation of the steam line. This level results from the balance of the rate of coolant makeup and the core reactivity coefficients. At this level the power exceeds the heat removal capacity for cooling the suppression pool. The pool heats up until at 1-1/3 hr the failure level of the containment is reached. Makeup flow to the vessel is subsequently lost due to cavitation of the emergency core cooling system pumps, the core becomes uncovered and fuel degradation occurs. It should be noted that the core stays at an elevated power level only while it is covered; as the core uncovers, the power level is reduced from the above equilibrium power level down to decay power level. Thus, while heatup of the suppression pool takes place due to the imbalance between core power and residual heat removal capability, core heatup and melting is driven by decay heating and the energy from the Zircaloy-water reaction. Table 6.2 indicates times of key events and conditions in the containment as predicted by the MARCH 2 code. Table 6.3 gives the core and primary system conditions at key times in the accident sequence as predicted by MARCH.

*All tables in this section of the report have been placed at the end of the section.

The flow path for fission product release within the reactor coolant system is illustrated in Figure 6.1. Figure 6.2 is a schematic of the breakdown of control volumes used in the MERGE analysis. After leaving the steam separators the flow splits, with a fraction (~85 percent) passing through the steam dryers and the balance bypassing the dryers. These flows rejoin at the steam line. The differences between the primary system geometries in the Peach Bottom and Grand Gulf reactor coolant systems are minor. The temperatures of selected fuel regions as calculated by MARCH are illustrated as a function of time in Figures 6.3a and 6.3b. In Figures 6.3a and 6.3b as well as subsequent plots of this type, the notation ROD(X,Y) denotes the fuel node at axial elevation X and radial region Y. The temperatures (Figures 6.4a-h) in the reactor coolant system derived from the MERGE analyses are therefore quite similar to those predicted for the same sequence in the Peach Bottom plant. Time zero in Figure 6.4 corresponds to the time of core uncovery or 88.2 minutes from the start of the accident.

After leaving the vessel, fission products are carried down the steam line and relief line to the suppression pool. Fission products that escape the pool disperse within the primary containment volume before being released through the hole in containment to the environment. The flow path from the vessel to the environment is illustrated in Figure 6.5. After melt-through of the reactor vessel, fission products released during concrete attack flow from the cavity to the drywell and through the pool before passing into the containment and to the environment.

Table 6.4 presents the reactor containment conditions at key times during the accident sequence as calculated by MARCH. The temperatures and pressures in the containment volumes during the sequence are shown in Figures 6.6 and 6.7. Table 6.5 summarizes the containment leak rates and related conditions derived from the MARCH analyses and used in the evaluation of fission product release to the environment.

6.1.2 Sequence TPI

In this transient sequence a relief valve is assumed to stick open following reactor shutdown, resulting in blowdown of the reactor vessel to the suppression pool. The emergency core cooling system supplies makeup to the reactor vessel, but the heat removal system for the suppression pool is also

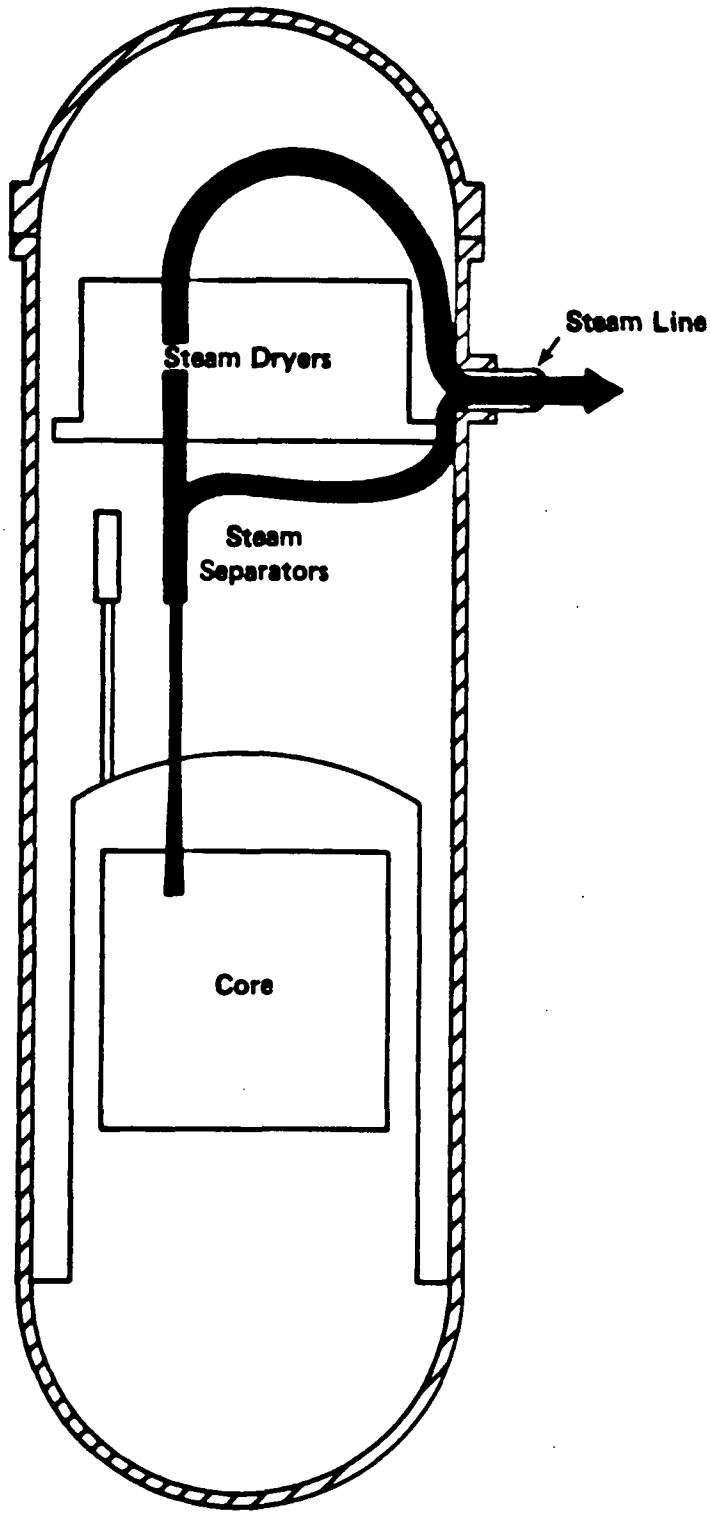

FIGURE 6.1. FLOWPATHS FOR FISSION PRODUCT TRANSPORT IN RCS - SEQUENCES TC, TQUV, AND TPI

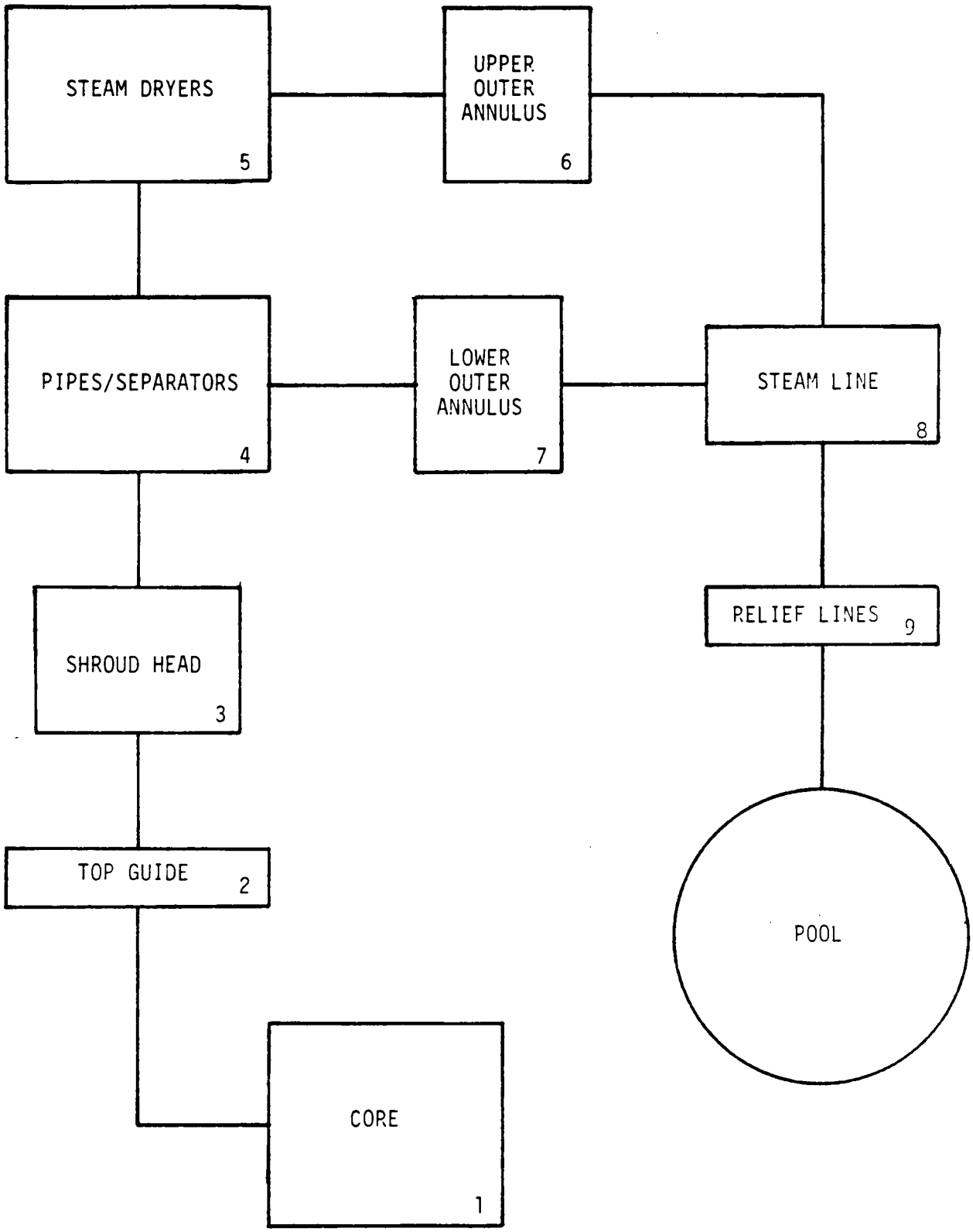

FIGURE 6.2. SCHEMATIC OF CONTROL VOLUMES FOR THE GRAND GULF SEQUENCES

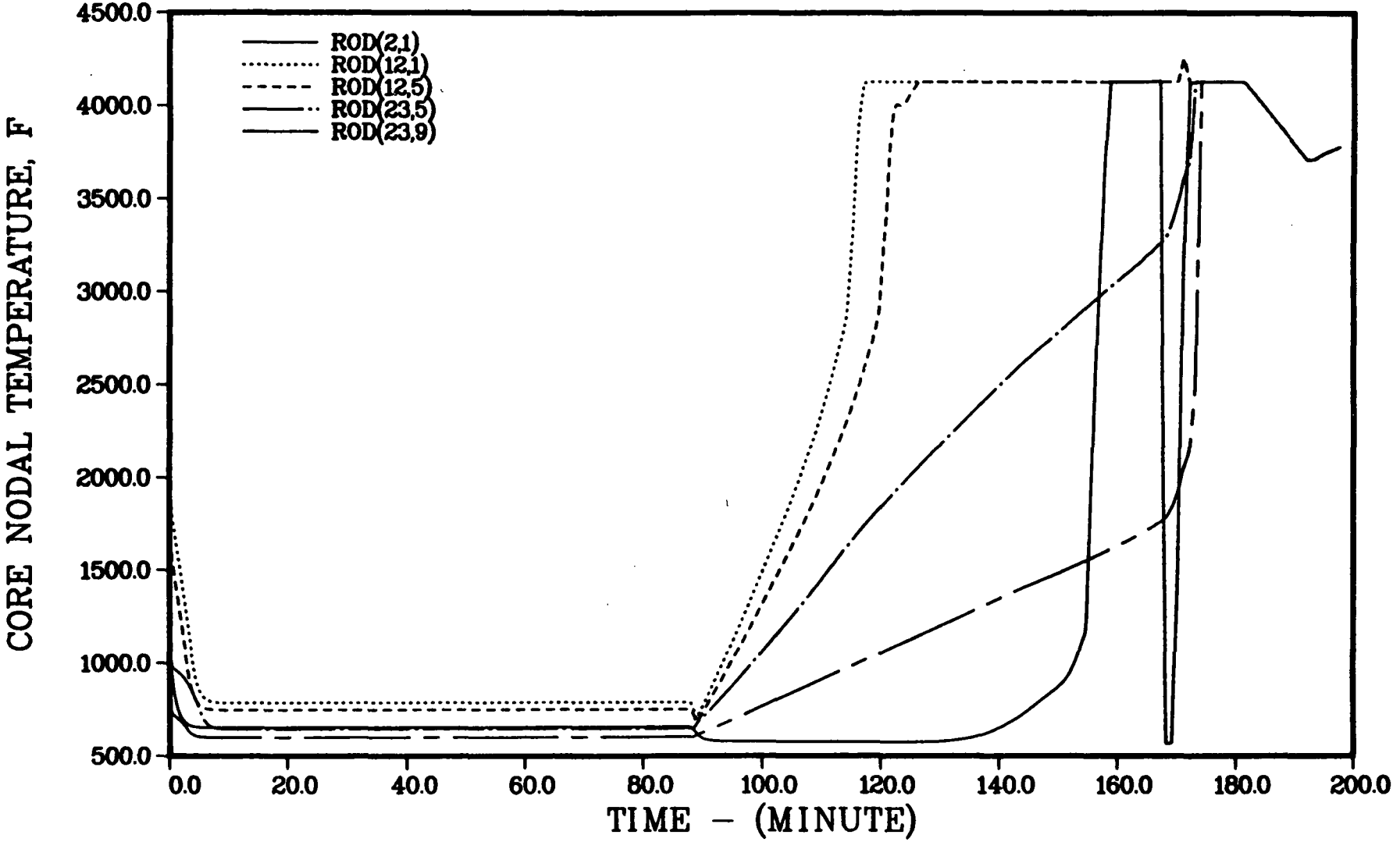

FIGURE 6.3a TEMPERATURES OF SELECTED CORE NODES - SEQUENCE TC

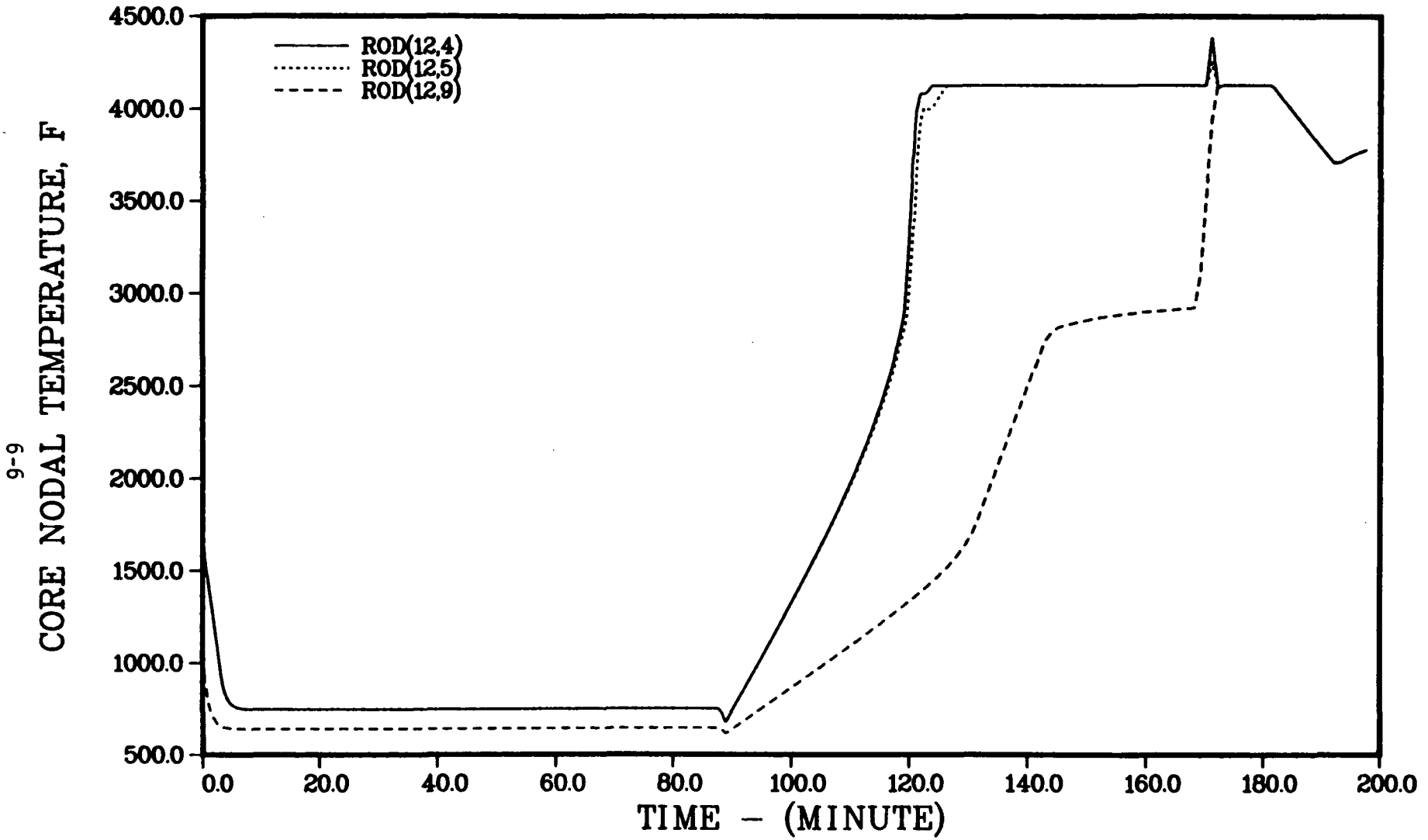

FIGURE 6.3b TEMPERATURES OF SELECTED CORE NODES - SEQUENCE TC

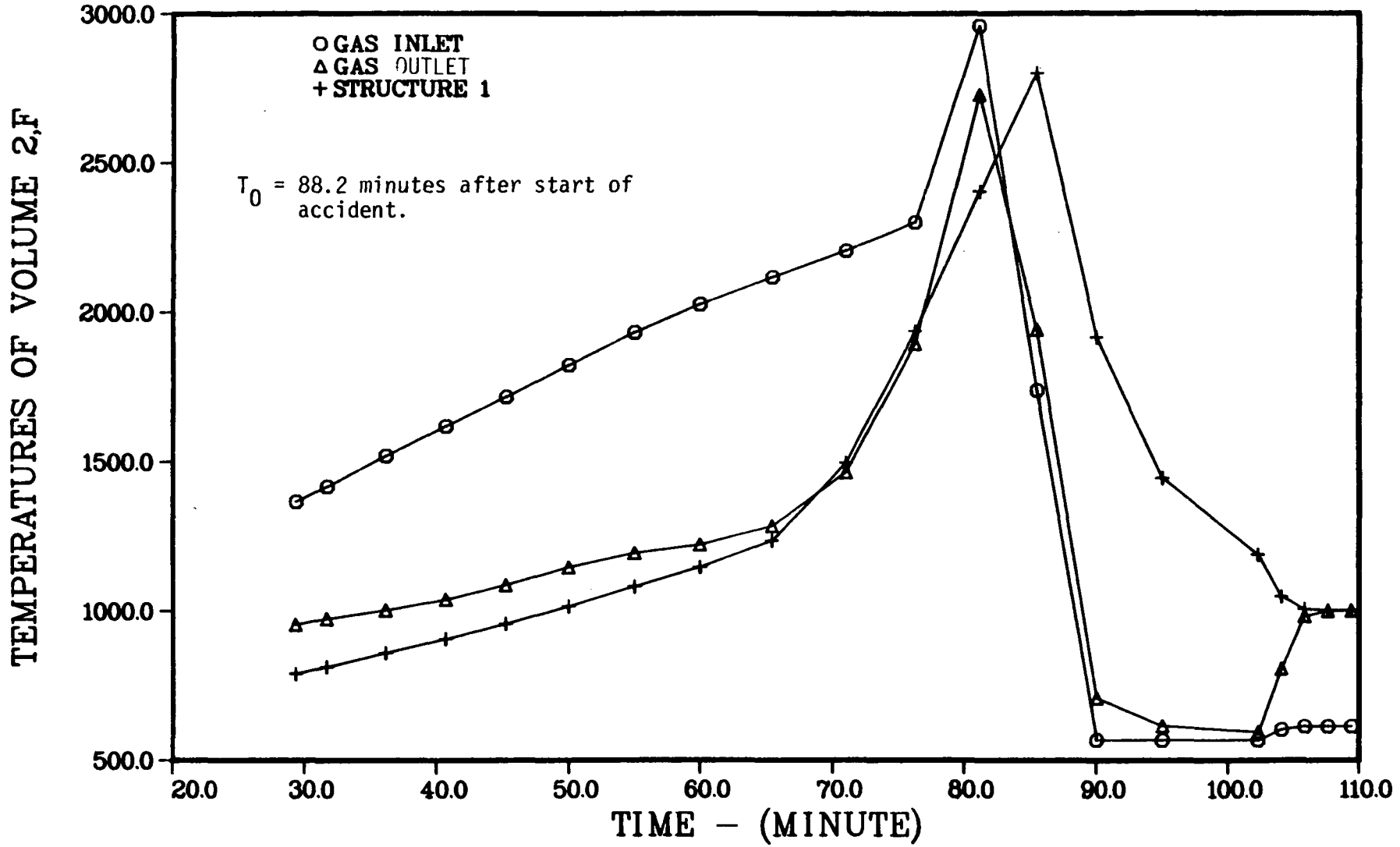

FIGURE 6.4a GAS AND STRUCTURE TEMPERATURES FOR THE TOP GUIDE IN GRAND GULF - SEQUENCE TC

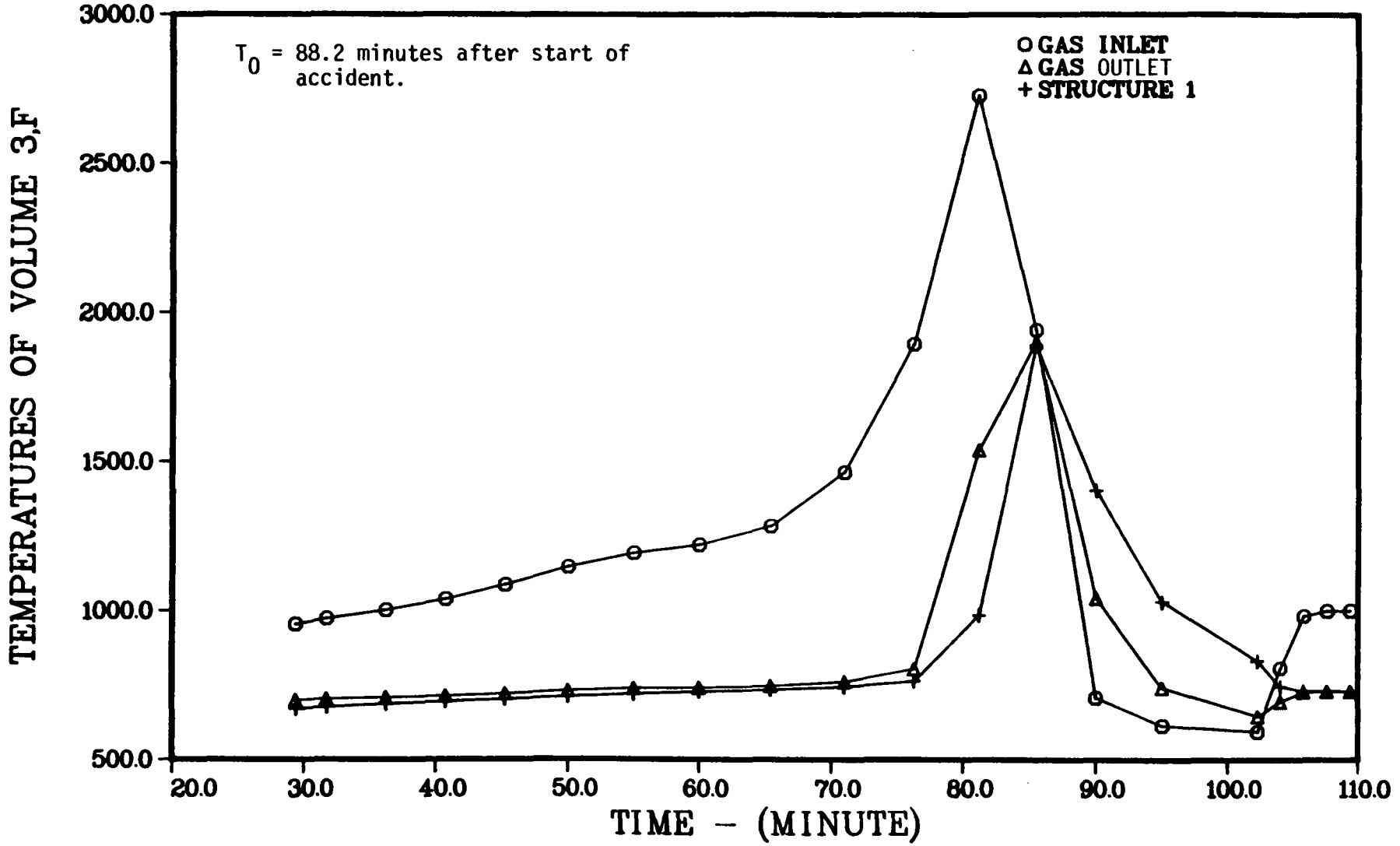

FIGURE 6.4b GAS AND STRUCTURE TEMPERATURES FOR THE SHROUD HEAD IN GRAND GULF - SEQUENCE TC

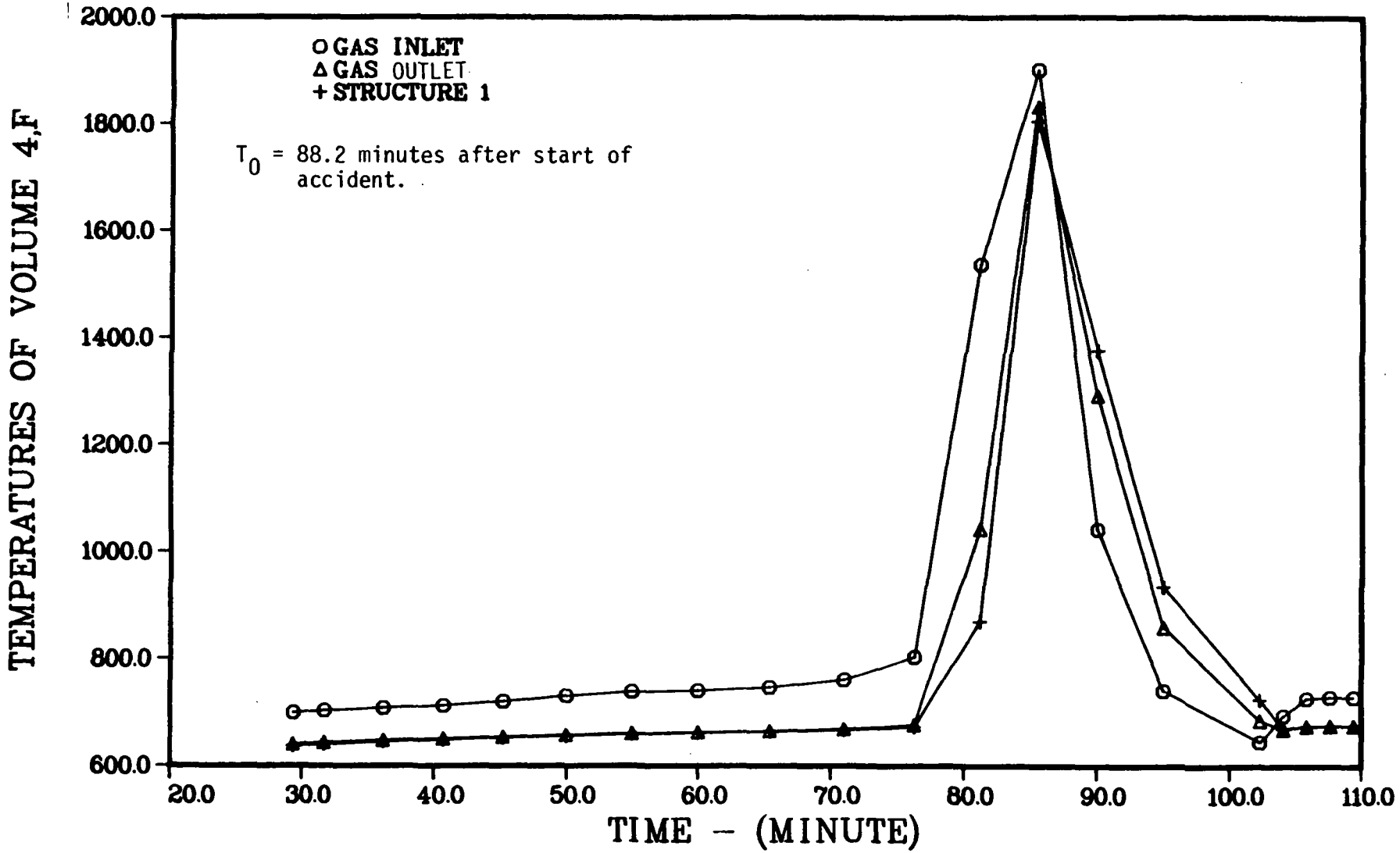

FIGURE 6.4c GAS AND STRUCTURE TEMPERATURES FOR THE STAND PIPES AND STEAM SEPARATORS IN GRAND GULF - SEQUENCE TC

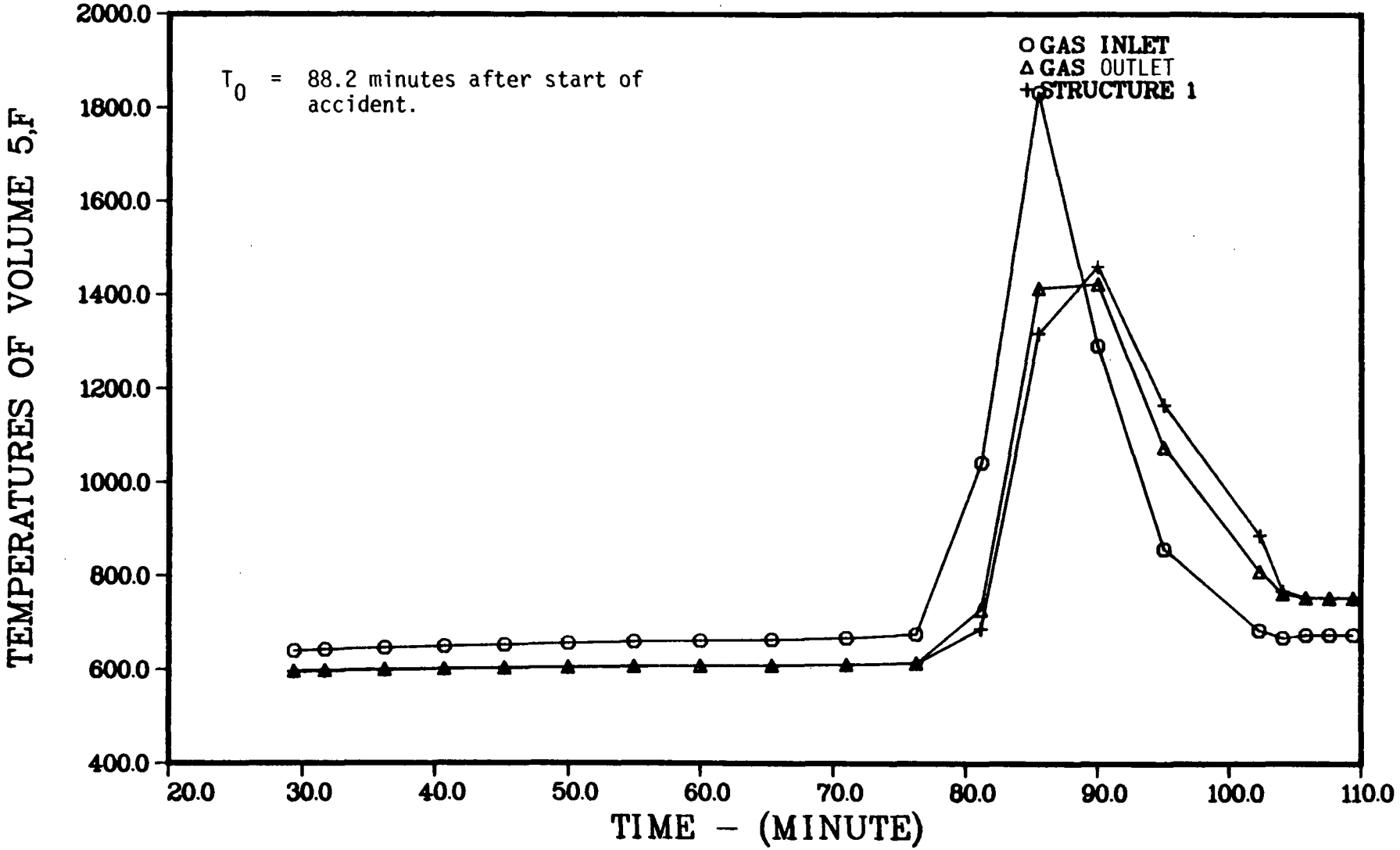

FIGURE 6.4d GAS AND STRUCTURE TEMPERATURES FOR THE STEAM DRYERS IN GRAND GULF - SEQUENCE TC

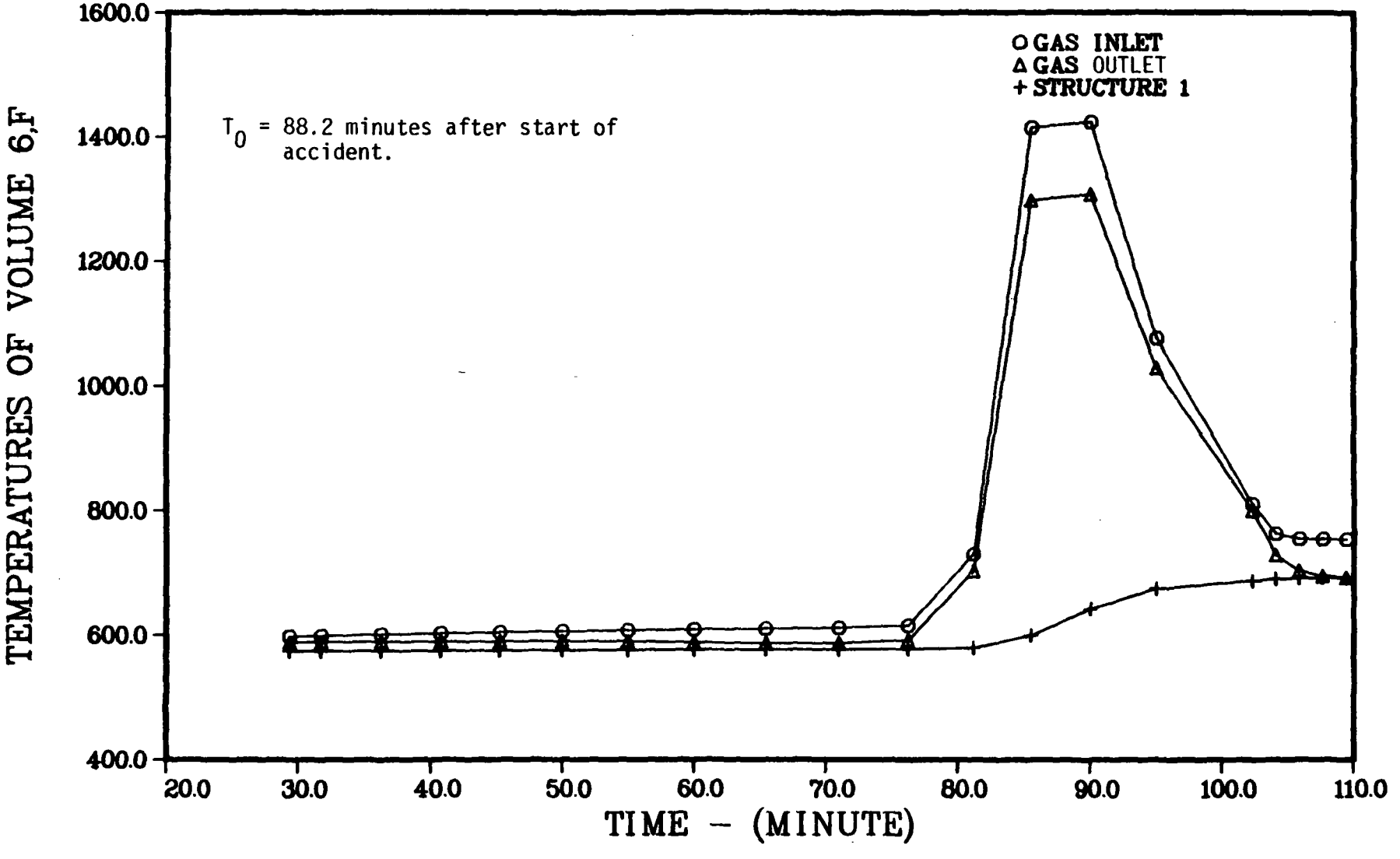

FIGURE 6.4e GAS AND STRUCTURE TEMPERATURES FOR THE UPPER OUTER ANNULUS IN GRAND GULF - SEQUENCE TC

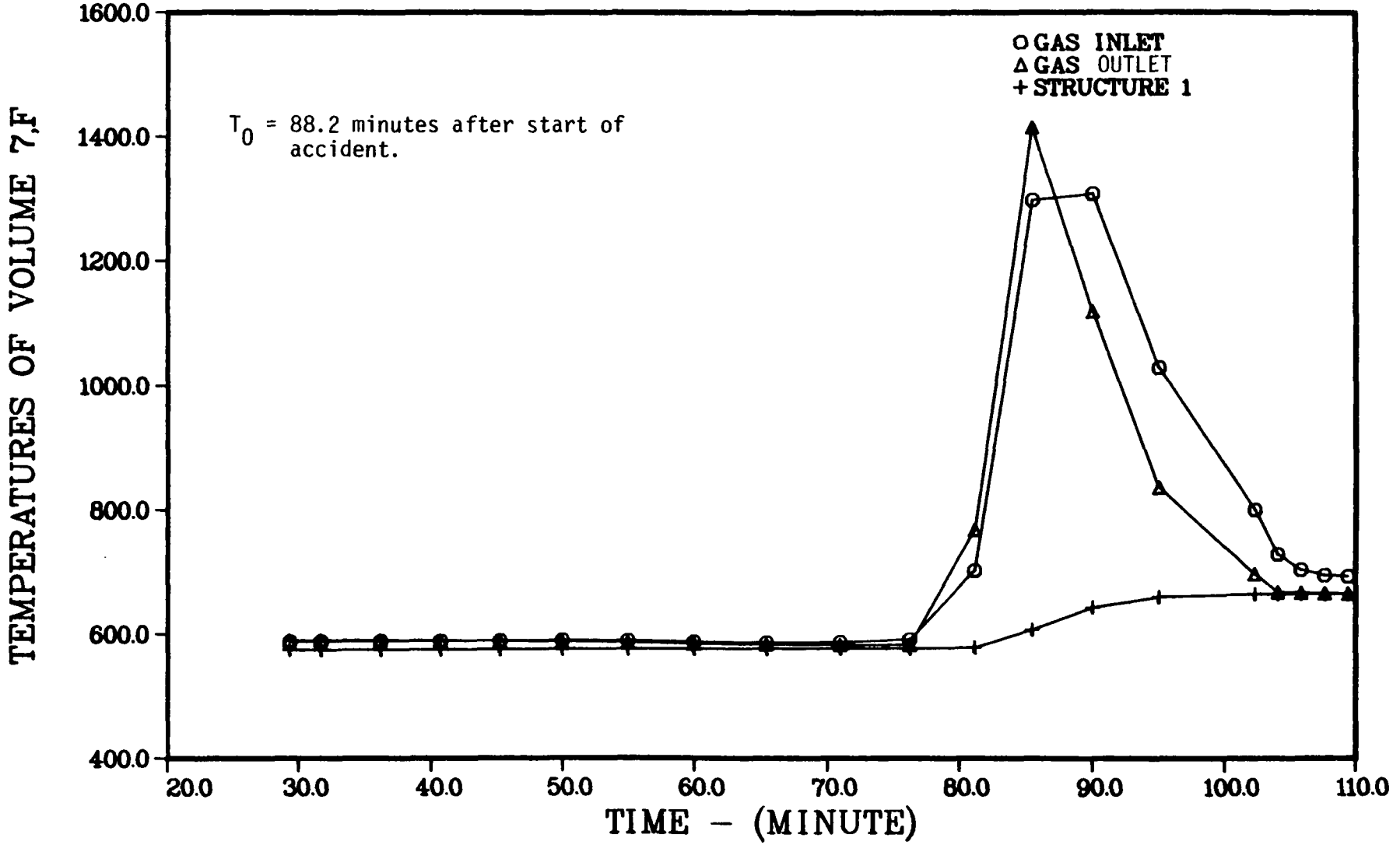

FIGURE 6.4f GAS AND STRUCTURE TEMPERATURES FOR THE LOWER OUTER ANNULUS IN GRAND GULF - SEQUENCE TC

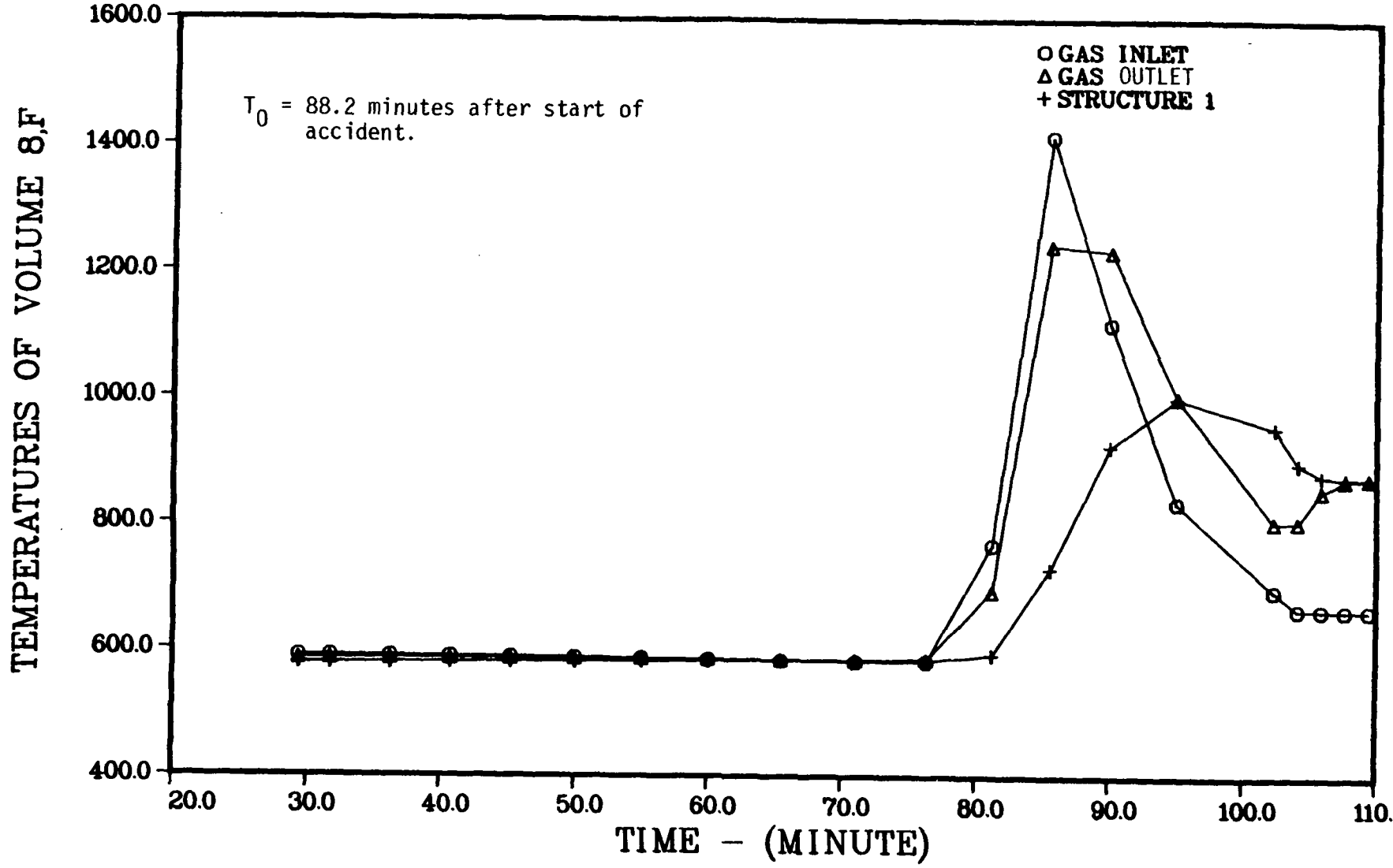

FIGURE 6.4g GAS AND STRUCTURE TEMPERATURES FOR THE STEAM LINE IN GRAND GULF - SEQUENCE TC

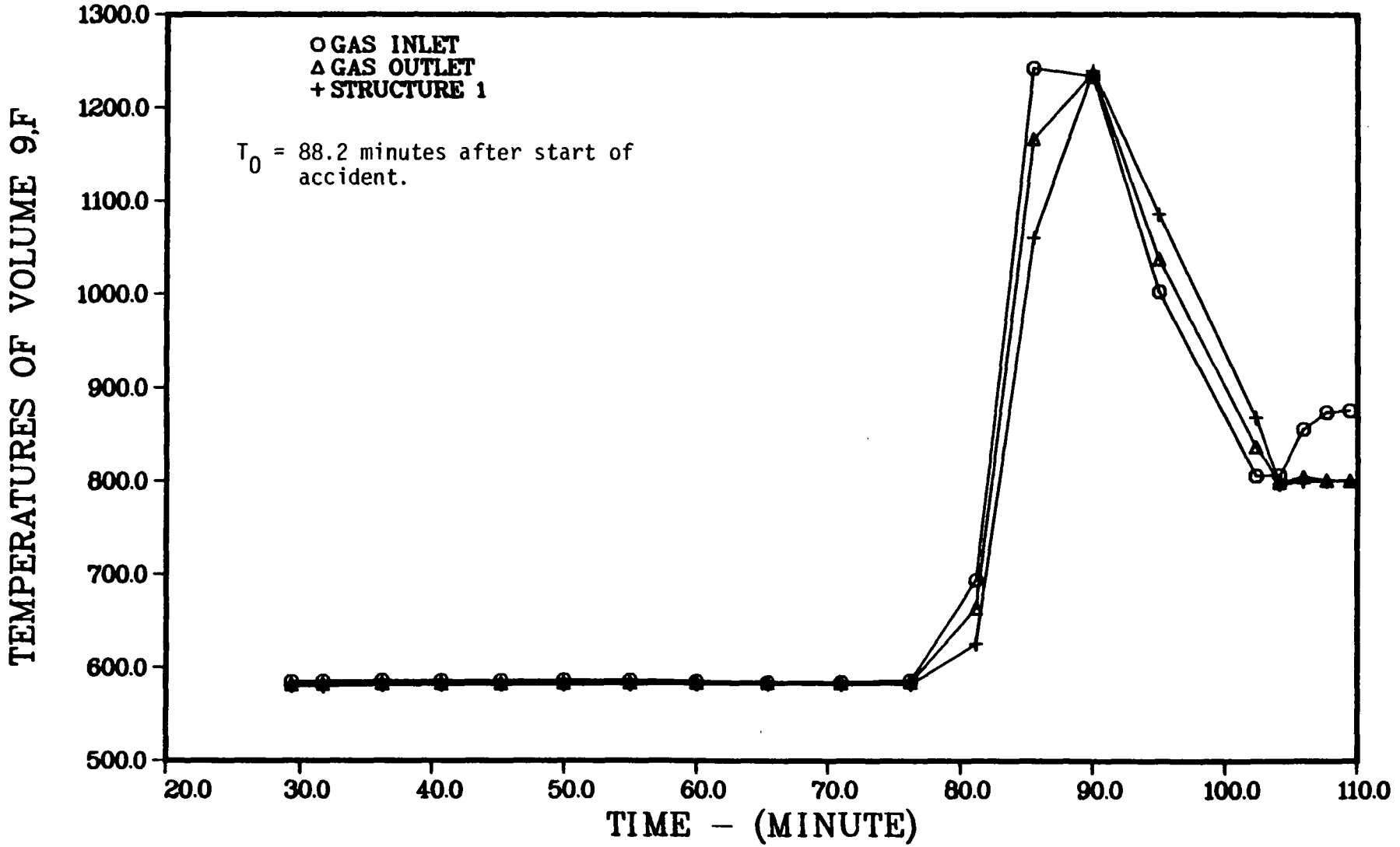

FIGURE 6.4h GAS AND STRUCTURE TEMPERATURES FOR THE RELIEF LINES IN GRAND GULF - SEQUENCE TC

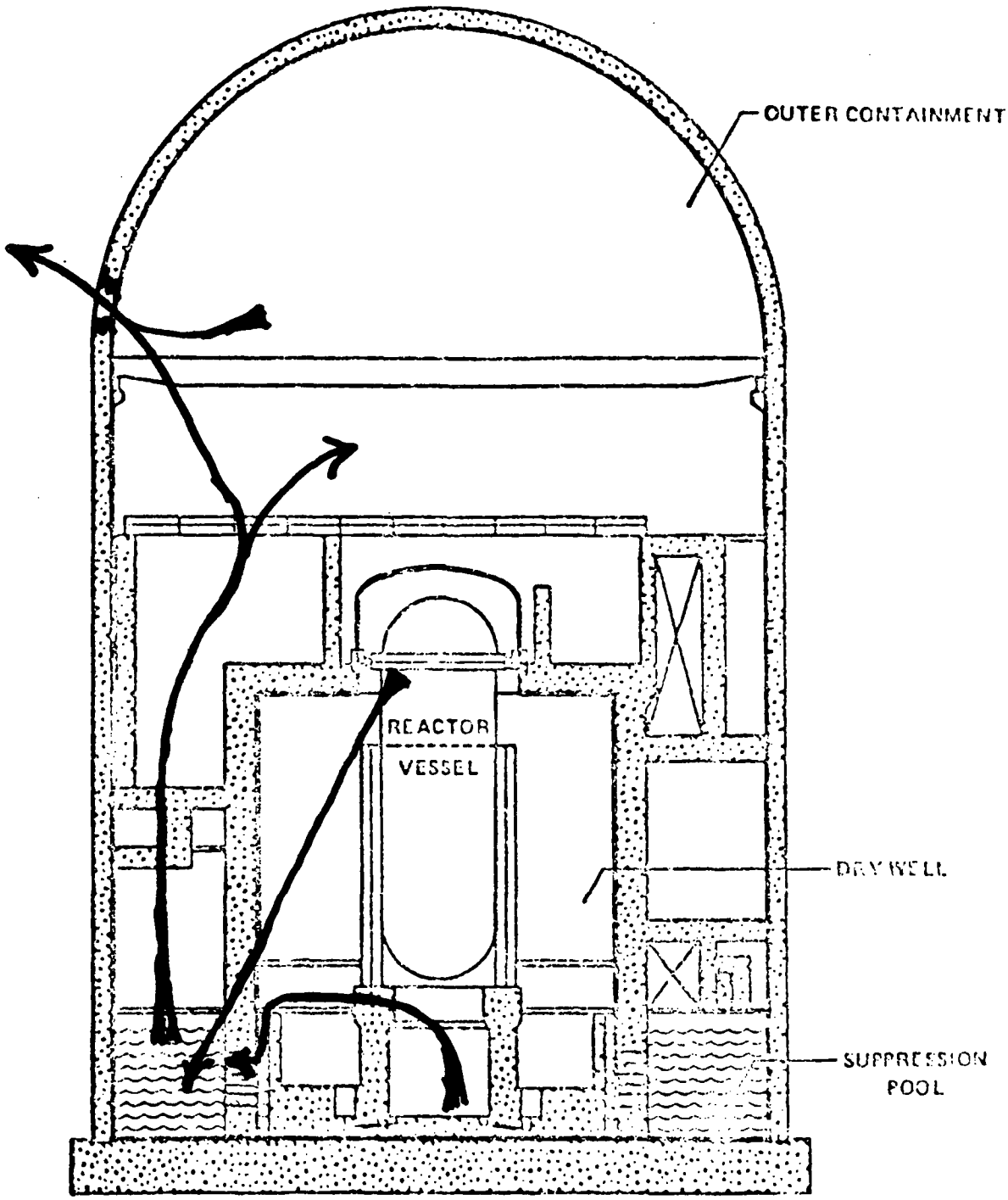

FIGURE 6.5. FLOWPATHS FROM THE VESSEL AND REACTOR CAVITY TO THE ENVIRONMENT

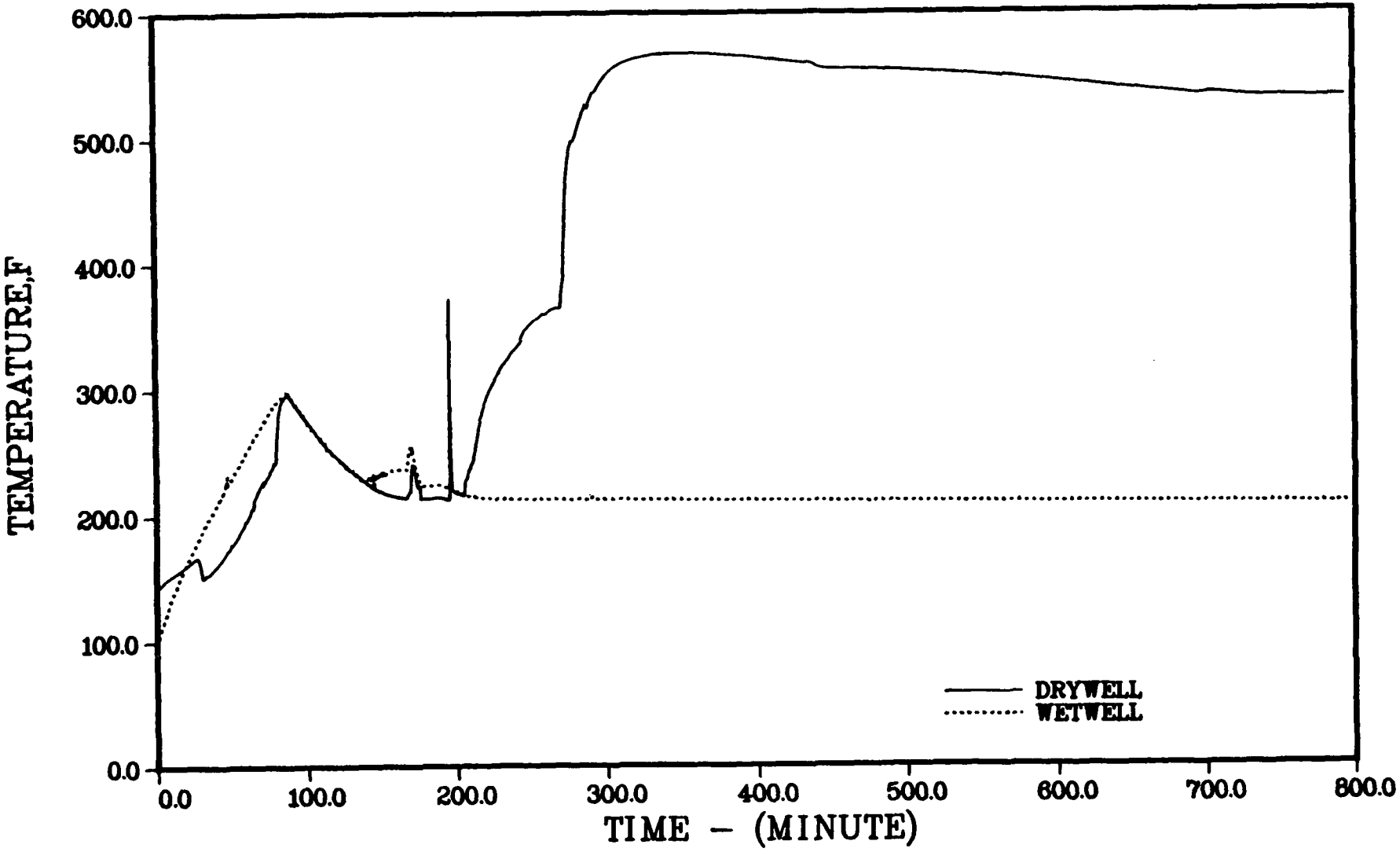

FIGURE 6.6. GAS TEMPERATURES IN CONTAINMENT VOLUMES - SEQUENCE TC

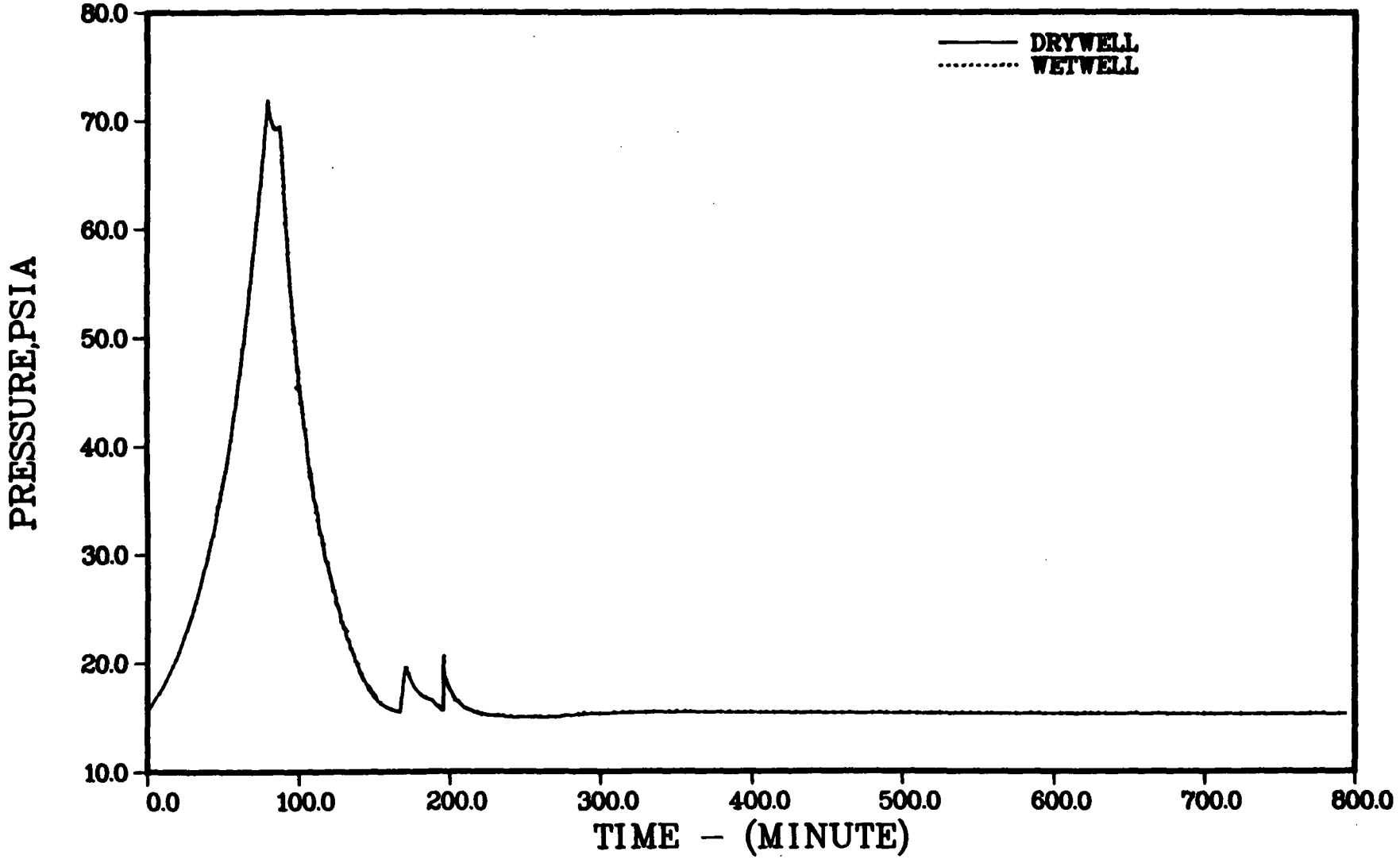

FIGURE 6.7. PRESSURES IN CONTAINMENT VOLUMES - SEQUENCE TC

assumed to fail, resulting in increasing pool temperature and containment pressure with time. At 1332 minutes, MARCH 2 predicts the containment to fail. Subsequently makeup flow to the vessel is lost due to pump cavitation, the core becomes uncovered and fuel degradation occurs. Table 6.2 gives the timing of the key events during the accident sequence; Table 6.3 presents the core and primary system conditions at key times during the sequence.

The flow paths for the TPI sequence are identical to those for the TC sequence. Temperatures in selected fuel regions as calculated by MARCH are given in Figures 6.8a and 6.8b. Gas temperatures and surface temperatures within subvolumes of the reactor coolant system as predicted by the MERGE code are illustrated in Figures 6.9a-h. Time zero in Figure 6.9 corresponds to the time of core uncovery or 1535.7 minutes after the start of the accident.

As in the preceding sequence, core melting in this sequence takes place within a failed containment, but the timing of events takes place over a much longer period of time. Table 6.4 gives the containment conditions at key times during the sequence. Figures 6.10 and 6.11 give the temperature and pressure histories in the containment. Table 6.5 summarizes the containment leakages and related parameters derived from the MARCH analyses and used in the evaluation of the fission product release to the environment.

6.1.3 Sequence TQUV

In the TQUV sequence, the various water supply systems capable of providing makeup to the vessel are all assumed to fail. The suppression pool heat removal systems are operating. Additionally, in the analysis of the TQUV sequence it was assumed that the system was equipped with hydrogen igniters and that the latter were operable. At the time of core uncovery the containment is intact. Based on our understanding of current BWR emergency operating procedures, the primary system was assumed to be depressurized when the level of water in the core reached the 2-ft level. The timing of key events for this sequence is provided in Table 6.2.

The primary system and containment flow paths for the TQUV sequence are very similar to those for the two other sequences illustrated in Figures 6.1 and 6.5 for the primary system and containment, respectively. In this sequence, however, core melting takes place with the containment intact and the pressure suppression pool water subcooled. Containment failure is due

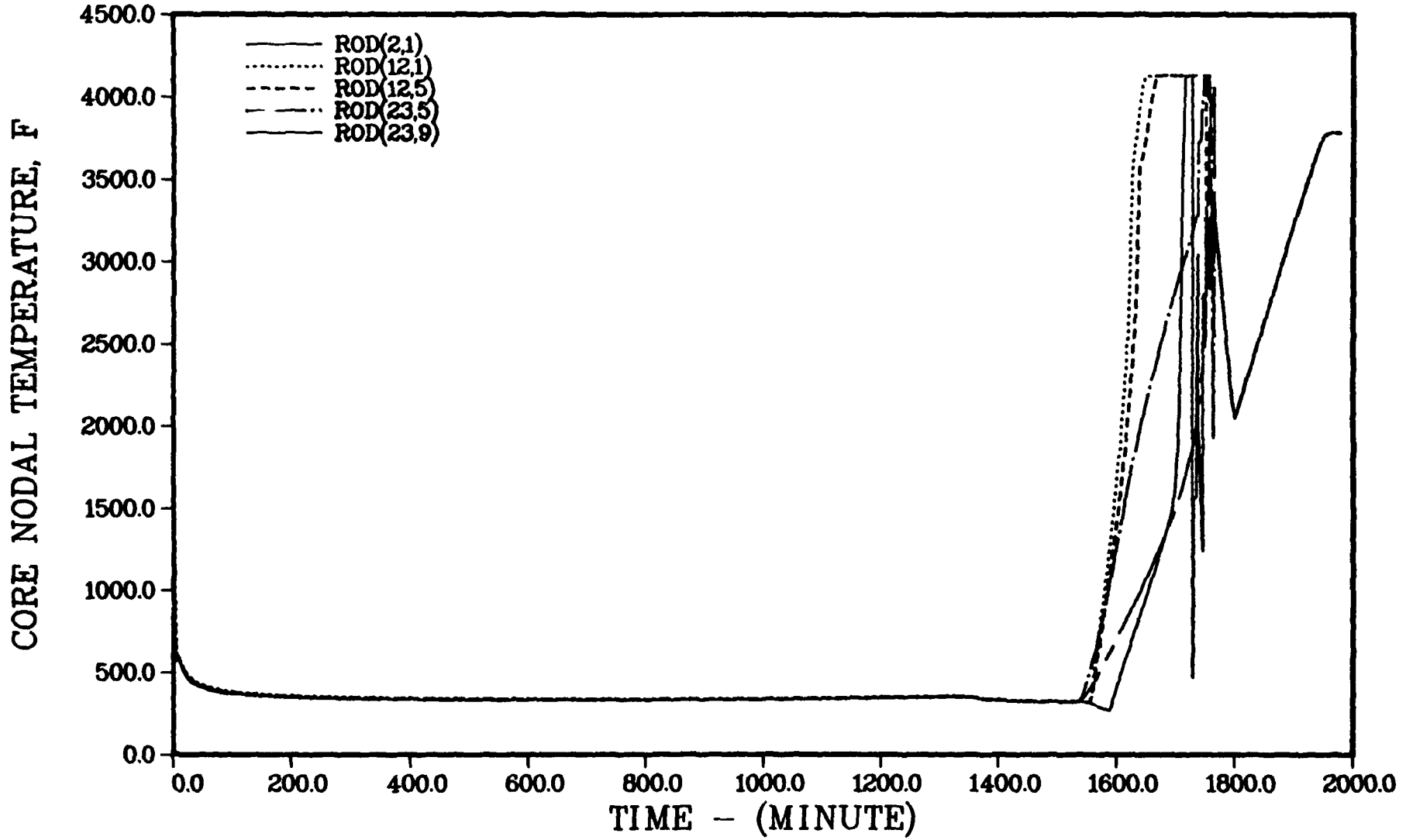

FIGURE 6.8a TEMPERATURES OF SELECTED CORE NODES - SEQUENCE TPI

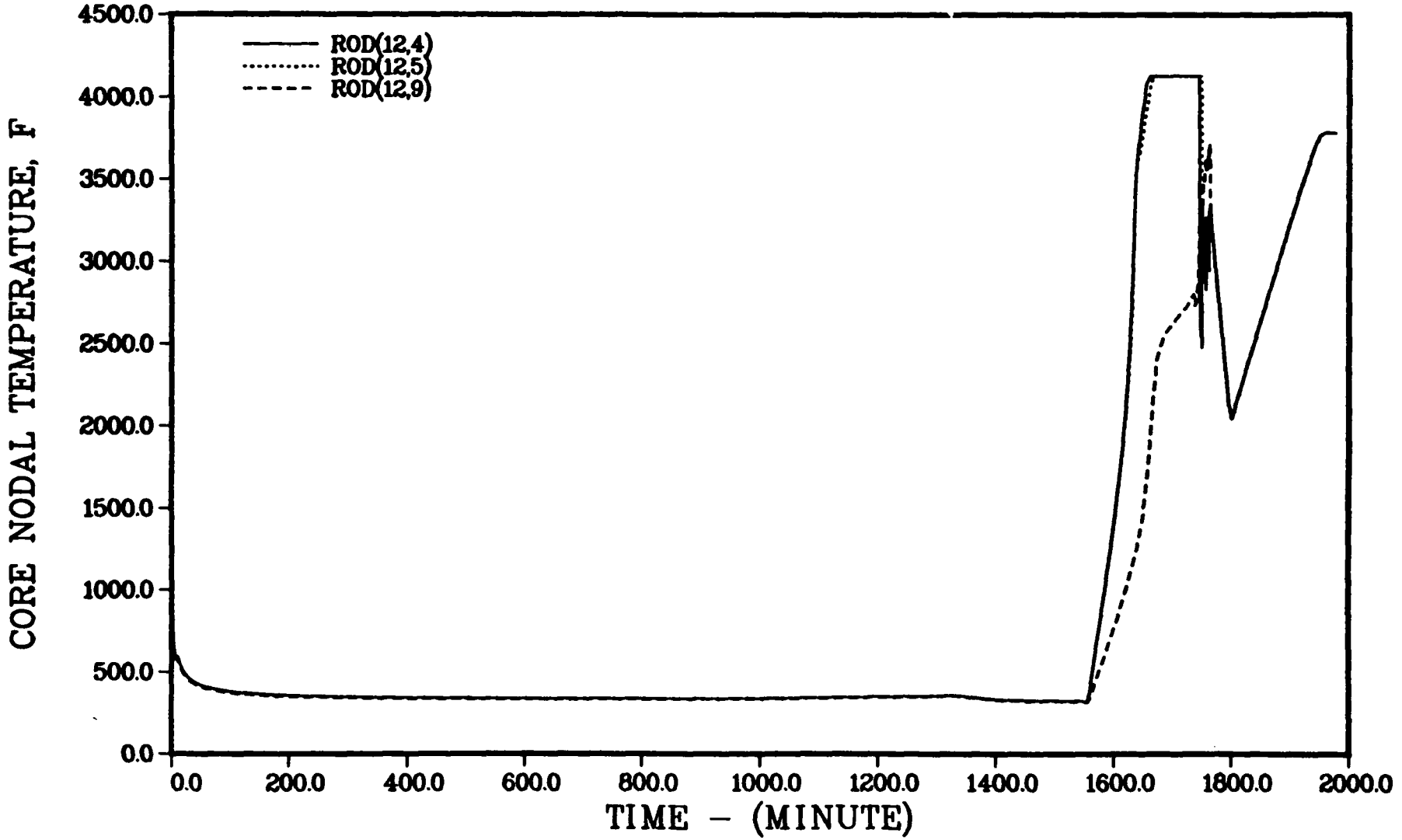

FIGURE 6.8b TEMPERATURES OF SELECTED CORE NODES - SEQUENCE TPI

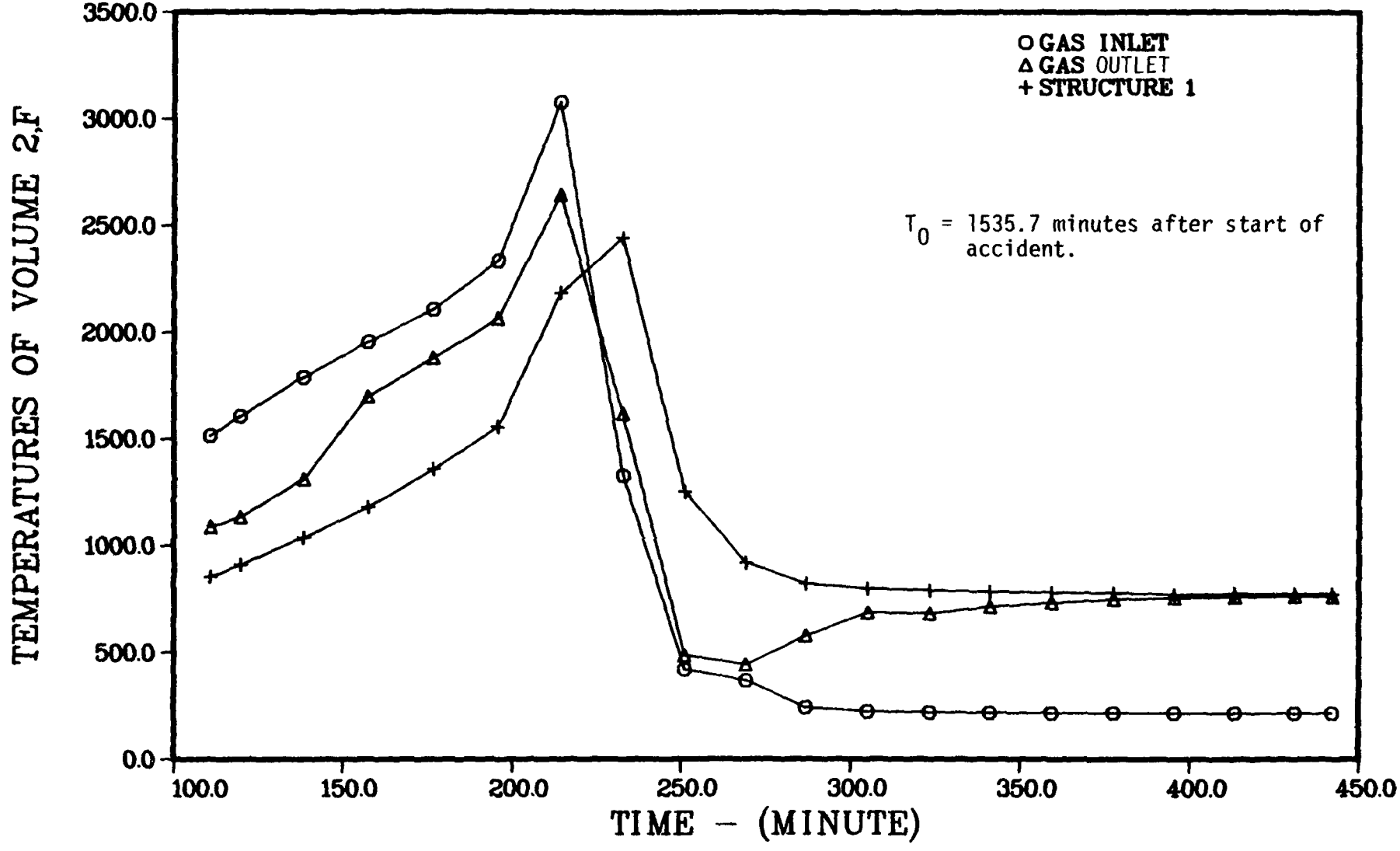

FIGURE 6.9a GAS AND STRUCTURE TEMPERATURES FOR THE TOP GUIDE IN GRAND GULF - SEQUENCE TPI

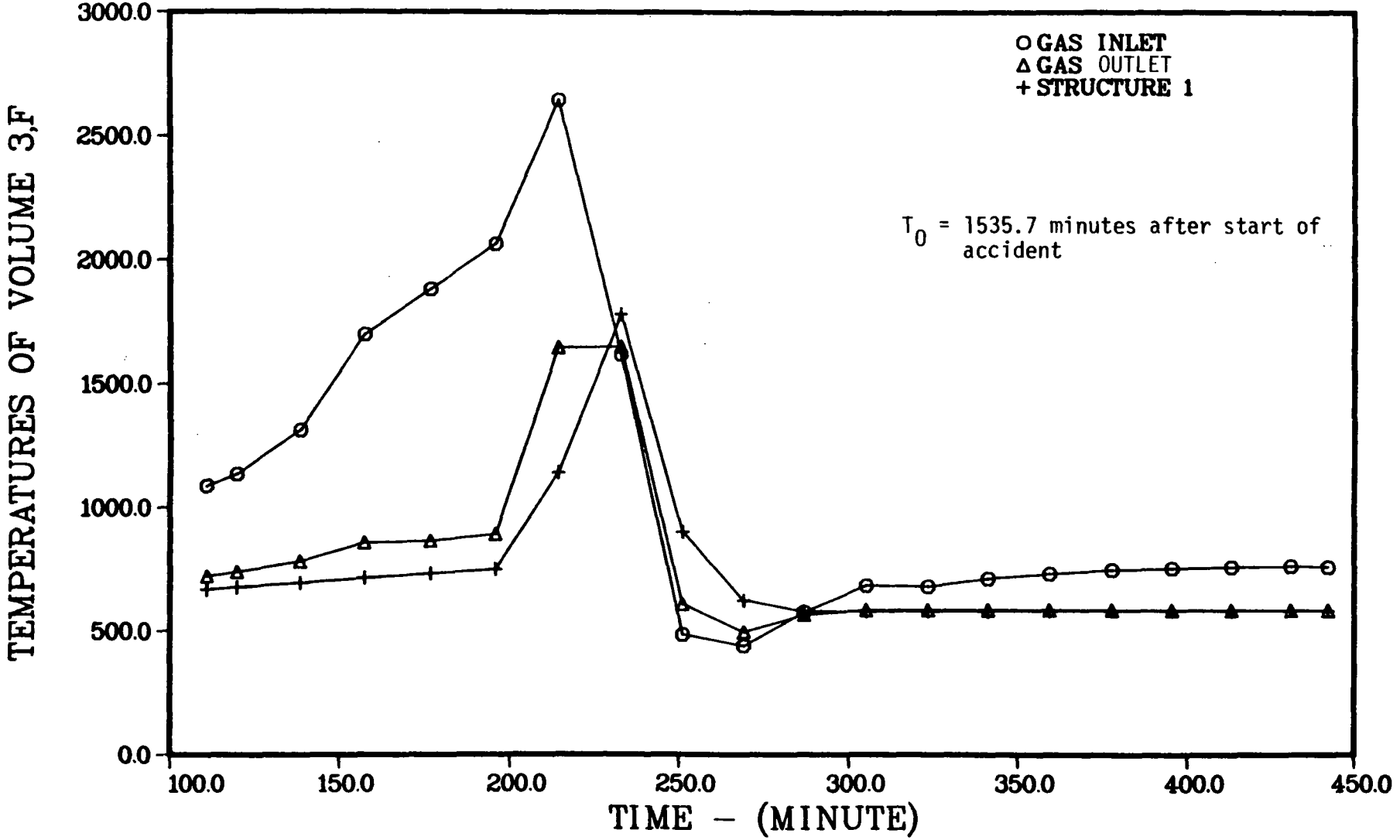

FIGURE 6.9b GAS AND STRUCTURE TEMPERATURES FOR THE SHROUD HEAD IN GRAND GULF - SEQUENCE TPI

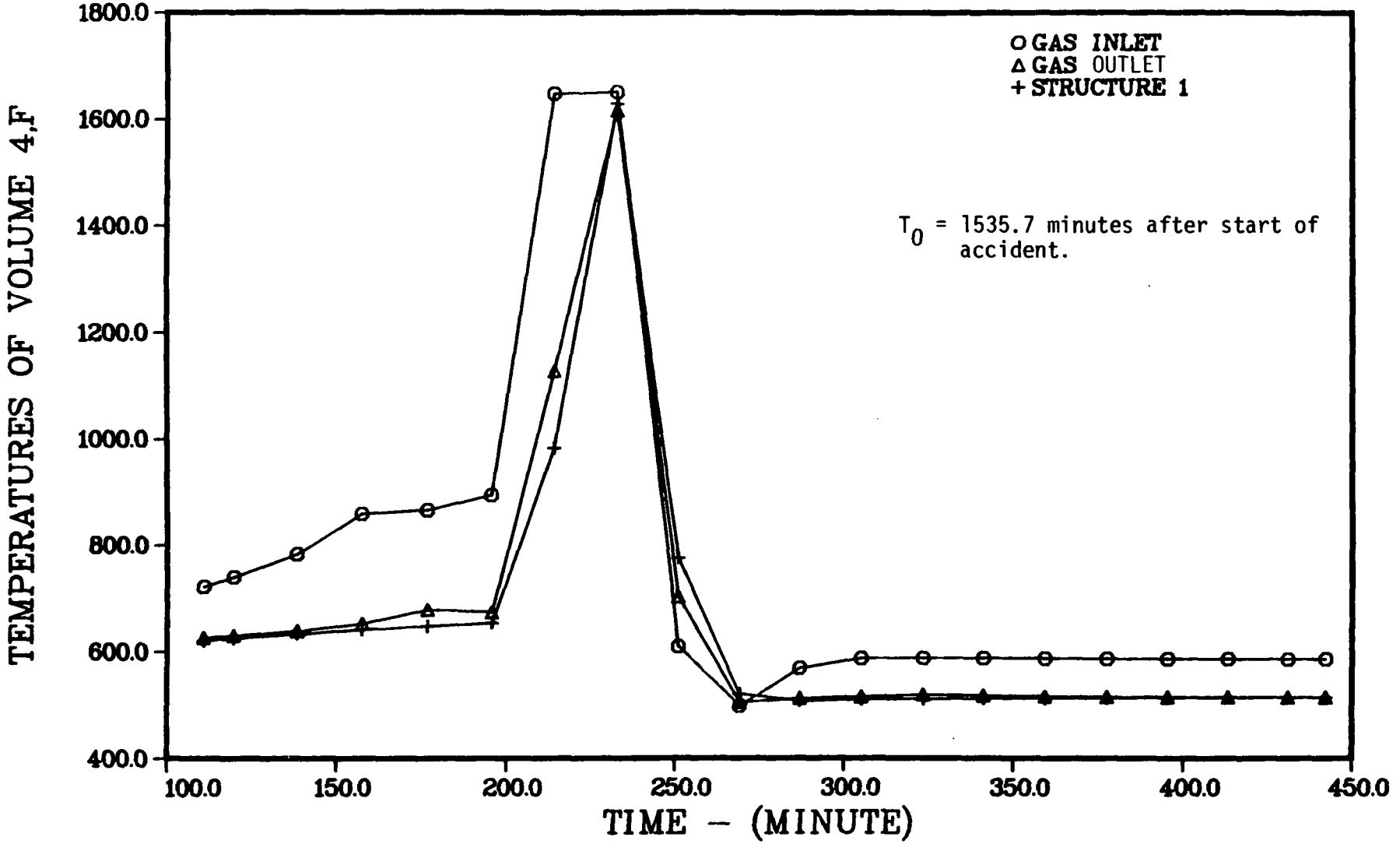

FIGURE 6.9c GAS AND STRUCTURE TEMPERATURES FOR THE STAND PIPES AND STEAM SEPARATORS IN GRAND GULF - SEQUENCE TPI

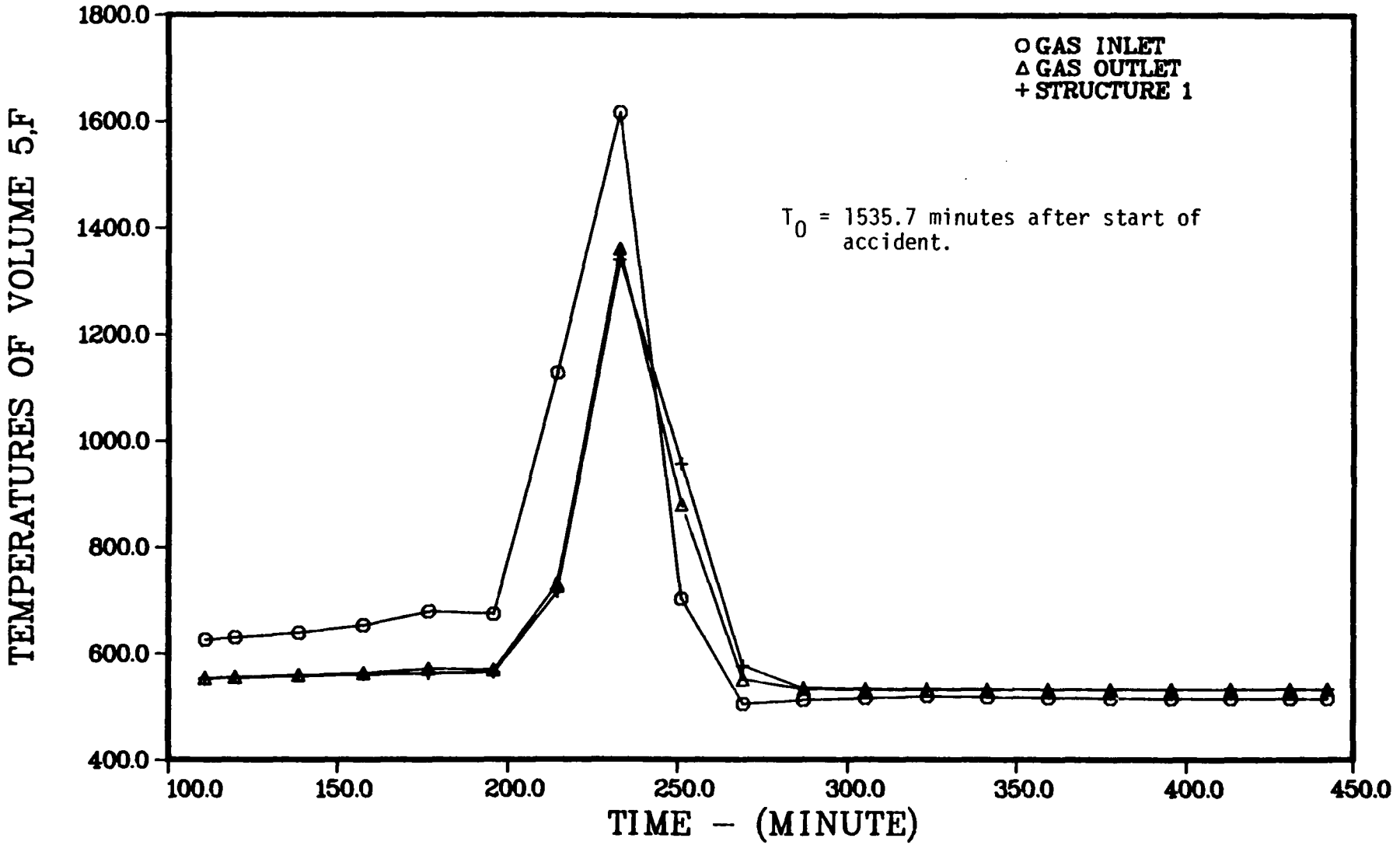

FIGURE 6.9d GAS AND STRUCTURE TEMPERATURES FOR THE STEAM DRYERS IN GRAND GULF - SEQUENCE TPI

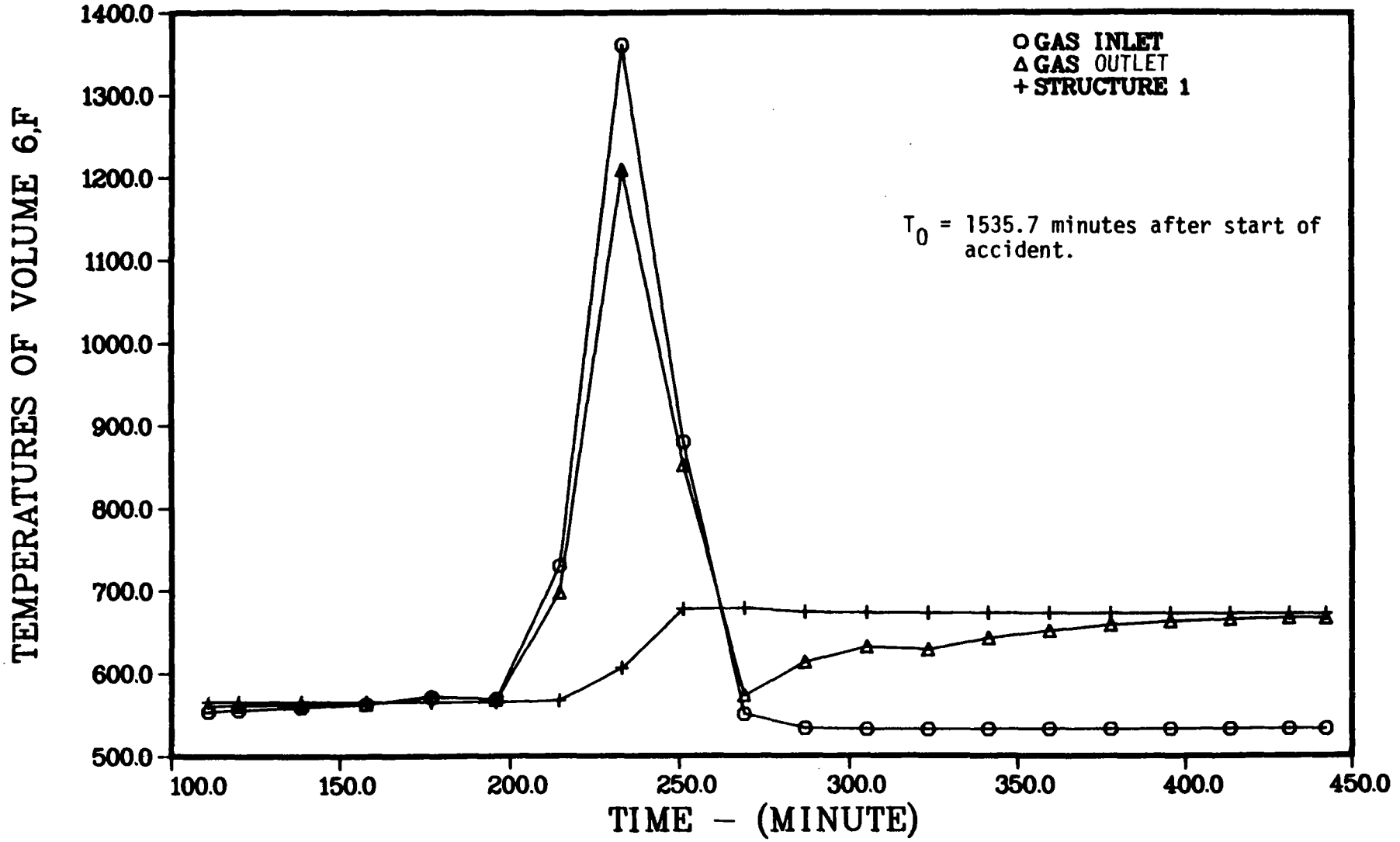

FIGURE 6.9e GAS AND STRUCTURE TEMPERATURES FOR THE UPPER OUTER ANNULUS IN GRAND GULF - SEQUENCE TPI

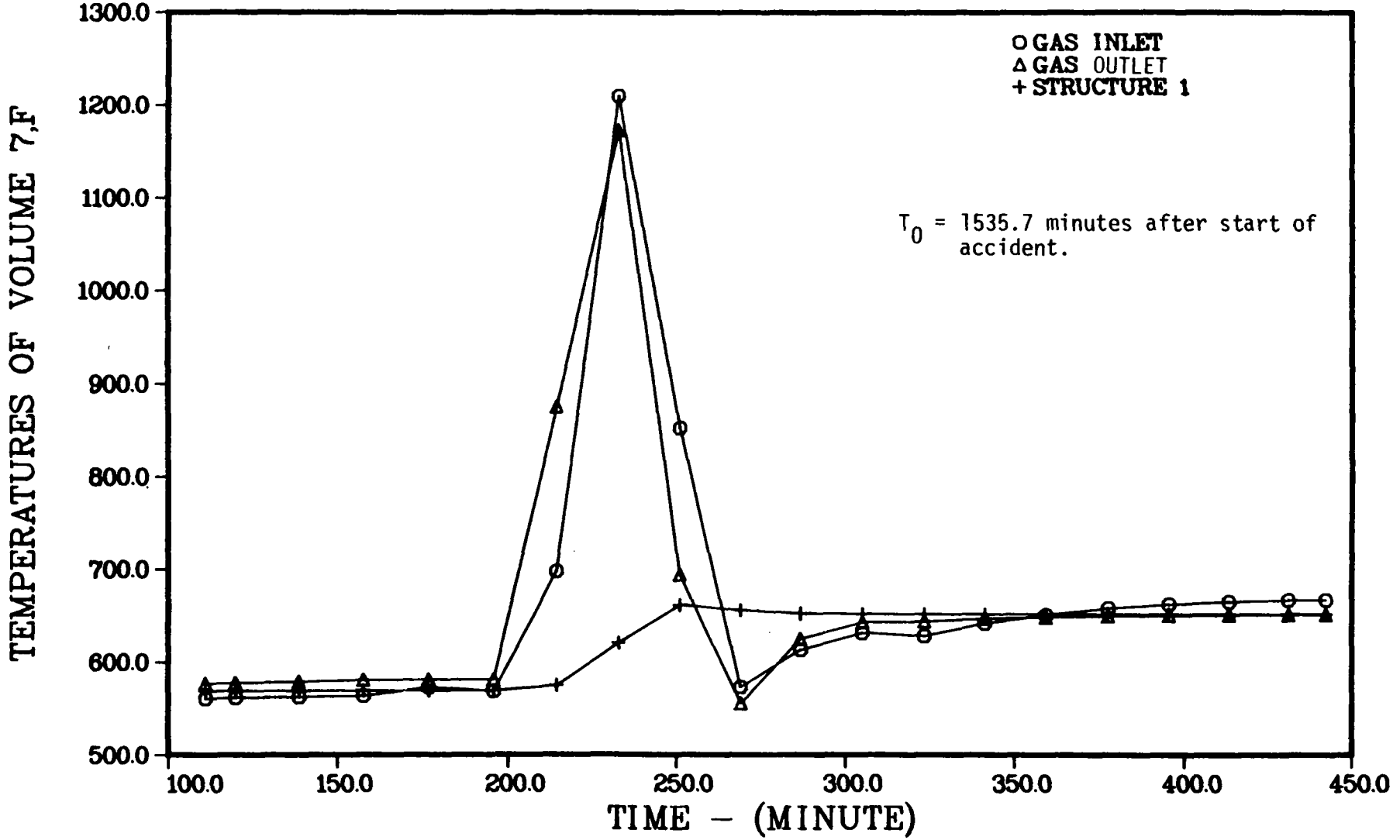

FIGURE 6.9f GAS AND STRUCTURE TEMPERATURES FOR THE LOWER OUTER ANNULUS IN GRAND GULF - SEQUENCE TPI

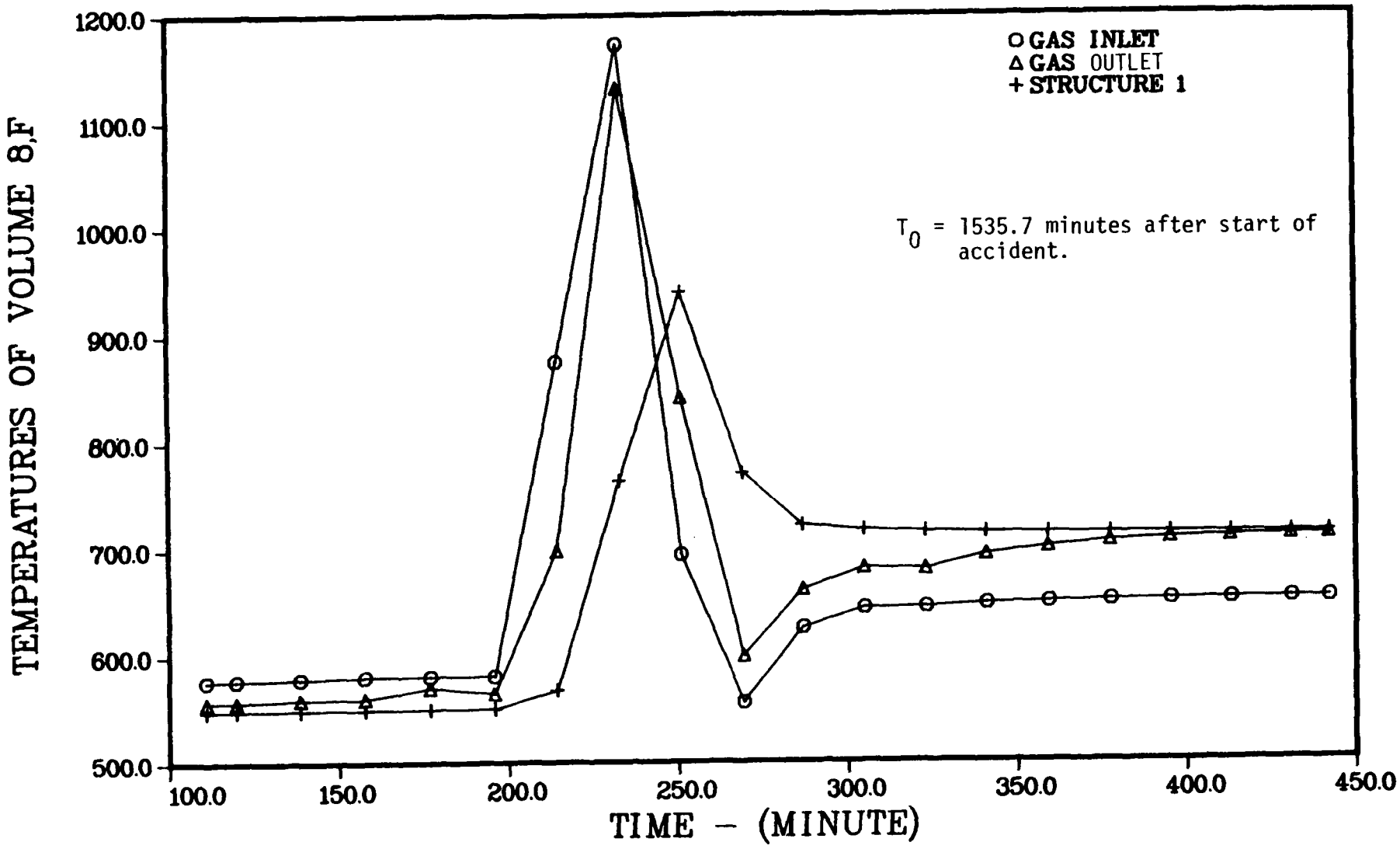

FIGURE 6.9g GAS AND STRUCTURE TEMPERATURES FOR THE STEAM LINE IN GRAND GULF - SEQUENCE TPI

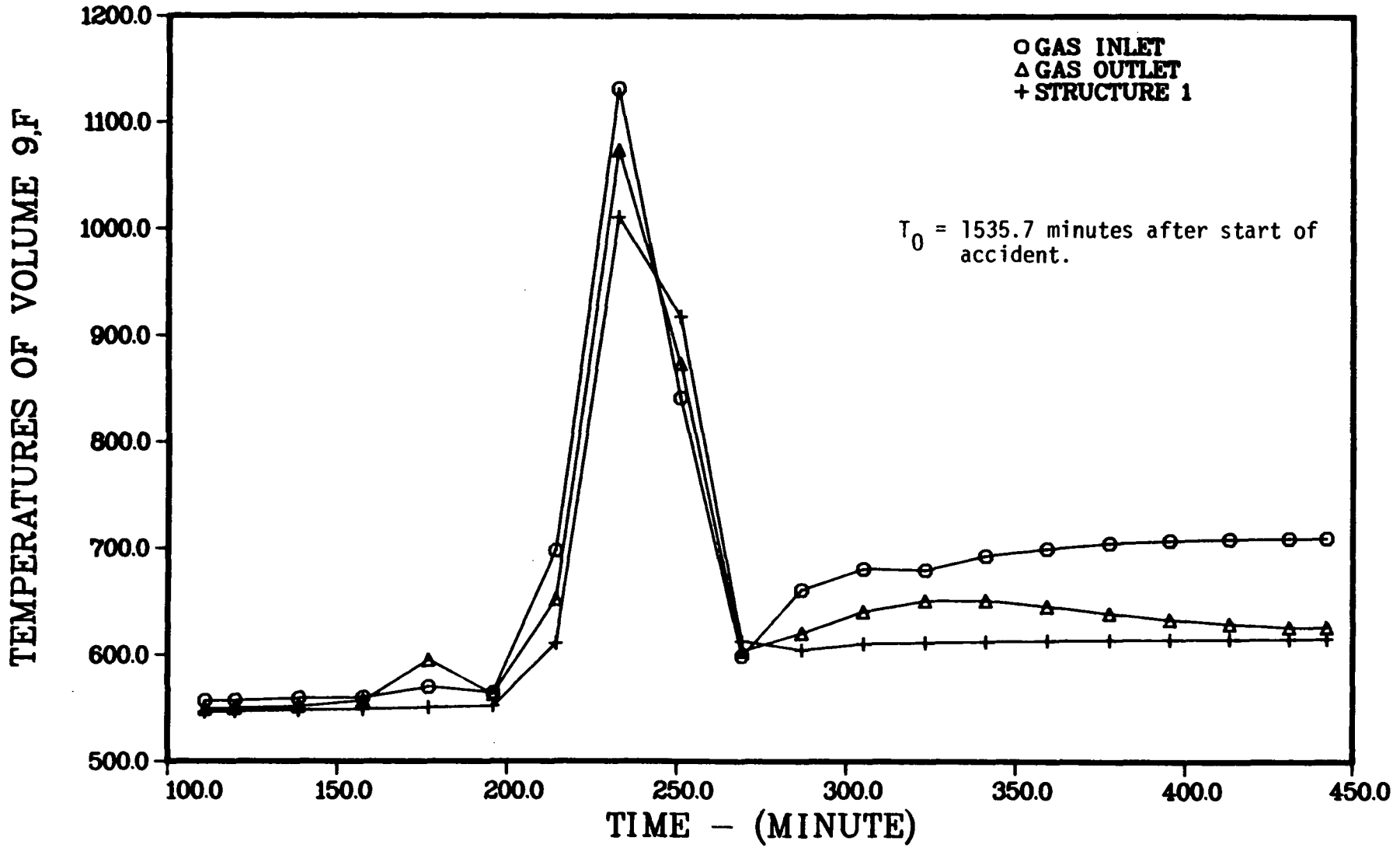

FIGURE 6.9h GAS AND STRUCTURE TEMPERATURES FOR THE RELIEF LINES IN GRAND GULF - SEQUENCE TPI

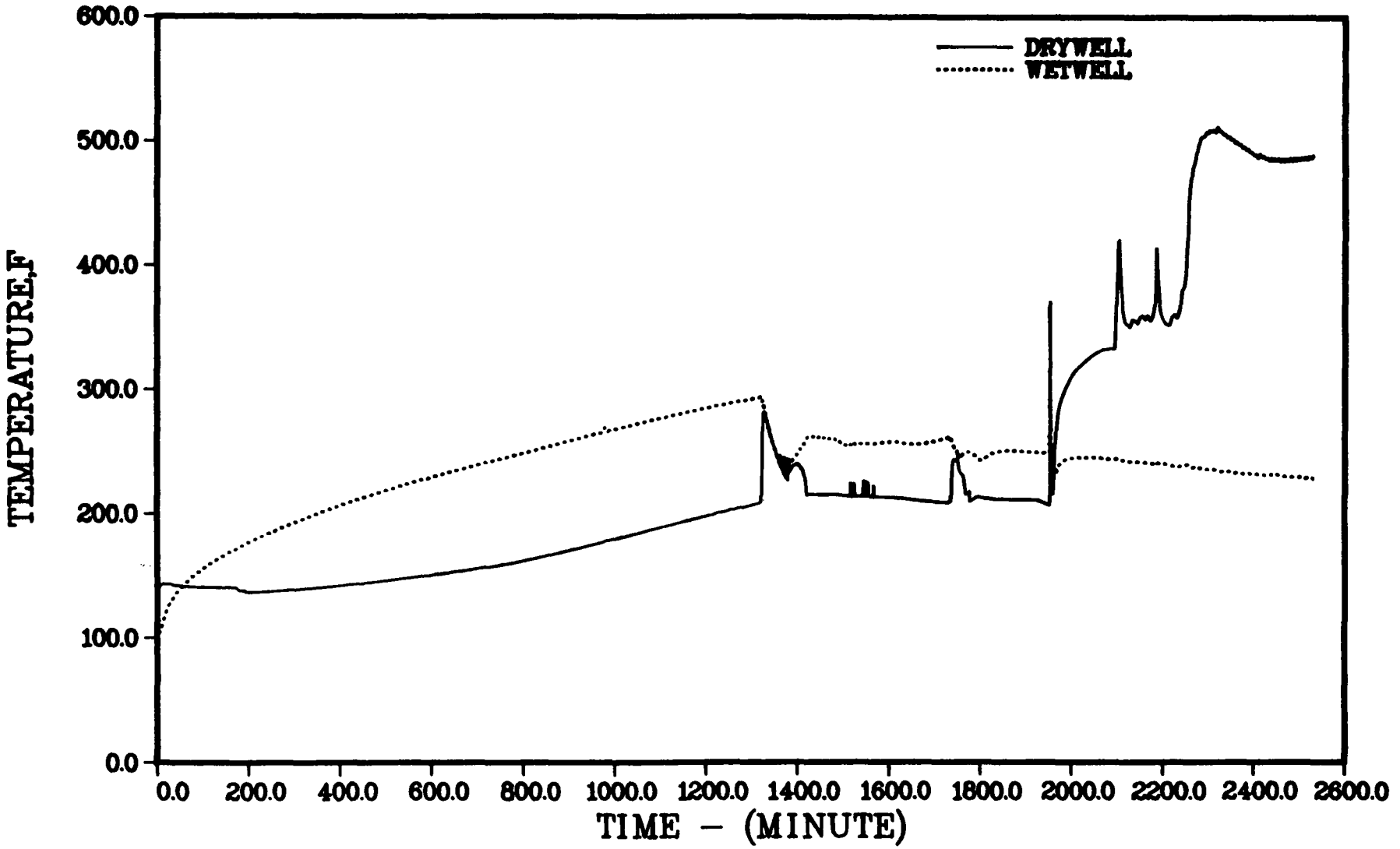

FIGURE 6.10. GAS TEMPERATURES IN CONTAINMENT VOLUMES - SEQUENCE TPI

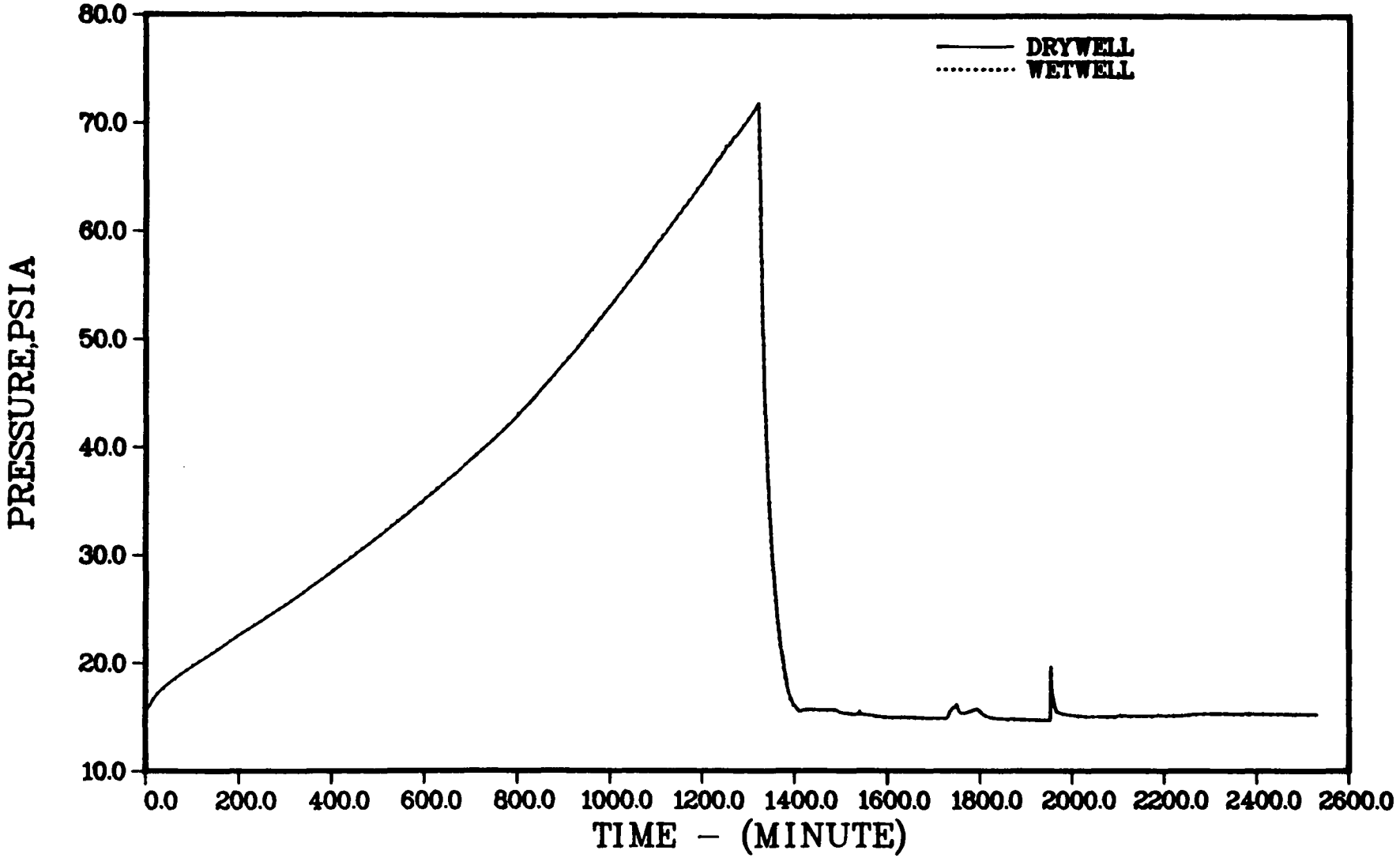

FIGURE 6.11. PRESSURES IN CONTAINMENT VOLUMES - SEQUENCE TPI

to the buildup of noncondensibles and is predicted to take place late in the accident sequence.

Table 6.3 gives the core and primary system conditions at key times during the sequence. Temperatures of selected fuel regions as calculated by MARCH are illustrated in Figures 6.12a and 6.12b. Gas and structure temperatures within the primary system as calculated by MERGE are shown in Figures 6.13a-h. Time zero in Figure 6.13 corresponds to the time of core uncovery or 47.0 minutes from the start of the accident.

Primary containment conditions during the sequence are given in Table 6.4. Temperatures and pressures in the containment volumes are illustrated in Figures 6.14 and 6.15. In the analyses of the TQUV sequence, it was assumed that hydrogen igniters were available to control the buildup of flammable gases in the containment. In the containment pressure history illustrated in Figure 6.15, it is interesting to note that relatively high pressures due to hydrogen burning are predicted even with the operation of the igniters. The containment was assumed to be able to withstand these burn pressures, but failed eventually due to the buildup of noncondensible gases. As has been noted in other volumes of this series, the predicted pressure loads from hydrogen burning can be sensitive to the rate and magnitude of hydrogen input to the containment, ignition thresholds, containment compartmentalization, etc. The containment leakages and related parameters derived from the MARCH analyses for use in the release of fission product release to the environment are summarized in Table 6.5.

6.1.4 Sequence S_2E

The S_2E sequence is initiated by a small break in the primary coolant system; the initiating event is accompanied by the failure of the emergency core cooling system. In the absence of coolant makeup, the primary coolant inventory would be lost through the break and lead to core uncovery and melting. Figure 6.16 illustrates schematically the fission product flow path in the primary system. The rate of coolant loss and the timing of core uncovery and subsequent melting would depend on the size and location of the break in the primary system. For the analyses presented here, a break size equal to a 2-inch diameter opening has been assumed. The actuation of the Automatic Depressurization System (ADS) which would tend to divert more of the primary

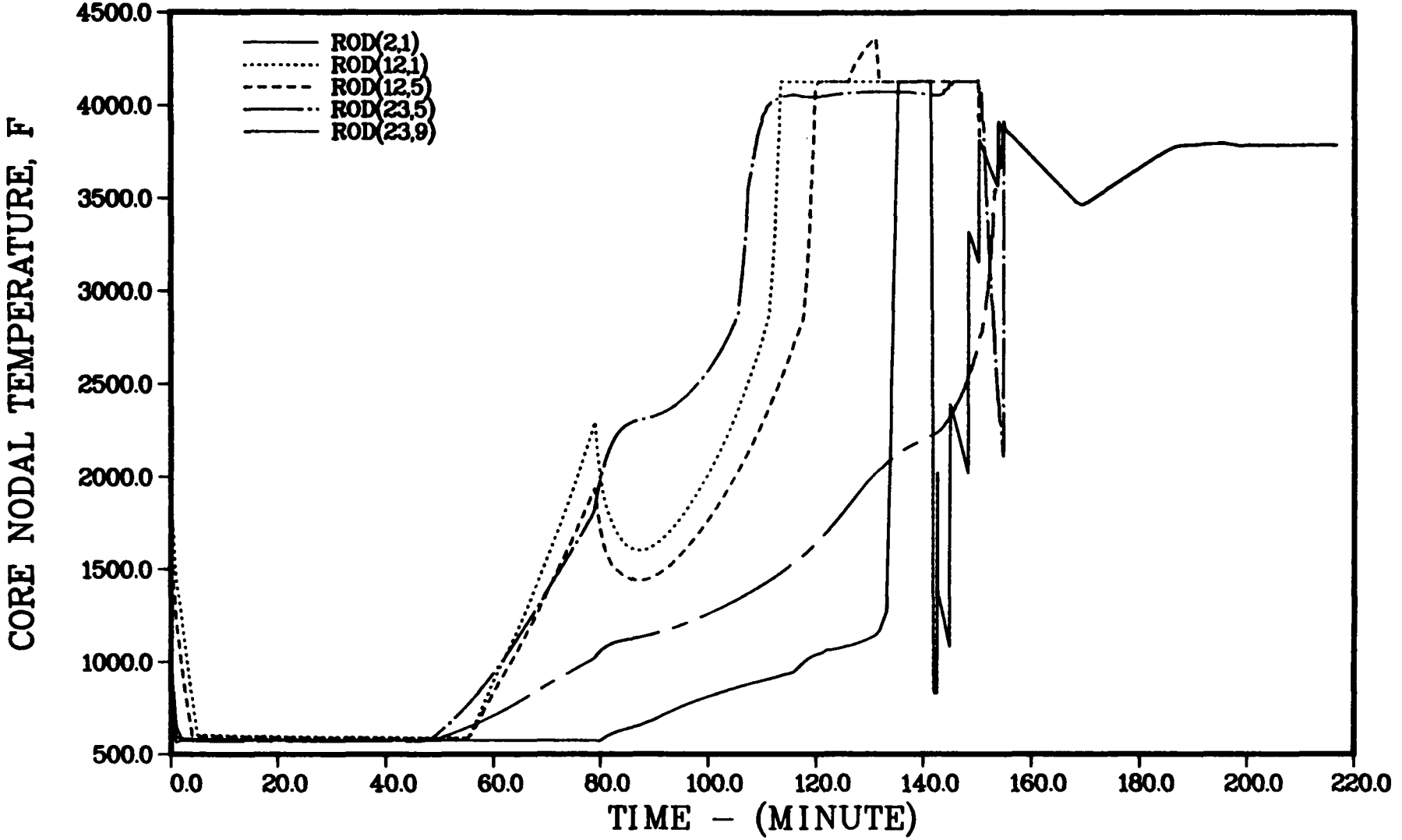

FIGURE 6.12a TEMPERATURES OF SELECTED CORE NODES - SEQUENCE TQUV

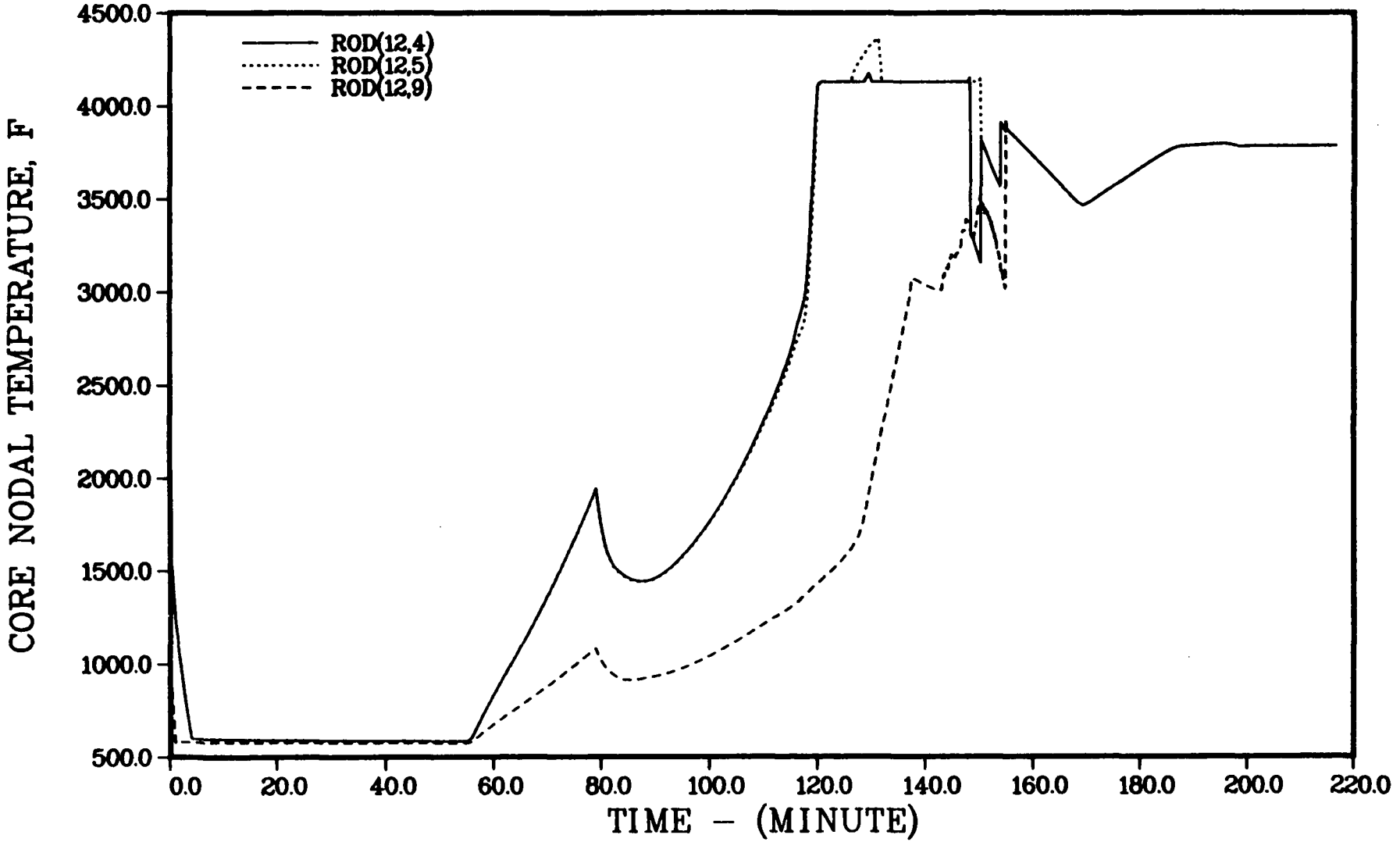

FIGURE 6.12b TEMPERATURES OF SELECTED CORE NODES - SEQUENCE TQUV

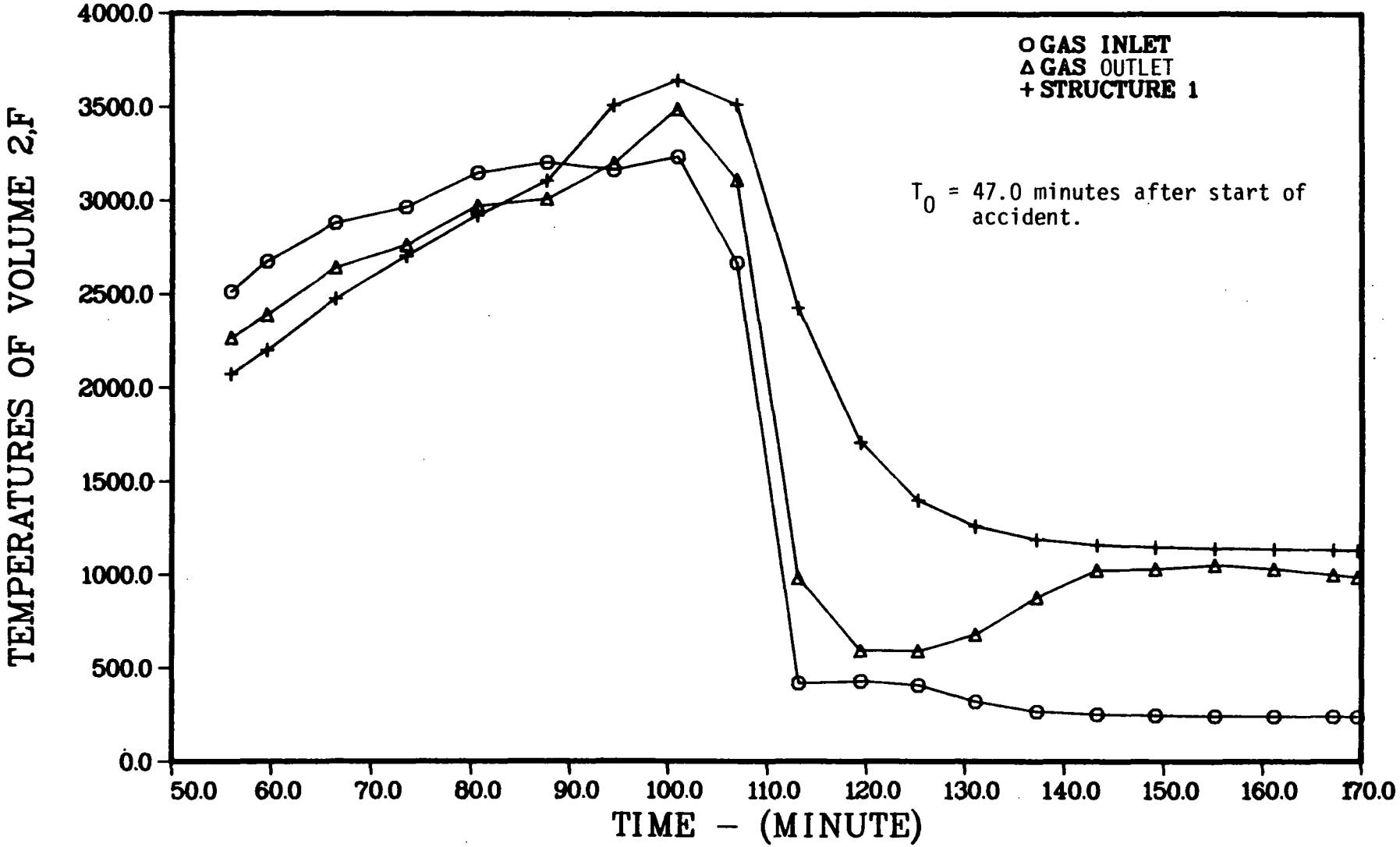

FIGURE 6.13a GAS AND STRUCTURE TEMPERATURES FOR THE TOP GUIDE IN GRAND GULF - SEQUENCE TQUV

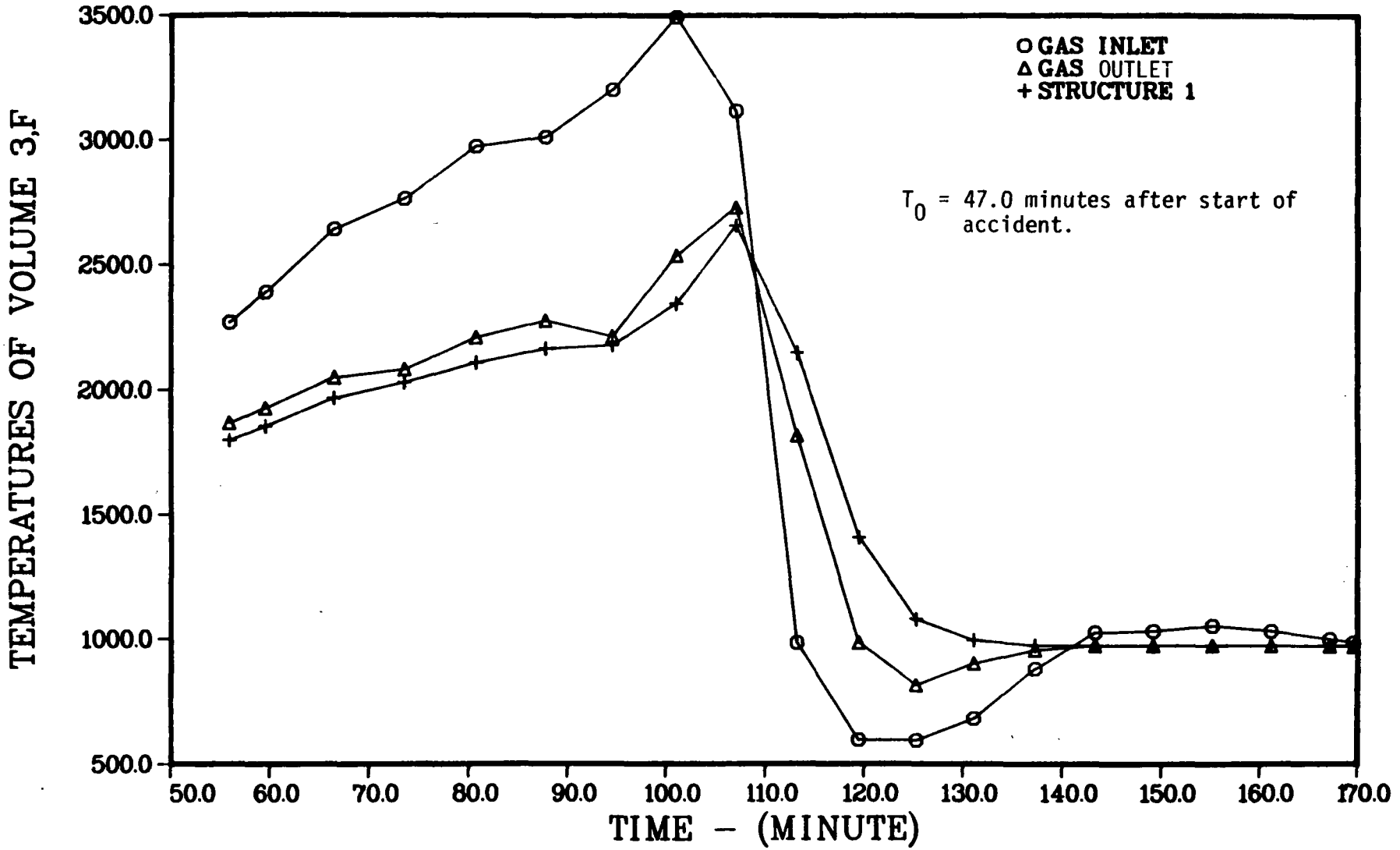

FIGURE 6.13b GAS AND STRUCTURE TEMPERATURES FOR THE SHROUD HEAD IN GRAND GULF - SEQUENCE TQUV

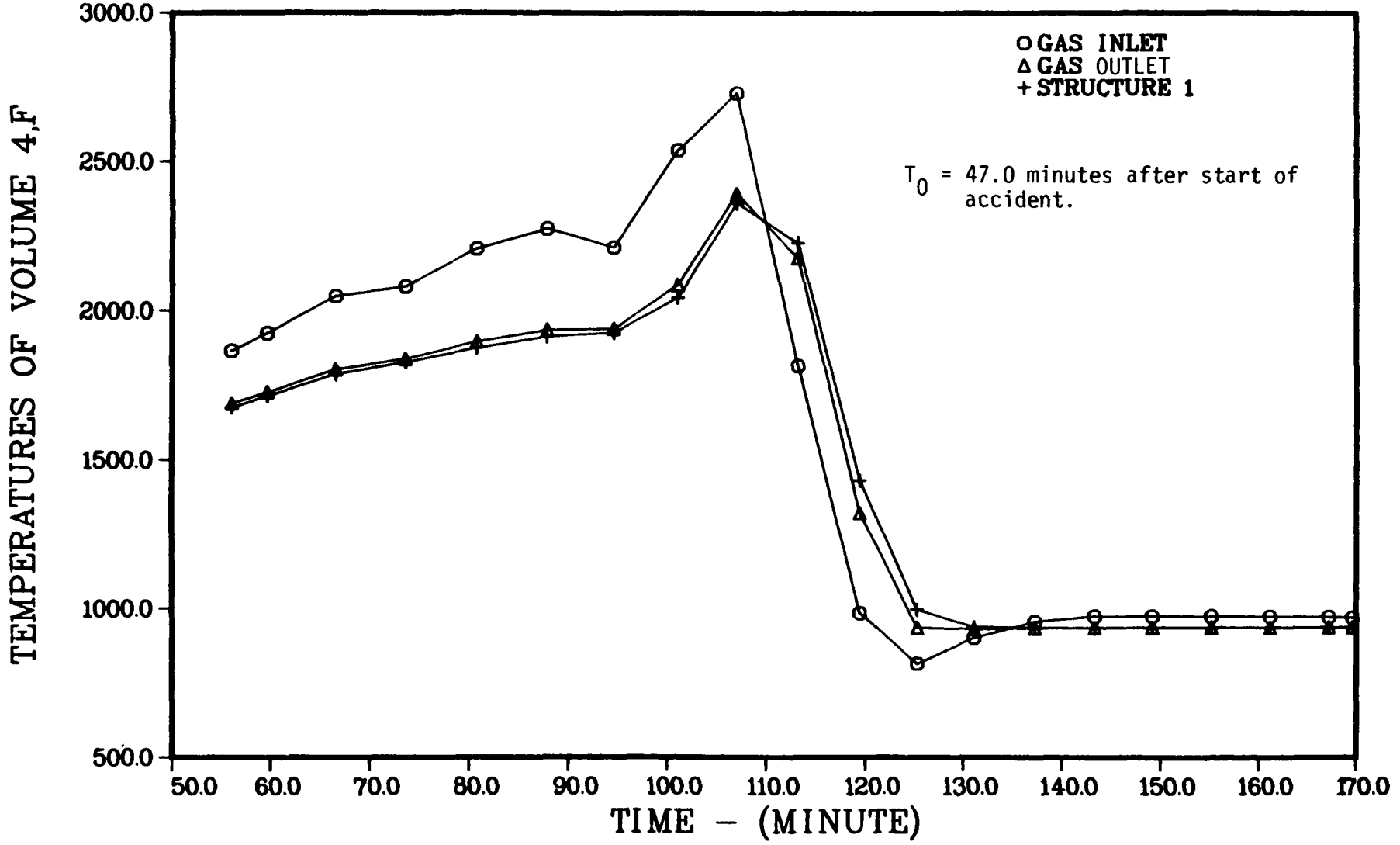

FIGURE 6.13c GAS AND STRUCTURE TEMPERATURES FOR THE STAND PIPES AND STEAM SEPARATORS IN GRAND GULF - SEQUENCE TQUV

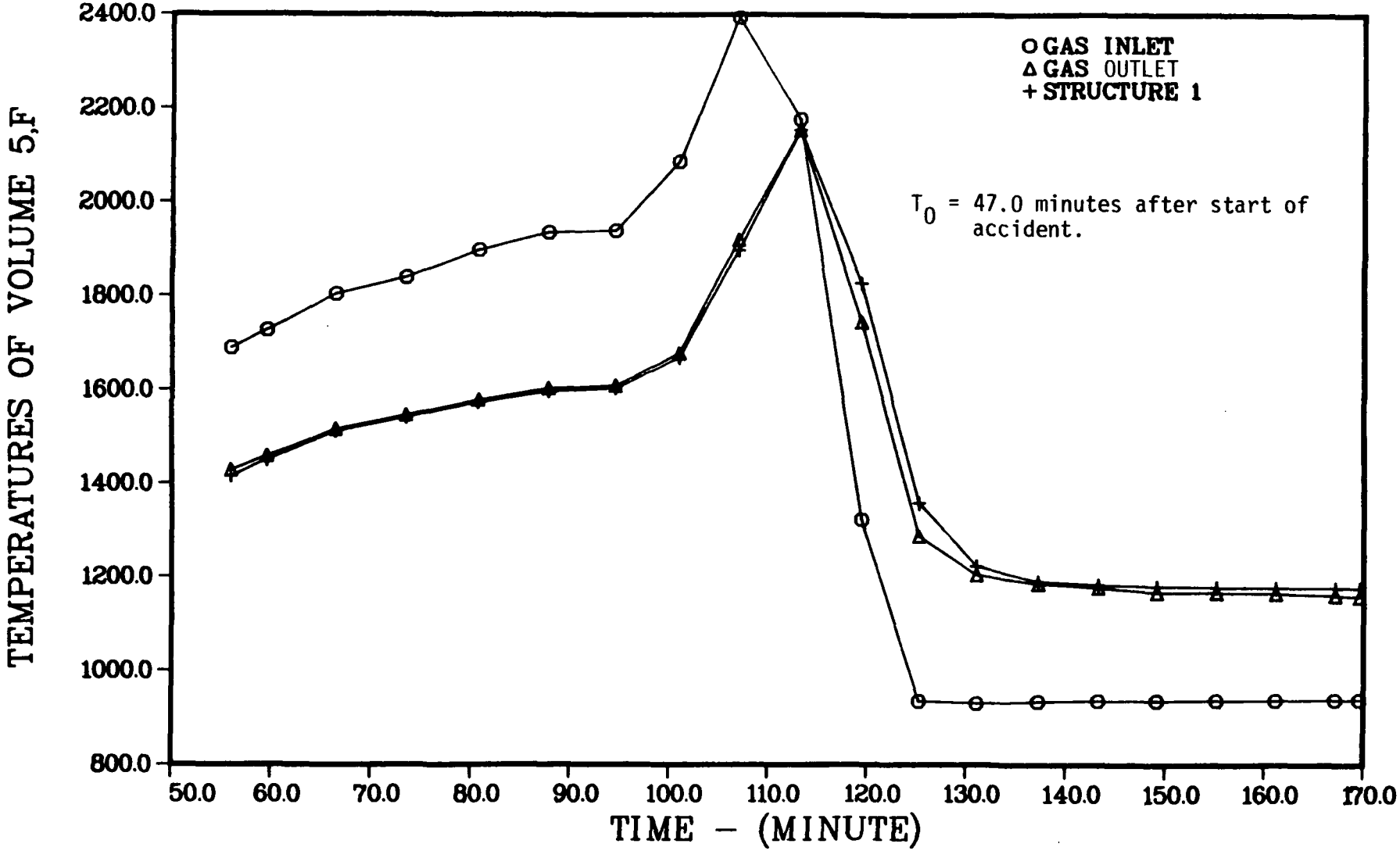

FIGURE 6.13d GAS AND STRUCTURE TEMPERATURES FOR THE STEAM DRYERS IN GRAND GULF - SEQUENCE TQUV

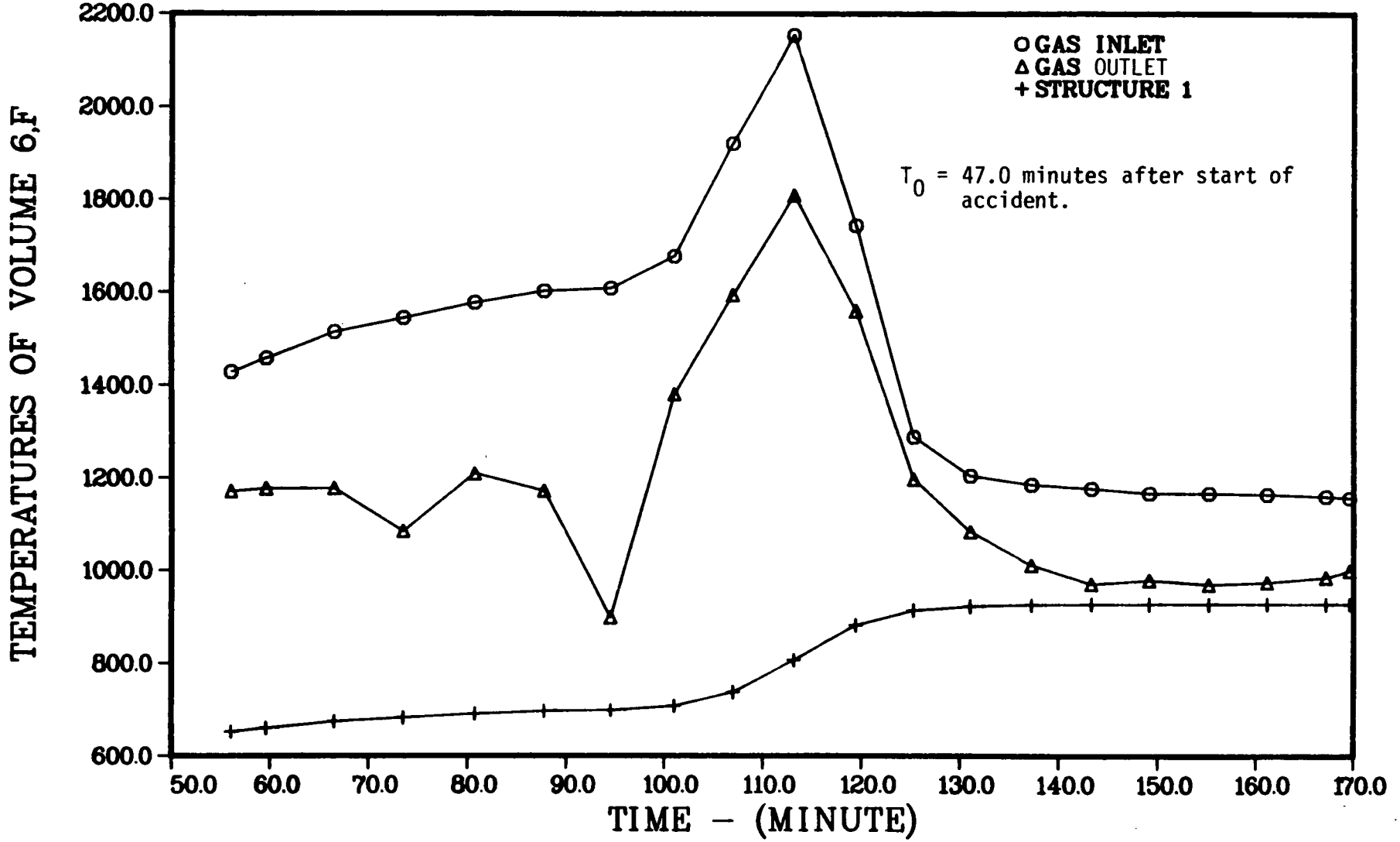

FIGURE 6.13e GAS AND STRUCTURE TEMPERATURES FOR THE UPPER OUTER ANNULUS IN GRAND GULF - SEQUENCE TQUV

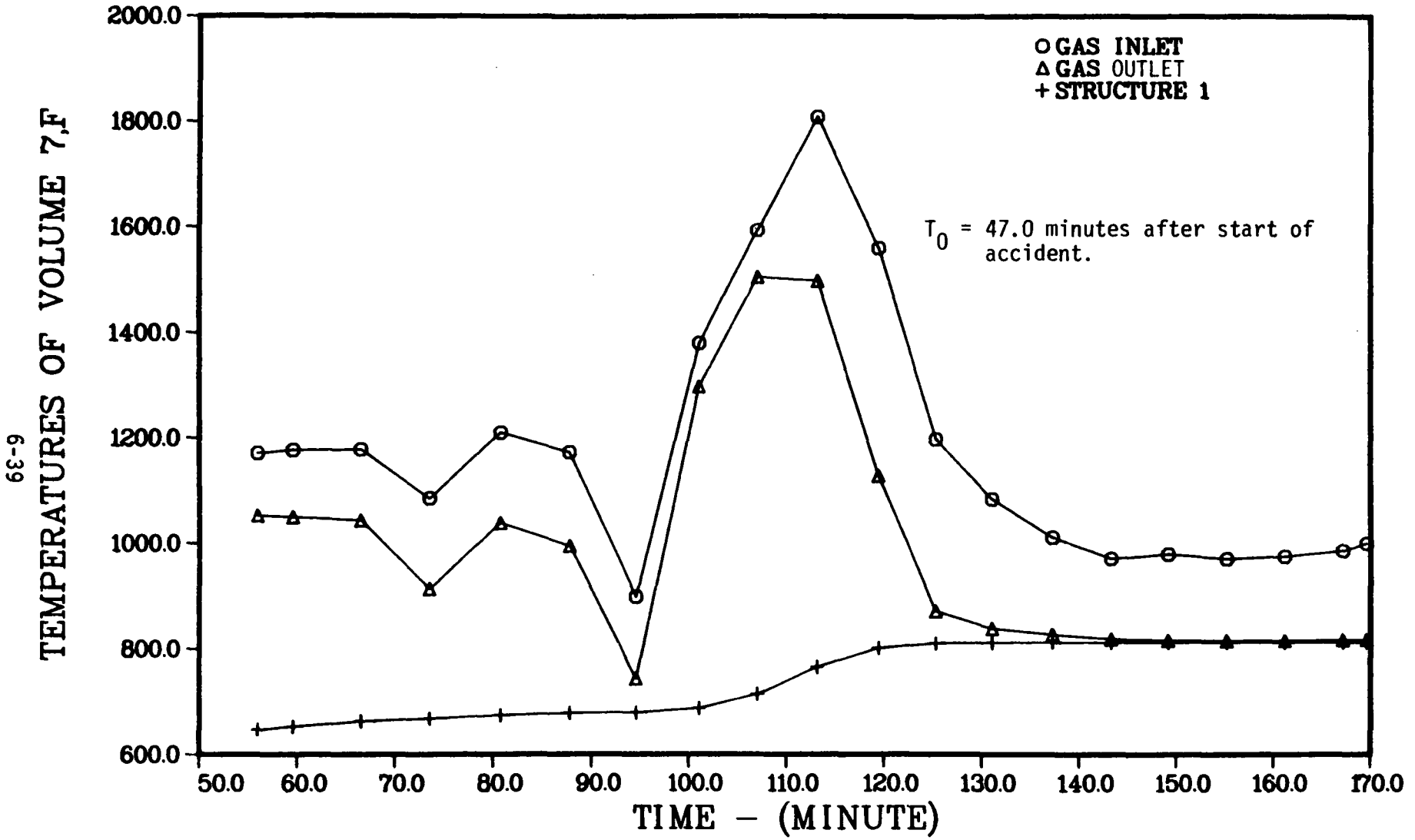

FIGURE 6.13f GAS AND STRUCTURE TEMPERATURES FOR THE LOWER OUTER ANNULUS IN GRAND GULF - SEQUENCE TQUV

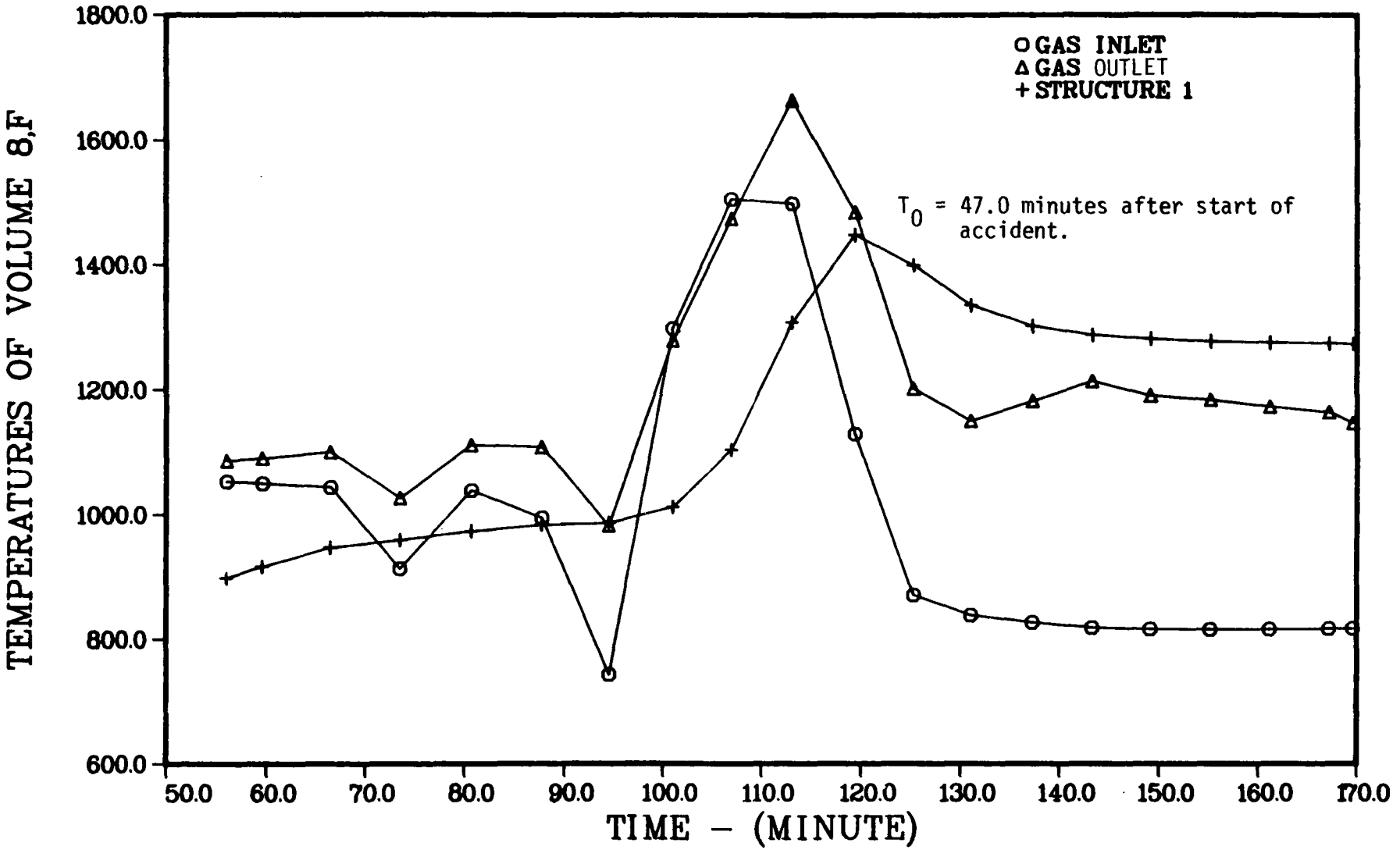

FIGURE 6.13g GAS AND STRUCTURE TEMPERATURES FOR THE STEAM LINE IN GRAND GULF - SEQUENCE TQUV

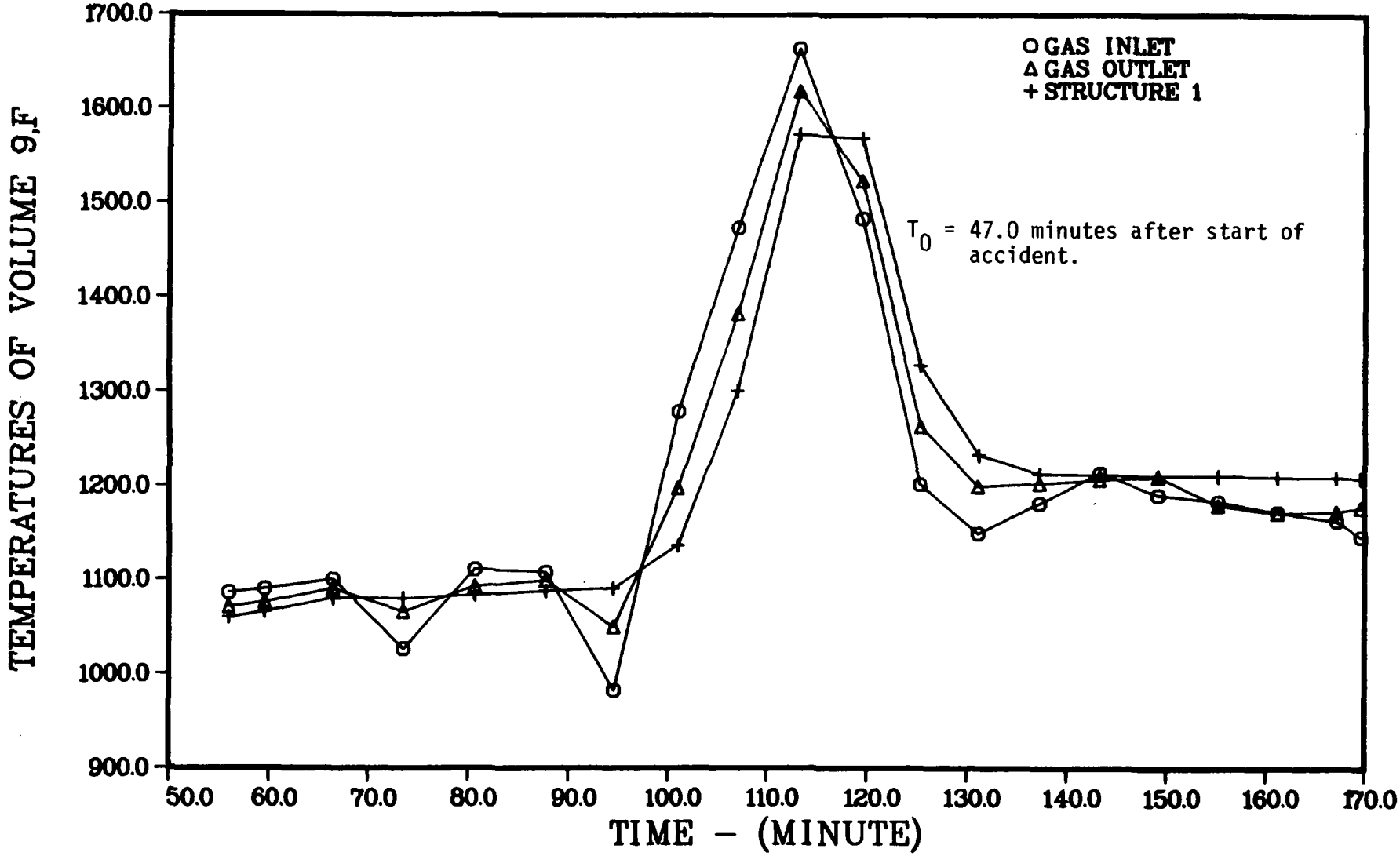

FIGURE 6.13h GAS AND STRUCTURE TEMPERATURES FOR THE RELIEF LINES IN GRAND GULF - SEQUENCE TQUV

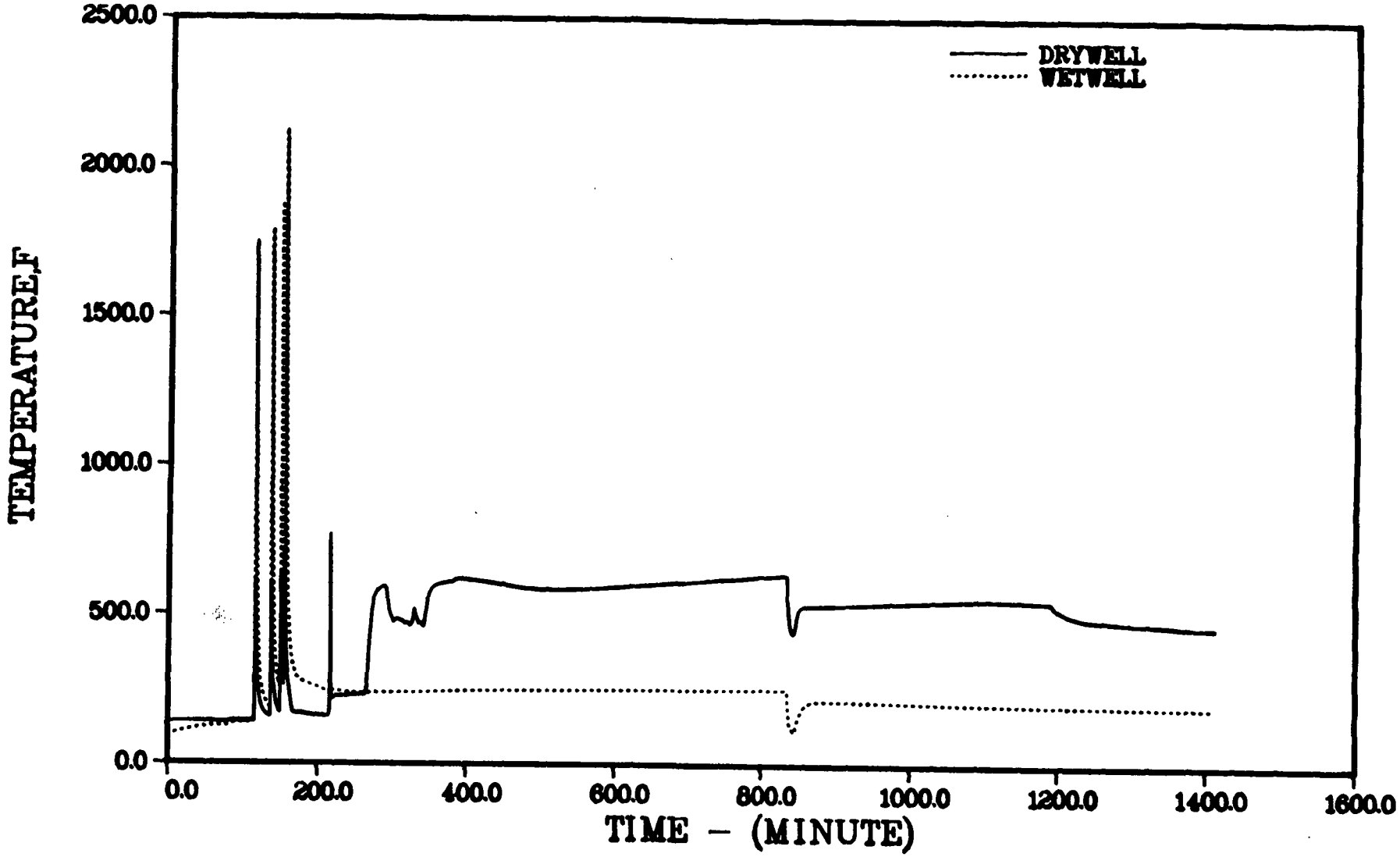

FIGURE 6.14. GAS TEMPERATURES IN CONTAINMENT VOLUMES - SEQUENCE TQUV

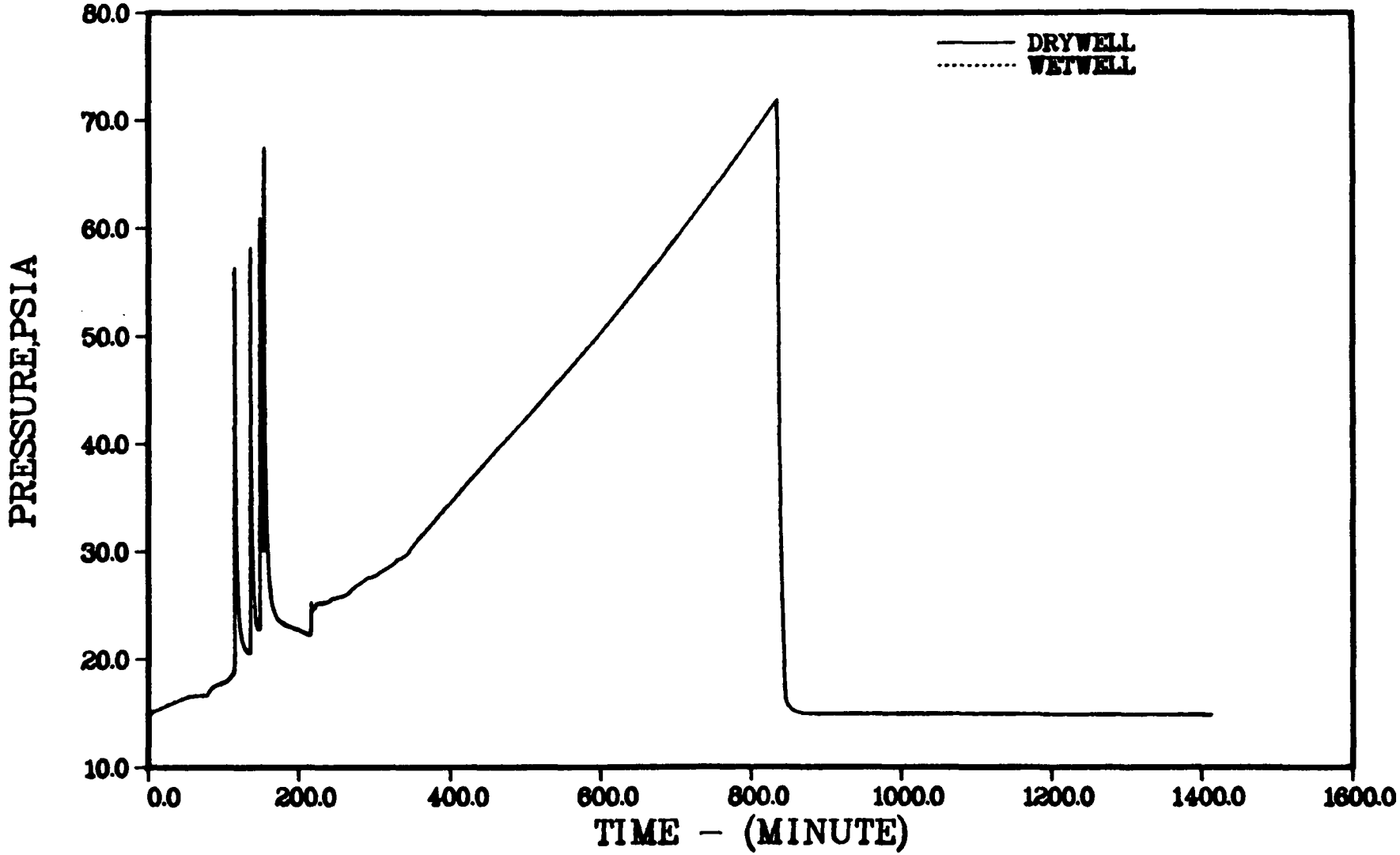

FIGURE 6.15. PRESSURES IN CONTAINMENT VOLUMES - SEQUENCE TQUV

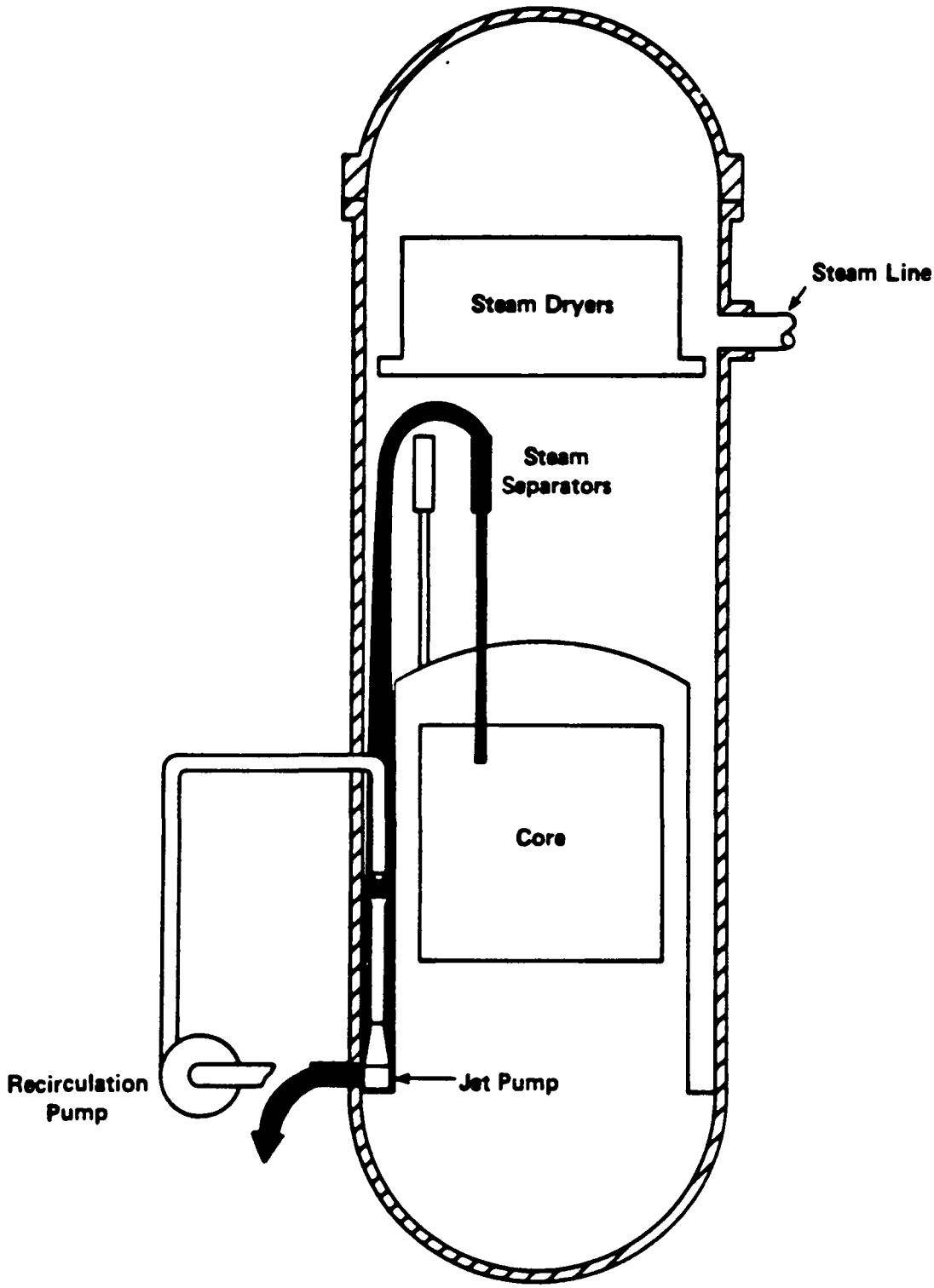

FIGURE 6.16 FLOWPATH FOR FISSION PRODUCT TRANSPORT THROUGH PRIMARY SYSTEM BREAK IN GRAND GULF - SEQUENCE S2E

system effluent to the suppression pool was not considered in the analyses described here.

In the S_2E sequence, the fission products released from the core would flow to the drywell through the break in the piping and then to the suppression pool by way of the horizontal vents. Since the suppression pool would be subcooled in this sequence, it would be very effective in the removal of fission products flowing through it. In order to investigate the effects of potential suppression pool bypass, some direct leakage from the drywell to the outer containment was considered in the analyses for the S_2E sequence. The effect on fission product release of two specific bypass leak rates was examined. The first case corresponds to possible nominal leakage from the drywell to the outer containment; the leak rate of 860 ft^3/min that was utilized is based on leakage data provided by the General Electric Company extrapolated to the conditions expected during the accident. The second case considered modeled a stuck open vacuum breaker between the outer containment and the drywell; a leak rate about a factor of 10 greater than the above nominal rate was utilized for this case.

The timing of key events for the S_2E sequence as predicted by MARCH 2 is given in Table 6.2. Figures 6.17a and 6.17b give the temperature histories of selected core nodes during this sequence. Table 6.3 gives the core and primary system conditions at key times during the accident sequence. Figure 6.18 gives the schematic representation of the primary system nodalization used in the MERGE analyses. Gas and structure temperatures within the primary system as calculated by MERGE are given in Figures 6.19a-d. In Figure 6.19 time zero corresponds to time of core uncovery or 5.6 minutes after the start of the accident.

The conditions in the containment at key times in the accident sequence are summarized in Table 6.4. The temperatures and pressures in the containment for the nominal bypass case are illustrated in Figures 6.20 and 6.21; the corresponding histories with the large pool bypass are given in Figures 6.22 and 6.23. It can be seen that suppression pool bypass at the levels considered has only a minimal impact on the overall containment pressure and temperature response.

In the S_2E sequence, as was the case for TQUV, the hydrogen igniters were assumed to be operable. For the S_2E sequence, however, pressures exceeding the assumed failure level were predicted from hydrogen burning. These pressures

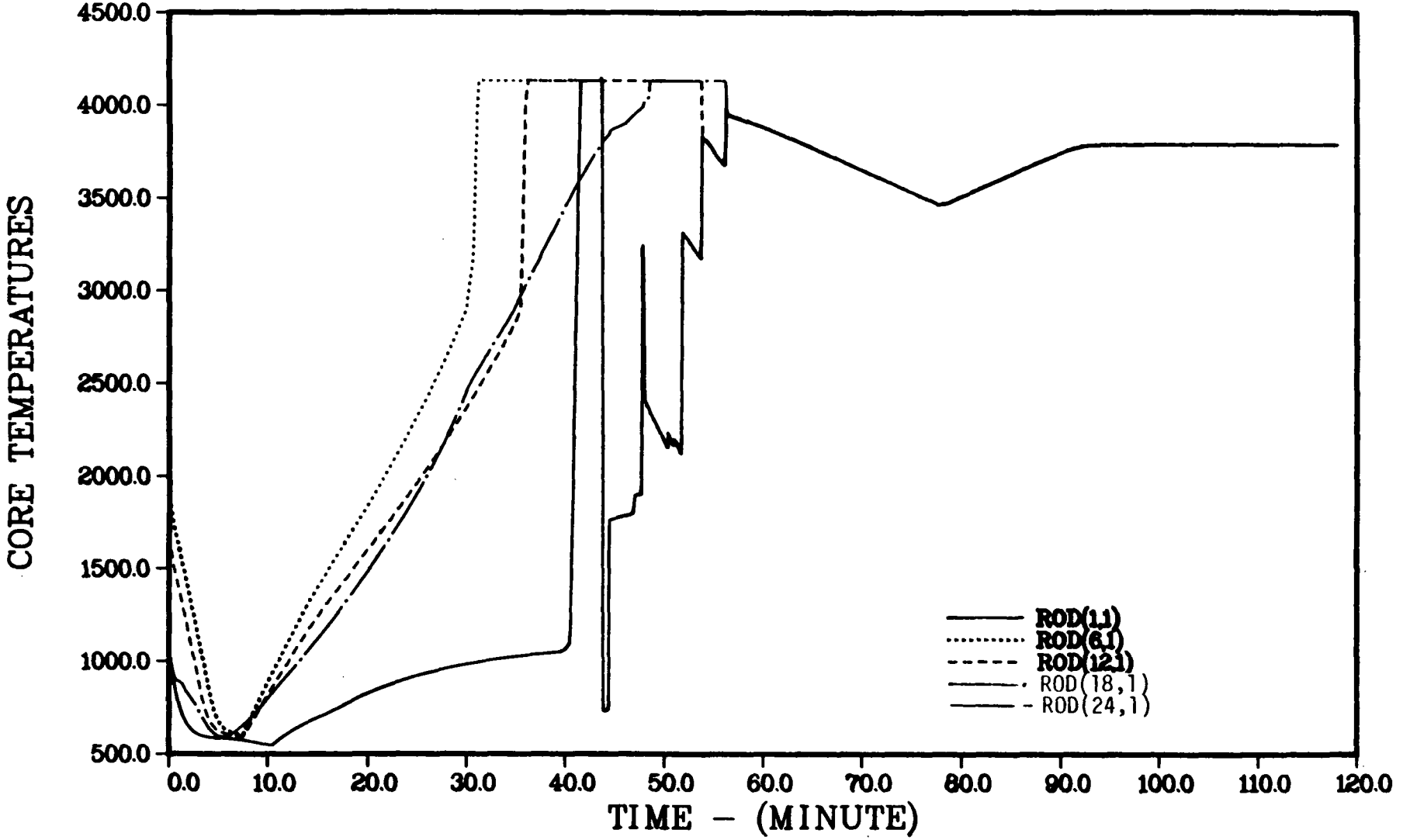

FIGURE 6.17a SELECTED CORE NODE TEMPERATURES FOR GRAND GULF - SEQUENCE S2E

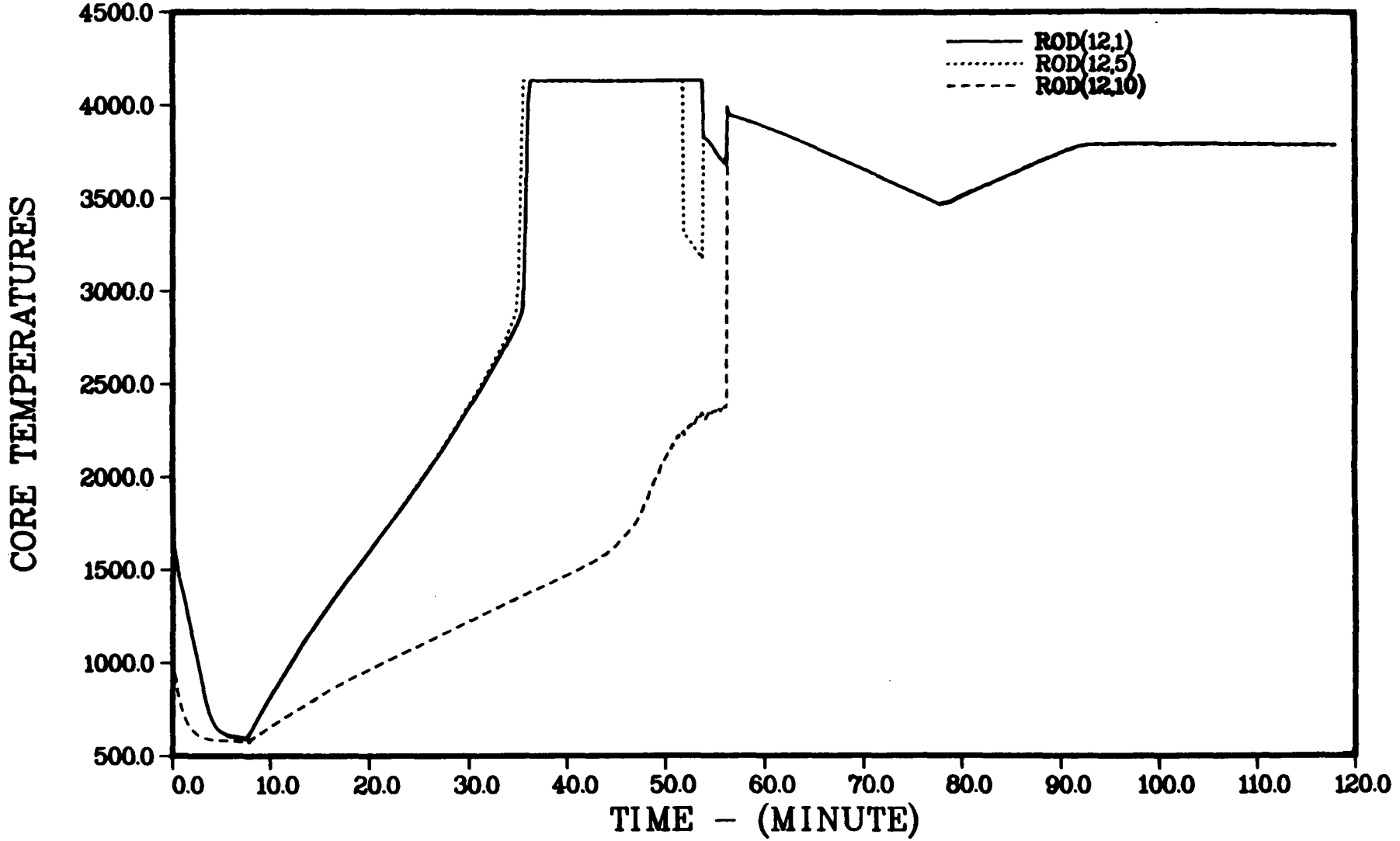

FIGURE 6.17b SELECTED CORE NODE TEMPERATURES FOR GRAND GULF - SEQUENCE S2E

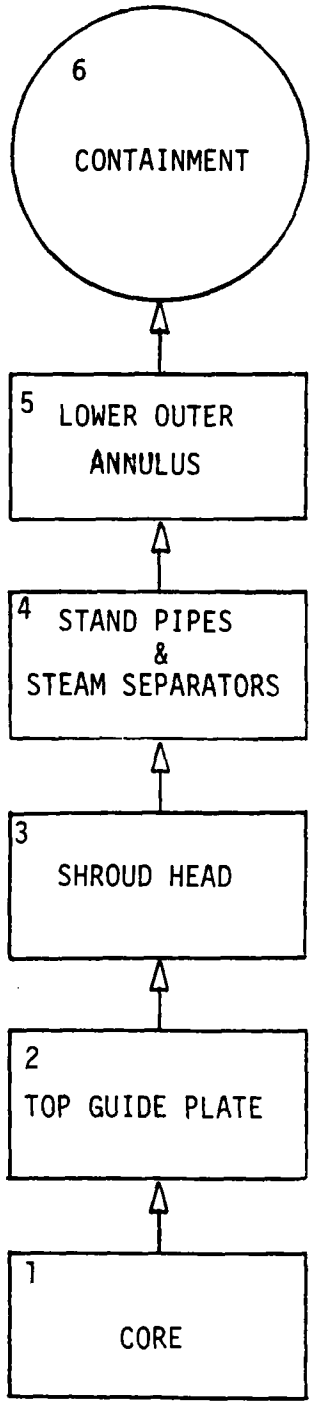

FIGURE 6.18 MERGE PRIMARY SYSTEM CONTROL VOLUMES FOR GRAND GULF - SEQUENCE S2E

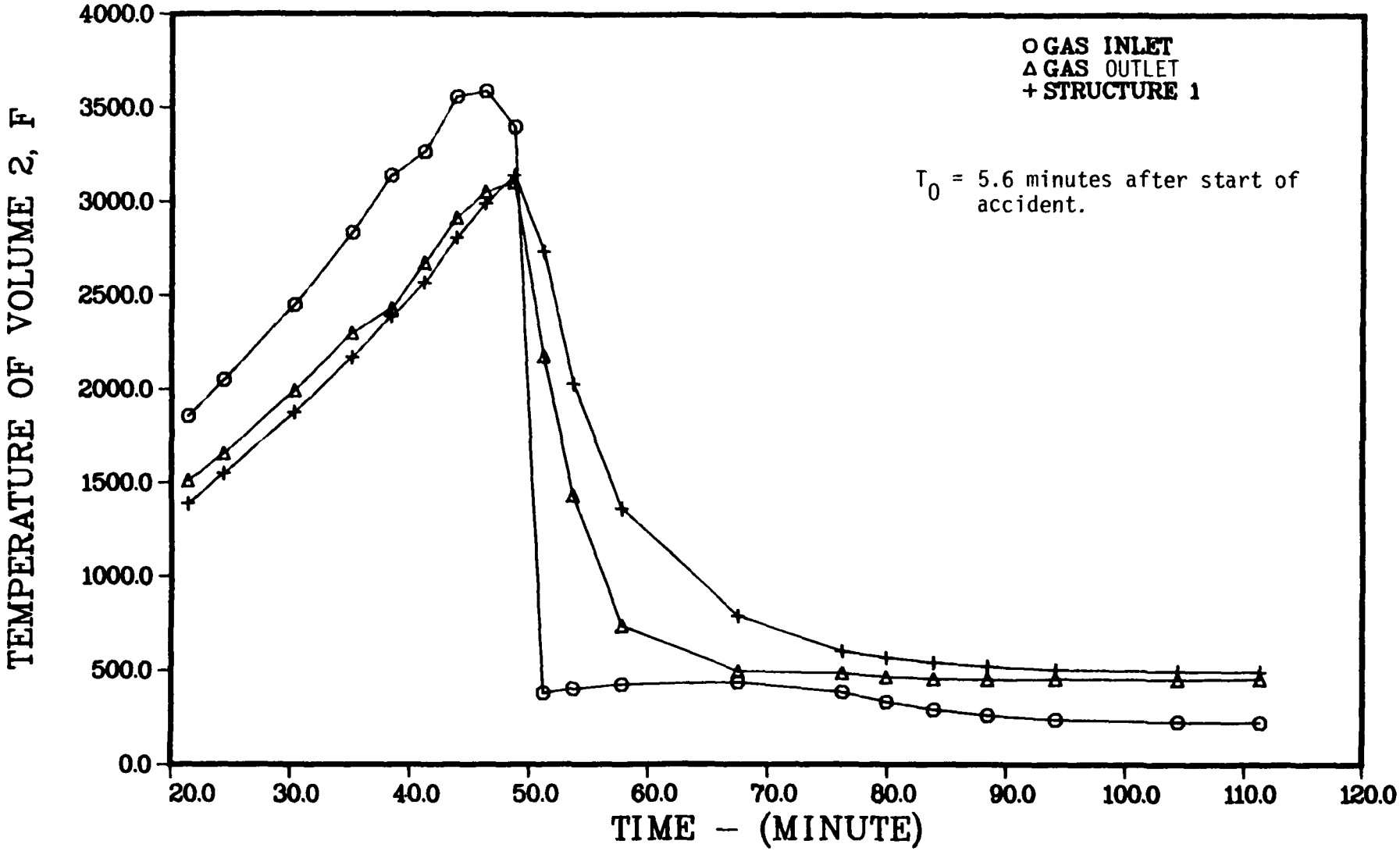

FIGURE 6.19a GAS AND STRUCTURE TEMPERATURES FOR THE TOP GUIDE PLATE IN GRAND GULF - SEQUENCE S2E

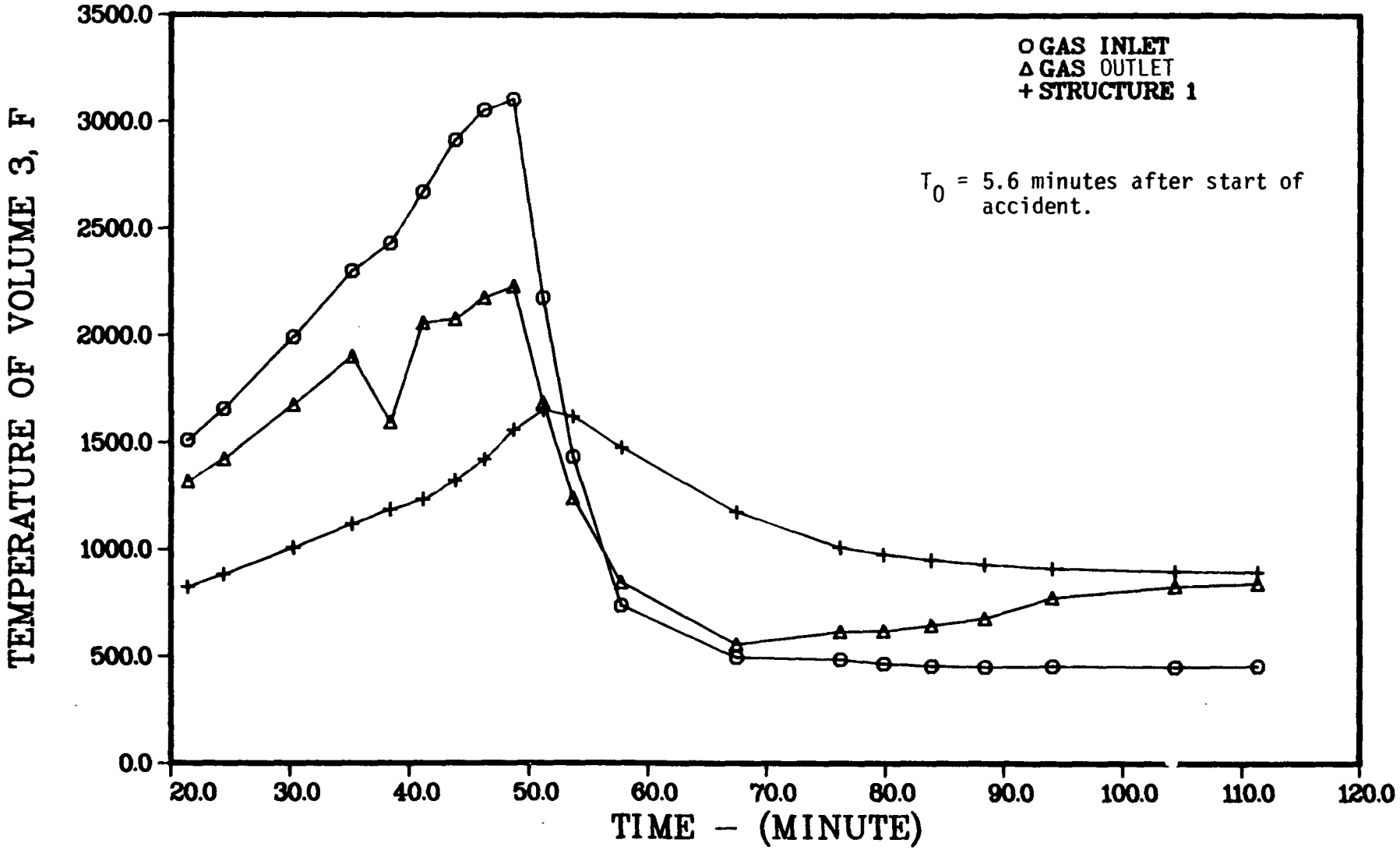

FIGURE 6.19b GAS AND STRUCTURE TEMPERATURES FOR THE SHROUD HEAD IN GRAND GULF - SEQUENCE S2E

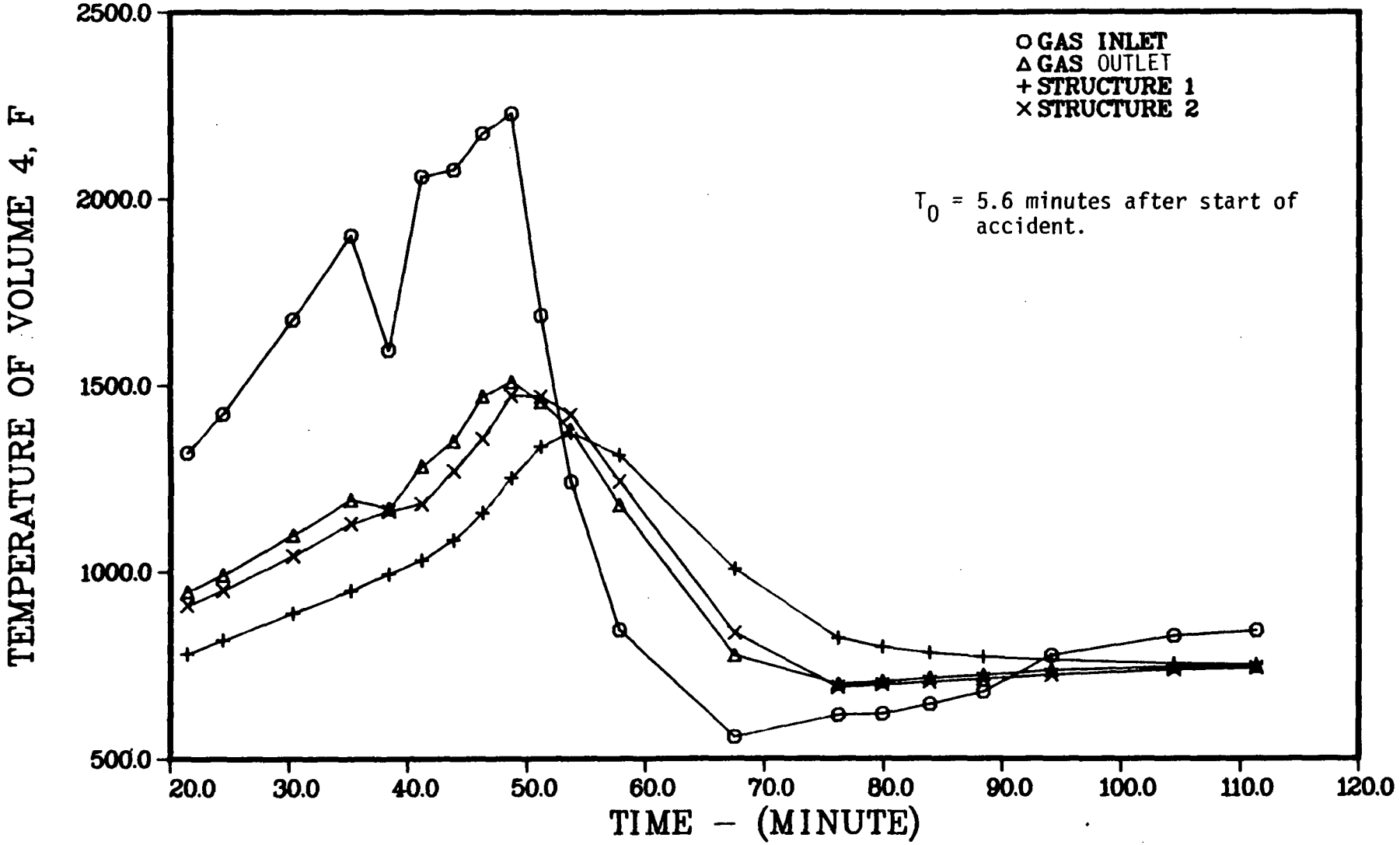

FIGURE 6.19c GAS AND STRUCTURE TEMPERATURES FOR THE STAND PIPES AND STEAM SEPARATORS IN GRAND GULF - SEQUENCE S2E

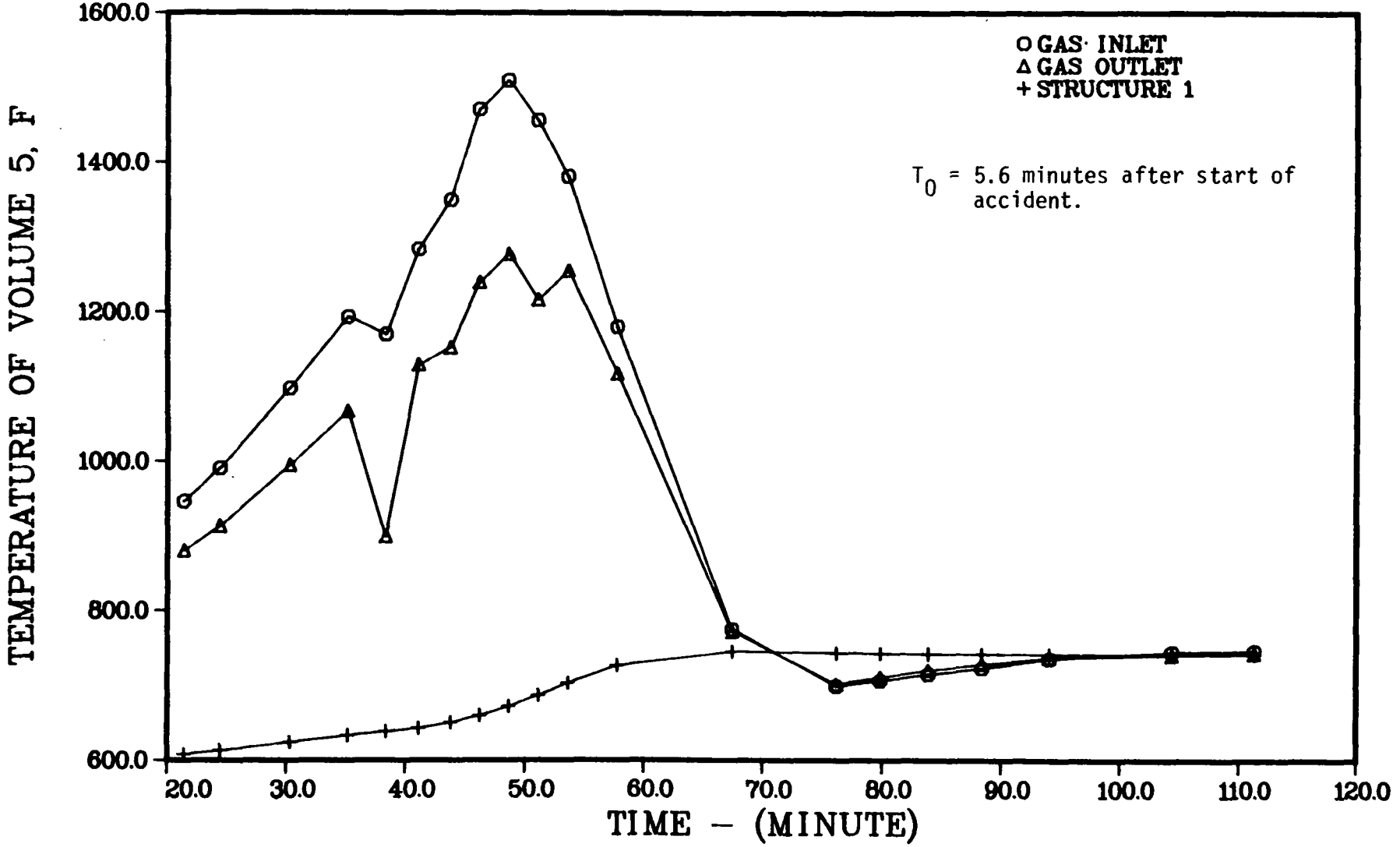

FIGURE 6.19d GAS AND STRUCTURE TEMPERATURES FOR THE LOWER OUTER ANNULUS IN GRAND GULF - SEQUENCE S2E

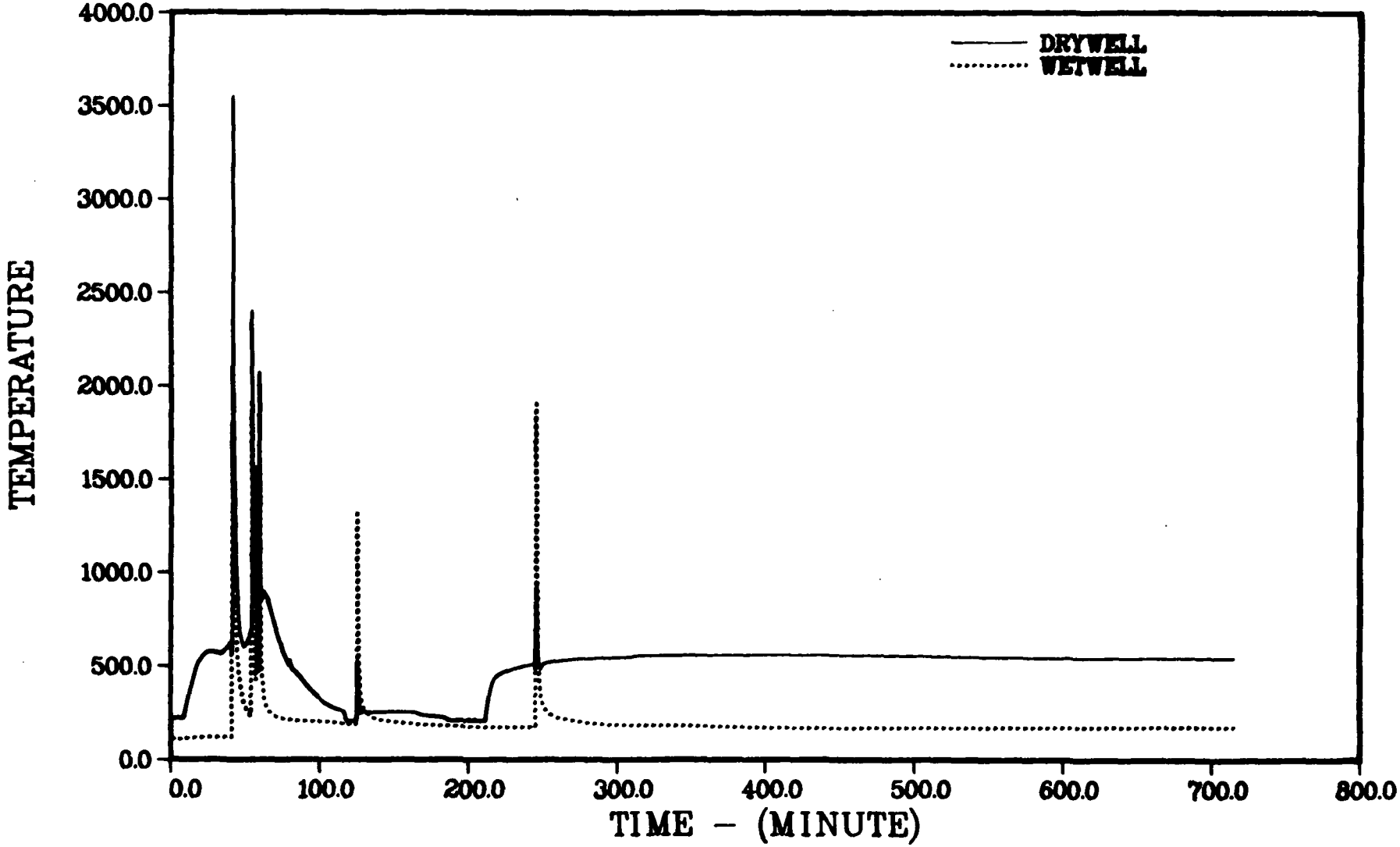

FIGURE 6.20 CONTAINMENT TEMPERATURES WITH NOMINAL POOL BYPASS FOR GRAND GULF - SEQUENCE S2E

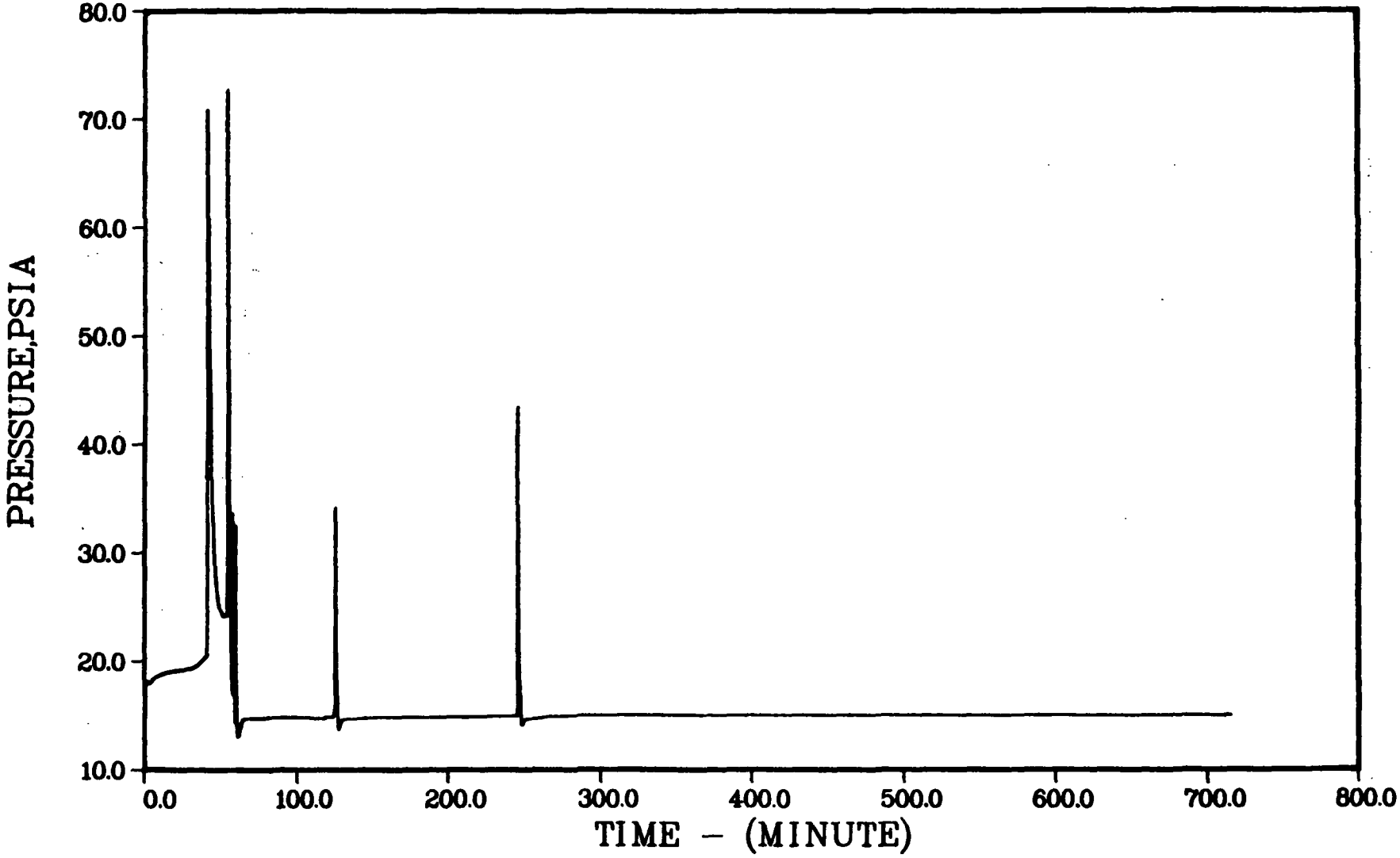

FIGURE 6.21 CONTAINMENT PRESSURE WITH NOMINAL POOL BYPASS FOR GRAND GULF - SEQUENCE S2E

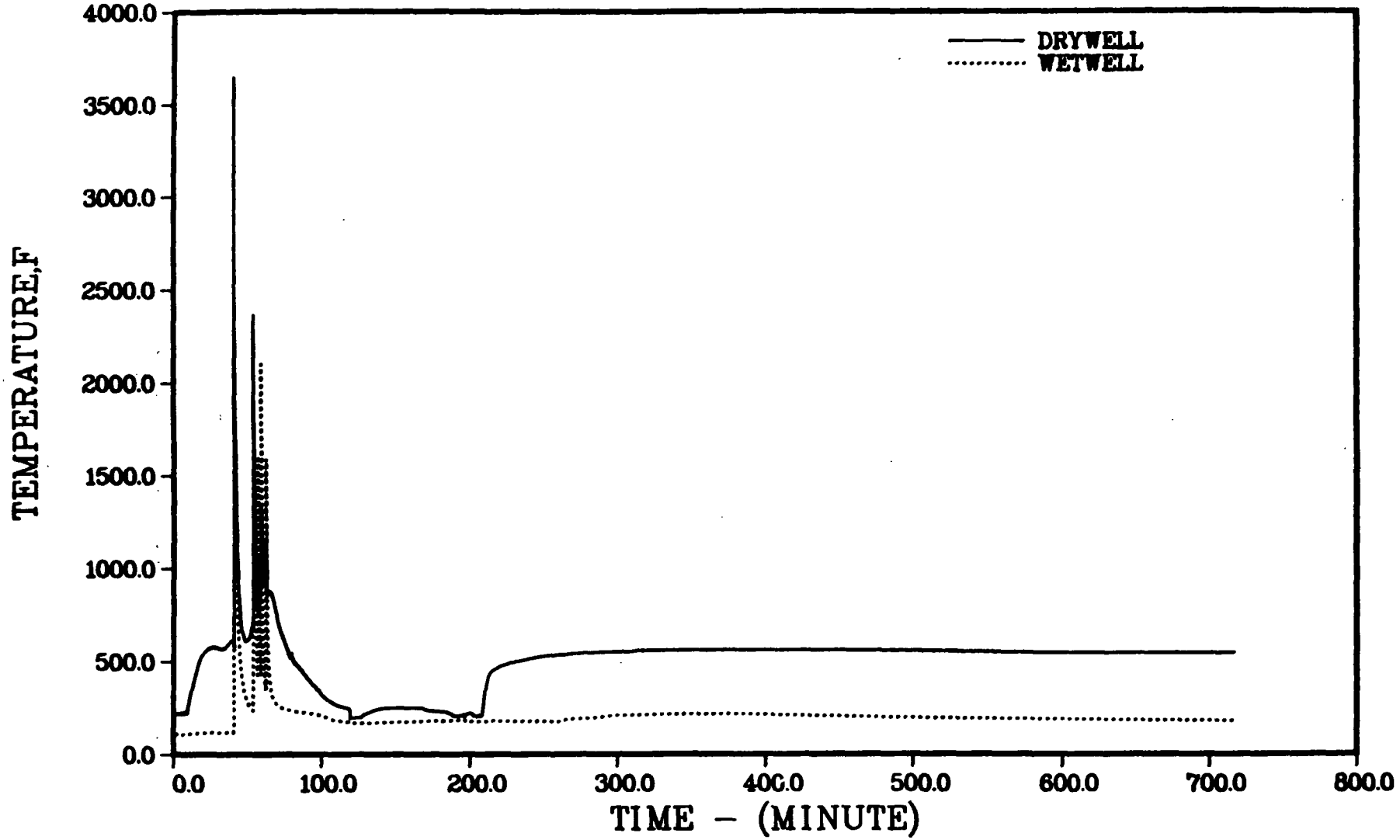

FIGURE 6.22 CONTAINMENT TEMPERATURES WITH LARGE POOL BYPASS FOR GRAND GULF - SEQUENCE S2E

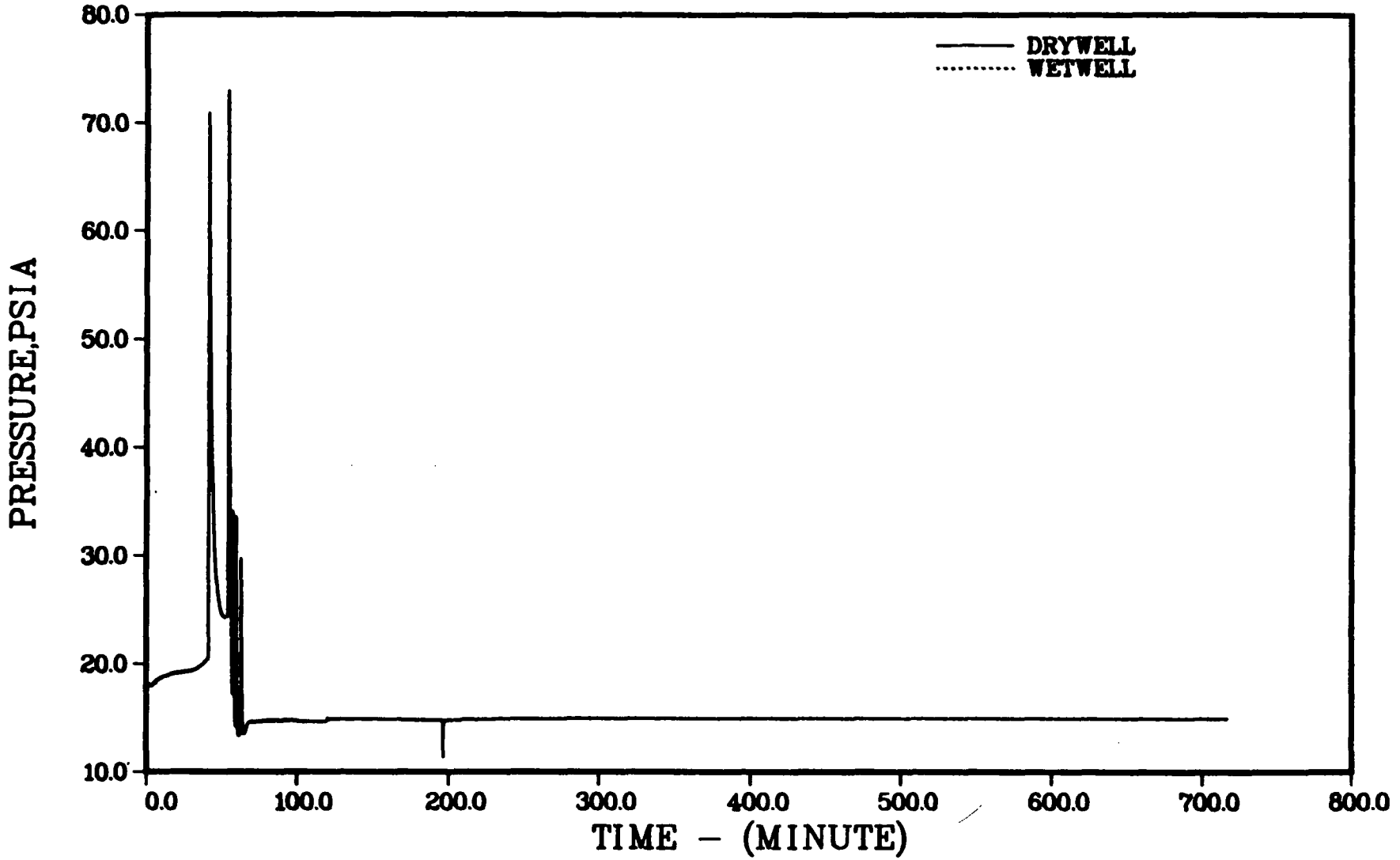

FIGURE 6.23 CONTAINMENT PRESSURE WITH LARGE POOL BYPASS FOR GRAND GULF - SEQUENCE S2E

were predicted to occur during the core slumping process when large amounts of hydrogen are generated and released to the containment. As has been noted previously, the prediction of containment loads due to hydrogen burns can be sensitive to the rate and magnitude of the hydrogen generation and release to the containment, the ignition threshold assumed, containment compartmentalization, etc. In the present analyses, an ignition threshold at 6 volume percent hydrogen was utilized.

The containment leakages and related parameters derived from the MARCH analyses for use in the fission product release and transport analyses are summarized in Table 6.5.

6.2 Radionuclide Sources

6.2.1 Source Within Pressure Vessel

Inventory

The fission product and structural materials inventories used in the analyses in this report are scaled from those used in the Peach Bottom analyses to account for the larger core in the Grand Gulf plant. The inventory for the Peach Bottom plant was based on results of the ORIGEN 2[6.1] code for the Browns Ferry Unit 1 reactor. The computer runs were performed by Oak Ridge National Laboratory in the station blackout study for Browns Ferry Unit 1[6.2]. An actual core loading (Cycle 4) involving seven different types of fuel assemblies are described in Table 6.6. For each type of fuel, two ORIGEN 2 calculations were performed, for the maximum axial power factor and for the minimum axial power factor. The fission product elemental inventories from the high and low power runs were weighted and summed to obtain the inventories for the average power for each type of fuel. Inventories for each fuel type were summed to determine the total core inventory.

The fission product inventories were distributed among nine radial zones according to the power peaking factors supplied by the General Electric Company. The total inventories used in these analyses are presented in Table 6.7.

Release from Fuel

The rates of release from the melting core were computed using the CORSOR code, which utilizes the MARCH predictions of core nodal temperatures as functions of time for each sequence. The MARCH predicted extent of Zr oxidation at each node as a function of time was also used in evaluating the Te release from the melting core. The fractions of inventory released prior to vessel failure are given for each species and sequence in Table 6.8. Release from molten core fragments is calculated up to the time of bottom head failure in these analyses, regardless of whether a given node is predicted to have slumped out of the core geometry. The calculated release rates are not considered by CORSOR to be affected by the location of the node during the progress of the melt, although it is likely that some change in emission rates will accompany the slumping of any portion of the core.

Tables 6.9 through 6.12 present the mass release rates for the species Cs, I, Te, and aerosol particles for the TC, TPI, TQUV, and S_2E sequences in the Grand Gulf plant. The particles are assumed to be composed of the sum of all nonfission product species, along with all fission products, excepting Cs, I, Te, and the noble gases.

The difference between the initial core inventory and the amount released represents the melt composition as it enters the drywell cavity and becomes a source of fission products within the containment.

Regrouping of Released Species

In order to track the Reactor Safety Study groups independently, an additional CORSOR run was performed for the TC sequence which produced release rates for all groups. A description of the makeup and methodology for release of each group follows.

- Group 1 (Xe, Kr) -- Xe and Kr releases were summed and a release rate computed. This group was not previously computed.
- Group 2 (I, Br) -- Br release was not considered due to an absence of data concerning Br release and its small inventory relative to I (1:16).
- Group 3 (Cs, Rb) -- Thermodynamic and physical properties of Rb justify treating it identically

to Cs. As a result, the Rb inventory was lumped into the Cs inventory for treatment by CORSOR. Releases for I and Cs were combined to produce release rates for CsI and CsOH which were the forms assumed to be transporting through the primary system. This assumption is based on the predicted temperatures and gas compositions combined with consideration of the likely chemical thermodynamic equilibrium states.[6.3,6.4]

- Group 4 (Te, Se, Sb) -- Se and Sb were not considered based on their small inventory and lack of data concerning their behavior. Their inclusion in this group would be further complicated by the dependence of Te release on Zircaloy oxidation.

- Group 5 (Ba, Sr) -- Ba and Sr were released separately and their releases summed to form the release rates for this group. Further, their releases were not included in the aerosol materials sum.

- Group 6 (Rh, Pd, Tc, Ru, Mo) -- Rh, Pd, and Tc inventories were added to the Ru inventory for purposes of release. The releases of Ru and Mo were then summed to produce release rates for this group. The aerosol materials sum does not include Mo or Ru releases.

- Group 7 (La, Y, Eu, Nd, Np, Sm, Pm, Pu, Zr, Ce, Nb, Pr) -- All members of Reactor Safety Study Group 7 with the exception of Zr were treated identically for purposes of release, using UO_2 release rate coefficients. Their release and the release of Zr were summed to produce release rates for this group. Table 6.7b lists initial inventories of Group 7 members not included in Table 6.7.

- Aerosol Materials (Fe, UO_2, Zr (cladding)), -- The release rate for this group includes only nonfission products.

Table 6.7c lists initial inventories and final CORSOR releases for the Reactor Safety Study groups and compares the results for the TC sequence with and without the RSS grouping.

It is necessary to select an initial particle size for those materials forming the aerosol species. It has been shown[6.5] that when significant agglomeration occurs, the initial aerosol size has a negligible effect on

subsequent aerosol behavior after agglomeration has proceeded for a very short time. Nevertheless, initial particle sizes were chosen to correspond to the best available information. Numerous reviews of experimental mean aerosol sizes from vaporizing and condensing fuel indicate that the sizes will be from slightly below 0.01 μm to about 0.1 μm with the most likely size being about 0.05 μm.[6.6,6.7] A number median radius of 0.05 μm and a geometric standard deviation of 1.7 were assumed for the primary particles in the current analyses, and a bulk density of 3 g/cc was assumed for the particles.

6.2.2 Sources Within the Containment

Release from the primary circuit is in general directed to the suppression pool for the sequences considered in this report. After passing through the suppression pool, the released source enters the containment. The source originated from the reactor vessel or from core-concrete interactions enters the drywell first, is subsequently passed through the suppression pool, and finally enters the containment. The flow paths among compartments and the timing of events which control the flows were discussed in Chapter 4 and in earlier sections of this chapter.

Release from Core-Concrete Interactions

The VANESA code was used to predict aerosol and gas release rates, particle size distribution, and compositions as a function of time. Composition of the core materials contacting the concrete was determined with the CORSOR code. These represent the materials remaining in the melt at the time of head melt-through. As mentioned before, the rates and compositions given by the VANESA code constitute the source to the drywell after vessel head failure. The total release rates and composition of the release are given in Tables 6.13, 6.14, and 6.15. These rates and compositions define the source to the drywell after vessel head failure.

Source Term for Volatile Iodides

In a previous section it was noted that the thermodynamics of the cesium-iodine-hydrogen-oxygen system indicate that iodine will be present

primarily as a nonvolatile iodide in the primary coolant system. After release from the primary system, a small fraction of the iodine inventory in the containment is believed to be present as volatile iodides.[6.3] The presence of volatile iodide species in containment-type systems has been observed in experiments[6.8] and in the TMI-2 post-accident containment atmosphere.[6.9] At present, the mechanisms responsible for the generation of these volatile iodides are not well understood. Since a theoretical model is not available, an empirical approach has been selected for the formulation of a source term for volatile iodides. This source term consists of two components. One component represents the fraction of the containment iodine inventory which is present as volatile iodides before containment failure. The second component represents a generation rate for volatile iodides after containment failure. The containment inventory of volatile iodides present prior to containment failure was estimated from levels observed in TMI-2[6.9] and from estimates of the probable detection limits in relevant experiments.[6.10] The volatile iodide generation rate was estimated from a conservative evaluation of the measurements of the airborne iodine levels in the TMI-2 containment over the time period from 100-2000 hours after reactor trip. Based on these estimates it has been assumed for this study that 0.05 percent of the containment iodine inventory will be present as volatile iodides prior to containment failure and after containment failure, additional volatile iodides will be generated at a rate of 2×10^{-7} fraction/hour of the containment iodine inventory.

Of this volatile iodine source, it is believed that a fraction of the iodine inventory in a reactor containment will be present as volatile organic iodides (predominantly CH_3I).[6.3] (Other volatile species may also be present.) Therefore, in the analysis of reactor accidents involving a radionuclide release from the reactor system and containment failure, formation in the containment and subsequent release of organic iodides should be considered. Unfortunately, the mechanism responsible for the generation of organic iodides has not yet been elucidated. As a result, it is not yet possible to establish a definitive source of organic iodides. Early estimates of the organic iodine source terms were based on a conservative interpretation of experimental systems studies.[6.8,6.11] Early thermodynamic studies predicted that organic iodides should be present in much smaller concentrations than observed in experiments.[6.12] These calculations predicted that CH_3I would comprise only 10^{-4} percent of the total gaseous iodine inventory modeled.

Experimental data[6.8] and "chemical species specific" measurements of the TMI-2 airborne iodine inventory[6.9] imply that the concentration of organic iodides present in a reactor containment during and following an accident may be higher than the concentrations predicted by thermodynamic calculations for an equilibrium system. Additionally, observations of the airborne iodine behavior at TMI-2[6.9] imply the presence of competing sources and sinks for volatile iodine species. In light of these data, a kinetic description may be required to adequately quantify the time dependence of the organic iodide concentration in reactor containments during and following reactor accidents. Pending results of studies, such as those which are currently under way,[6.4] use of a general source term for volatile iodides rather than separate source terms for CH_3I, I_2, etc., has been assumed as noted above.

References

(6.1) Groff, A. G., "ORIGEN 2 -- A Revised and Updated Version of the Oak Ridge Isotope Generation and Depletion Code", ORNL-5621 (July, 1980).

(6.2) Wichner, R. P., et al, "Station Blackout at Browns Ferry Unit One -- Iodine and Noble Gas Distribution and Release", NUREG/CR-2181 (August, 1982).

(6.3) Technical Base for Estimating Fission Product Behavior During LWR Accidents, NUREG-0772, (June, 1981).

(6.4) Torgerson, D. F., et al., Fission Product Chemistry Under Reactor Accident Conditions, presented at the International Meeting on Thermal Nuclear Reactor Safety, Chicago, Illinois, U.S.A. (September, 1982).

(6.5) Jordan, H., Schumacher, P. M., and Gieseke, J. A., "Comparison of QUICK Predictions with Results of Selected, Recent Aerosol Behavior Experiments", NUREG/CR-2922, BMI-2089 (September, 1982).

(6.6) Gieseke, J. A., et al, "Aerosol Source Term for Fast Reactor Safety Analysis", BMI-X-637 (August 11, 1972).

(6.7) Nuclear Aerosols in Reactor Safety, CSNI/SOAR No. 1 (June, 1979).

(6.8) Postma, A. K. and Zavodoski, R. W., Review of Organic Iodide Formation Under Accident Conditions in Water-Cooled Reactors, WASH-1233 (1972).

(6.9) Pelletier, C. A., et al., Preliminary Radioiodine Source Term and Inventory Assessment for TMI-2, SAI-139-82-12-RV (September, 1982).

(6.10) Lin, C. C., Chemical Effecs of Gamma Radiation on Iodine in Aqueous Solutions, J. Inorg. Nucl. Chem., 42, pp. 1101-1107 (1980).

(6.11) Reactor Safety Study: An Assessment of Accident Risks in U.S. Commercial Nuclear Power Plants, WASH-1400 (1974).

(6.12) Barnes, R. H., Kircher, J. F., and Townley, C. W., Chemical Equilibrium Studies of Organic Iodide Formation Under Nuclear Reactor Accident Conditions, BMI-1816 (1966).

TABLE 6.1 REACTOR CHARACTERISTICS, CONTAINMENT PARAMETERS, AND MARCH OPTIONS FOR THE BWR MARK III CONTAINMENT

Weight Zircaloy in Core:	174,700 lbm (79,242 kg)
Weight Other Metal in Core:	30,450 lbm (13,812 kg)
Weight UO_2 in Core:	366,400 lbm (166,195 kg)
Weight of Grids Included in Debris:	122,900 lbm (55,746 kg)
Weight of Bottom Head:	207,600 lbm (94,165 kg)
Bottom Head Diameter:	21 ft (6.4 m)
Bottom Head Thickness:	0.538 ft (0.164 m)

Containment Parameters

Number of Compartments: 2

Compartment 1: Drywell

Compartment 2: Primary Containment

	Free Volume		Initial Temperature		Initial Pressure	
	ft^3	m^3	°F	°C	psia	MPa
Drywell	270,100	7,649	135	57.2	14.7	0.1
Primary Containment	1.4×10^6	39,650	90	32.2	14.7	0.1

	Thermal Conductivity		Heat Capacity		Density	
Material	Btu/hr ft F	W/cm C	Btu/lb F	J/kg K	lb/ft^3	kg/m^3
Iron	25.	0.4325	0.110	460.5	487	7801.7
Concrete	0.8	0.01384	0.252	1055.1	151	2419.1

	Iron Thickness		Concrete Thickness		Heat Transfer Area	
Slab	ft	cm	ft	m	ft^2	m^2
1. Drywell Floor	--	--	26.	7.92	3,402	316
2. Wetwell Floor	0.08	2.44	16.	4.88	5,900	548
3. Shield Wall	--	--	1.	0.305	9,603	892
4. Pedestal	--	--	3.	0.914	3,158	293

TABLE 6.1 (Continued)

Slab	Iron Thickness ft	Iron Thickness cm	Concrete Thickness ft	Concrete Thickness m	Heat Transfer Area ft^2	Heat Transfer Area m^2
5. Wetwell Wall	0.14	4.27	--	--	80,490	7,478
6. Drywell Wall-Top	--	--	5.	1.524	23,920	2,222
7. Drywell Wall-Bottom	0.08	2.44	5.1	1.554	6,313	586
8. Miscellaneous Concrete	--	--	2.	0.610	16,880	1,568

Steel/Concrete Interface Coefficient: 100 Btu/hr/ft^2/F (0.0568 W/cm^2/C)
Initial Temperature Range of Slabs: 90-135 F (32.2-57.2 C)

Concrete Composition

Weight fraction $CaCO_3$	0.8
Weight fraction $Ca(OH)_2$	0.15
Weight fraction SiO_2	0.01
Weight fraction Al_2O_3	0.01
Weight fraction free H_2O	0.03
Gm rebar per gm concrete	0.135

Engineered Safety Systems

ECC Pump	Rated Flow GPM	Rated Flow ℓ/s	Pressure psia	Pressure MPa
High Head	7120	449.1	2000	13.8
Low Head	7500	473.1	550	3.8
Safety Injection	800	50.5	2000	13.8

Suppression Pool Heat Exchanger

Capacity, Btu/hr	1.847×10^8 (5.412×10^7 W)
Primary flow, lb/min	61,090 (461.8 kg/s)
Secondary flow, lb/min	65,830 (497.7 kg/s)
Primary inlet, F	185 F (85 C)
Secondary inlet, F	90 F (32.2 C)

TABLE 6.1 (Continued)

ECC Storage and Injection Tanks

	CST	
Weight of Water	3. x 10^6 lb	1.36 x 10^6 kg
Initial Pressure	14.7 psia	0.1 MPa
Temperature	100 F	37.8 C

Fractional Value of RWST to Start ECC Recirculation: 0.43

Calculated Model Input

Core Heatup Section

Number of radial zones: 9

Number of axial zones: 24

Meltdown model: BOIL Model A

Core slumping starts when lowest node in region is molten.

Core collapse occurs when 75% of core has melted, or core support reaches melting temperature.

Zircaloy-water reaction: Urbanic-Heidrick reaction rate data, steam limited, continues for melted nodes, convective heat transfer in molten regions, reaction of Zircaloy with water in bottom head calculated.

TABLE 6.2 ACCIDENT EVENT TIMES

Event	Time, minutes
Grand Gulf TPIY	
ECC Recirculation On	1278.8
Containment Fail	1331.8
ECC Off	1332.9
Core Uncover	1535.7
Start Melt	1645.7
Core Slump	1729.5
Core Collapse	1765.2
Bottom Head Dry	1801.0
Bottom Head Fail	1978.0
Reactor Cavity Dry	1978.0
Start Concrete Attack	1978.0
End Calculation	2579.0
Grand Gulf TQUVY	
Containment Heat Removal On	11.0
Core Uncover	47.0
Activate ADS	79.0
Start Melt	103.0
Hydrogen Burn	115.5
Hydrogen Burn	136.4
Core Slump	142.0
Hydrogen Burn	149.3
Hydrogen Burn	154.2
Core Collapse	155.0
Bottom Head Dry	170.6
Bottom Head Fail	216.6
Reactor Cavity Dry	216.6
Start Concrete Attack	216.6
Containment Fail	834.3
End Calculation	1416.7

TABLE 6.2 (Continued)

Event	Time, minutes
	Grand Gulf TCγ
Containment Heat Removal On	10.0
ECC Recirculation On	76.9
Containment Fail	80.6
ECC Off	80.8
Core Uncover	88.2
Start Melt	117.5
Core Slump	168.1
Core Collapse	175.1
Bottom Head Dry	195.3
Bottom Head Fail	197.6
Reactor Cavity Dry	197.6
Start Concrete Attack	197.6
End Calculation	798.8

TABLE 6.2 (Continued)

Event	Time, minutes
	Grand Gulf S2E
Core Uncover	5.6
Start Melt	27.8
Hydrogen Burn	41.4
Start Slump	45.6
Hydrogen Burn	54.4
Containment Fail	54.4
Core Collapse	57.6
Hydrogen Burn	57.6
Hydrogen Burn	59.6
Vessel Head Dry	80.7
Head Fail	119.2
Concrete Attack	119.2
Hydrogen Burn	125.6
Cavity Dry	213.7
Hydrogen Burn	245.5
End Calculation	720.3

TABLE 6.3 CORE AND PRIMARY SYSTEM RESPONSE

Accident Event	Time, minutes	Primary System Pressure, psia	Primary System Water Inventory, lbm	Average Core Temperature, F	Peak Core Temperature, F	Fraction Core Melted	Fraction Zircaloy Reacted *
			Grand Gulf TPIY				
Containment Fail	1331.8	136	6.78×10^5	355	359	0.	0.
Core Uncover	1535.7	85	3.36×10^5	322	326	0.	0.
Start Melt	1645.7	20	2.67×10^5	2128	4130	0.	0.038
Start Slump	1729.5	17	2.62×10^5	3389	4130	0.310	0.090
Core Collapse	1765.2	295	2.19×10^5	3314	4130	0.791	0.423
Bottom Head Dry	1801.0	281	0.	2044	---	---	0.423
Bottom Head Fail	1978.0	15	0.	3779	---	---	0.423
			Grand Gulf TQUVY				
Core Uncover	47.0	1201	2.80×10^5	579	593	0.	0.
Actuate ADS	79.0	1202	2.25×10^5	1401	2697	0.	0.006
Start Melt	103.0	101	1.53×10^5	1688	4130	0.001	0.028
Start Slump	142.0	30	1.37×10^5	3332	4130	0.450	0.184
Core Collapse	155.0	250	1.14×10^5	3873	4130	0.766	0.381
Bottom Head Dry	170.6	307	0.	3478	---	---	0.403
Bottom Head Fail	216.6	25	0.	3786	---	---	0.403

TABLE 6.3 (Continued)

Accident Event	Time, minutes	Primary System Pressure, psia	Primary System Water Inventory, lbm	Average Core Temperature, F	Peak Core Temperature, F	Fraction Core Melted	Fraction Zircaloy Reacted *
			Grand Gulf TCY				
Containment Fail	80.6	1257	6.77×10^5	683	790	0.	0.
Core Uncover	88.2	1255	3.08×10^5	684	791	0.	0.
Start Melt	117.5	1215	2.19×10^5	1712	4130	0.	0.016
Start Slump	168.1	1200	2.12×10^5	3509	4130	0.408	0.110
Core Collapse	175.1	1202	1.77×10^5	4130	4130	0.894	0.418
Bottom Head Dry	195.3	1200	0.	3748	---	---	0.418
Bottom Head Fail	197.6	1203	0.	3779	---	---	0.418

TABLE 6.3 (Continued)

Accident Event	Time, minutes	Primary System Pressure, psia	Primary System Water Inventory, lbm	Average Core Temperature, F	Peak Core Temperature, F	Fraction Core Melted	Fraction Clad Reacted*
			Grand Gulf S_2E				
Core Uncover	5.6	1166	2.71E5	594	670	0.	0.
Start Melt	27.8	162	1.78E5	1743	4130	0.00	0.02
Start Slump	45.6	56	1.60E5	3151	4139	0.44	0.17
Core Collapse	57.6	265	1.42E5	4130	---	0.77	0.38
Vessel Head Dry	80.7	357	0.	3508	---	---	0.38
Head Fail	119.2	18	0.	3785	---	---	0.38

*Based on the total Zircaloy in the core, including channel boxes as well as the cladding.

TABLE 6.4 CONTAINMENT RESPONSE

Accident Event	Time, minutes	Compartment Pressure, psia		Compartment Temperature, F		RWST or CST Water Mass, lbm	Suppression Pool Water		Reactor Cavity Water Mass, lbm	Reactor Cavity Water Temp., F	Steam Cond. on Walls lbm/min
		1	2	1	2		Mass, lbm	Temp., F			
Grand Gulf TPIY											
ECC Recirc. On	1278.8	68.6	68.6	204	291	8.13×10^4	1.08×10^7	291	4.94×10^4	176	84/297*
Containment Fail	1331.8	72.0	72.0	210	295	8.13×10^4	1.07×10^7	295	5.48×10^4	179	89/256
ECC Off	1332.9	72.4	72.4	227	295	8.13×10^4	1.07×10^7	292	5.48×10^4	179	346/208
Core Uncover	1535.7	15.2	15.2	183	256	8.13×10^4	9.83×10^6	212	5.70×10^4	162	0/0
Start Melt	1645.7	14.9	14.9	179	257	8.13×10^4	9.78×10^6	209	6.00×10^4	163	18/0
Start Slump	1729.5	14.9	14.9	179	761	8.13×10^4	9.76×10^6	206	6.16×10^4	163	22/0
Core Collapse	1765.3	15.4	15.4	189	242	8.13×10^4	9.70×10^6	202			0/0
Bottom Head Dry	1801.0	16.1	16.1	189	246	8.13×10^4	9.73×10^6	214	6.34×10^4	164	52/0
Bottom Head Fail	1978.0	14.9	14.9	189	247	8.13×10^4	9.71×10^6	211	6.84×10^4	165	194/0
Cavity Dryout	1978.0	19.8	19.8	384	294	8.13×10^4	9.75×10^6	216	0.	---	0/0
Start Concrete Attack	1978.0	20.3	20.3	365	298	8.13×10^4	9.75×10^6	217	348.	229	0/0
End Calculation	2579.0	15.3	15.3	474	225	8.13×10^4	9.40×10^6	214	0.	---	0/0
Grand Gulf TQUVY											
Containment Heat Removal On	11.0	15.3	15.3	139	101	2.49×10^6	1.10×10^7	105	0.	---	0/167*
Core Uncover	47.0	16.4	16.4	139	121	2.49×10^6	1.12×10^7	124	0.	---	0/352
Start Melt	103.0	17.9	17.9	140	136	2.49×10^6	1.14×10^7	137	0.	---	0/271

* Volume 1/Volume 2

TABLE 6.4 (Continued)

Accident Event	Time, minutes	Compartment Pressure, psia		Compartment Temperature, F		RWST or CST Water Mass, lbm	Suppression Pool Water		Reactor Cavity Water Mass, lbm	Reactor Cavity Water Temp., F	Steam Cond. on Walls lbm/min
		1	2	1	2		Mass, lbm	Temp., F			
						Grand Gulf TQUVY (Continued)					
Hydrogen Burn	115.4	56.3	56.3	603	1749	2.49×10^6	1.14×10^7	135	0.	---	0/0*
Hydrogen Burn	136.4	58.2	58.2	611	1791	2.49×10^6	1.14×10^7	135	0.	---	0/0
Core Slump	142.0	25.4	25.4	233	404	2.49×10^6	1.14×10^7	135	0.	---	0/0
Hydrogen Burn	149.3	61.2	61.2	633	1894	2.49×10^6	1.14×10^7	135	0.	---	0/0
Hydrogen Burn	154.2	67.7	67.7	716	2132	2.49×10^6	1.14×10^7	136	0.	---	0/0
Core Collapse	155.0	54.2	54.2	588	1509	2.49×10^6	1.14×10^7	136	0.	---	0/0
Bottom Head Dry	170.6	24.0	24.0	166	296	2.49×10^6	1.14×10^7	143	453.	166	59/0
Bottom Head Fail	216.6	23.0	23.0	180	242	2.49×10^6	1.15×10^7	140	1018.	157	494/0
Start Debris/ Water Interaction	216.6	23.2	23.2	183	242	2.49×10^6	1.15×10^7	140	1018.	157	486/0
Cavity Dryout	216.6	23.6	23.6	186	245	2.49×10^6	1.15×10^7	140	0.	---	720/0
Start Concrete Attack	216.6	25.3	25.3	763	254	2.49×10^6	1.15×10^7	141	83.9	236	0/0
Containment Fail	834.3	72.0	72.0	639	254	2.49×10^6	1.16×10^7	114	0.	---	0/0
End Calculation	1417.0	14.9	14.9	466	196	2.49×10^6	1.16×10^7	134	0.	---	0/0

* Volume 1/Volume 2

TABLE 6.4 (Continued)

Accident Event	Time, minutes	Compartment Pressure, psia		Compartment Temperature, F		RWST or CST Water Mass, lbm	Suppression Pool Water		Reactor Cavity Water Mass, lbm	Reactor Cavity Water Temp., F	Steam Cond. on Walls lbm/min
		1	2	1	2		Mass, lbm	Temp., F			
						Grand Gulf TCY					
Containment Heat Removal On	10.0	17.0	17.0	150	130	2.01×10^6	8.85×10^6	132	0.	---	0/1137*
ECC Recirc. On	76.9	66.0	66.0	237	284	1.37×10^5	1.08×10^7	284	8.14×10^3	189	0/2210
Containment Fail	80.6	72.0	72.1	248	291	---	1.07×10^7	291	---	---	633/2155
ECC Off	80.8	71.5	71.5	246	291	8.04×10^4	1.07×10^7	291	---	---	524/1738
Core Uncover	88.2	69.6	69.6	242	299	8.04×10^4	1.08×10^7	297	1.46×10^4	212	419/1894
Start Melt	117.6	29.6	29.6	196	248	8.04×10^4	1.02×10^7	249	1.81×10^4	192	56/50
Start Slump	168.1	15.2	15.2	193	243	8.04×10^4	9.89×10^6	213	2.25×10^4	188	111/0
Core Collapse	175.1	16.9	16.9	199	249	8.04×10^4	---	214	---	---	193/0
Bottom Head Dry	195.3	15.1	15.1	198	209	8.04×10^4	9.87×10^6	214	2.95×10^4	191	119/9
Bottom Head Fail	197.6	17.6	17.6	220	234	8.04×10^4	9.96×10^6	220	2.95×10^4	191	1913/0
Start Debris/ Water Interaction	197.6	20.2	20.2	226	251	8.04×10^4	9.96×10^6	220	2.95×10^4	191	2605/0
Cavity Dryout	197.6	21.9	21.9	344	274	8.04×10^4	---	222	0.	---	0/0
Start Concrete Attack	197.6	21.9	21.9	343	273	8.04×10^4	9.99×10^6	222	0.	---	0/0
End Calculation	798.8	15.2	15.2	539	198	8.04×10^4	9.50×10^6	199	0.	---	0/43

* Volume 1/Volume 2

TABLE 6.4 CONTAINMENT RESPONSE

Accident Event	Time, minutes	Compartment Pressure, psia		Compartment Temperature, F		RWST or CST Water Mass, lbm	Suppression Pool Water		Reactor Cavity Water Mass, lbm	Reactor Cavity Water Temp., F	Steam Cond. on Walls lbm/min
		1	2	1	2		Mass, lbm	Temp., F			
						Grand Gulf S_2E					
Core Uncover	5.6	18.2	18.2	223	106	2.49×10^6	1.09×10^7	101	---	---	933/292*
Spray Recir. On	10.1	18.7	18.7	256	113	2.49×10^6	1.11×10^7	119	1.30×10^5	213	0/449
Start Melt	27.8	19.3	19.3	580	120	2.49×10^6	1.12×10^7	122	1.29×10^5	203	0/372
Start Slump	45.6	30.5	30.5	751	513	2.49×10^6	1.12×10^7	123	1.24×10^5	168	0/0
Containment Fail	54.4	72.8	72.8	2272	1925	2.49×10^6	1.12×10^7	124	1.23×10^5	153	0/0
Core Collapse	57.6	17.1	17.1	792	425	2.49×10^6	1.12×10^7	125	1.22×10^5	147	0/0
Vessel Head Dry	80.7	14.8	14.8	524	213	2.49×10^6	1.13×10^7	133	1.21×10^5	143	0/0
Head Fail	119.2	14.7	14.7	210	191	2.49×10^6	---	---	1.21×10^5	143	0/0
Start Concrete Attack	119.2	14.8	14.8	208	192	2.49×10^6	1.13×10^7	139	1.20×10^5	213	0/0
Cavity Dry	213.7	14.8	14.8	315	174	2.49×10^6	1.14×10^7	155	0.	---	0/0
End Calculation	720.3	15.0	15.0	546	179	2.49×10^6	1.14×10^7	173	0.	---	0/0

*Volume 1/Volume 2.

TABLE 6.5 CONTAINMENT LEAKAGE

Subsequence	Time, min	Leak Rate[a] v/min	Drywell Pressure MPa	Drywell Pressure psia	Drywell Temp. °F	Drywell Temp. °C	Wetwell Pressure MPa	Wetwell Pressure psia	Wetwell Temp. °F	Wetwell Temp. °C	Remarks
TPIY	1332	6.9×10^{-6}	0.50	72.0	210	99	0.50	72.0	295	146	Containment fails
	1332-1535.7	0.13	0.18	26.5	178	81	0.18	26.5	253	123	Core heats
	1535.7-1765.2	0.03	0.10	15.1	180	82	0.10	15.1	257	125	Core heats and melts
	1765.2-1977+	0.02	0.10	15.0	186	86	0.10	15.0	247	119	Vessel heats and dries out
	1977+	0.02	0.10	15.0	189	87	0.10	15.0	247	119	Bottom head fails
	1977+-1998	0.07	0.13	18.5	324	162	0.13	18.5	282	139	Initial concrete attack
	1998-2008	0.03	0.11	16.0	214	101	0.11	16.0	238	114	Concrete decomposition
	2008-2579	0.015	0.10	15.2	398	203	0.10	15.2	238	114	Concrete decomposition
TQUVY	0-103	6.9×10^{-6}	0.11	16.7	139	60	0.11	16.7	121	50	Core heats
	103-115.5	6.9×10^{-6}	0.12	18.3	141	61	0.12	18.3	137	58	Core melts and slumps
	115.5-115.6	6.9×10^{-6}	0.37	54.8	597	314	0.37	54.8	1668	909	Hydrogen burns
	115.6-136.4	6.9×10^{-6}	0.17	24.4	223	106	0.17	24.4	360	182	Core melts and slumps
	136.4-136.5	6.9×10^{-6}	0.39	57.7	611	322	0.39	57.7	1764	962	Hydrogen burn
	136.5-149.3	6.9×10^{-6}	0.19	28.1	262	128	0.19	28.1	504	262	Core melts and slumps
	149.3	6.9×10^{-6}	0.41	61.0	634	334	0.41	61.0	1881	1027	Hydrogen burns
	149.3-154.2	6.9×10^{-6}	0.27	39.2	389	198	0.27	39.2	899	481	Core melts and slumps
	154.2	6.9×10^{-6}	0.46	67.6	714	379	0.46	67.6	2130	1165	Hydrogen burns
	154.2-170.5	6.9×10^{-6}	0.21	30.9	276	135	0.21	30.9	560	293	Vessel dries out
	170.5-216.6	6.9×10^{-6}	0.16	22.9	162	72	0.16	22.9	261	127	Vessel melts
	216.6	6.9×10^{-6}	0.16	23.0	179	82	0.16	23.0	242	117	Bottom head fails
	216.6-217.0	6.9×10^{-6}	0.16	24.2	369	187	0.16	24.2	264	129	Initial concrete attack

(a) Normalized to a wetwell free volume of 1.4×10^6 ft^3. Units are volume fraction/minute.

TABLE 6.5 (Continued)

Subsequence	Time, min	Leak Rate[a] v/min	Drywell Pressure MPa	Drywell Pressure psia	Drywell Temp. °F	Drywell Temp. °C	Wetwell Pressure MPa	Wetwell Pressure psia	Wetwell Temp. °F	Wetwell Temp. °C	Remarks
TQUVY	217.0-277.1	6.9×10^{-6}	0.17	25.6	277	136	0.17	25.6	238	115	Concrete decomposition
(Continued)	277.1-637.8	6.9×10^{-6}	0.27	39.2	580	304	0.27	39.2	246	119	Concrete decomposition
	637.8-834.3	6.9×10^{-6}	0.43	62.5	620	327	0.43	62.5	252	122	Concrete decomposition
	834.3	6.9×10^{-6}	0.49	72.0	638	337	0.49	72.0	253	123	Containment fails
	834.3-844.4	0.13	0.24	35.6	498	259	0.24	35.6	154	68	Concrete decomposition
	844.4-1417	0.005	0.10	15.0	521	272	0.10	15.0	203	95	Concrete decomposition
TCY	80.6	6.9×10^{-6}	0.50	72.0	248	120	0.50	72.0	291	144	Containment fails
	80.6-117.5	0.20	0.34	50.2	218	104	0.34	50.2	277	136	Core heats
	117.5-175.1	0.10	0.13	19.2	194	90	0.13	19.2	235	113	Core melts and slumps
	175.1-195.3	0.10	0.11	16.3	196	92	0.11	16.3	223	106	Vessel dries out
	195.3-197.6	0.11	0.11	16.6	200	94	0.11	16.6	229	109	Vessel melts
	197.6	0.13	0.13	18.9	223	106	0.13	18.9	233	112	Bottom head fails
	197.6-207.0	0.14	0.12	17.9	219	104	0.12	17.9	219	104	Initial concrete attack
	207.0-227.9	0.04	0.10	15.3	272	133	0.10	15.3	212	100	Concrete decomposition
	227.9-798.8	0.02	0.10	15.3	542	283	0.10	15.3	202	95	Concrete decomposition

(a) Normalized to a wetwell free volume of 1.4×10^6 ft^3. Units are volume fraction/minute.

TABLE 6.5 (Continued)

Subsequence	Time, min	Leak Rate[a] v/min	Drywell Pressure MPa	Drywell Pressure psia	Drywell Temp. °F	Drywell Temp. °C	Wetwell Pressure MPa	Wetwell Pressure psia	Wetwell Temp. °F	Wetwell Temp. °C	Remarks
S2E (Nominal Pool Bypass)	5.6	6.9×10^{-6}	0.12	18	223	106	0.12	18	106	41	Core uncovers
	5.6-27.8	6.9×10^{-6}	0.13	19	432	222	0.13	19	117	47	Core heats
	27.8-41.4	6.9×10^{-6}	0.14	20	592	311	0.14	20	124	51	Core melts
	41.4	6.9×10^{-6}	0.49	71	3231	1777	0.49	71	1819	993	Hydrogen burns
	41.4-45.6	6.9×10^{-6}	0.30	43	1335	724	0.30	43	939	504	Core melts
	45.6-54.4	6.9×10^{-6}	0.18	26	644	340	0.18	26	316	158	Core slumps
	54.4	6.9×10^{-6}	0.50	73	2272	1244	0.50	73	1925	1052	Containment fails/H burns
	54.4-57.6	0.20	0.24	35	1211	655	0.24	35	946	508	Core melts
	57.6	0.13	0.12	17	792	422	0.12	17	425	218	Core collapses
	57.6	0.24	0.23	34	1060	571	0.23	34	1571	855	Hydrogen burns
	57.6-59.6	0.14	0.14	20	898	481	0.14	20	831	444	Reactor vessel heating
	59.6	0.26	0.23	33	1225	663	0.23	33	2076	1136	Hydrogen burn
	59.6-80.7	0.01	0.10	15	720	382	0.10	15	313	156	Reactor vessel heating
	80.7-119.2	2.2×10^{-3}	0.10	15	347	175	0.10	15	203	95	Reactor vessel dry
	119.2	6.9×10^{-6}	0.10	15	210	99	0.10	15	191	88	Reactor vessel fails
	119.2-125.6	2.5×10^{-3}	0.10	15	208	98	0.10	15	192	89	Concrete decomposition
	125.6	0.21	0.10	15	522	272	0.10	15	1333	723	Hydrogen burns
	125.6-213.7	6.2×10^{-3}	0.10	15	241	116	0.10	15	210	99	Concrete decomposition
	213.7-245.5	3.4×10^{-3}	0.10	15	477	247	0.10	15	176	80	Concrete decomposition
	245.5	0.23	0.30	43	910	488	0.30	43	1904	1040	Hydrogen burns
	245.5-720.3	6.8×10^{-3}	0.10	15	550	288	0.10	15	185	85	Concrete decomposition

(a) Normalized to a wetwell free volume of 1.4×10^{6} ft^3. Units are volume fraction/minute.

TABLE 6.5 (Continued)

Subsequence	Time, min	Leak Rate[a] v/min	Drywell Pressure MPa	Drywell Pressure psia	Drywell Temp. °F	Drywell Temp. °C	Wetwell Pressure MPa	Wetwell Pressure psia	Wetwell Temp. °F	Wetwell Temp. °C	Remarks
S2E	5.6	6.9×10^{-6}	0.13	18.3	223	106	0.13	18.3	107	42	Core uncovers
(Stuck Open Vacuum Breaker)	5.6-10.0	6.9×10^{-6}	0.13	18.6	226	108	0.13	18.6	111	44	Core heats
	10.0-27.8	6.9×10^{-6}	0.13	19.1	484	251	0.13	19.1	119	48	Core heats
	27.8-41.31	6.9×10^{-6}	0.13	19.8	586	308	0.13	19.8	122	50	Core melts
	41.31-41.34	6.9×10^{-6}	0.33	47.2	2404	1318	0.33	47.2	983	528	Hydrogen burns
	41.34-45.7	6.9×10^{-6}	0.30	43.0	1316	713	0.30	43.0	925	496	Core melts
	45.7-54.28	6.9×10^{-6}	0.18	25.5	646	341	0.18	25.5	314	156	Core slumps
	54.28-54.32	6.9×10^{-6}	0.36	52.3	1751	955	0.36	52.3	1181	638	Hydrogen burns
	54.32	6.9×10^{-6}	0.51	73.4	4105	2263	0.51	73.4	3544	1951	Containment fails
	54.32-57.48	0.20	0.24	34.7	1205	652	0.24	34.7	957	514	Core melts
	57.48-57.5	0.20	0.19	28.1	908	486	0.19	28.1	1176	635	Hydrogen burns
	57.5-58.7	0.21	0.16	23.6	919	493	0.16	23.6	1049	565	Core melts
	58.7-58.8	0.18	0.11	16.1	835	446	0.11	16.1	631	333	Core collapses
	58.8-59.75	0.02	0.10	14.6	894	479	0.10	14.6	492	256	Reactor vessel heats
	59.75-59.77	0.19	0.17	25.1	1078	581	0.17	25.1	1340	727	Hydrogen burns
	59.77-63.04	0.07	0.11	16.3	993	534	0.11	16.3	742	394	Vessel heats
	63.04-63.07	0.17	0.16	23.3	1021	550	0.16	23.3	1077	581	Hydrogen burns
	63.07-120.2	4.6×10^{-3}	0.10	14.8	458	237	0.10	14.8	244	118	Vessel heats
	120.2	0.02	0.10	14.8	197	92	0.10	14.8	169	76	Reactor vessel fails
	120.2-120.22	0.03	0.10	15.0	198	92	0.10	15.0	170	76.5	Boiloff of water
	120.22-121.8	0.02	0.10	14.9	200	94	0.10	14.9	169	76	Initial concrete attack
	121.8-215.0	4.2×10^{-3}	0.10	14.9	244	118	0.10	14.9	179	82	Concrete decomposition
	215.0-720.9	0.02	0.10	15.0	551	288	0.10	15.0	198	92	Concrete decomposition

(a) Normalized to a wetwell free volume of 1.4×10^6 ft^3. Units are volume fraction/minute.

TABLE 6.6 FUEL CHARACTERISTICS IN CYCLE 4 AT BROWNS FERRY UNIT 1[6.2]

Fuel Type	Number of Assemblies	Cycle Inserted	Array Size	Initial U Loading (kg)	Enrichment (%)	Initial Gd Loading (g)	Approximate Burnup[a] (MWd/MT)
2	87	1	7 x 7	187.06	2.50	441	30,400
3	127	1	7 x 7	186.93	2.50	547	23,800
4	140	2	8 x 8	183.361	2.74	292	22,900
5	23	2	8 x 8	183.361	2.74	442	24,000
6	87	3	8 x 8	182.52	2.65	355	16,600
7	68	3	8 x 8	182.32	2.65	537	16,900
8	232	4	8 x 8	182.185	2.84	330	8,900

(a) Burnup calculated through 11 months of Cycle 4 operation.

TABLE 6.7a. INVENTORIES OF RADIONUCLIDES AND STRUCTURAL MATERIALS FOR GRAND GULF DURING IN-VESSEL PERIOD OF MELTING

Fission Products		Actinides/Structural	
Element	Mass (kg)	Element	Mass (kg)
Kr	27.3	U	147,000
Rb	24.8	Pu	790
Sr	66.7	Cr	2,570
Y	38.5	Mn	268
Zr	284	Fe	9,410
Mo	252	Ni	1,590
Tc	62.6	Zr	78,200
Ru	183	Sn	1,190
Rh	35.3		
Pd	88.5		
Te	37.1		
I	17.7		
Xe	412		
Cs	220		
Ba	112		
La	105		
Ce	221		
Pr	85.5		
Nd	288		
Sm	57.2		

TABLE 6.7b. INITIAL INVENTORIES OF ADDITIONAL SPECIES INCLUDED IN GROUPED RELEASE CALCULATIONS

Element	Mass (kg)
Eu	15.0
Nb	4.6
Np	43.8
Pm	12.2

TABLE 6.7c. CORSOR RESULTS WITH AND WITHOUT RSS GROUPING FOR THE TC SEQUENCE

	Without RSS Grouping		With RSS Grouping	
Group	Initial Inventory (kg)	Final CORSOR Releases (kg)	Initial Inventory (kg)	Final CORSOR Releases (kg)
Xe	439	439	439	439
I	17.7	17.7*	17.7	17.7*
Cs	220	220*	245	245*
Te	37.0	12.6	37.0	9.3
Sr	NA	NA	179	40.5
Ru	NA	NA	621	45.0
La	NA	NA	1945	1.02
Aerosol	236698	1263	235800	1095
	Not Grouped		Grouped	
CsI	13.1		13.1	
CsOH	227		255	

*CORSOR releases these species in the form of CsI and CsOH.

TABLE 6.8. CORSOR PREDICTIONS OF FRACTION OF INVENTORY EMITTED BY CORE PRIOR TO VESSEL FAILURE FOR THE THREE ACCIDENT SEQUENCES FOR GRAND GULF

Species	TC	TPI	TQUV	S_2E
Xe	1.00	1.00	1.00	1.00
Kr	1.00	1.00	1.00	1.00
I	1.00	1.00	1.00	1.00
Cs	1.00	1.00	1.00	1.00
Te	0.34	0.57	0.43	0.27
Sr	0.12	0.23	0.16	0.12
Ba	0.29	0.49	0.37	0.29
Ru	0.01	0.02	0.02	0.01
Mo	0.16	0.33	0.23	0.20
Zr (FP)	--	--	--	--
UO_2[(a)]	--	--	--	--
Sn[(a)]	0.67	0.87	0.80	0.70
Zr[(a)] Clad	--	--	--	--
Fe[(a)]	0.03	0.06	0.04	0.03

(a) Nonfission product species.

TABLE 6.9. CORE RELEASE RATES INTO PRIMARY SYSTEM PREDICTED BY CORSOR FOR TC SEQUENCE FOR THE GRAND GULF PLANT

Time (s)	Mass Release Rate (g/s)			
	Cs	I	Te	Aerosol
0	388	20.3	1.1	114
96	57.6	4.8	0.5	60.2
276	68.6	5.7	0.9	107
444	72.4	6.0	1.3	150
612	71.6	5.8	1.6	188
780	70.4	5.9	2.0	225
960	64.6	5.4	2.3	258
1150	60.9	5.1	2.6	290
1340	56.9	4.7	2.9	315
1550	50.3	4.2	3.2	336
1780	47.5	4.0	3.4	348
2070	41.8	3.5	3.7	363
2440	36.2	3.0	3.4	372
2810	33.5	2.8	4.1	380
3110	73.4	6.1	4.0	393
3290	93.3	7.8	4.3	438
3490	41.5	3.5	3.0	335
3760	5.8	0.5	1.8	171
4020	1.6	0.1	1.1	91.7
5350	0.5	--	0.9	71.8

TABLE 6.10. CORE RELEASE RATES INTO PRIMARY SYSTEM PREDICTED BY CORSOR FOR TPI SEQUENCE FOR THE GRAND GULF PLANT

Time (s)	Mass Release Rate (g/s)			
	Cs	I	Te	Aerosol
0	570	42.1	6.2	725
221	42.8	3.5	1.3	151
603	38.4	3.2	1.8	194
1100	33.6	2.8	2.1	221
1570	25.5	2.1	2.4	240
1980	27.0	2.2	2.5	244
2520	21.1	1.8	2.7	249
3220	17.6	1.5	2.8	247
3970	15.0	1.2	2.8	244
4780	13.4	1.1	2.5	216
5630	14.1	1.8	1.8	159
6290	22.0	1.8	1.9	179
6810	14.8	1.2	1.3	120
7360	3.92	0.3	0.3	20.4
7920	0.9	0.1	0.1	5.4
8510	0.2	--	--	1.3
9130	--	0.0	0.0	0.3
9780	--	0.0	0.0	0.3
10500	0.1	--	0.0	0.5
18100	0.7	0.1	0.3	26.8
19700	0.8	0.1	1.9	350

TABLE 6.11. CORE RELEASE RATES INTO THE PRIMARY SYSTEM PREDICTED BY CORSOR FOR TQUV SEQUENCE FOR THE GRAND GULF PLANT

Time (s)	Mass Release Rate (g/s)			
	Cs	I	Te	Aerosol
0	319	17.6	2.9	185
130	52.6	4.4	0.9	74.1
325	90.6	7.6	1.5	157
451	103	8.6	1.9	218
577	107	8.9	2.3	272
704	105	8.7	2.8	325
886	62.2	5.1	3.0	341
1090	68.4	5.7	3.2	356
1230	94.8	7.9	3.7	404
1380	73.4	6.1	4.1	444
1590	61.5	5.1	4.5	475
1860	47.5	4.0	4.7	470
2230	28.3	2.4	4.3	413
2670	27.4	2.3	2.7	252
3040	41.6	3.5	2.7	262
3340	40.2	3.4	2.7	278
3630	78.0	0.7	1.7	153
3940	2.08	0.2	1.1	85.0
4300	1.09	0.1	1.2	90.8
6840	0.2	--	1.9	168

TABLE 6.12. CORE RELEASE RATES INTO THE PRIMARY SYSTEM PREDICTED BY CORSOR FOR S_2E SEQUENCE FOR THE GRAND GULF PLANT

Time (s)	Mass Release Rate (g/s)			
	Cs	I	Te	Aerosol
0	95.8	2.5	0.0	105
180	5.4	0.3	0.1	15.9
450	76.5	6.3	0.6	92.8
630	128	10.6	1.1	172
780	160	13.3	1.5	238
900	170	14.1	1.8	306
1020	158	12.9	2.2	375
1143	150	12.4	2.5	428
1280	109	9.0	2.5	469
1462	69.1	5.7	2.4	400
1708	54.7	4.5	2.0	333
2020	50.3	4.2	2.3	319
2315	60.1	5.0	2.6	352
2834	4.9	0.4	1.9	204
3856	0.3	0.2	1.5	132
4878	--	--	1.9	191
5478	--	--	1.8	175
5867	--	--	1.8	171

TABLE 6.13. (Continued)

Species, %	Time (s)												
	14400	15600	16800	18000	19200	20400	21600	22800	24000	25200	26400	27600	28800
FeO	22.8	23.2	23.5	23.9	24.1	24.3	25.1	3.15	3.52	2.58	2.13	1.99	2.13
Cr_2O_3	0.06	0.06	0.06	0.06	0.05	0.05	0.04	1.74	2.10	1.08	7×10^{-3}	9×10^{-3}	0.01
Ni	0.54	0.52	0.49	0.47	0.45	0.43	0.41	4.71	4.28	2.33	1.82	1.70	1.60
Mo	2×10^{-7}	2×10^{-7}	2×10^{-7}	1×10^{-7}	1×10^{-7}	1×10^{-7}	1×10^{-3}	1×10^{-3}	1×10^{-3}	8×10^{-4}	1×10^{-3}	3×10^{-3}	6×10^{-3}
Ru	2×10^{-6}	2×10^{-6}	2×10^{-6}	1×10^{-6}	1×10^{-6}	1×10^{-6}	1×10^{-6}	1×10^{-5}	1×10^{-5}	4×10^{-6}	3×10^{-6}	2×10^{-6}	2×10^{-6}
Sn	0.46	0.45	0.43	0.42	0.41	0.39	0.39	14.19	13.92	9.78	10.1	12.7	14.7
Sb	--	--	--	--	--	--	--	--	--	--	--	--	--
Te	0.46	0.44	0.42	0.40	0.38	0.36	0.35	4.04	3.67	2.85	2.51	2.50	2.46
Ag	--	--	--	--	--	--	--	--	--	--	--	--	--
Mn	3.63	3.47	3.30	3.16	3.01	2.87	2.80	31.8	29.0	19.61	16.6	16.4	16.0
CaO	23.4	23.7	24.1	24.4	24.6	24.8	25.6	6.25	6.09	5.92	6.39	6.48	6.46
Al_2O_3	1×10^{-4}	2×10^{-4}	2×10^{-4}	2×10^{-4}	2×10^{-4}	2×10^{-4}	2×10^{-4}	3×10^{-4}	3×10^{-3}	4×10^{-3}	5×10^{-3}	5×10^{-3}	6×10^{-3}
Na_2O	1.58	1.62	1.65	1.70	1.77	1.86	1.70	1.26	1.53	2.95	3.15	2.85	2.64
K_2O	13.1	13.4	13.9	14.2	15.2	16.1	15.43	15.3	19.6	43.5	49.3	46.8	45.0
SiO_2	29.9	30.5	29.2	28.8	28.1	27.4	27.3	3.20	2.74	2.11	1.61	1.07	0.79
UO_2	0.33	0.30	0.28	0.25	0.23	0.21	0.20	13.9	13.1	6.98	6.13	7.26	7.86
ZrO_2	0.02	0.02	0.02	0.02	0.02	0.02	0.03	0.30	0.27	0.23	0.20	0.21	0.21
Cs_2O	--	--	--	--	--	--	--	--	--	--	--	--	--
BaO	1.48	1.29	1.10	0.93	0.74	0.53	0.26	0.12	0.12	0.08	0.07	0.07	0.08
SrO	1.26	1.06	0.88	0.72	0.55	0.39	0.19	0.01	8×10^{-3}	5×10^{-3}	4×10^{-3}	4×10^{-3}	4×10^{-3}
La_2O_3	3×10^{-4}	2×10^{-4}	2×10^{-4}	2×10^{-4}	2×10^{-4}	2×10^{-4}	2×10^{-4}	3×10^{-3}	2×10^{-3}	2×10^{-3}	2×10^{-3}	2×10^{-3}	2×10^{-3}
CeO_2	0.99	0.83	0.68	0.55	0.42	0.29	0.13	5×10^{-3}	4×10^{-3}	3×10^{-3}	3×10^{-3}	2×10^{-3}	2×10^{-3}
Nb_2O_5	1×10^{-5}	1×10^{-5}	1×10^{-5}	1×10^{-5}	1×10^{-5}	1×10^{-5}	1×10^{-6}	1×10^{-5}	1×10^{-5}	1×10^{-5}	1×10^{-5}	1×10^{-5}	1×10^{-5}
CsI	--	--	--	--	--	--	--	--	--	--	--	--	--
Source Rate, g/sec	121.	121.	121.	121.	122.	120.	114.	9.3	13.1	15.6	13.8	11.5	10.6

TABLE 6.13. AEROSOL COMPOSITION AND TOTAL RELEASE RATE FOR GRAND GULF, TC

Species, %	Time (s) 0	1200	2400	3600	4800	6000	7200	8400	9600	10800	12000	13200
FeO	21.2	15.7	19.2	19.3	19.1	19.9	20.3	20.8	21.2	21.6	22.0	22.4
Cr_2O_3	--	0.06	0.15	0.13	0.10	0.10	0.09	0.08	0.08	0.07	0.07	0.07
Ni	0.65	1.14	0.94	0.82	0.76	0.74	0.69	0.65	0.62	0.60	0.58	0.56
Mo	--	1×10^{-6}	6×10^{-7}	5×10^{-7}	5×10^{-7}	4×10^{-7}	4×10^{-7}	3×10^{-7}	3×10^{-7}	3×10^{-7}	3×10^{-7}	2×10^{-7}
Ru	7×10^{-8}	9×10^{-6}	6×10^{-6}	4×10^{-6}	4×10^{-6}	4×10^{-6}	3×10^{-6}	3×10^{-6}	3×10^{-6}	2×10^{-6}	2×10^{-6}	2×10^{-6}
Sn	0.15	0.72	0.68	0.61	0.58	0.57	0.54	0.52	0.50	0.49	0.48	0.47
Sb	--	--	--	--	--	--	--	--	--	--	--	--
Te	0.38	0.72	0.75	0.68	0.63	0.62	0.59	0.56	0.54	0.52	0.50	0.48
Ag	--	--	--	--	--	--	--	--	--	--	--	--
Mn	1.43	6.50	6.14	5.45	5.04	4.89	4.59	4.34	4.16	4.07	3.92	3.78
CaO	--	15.8	19.4	19.6	19.4	20.3	20.76	21.2	21.7	22.1	22.5	22.9
Al_2O_3	--	0.13	2×10^{-5}	3×10^{-5}	5×10^{-5}	6×10^{-5}	7×10^{-5}	9×10^{-5}	1×10^{-4}	1×10^{-4}	1×10^{-4}	1×10^{-4}
Na_2O	--	0.77	0.68	1.28	1.57	1.43	1.49	1.52	1.52	1.53	1.55	1.54
K_2O	--	5.32	5.66	10.7	13.1	11.9	12.42	12.74	12.73	12.8	13.9	13.0
SiO_2	--	18.97	23.43	25.01	26.4	28.1	28.9	29.4	29.8	30.1	30.1	30.1
UO_2	0.11	1.31	1.01	0.81	0.71	0.65	0.57	0.51	0.46	0.42	0.39	0.36
ZrO_2	0.01	0.05	0.02	0.02	0.02	0.02	0.02	0.02	0.02	0.02	0.02	0.02
Cs_2O	58.7	--	--	--	--	--	--	--	--	--	--	--
BaO	5.11	6.04	6.02	4.93	4.09	3.62	3.15	2.76	2.44	2.16	1.91	1.67
SrO	5.66	11.25	9.56	6.96	5.32	4.38	3.55	2.92	2.45	2.07	1.75	1.49
La_2O_3	3×10^{-4}	2.30	1.67	3×10^{-4}	3×10^{-4}	3×10^{-4}	3×10^{-4}	3×10^{-4}	3×10^{-4}	3×10^{-4}	3×10^{-4}	3×10^{-4}
CeO_2	0.32	6.26	4.74	3.68	3.11	2.76	2.32	1.98	1.72	1.51	1.32	1.15
Nb_2O_5	2×10^{-6}	6×10^{-5}	4×10^{-5}	3×10^{-5}	3×10^{-5}	2×10^{-5}	2×10^{-5}	2×10^{-5}	2×10^{-5}	2×10^{-5}	1×10^{-5}	1×10^{-5}
CsI	6.83	6.86	4×10^{-3}	--	--	--	--	--	--	--	--	--
Source Rate, g/sec	65.5	145.	160.	147.	142.	137.	133.	129.	127.	125.	123.	121.

TABLE 6.14. (Continued)

Species, %	Time, sec										
	12000	13200	14400	15600	16800	18000	19200	20400	21600	22800	24000
FeO	20.9	21.0	20.9	20.9	20.9	20.9	20.9	21.0	21.1	21.3	21.4
Cr_2O_3	0.03	0.02	0.02	0.02	0.02	0.02	0.02	0.02	0.02	0.02	0.02
Ni	0.25	0.24	0.24	0.25	0.26	0.26	0.27	0.27	0.26	0.25	0.25
Mo	4×10^{-8}	4×10^{-8}	4×10^{-8}	4×10^{-8}	4×10^{-8}	4×10^{-8}	4×10^{-8}	4×10^{-8}	4×10^{-8}	4×10^{-8}	4×10^{-8}
Ru	4×10^{-7}	4×10^{-7}	4×10^{-7}	4×10^{-7}	5×10^{-7}	5×10^{-7}	5×10^{-7}	5×10^{-7}	5×10^{-7}	4×10^{-7}	4×10^{-7}
Sn	0.08	0.08	0.08	0.08	0.08	0.08	0.08	0.08	0.08	0.08	0.08
Sb	--	--	--	--	--	--	--	--	--	--	--
Te	0.26	0.26	0.25	0.25	0.25	0.25	0.25	0.24	0.24	0.23	0.23
Ag	--	--	--	--	--	--	--	--	--	--	--
Mn	2.40	2.34	2.34	2.36	2.37	2.39	2.40	2.38	2.34	2.29	2.24
CaO	21.3	21.3	21.4	21.4	21.4	21.4	21.4	21.5	21.6	21.8	22.0
Al_2O_3	1×10^{-4}	1×10^{-4}	2×10^{-4}	2×10^{-4}	2×10^{-4}	2×10^{-4}	2×10^{-4}	2×10^{-4}	2×10^{-4}	2×10^{-4}	2×10^{-4}
Na_2O	3.31	3.31	3.33	3.37	3.42	3.47	3.49	3.50	3.48	3.45	3.43
K_2O	19.1	19.2	19.2	19.2	19.2	19.2	19.2	19.3	19.4	19.6	19.7
SiO_2	28.9	29.1	29.3	29.5	29.6	29.7	29.7	29.6	29.4	29.2	23.0
UO_2	0.18	0.17	0.16	0.16	0.16	0.16	0.16	0.15	0.14	0.14	0.13
ZrO_2	0.02	0.02	0.02	0.02	0.02	0.02	0.02	0.02	0.02	0.02	0.02
Cs_2O	--	--	--	--	--	--	--	--	--	--	--
BaO	1.32	1.20	1.10	1.02	0.95	0.89	0.83	0.77	0.72	0.67	0.62
SrO	1.56	1.39	1.27	1.17	1.08	1.01	0.94	0.87	0.80	0.73	0.67
La_2O_3	2×10^{-4}	1×10^{-4}	1×10^{-4}	1×10^{-4}	1×10^{-4}	1×10^{-4}	1×10^{-4}	1×10^{-4}	1×10^{-4}	1×10^{-4}	1×10^{-4}
CeO_2	0.39	0.35	0.33	0.32	0.31	0.30	0.29	0.27	0.25	0.23	0.21
Nb_2O_5	1×10^{-6}	1×10^{-6}	1×10^{-6}	1×10^{-6}	1×10^{-6}	1×10^{-6}	1×10^{-6}	1×10^{-6}	1×10^{-6}	1×10^{-6}	1×10^{-6}
CsI	--	--	--	--	--	--	--	--	--	--	--
Source Rate g/sec	87.	82.	76.4	71.6	68.3	68.1	69.0	70.7	72.8	74.3	75.6

TABLE 6.14. AEROSOL COMPOSITION AND TOTAL RELEASE RATE FOR GRAND GULF, TPI

Species, %	Time, sec									
	0	1200	2400	3600	4800	6000	7200	8400	9600	10800
FeO	90.2	42.8	27.4	22.9	20.3	19.70	19.60	20.3	20.6	20.8
Cr_2O_3	--	--	0.02	0.01	0.03	0.05	0.06	0.05	0.04	0.03
Ni	0.03	0.09	0.23	0.39	0.50	0.58	0.54	0.37	0.30	0.27
Mo	--	--	3×10^{-8}	8×10^{-8}	1×10^{-7}	2×10^{-7}	2×10^{-7}	8×10^{-8}	6×10^{-8}	5×10^{-8}
Ru	--	6×10^{-8}	3×10^{-7}	9×10^{-7}	1×10^{-6}	2×10^{-6}	2×10^{-6}	9×10^{-7}	6×10^{-7}	5×10^{-7}
Sn	0.05	0.06	0.09	0.12	0.13	0.14	0.14	0.11	0.09	0.09
Sb	--	--	--	--	--	--	--	--	--	--
Te	0.44	0.37	0.36	0.37	0.36	0.37	0.35	0.31	0.29	0.28
Ag	--	--	--	--	--	--	--	--	--	--
Mn	1.33	1.96	2.76	3.54	3.85	4.06	3.89	3.12	2.74	2.54
CaO	--	0.80	3.91	14.4	20.4	19.9	19.9	20.6	20.9	21.1
Al_2O_3	--	2×10^{-6}	4×10^{-6}	1×10^{-5}	2×10^{-5}	4×10^{-5}	6×10^{-6}	8×10^{-5}	1×10^{-4}	1×10^{-4}
Na_2O	--	2.89	3.30	3.71	3.41	3.24	3.16	3.23	3.31	3.31
K_2O	--	35.6	23.4	19.8	17.8	17.42	17.5	18.2	18.6	18.9
SiO_2	--	6.87	29.7	25.7	24.5	26.13	27.6	28.2	28.5	28.8
UO_2	0.23	0.17	0.25	0.38	0.47	0.53	0.46	0.30	0.24	0.20
ZrO_2	0.06	0.03	0.02	0.02	0.02	0.02	0.02	0.02	0.02	0.02
Cs_2O	--	--	--	--	--	--	--	--	--	--
BaO	2.78	3.56	3.46	3.12	2.74	2.51	2.22	1.91	1.66	1.47
SrO	4.90	4.45	4.44	4.57	4.25	3.94	3.35	2.59	2.10	1.79
La_2O_3	7×10^{-4}	4×10^{-4}	3×10^{-4}	2×10^{-4}	2×10^{-4}	2×10^{-4}	2×10^{-4}	2×10^{-4}	2×10^{-4}	2×10^{-4}
CeO_2	1×10^{-3}	0.22	0.58	1.01	1.26	1.40	1.21	0.76	0.56	0.46
Nb_2O_5	6×10^{-6}	3×10^{-6}	2×10^{-6}	9×10^{-6}	1×10^{-5}	2×10^{-5}	1×10^{-5}	8×10^{-6}	1×10^{-6}	1×10^{-6}
CsI	--	--	--	--	--	--	--	--	--	--
Source Rate g/sec	0.71	3.72	8.49	39.9	64.3	82.7	101.	104.	95.	90

100.0 ✓

TABLE 6.15. AEROSOL COMPOSITION AND TOTAL RELEASE RATE FOR GRAND GULF, TQUV

Species, %	Time, sec										
	0	1200	2400	3600	4800	6000	7200	8400	9600	10800	12000
FeO	--	17.6	18.9	19.2	19.1	19.0	19.1	19.4	19.7	20.0	20.3
Cr_2O_3	--	--	--	--	--	--	--	--	--	--	--
Ni	4.36	1.19	0.75	0.62	0.61	0.62	0.60	0.56	0.52	0.50	0.48
Mo	1×10^{-6}	6×10^{-7}	3×10^{-7}	2×10^{-7}	2×10^{-7}	2×10^{-7}	2×10^{-7}	2×10^{-7}	1×10^{-7}	1×10^{-7}	1×10^{-7}
Ru	1×10^{-5}	5×10^{-6}	2×10^{-6}	2×10^{-6}	2×10^{-6}	2×10^{-6}	2×10^{-6}	1×10^{-6}	1×10^{-6}	1×10^{-6}	1×10^{-6}
Sn	1.24	0.29	0.21	0.19	0.18	0.18	0.18	0.17	0.16	0.16	0.16
Sb	--	--	--	--	--	--	--	--	--	--	--
Te	2.48	0.46	0.41	0.37	0.36	0.35	0.34	0.32	0.31	0.30	0.30
Ag	--	--	--	--	--	--	--	--	--	--	--
Mn	22.0	4.72	3.63	3.21	3.11	3.05	2.96	2.86	2.72	2.63	2.54
CaO		17.9	19.3	19.7	19.7	19.7	19.9	20.2	20.5	20.8	21.1
Al_2O_3		3×10^{-5}	7×10^{-5}	1×10^{-4}	1×10^{-4}	1×10^{-4}	2×10^{-4}	2×10^{-4}	2×10^{-4}	2×10^{-4}	2×10^{-4}
Na_2O		2.89	2.92	3.06	3.10	3.15	3.17	3.19	3.22	3.23	3.22
K_2O		15.6	17.0	17.4	17.4	17.4	17.5	17.8	18.2	18.4	18.7
SiO_2		25.8	28.8	30.2	31.3	31.9	32.2	32.0	31.7	31.3	30.9
UO_2	4.59	1.18	0.66	0.49	0.45	0.43	0.39	0.34	0.31	0.28	0.26
ZrO_2	0.09	0.05	0.02	0.02	0.02	0.02	0.02	0.02	0.02	0.02	0.02
Ca_2O	--	--	--	--	--	--	--	--	--	--	--
BaO	21.4	3.14	2.54	2.06	1.75	1.52	1.34	1.18	1.05	0.93	0.83
SrO	32.1	4.86	3.28	2.43	1.98	1.68	1.42	1.21	1.03	0.89	0.77
La_2O_3	1×10^{-3}	1.45	2×10^{-4}	2×10^{-4}	2×10^{-4}	1×10^{-4}	1×10^{-4}	1×10^{-4}	1×10^{-4}	1×10^{-4}	1×10^{-4}
CaO_2	11.7	2.90	1.56	1.13	0.99	0.90	0.80	0.67	0.57	0.49	0.43
Nb_2O_5	2×10^{-4}	6×10^{-5}	3×10^{-5}	2×10^{-5}	2×10^{-5}	2×10^{-5}	2×10^{-5}	1×10^{-5}	1×10^{-5}	1×10^{-5}	1×10^{-5}
CsI	--	--	--	--	--	--	--	--	--	--	--
Source Rate, g/sec	25.4	171.	164.	141.	128.	127.	126.	124.	123.	122.	122.

TABLE 6.15. (Continued)

Species, %	Time, sec										
	13200	14400	15600	16800	18000	19200	20400	21600	22800	24000	25200
FeO	20.6	20.9	21.2	21.6	21.9	22.4	22.8	23.33	1.09	1.63	2.06
Cr_2O_3	--	--	--	--	--	--	--	--	0.95	1.52	1.70
Ni	0.47	0.45	0.44	0.42	0.41	0.38	0.37	0.36	3.62	3.44	3.30
Mo	1×10^{-7}	1×10^{-7}	9×10^{-8}	9×10^{-8}	8×10^{-8}	7×10^{-8}	7×10^{-8}	6×10^{-8}	5×10^{-4}	5×10^{-4}	5×10^{-4}
Ru	1×10^{-6}	1×10^{-6}	9×10^{-7}	8×10^{-7}	8×10^{-7}	7×10^{-7}	6×10^{-7}	6×10^{-7}	6×10^{-6}	5×10^{-6}	5×10^{-6}
Sn	0.15	0.15	0.15	0.14	0.14	0.13	0.13	0.13	4.34	4.34	4.37
Sb	--	--	--	--	--	--	--	--	--	--	--
Te	0.29	0.28	0.28	0.27	0.26	0.25	0.25	0.24	2.54	2.46	2.39
Ag	--	--	--	--	--	--	--	--	--	--	--
Mn	2.48	2.41	2.34	2.27	2.21	2.12	2.06	2.01	20.7	19.9	19.3
CaO	21.4	21.7	22.1	22.4	22.8	23.2	23.6	24.2	8.62	8.38	8.58
Al_2O_3	2×10^{-4}	2×10^{-4}	3×10^{-4}	3×10^{-4}	3×10^{-4}	3×10^{-4}	3×10^{-4}	3×10^{-4}	4×10^{-3}	4×10^{-3}	4×10^{-3}
Na_2O	3.24	3.26	3.28	3.28	3.28	3.24	3.15	2.80	1.34	1.70	1.92
K_2O	18.9	19.2	19.5	19.8	20.0	20.3	20.5	20.7	42.1	42.9	43.4
SiO_2	30.4	29.8	29.2	28.5	27.8	27.1	26.4	25.8	5.69	5.19	4.74
UO_2	0.24	0.22	0.20	0.19	0.18	0.16	0.15	0.14	8.66	8.26	8.01
ZrO_2	0.02	0.02	0.02	0.02	0.02	0.02	0.02	0.02	0.20	0.20	0.19
Ca_2O	--	--	--	--	--	--	--	--	--	--	--
BaO	0.74	0.66	0.58	0.50	0.43	0.35	0.26	0.16	6×10^{-2}	6×10^{-2}	6×10^{-2}
SrO	0.67	0.58	0.50	0.43	0.36	0.29	0.21	0.12	5×10^{-3}	5×10^{-3}	4×10^{-3}
La_2O_3	1×10^{-4}	1×10^{-4}	1×10^{-4}	1×10^{-4}	1×10^{-4}	1×10^{-4}	1×10^{-4}	1×10^{-4}	1×10^{-3}	1×10^{-3}	1×10^{-3}
CaO_2	0.38	0.32	0.28	0.23	0.19	0.15	0.10	0.06	2×10^{-3}	2×10^{-3}	2×10^{-3}
Nb_2O_5	1×10^{-5}	1×10^{-5}	9×10^{-6}	9×10^{-5}	8×10^{-6}	8×10^{-6}	8×10^{-6}	9×10^{-7}	9×10^{-6}	9×10^{-6}	9×10^{-6}
CsI								--	--	--	
Source Rate, g/sec	118.	117.	118.	119.	119.	119.	119.	115.	10.4	10.2	--

7. RESULTS AND DISCUSSION

7.1 Introduction

Results of calculations for the transport and deposition of radionuclides are presented and discussed in this section. The plants and sequences selected for consideration were discussed in Chapter 4, the analytical and calculational methods were described in Chapter 5, and the assumptions and bases for the calculations were described in Chapter 6. Results presented in this chapter include the deposition and release from the reactor coolant system of radionuclides leaving the core region. These results are based on TRAP-MELT code calculations. Also included are the results for the masses of radionuclides airborne and deposited in the containment and suppression pool, as well as the airborne materials leaked to the environment. These results are based on SPARC calculations for retention in the suppression pool and NAUA-4 calculations for transport in the containment and reactor buildings.

7.2 Transport and Deposition in Reactor Coolant System (RCS)

The analyses of the transport and deposition within the RCS of materials released from the melting core have been performed using the TRAP-MELT code which was described earlier in this report. The time frame of interest in the RCS for core meltdown accidents such as those considered here spans the period of time starting with the onset of core melting and ending with failure of the bottom head of the RPV. For accidents involving only minor fuel damage, the gap release term, which occurs prior to melting of fuel, may be the major release and require careful consideration. For the accidents examined here, however, this release term is insignificant in comparison with the melt release and the period immediately prior to the onset of core melting is not considered. Rather, the gap releases calculated by CORSOR are added to the initial material emitted by the melting core.

Releases from the melting core and their behavior in the RCS are calculated beyond the time of core collapse in these analyses. This differs from the evaluations presented in Volume I of this report wherein the source to the RCS was assumed to go to zero when the core slumped into the residual

water in the lower plenum. As in the analyses of the Peach Bottom sequences, the slumping of the core has been simulated in MARCH on a nodal basis. This factor and the presence of much greater below core structures in the BWR pressure vessel dictate that emission from nodes which have left the core be included in the analyses.

As was pointed out in Section 4.2, during the in-vessel portion of the three transient sequences analyzed, the flow pathway through the RCS is the same. Namely, the flow leaves the core region and passes through the steam separators, splitting into two portions. These analyses treat the case where 85 percent of the flow passes through the steam dryers and the remainder bypasses those units through the outer annulus. The flows then merge and exit the pressure vessel through the steam lines and are led to the suppression pool through the safety relief lines. In the S_2E sequence the flow passes from the core region through the steam separators, through the lower outer annulus, and out the break in the primary system piping. The thermal hydraulic information pertaining to each of the sequences was presented in Section 6 of this document.

7.2.1 RCS Transport and Deposition for Sequence TC

In the TC sequence, the transient with failure to scram, the RCS remains at high pressure (~1200 psia) up to the time of vessel failure, and the released activity leaves the primary system through the safety valves into the suppression pool. The total masses of the species of interest emitted from the core as a function of time are presented in Table 7.1, along with the total masses retained in the RCS.

By examining the Total columns for CsI and CsOH, one can see that nearly the entire ivnentory of Cs and I are released by t = 3760, whereas Te and the less volatile species which form the aerosol particles continue to be released from the core. This table also indicates that only about one-third of the Te inventory is released from the fuel during the in-vessel period of the melt due to the presence of a large amount of unoxidized Zr in the melting core. From t = 3370 to t = 3760 there are significant decreases in the masses of the Cs species retained in the RCS. The reason for this is that the MERGE predicted surface temperatures increase greatly during this period due to a high mass flow rate of steam and hydrogen from the core. For example, the

TABLE 7.1. CORSOR PREDICTIONS OF MASSES OF SPECIES RELEASED FROM THE CORE (TOT) AND TRAP-MELT PREDICTION OF MASSES RETAINED IN THE RCS (RET) FOR WASH-1400 SPECIES GROUPS* DURING THE TC SEQUENCE FOR THE GRAND GULF PLANT

(Times Measured from Start of Core Melting)

Time (s)	CsI		CsOH		Te		Aerosol	
	Ret (kg)	Tot (kg)	Ret (kg)	Tot (kg)	Ret (kg)	Tot (kg)	Ret (kg)	Tot (kg)
200	--	3.2	--	30.5	--	0.1	--	9.8
590	0.4	7.7	3.6	61.2	0.1	0.4	19.0	49.5
990	2.2	12.2	18.2	73.9	0.1	0.8	80.7	118
1390	2.8	16.3	22.5	120	0.2	1.5	166	211
1780	3.5	19.7	27.5	143	0.3	2.2	272	320
2180	4.2	22.5	33.1	163	0.4	3.1	389	438
2580	4.8	25.1	37.1	180	0.5	4.1	508	558
2970	10.4	27.6	77.0	198	2.6	5.1	623	683
3370	14.2	32.2	149	228	6.2	6.3	690	827
3760	8.6	35.8	139	252	7.1	7.3	712	947
4160	6.8	36.3	131	256	7.7	7.9	719	999
4560	6.8	36.4	131	257	8.0	8.3	722	1022
4950	6.8	36.5	131	257	8.1	8.8	743	1050
5350	6.8	36.5	131	257	8.1	9.0	761	1069

*See Chapter 6

surface temperature of the steam dryers increases from 365 C, at t = 3100 s to 795 C at t = 3630 s. This results in the evaporation of condensed materials on the system surfaces and their transport through the RCS.

The RCS retention information for this sequence is presented in Table 7.2 in terms of retention fractions for the system and for specific volumes of the RCS. These values are defined to be the ratio of the mass of a species retained on the surfaces of a volume to the total mass of that species emitted up to a given time. Thus, these figures would underestimate retention efficiencies of volumes other than the first one in the flow path. The final entry in the table indicates the fraction of the core-emitted materials retained in the RCS and selected components at the time of vessel failure. Thus, for this sequence, TRAP-MELT predicts that 0.19 of the CsI and 0.51 of the CsOH are retained in the RCS. One can see the drop in the retention factor which accompanies the system temperature rise discussed above reflected in Figures 7.1 and 7.2. The major reason for the different RFs predicted for these two species is the chemical reaction of CsOH with system surfaces, which accounts for an RF of 0.25. The remainder of the retained CsOH is either condensed from the vapor (principally in the steam dryers) or condensed on particles which are subsequently retained. This latter mechanism is dominant for both CsOH and CsI retention.

The retention of Te in the RCS is depicted in Figure 7.3 and is almost totally due to chemical reaction with system surfaces, which results in very high RFs for the Te which is released from the core while it resides in the RCS.

Aerosol retention is fairly high for this sequence, due in large part to the lengthy residence time which most of the emitted aerosol experiences. The high pressure in this sequence leads to low flow velocities through the system through much of the in-vessel melt period. An exception can be noted in Figure 7.4 during the period $2970 < t < 4560$ s, during which time the RF for the system drops from 0.91 to 0.72. During this period the mass flow rate through the system is two orders of magnitude greater than at other times, resulting in reduced residence times. The aerosol mass escaping the RCS during this period is approximately 297 kg, while just over 1 kg had escaped prior to 2970 s. At the time of bottom head failure, 25.4 kg are suspended in the RCS and injected into the drywell during the puff release which accompanies system depressurization. This represents the first aerosol mass not passing through

TABLE 7.2 TRAP-MELT PREDICTIONS OF PRIMARY SYSTEM RETENTION FACTORS (RF) AND VOLUME SPECIFIC RETENTION FACTORS AS A FUNCTION OF TIME FOR THE TC SEQUENCE FOR THE GRAND GULF PLANT

(Times Measured from Start of Core Melting)

Time (s)	CsI			CsOH			Te			Aerosol			
	RF	Steam Dryers	Lower Annulus	RF	Steam Sep	Steam Dryers	RF	Steam Sep	Steam Dryers	RF	Core	Steam Sep	Steam Dryers
200	--	--	--	--	--	--	.08	.08	--	--	--	--	--
590	.05	--	--	.06	.05	--	.12	.12	--	.38	.36	.03	--
990	.18	.01	--	.25	.23	.02	.14	.14	--	.69	.61	.07	--
1390	.17	.01	--	.19	.17	.01	.13	.13	--	.79	.74	.05	--
1780	.18	.01	--	.19	.18	.01	.13	.13	--	.85	.81	.04	--
2180	.19	.01	--	.20	.19	.01	.13	.12	--	.89	.85	.03	--
2580	.19	.01	--	.21	.19	.02	.12	.11	--	.91	.88	.03	--
2970	.38	.03	--	.39	.35	.03	.51	.48	.02	.91	.86	.04	--
3370	.44	.21	.04	.65	.39	.22	.97	.90	.07	.84	.72	.08	.03
3760	.24	.16	.05	.55	.17	.31	.97	.89	.07	.75	.63	.07	.03
4160	.19	.11	.05	.51	.16	.27	.98	.90	.07	.72	.60	.07	.03
4560	.19	.11	.06	.51	.16	.28	.97	.87	.08	.71	.59	.06	.03
4950	.19	.11	.06	.51	.16	.28	.92	.83	.08	.71	.59	.06	.03
5350	.19	.11	.06	.51	.16	.28	.90	.81	.07	.71	.60	.06	.03

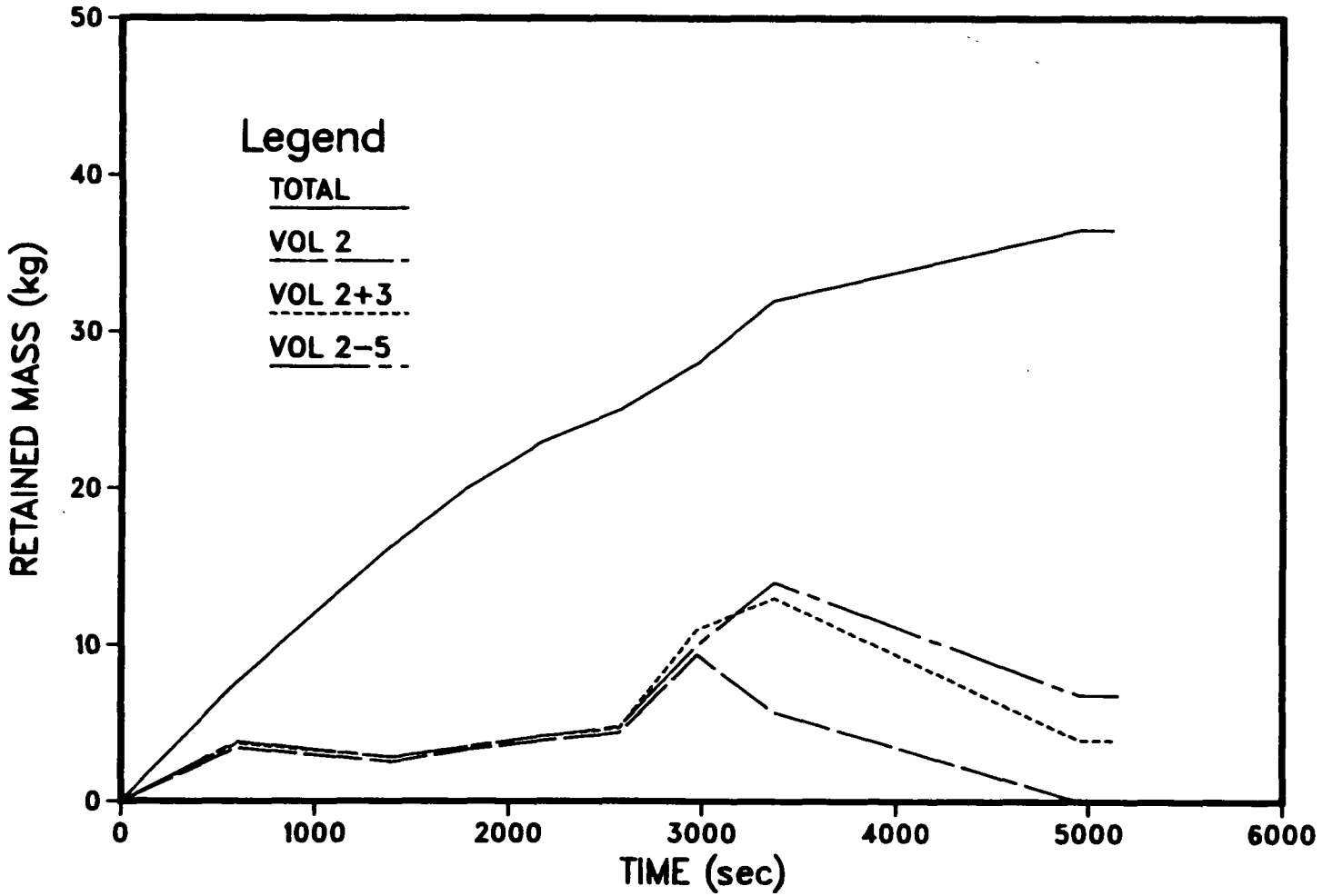

FIGURE 7.1. MASSES OF CsI EMITTED FROM CORE AND RETAINED IN THE RCS CONTROL VOLUMES AS FUNCTIONS OF TIME FOR THE TC SEQUENCE (Vol 1 = Core, Vol 2 = Steam Separators, Vol 3 = Steam Dryers, Vol 4 = Upper Annulus, Vol 5 = Relief Lines). Times Measured from Start of Core Melting.

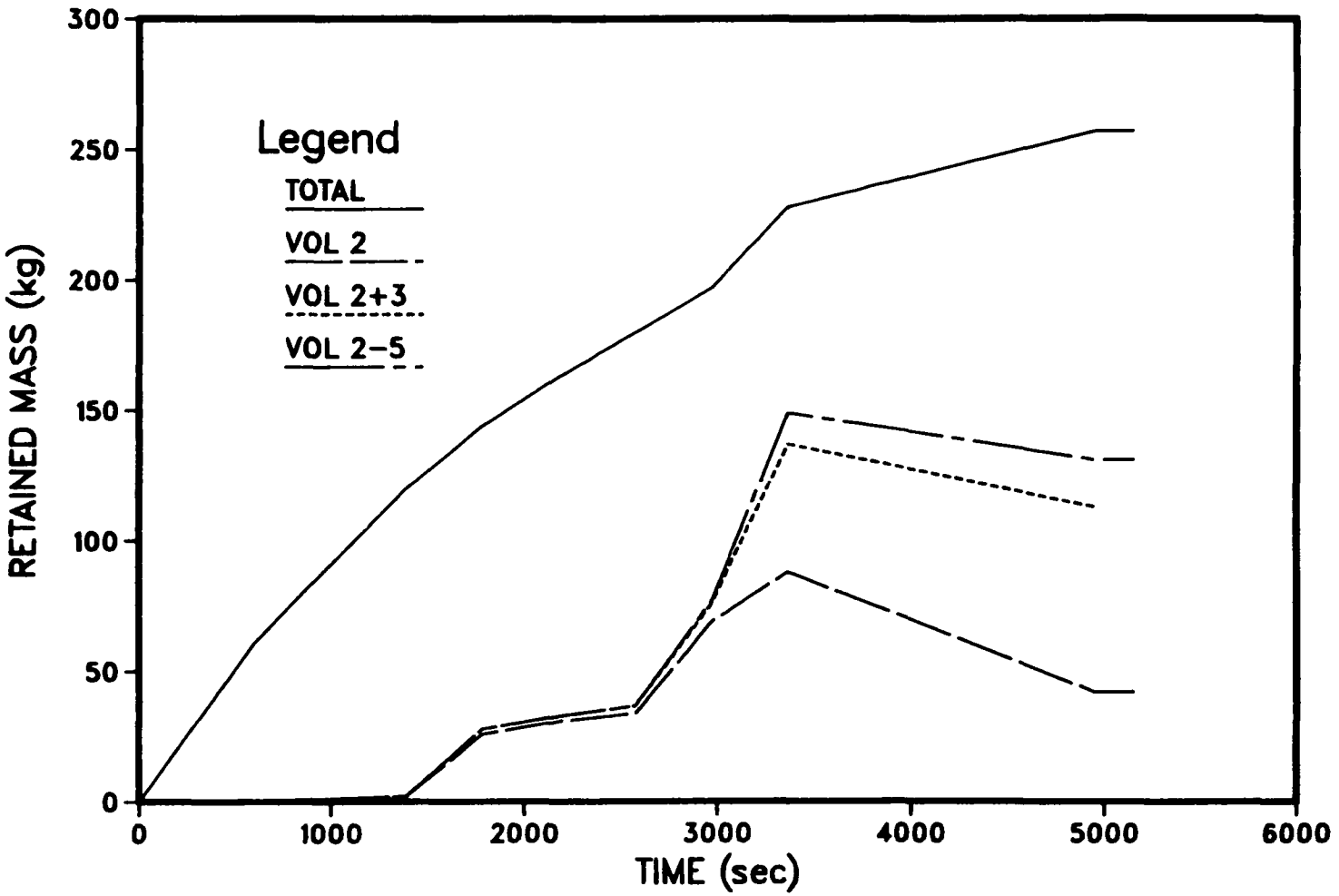

FIGURE 7.2. MASSES OF CsOH EMITTED FROM CORE AND RETAINED IN THE RCS CONTROL VOLUMES AS FUNCTIONS OF TIME FOR THE TC SEQUENCE (Vol 1 = Core, Vol 2 = Steam Separators, Vol 3 = Steam Dryers, Vol 4 = Upper Annulus, Vol 5 = Relief Lines). Times Measured from Start of Core Melting.

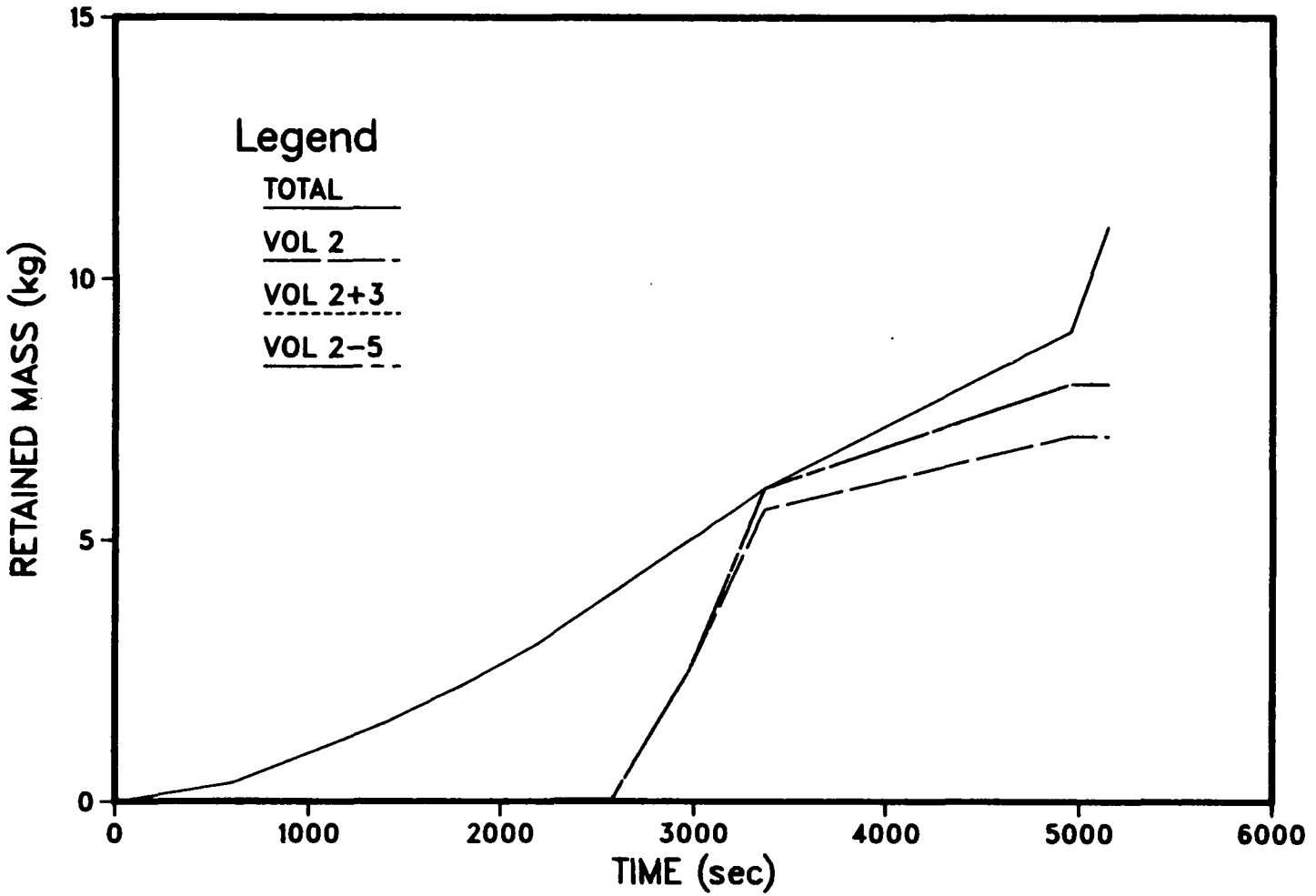

FIGURE 7.3. MASSES OF Te EMITTED FROM CORE AND RETAINED IN THE RCS CONTROL VOLUMES AS FUNCTIONS OF TIME FOR THE TC SEQUENCE (Vol 1 = Core, Vol 2 = Steam Separators, Vol 3 = Steam Dryers, Vol 4 = Upper Annulus, Vol 5 = Relief Lines). Times Measured from Start of Core Melting.

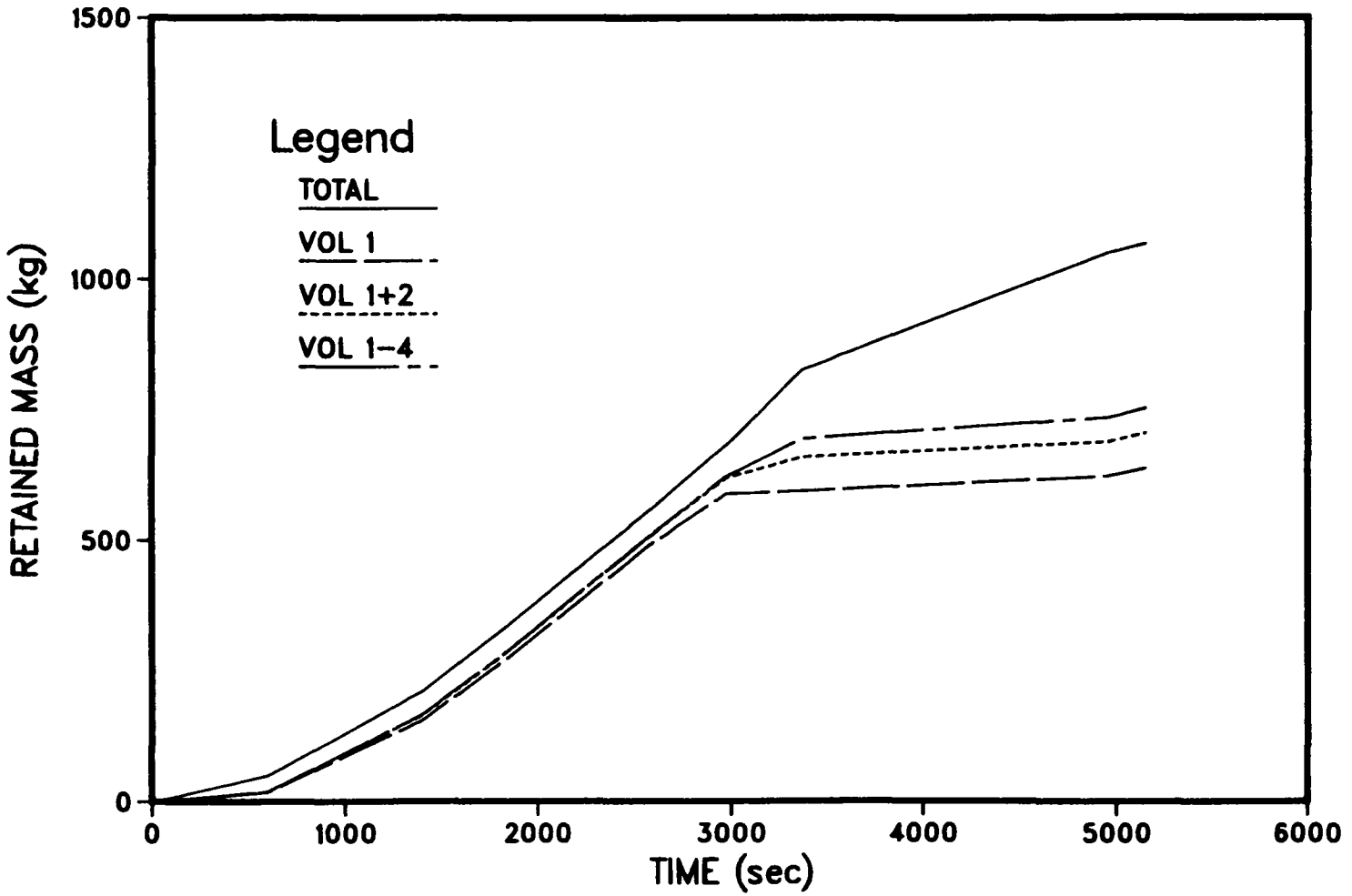

FIGURE 7.4. MASSES OF AEROSOL EMITTED FROM CORE AND RETAINED IN THE RCS CONTROL VOLUMES AS FUNCTIONS OF TIME FOR THE TC SEQUENCE (Vol 1 = Core, Vol 2 = Steam Separators, Vol 3 = Steam Dryers, Vol 4 = Upper Annulus, Vol 5 = Relief Lines). Times Measured from Start of Core Melting.

the suppression pool in this sequence. The aerosol size distribution has a mass median diameter at this time (and during much of the in-vessel part of the sequence) of approximately 2.0 μm.

A simulation of the TC sequence was performed using TRAP-MELT to track the RCS retention of the WASH-1400 groups as defined in Chapter 6. The Cs, I, and Te retention behavior was as discussed for CsI, CsOH, and Te in the above. Likewise, these results for the grouped species, summarized in Table 7.2a, indicate the extent of retention of Sr, Ru, and La is very nearly the same as that of the total aerosol, indicating no significant differences in the timing of the releases of these species.

7.2.2 RCS Transport and Deposition in Sequence TPI

In this sequence, the in-vessel portion of the accident during core melting is characterized by a low pressure due to the stuck open safety relief valve. The duration of this phase of the accident is over 5 h since the start of core melting occurs a long time from the initiation of the accident, but the variations in the steam and hydrogen flow rates do not permit a long RCS residence time to all the core-emitted materials.

Table 7.3 presents the total masses of the species of interest emitted as functions of time and the total masses retained in the RCS. As in the TC sequence discussed above, the depletion of the Cs and I inventories is apparent less than halfway through the time period. The longer duration of this accident's in-vessel phase leads to an increase in the amount of Te released from the core, but still only about one half of the inventory is released in-vessel. The aerosol emitted from the core is also greater than for the TC sequence due to the longer time frame here, but does not show as large an increase as one might expect due to a protracted period of low emission rates from about 6900 to 17700 s.

As was seen in the TC case, the heatup of the RCS surfaces which accompanies a period of high flow rate leads to the evaporation of CsI and CsOH which had previously condensed on system surfaces which is evident in Figures 7.5 and 7.6. This period of high flow rates is coupled with a cooling of the molten core which results in a reduced Te and aerosol emission rate. Thus, the mass of aerosol retained in the RCS does not increase much until

TABLE 7.2a. CORSOR PREDICTIONS OF RELEASE FROM CORE AND TRAP-MELT PREDICTIONS OF PRIMARY SYSTEM RETENTION OF WASH-1400 GROUPS FOR TC SEQUENCE

Group	Released (kg)	Retained (kg)
I	17.9	3.3
Cs	247	120
Te	9.0	8.1
Sr	39.4	27.7
Ru	43.3	27.5
La	0.91	0.65

*Groups are defined in Chapter 6.

TABLE 7.3. CORSOR PREDICTIONS OF MASSES OF SPECIES RELEASED FROM THE CORE (TOT) AND TRAP-MELT PREDICTIONS OF MASSES RETAINED IN THE RCS (RET) DURING THE TPI SEQUENCE FOR THE GRAND GULF PLANT

(Times Measured from Start of Core Melting)

Time (s)	CsI		CsOH		Te		Aerosol	
	Ret (kg)	Tot (kg)	Ret (kg)	Tot (kg)	Ret (kg)	Tot (kg)	Ret (kg)	Tot (kg)
1040	12.6	16.0	83.6	105	1.7	2.2	177	248
2080	17.9	21.2	116	137	3.7	4.6	412	490
3120	22.0	25.1	141	160	6.3	7.4	675	747
4160	24.4	28.0	155	178	8.6	10.3	920	1000
5200	27.3	30.5	173	193	11.7	13.0	1140	1230
6240	28.4	33.3	181	210	14.4	14.9	1190	1410
7280	8.2	36.0	109	226	15.7	16.3	1200	1540
8320	3.0	36.3	57.6	228	15.9	16.5	1200	1550
11400	2.9	36.4	55.4	228	15.9	16.5	1200	1560
15600	2.9	36.6	55.6	230	16.1	17.0	1240	1600
19800	3.1	37.0	56.8	232	16.7	19.4	1560	1940

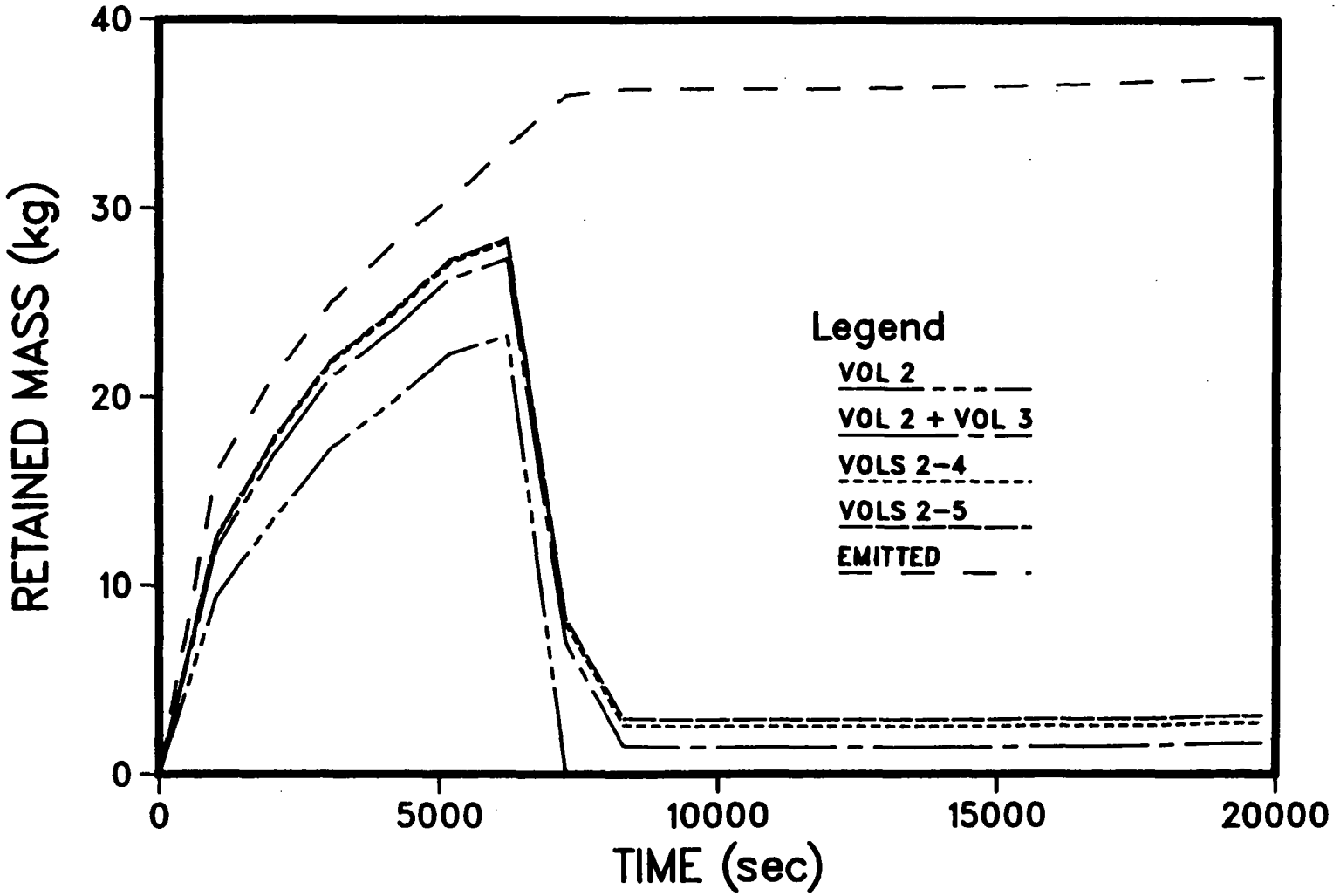

FIGURE 7.5. MASSES OF CsI EMITTED FROM CORE AND RETAINED IN THE RCS CONTROL VOLUMES AS FUNCTIONS OF TIME FOR THE TPI SEQUENCE (Vol 1 = Core, Vol 2 = Steam Separators, Vol 3 = Steam Dryers, Vol 4 = Upper Annulus, Vol 5 = Relief Lines). Times Measured from Start of Core Melting.

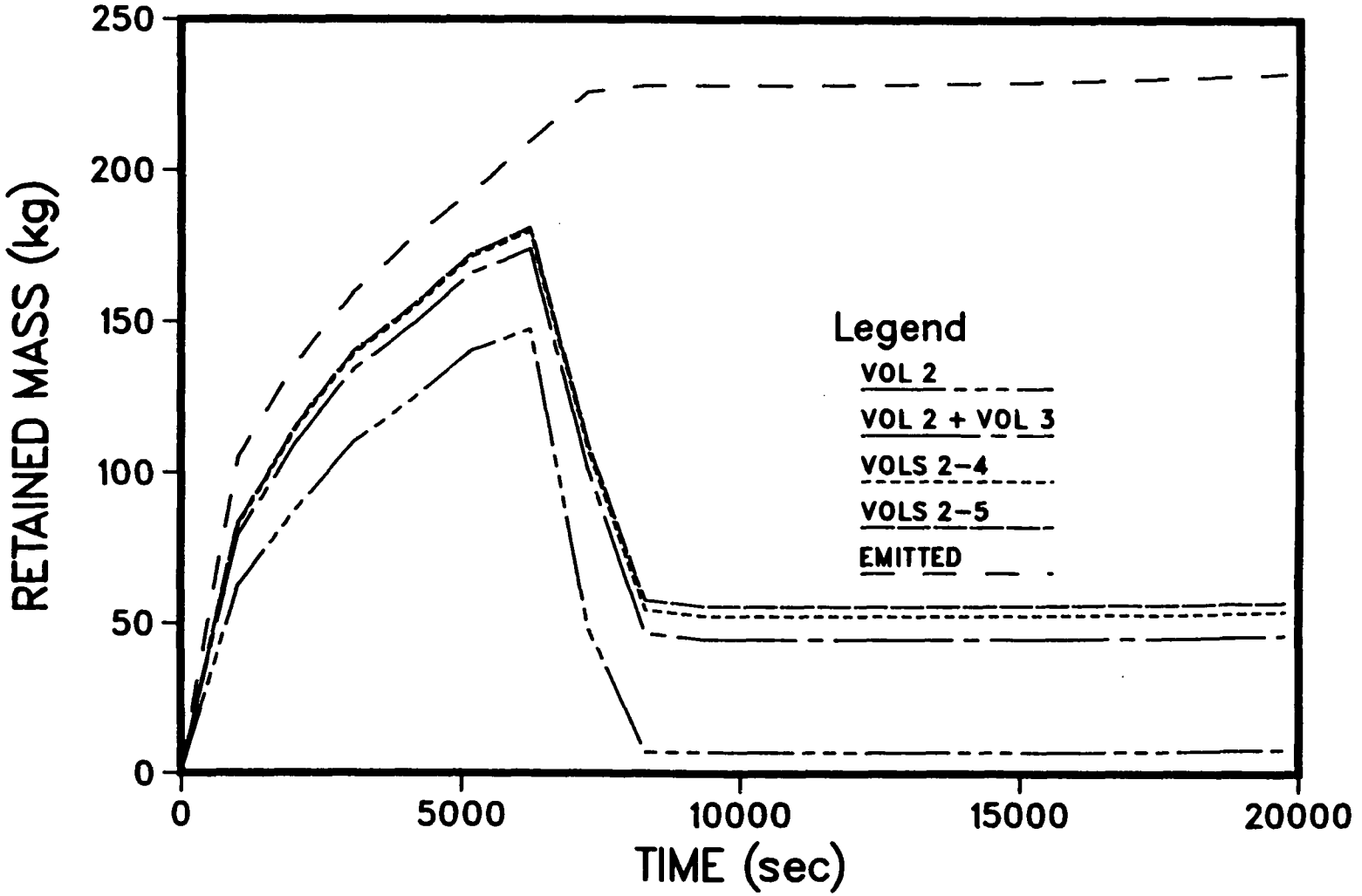

FIGURE 7.6. MASSES OF CsOH EMITTED FROM CORE AND RETAINED IN THE RCS CONTROL VOLUMES AS FUNCTIONS OF TIME FOR THE TPI SEQUENCE (Vol 1 = Core, Vol 2 = Steam Separators, Vol 3 = Steam Dryers, Vol 4 = Upper Annulus, Vol 5 = Relief Lines). Times Measured from Start of Core Melting.

very near the time at which the bottom head fails, as it is not until this time that the release rate of aerosol from the core is "revived".

Table 7.4 contains the RCS retention predictions for the TPI sequence, expressed in terms of the specific volumes considered in the analyses. Those volumes which contribute but little to the total retention are omitted from the table for the sake of clarity. As for TC, the difference in CsOH and CsI retention is due to the chemical reaction of the hydroxide with the system surfaces. And, as before, retention via deposition on particles which are retained dominates the material which condenses directly on the surfaces. The retention of Te is depicted in Figure 7.7 and is due almost entirely to chemical reaction with the RCS surfaces. The somewhat reduced efficiency of retention of these vapor species, as compared with TC, is caused by the different flow rates through the RCS during the time period in which these materials are emitted. The residence time these species have in the RCS volumes is reduced by an order of magnitude due to the higher flow velocities which pertain to the TPI sequence. This obviously leads to reduced interaction of the vapors with the surfaces. The aerosol retention shown in Figure 7.8 in the RCS is fairly high, as was observed to be the case for the TC sequence. During the period of high flow rates through the system, approximately 6240 to 10600 s, the RCS is purged of nearly all suspended materials, but just prior to vessel failure, the aerosol generation rate increases substantially, resulting in about 29 kg of aerosol being present in the release to the drywell at the time of bottom head failure. Prior to this time, 356 kg had been routed to the suppression pool via the relief lines.

7.2.3 RCS Transport and Deposition for Sequence TQUV

This sequence is not as simple to classify as the previous two. The system pressure varies throughout the melt period and the gas flow rate through the system varies through over two orders of magnitude in a cyclic fashion so that the RCS environment experienced by a particular species cannot be generalized. The masses of each species emitted from the core and the masses retained are presented in Table 7.5. Due to the somewhat longer melt period, compared to TC, a bit more Te and aerosol mass are released from the core.

Table 7.6 contains the RFs for the primary system and some of its components. Of the 0.54 value for the CsOH RF, 0.50 is due to chemical

TABLE 7.4. TRAP-MELT PREDICTIONS OF PRIMARY SYSTEM RETENTION FACTORS (RF) AND VOLUME SPECIFIC RETENTION FACTORS AS A FUNCTION OF TIME FOR THE TPI SEQUENCE FOR THE GRAND GULF PLANT

(Times Measured from Start of Core Melting)

Time (s)	CsI			CsOH			Te			Aerosol		
	RF	Steam Sep	Steam Dryers	RF	Steam Sep	Steam Dryers	RF	Steam Sep	Steam Dryers	RF	Steam Sep	Steam Dryers
1040	.78	.59	.16	.79	.60	.16	.75	.63	.10	.71	.07	.50
2080	.84	.64	.16	.85	.65	.16	.81	.70	.09	.84	.17	.54
3120	.88	.69	.15	.88	.69	.15	.85	.76	.07	.90	.27	.52
4160	.87	.70	.14	.87	.70	.14	.83	.76	.06	.92	.36	.47
5200	.89	.73	.13	.89	.73	.13	.90	.84	.05	.92	.39	.46
6240	.85	.70	.12	.86	.70	.13	.96	.88	.07	.84	.34	.43
7280	.23	.00	.19	.48	.21	.23	.96	.82	.12	.78	.32	.39
8320	.08	-	.04	.25	.03	.17	.97	.82	.12	.77	.32	.39
11400	.09	-	.04	.24	.03	.16	.97	.82	.12	.77	.32	.39
15600	.08	-	.04	.24	.03	.16	.95	.80	.12	.77	.33	.38
19800	.08	.01	.04	.24	.04	.16	.86	.73	.11	.80	.43	.31

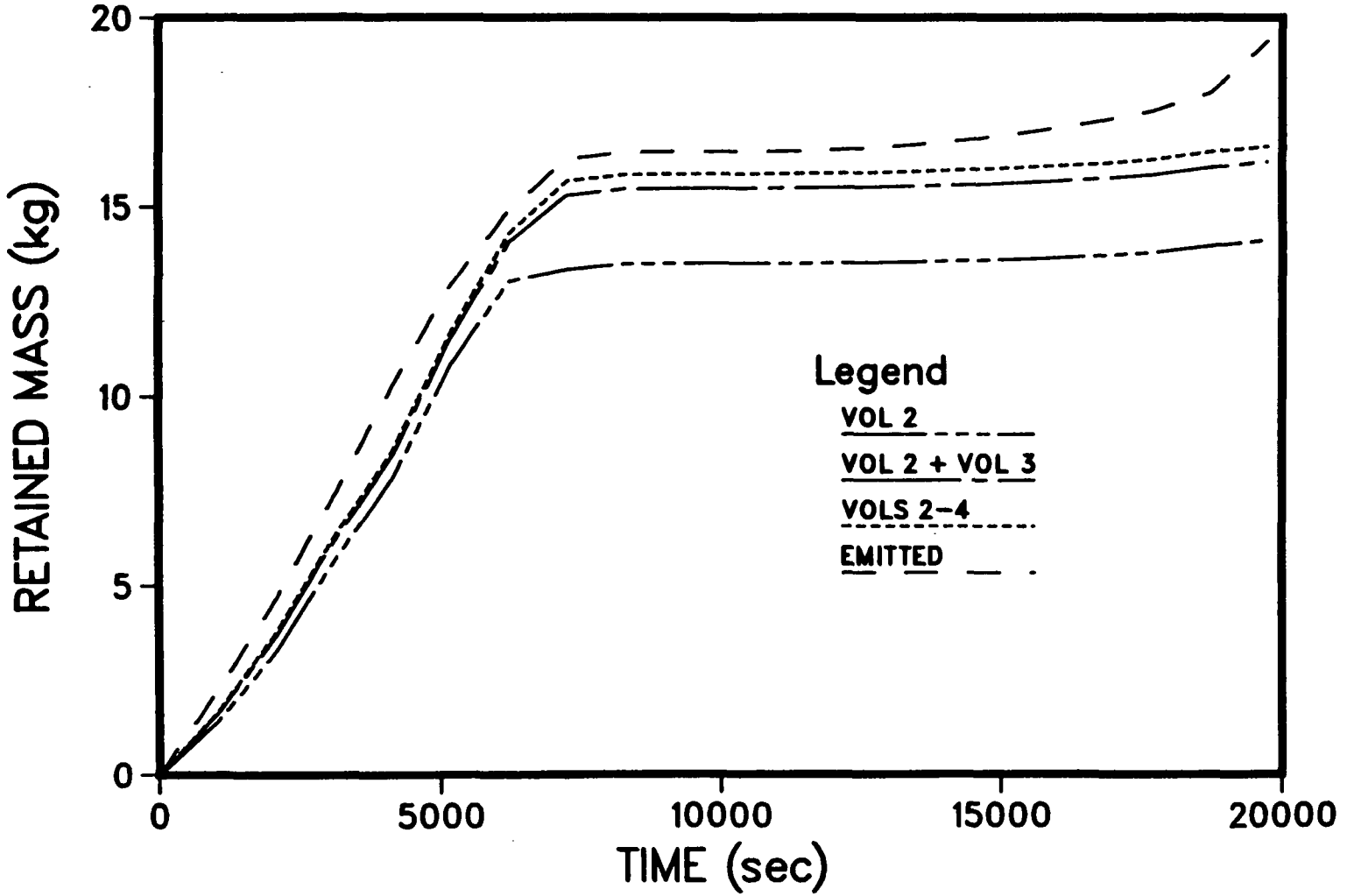

FIGURE 7.7. MASSES OF Te EMITTED FROM CORE AND RETAINED IN THE RCS CONTROL VOLUMES AS FUNCTIONS OF TIME FOR THE TPI SEQUENCE (Vol 1 = Core, Vol 2 = Steam Separators, Vol 3 = Steam Dryers, Vol 4 = Upper Annulus, Vol 5 = Relief Lines). Times Measured from Start of Core Melting.

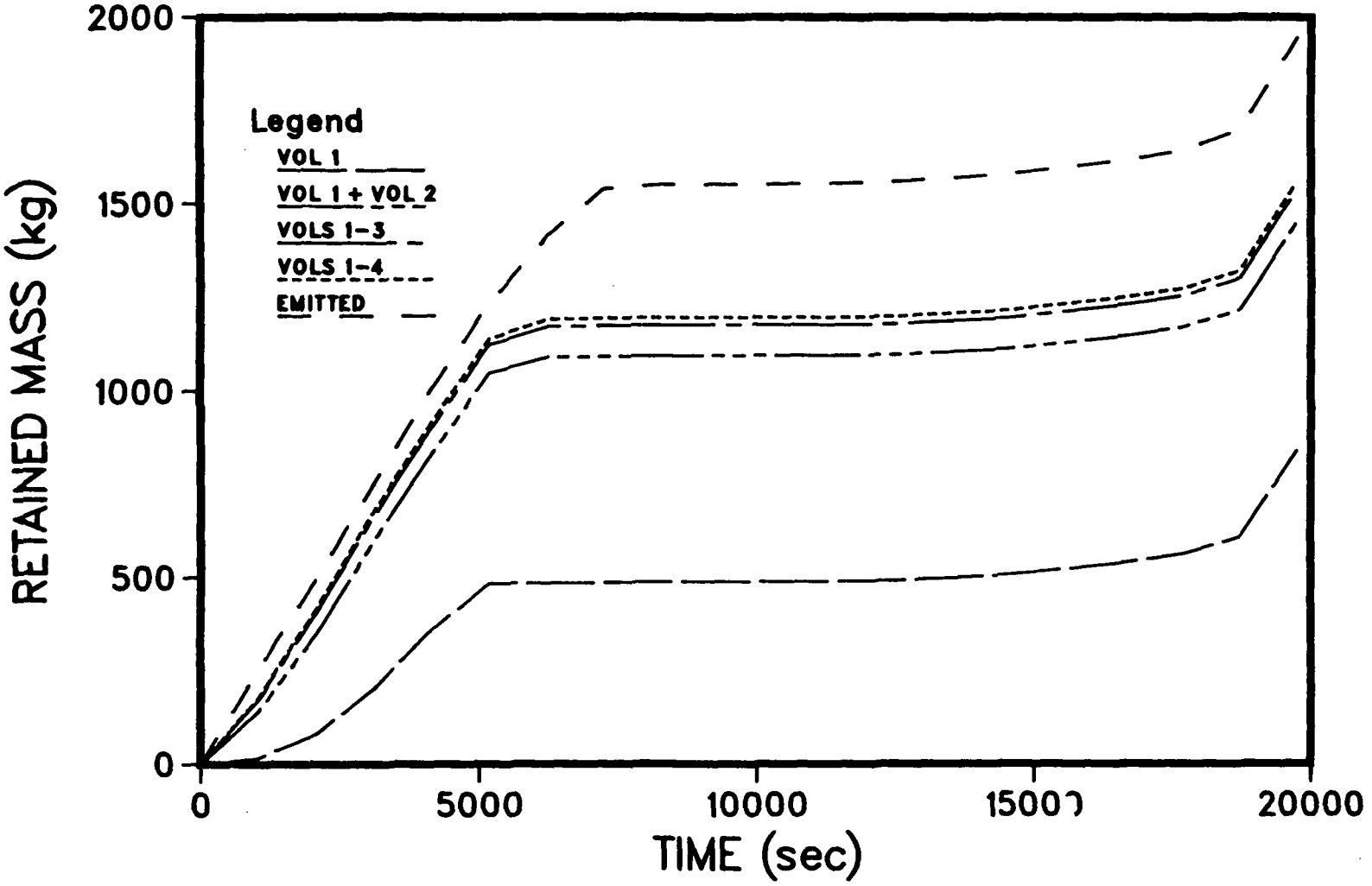

FIGURE 7.8. MASSES OF AEROSOL EMITTED FROM CORE AND RETAINED IN THE RCS CONTROL VOLUMES AS FUNCTIONS OF TIME FOR THE TPI SEQUENCE (Vol 1 = Core, Vol 2 = Steam Separators, Vol 3 = Steam Dryers, Vol 4 = Upper Annulus, Vol 5 = Relief Lines). Times Measured from Start of Core Melting.

TABLE 7.5. CORSOR PREDICTIONS OF MASSES OF SPECIES RELEASED FROM THE CORE (TOT) AND TRAP-MELT PREDICTIONS OF MASSES RETAINED IN THE RCS (RET) DURING THE TQUV SEQUENCE FOR THE GRAND GULF PLANT

(Times Measured from Start of Core Melting)

Time (s)	CsI		CsOH		Te		Aerosol	
	Ret (kg)	Tot (kg)	Ret (kg)	Tot (kg)	Ret (kg)	Tot (kg)	Ret (kg)	Tot (kg)
400	0.1	6.6	14.5	47.7	0.6	0.6	16.7	52.1
800	0.1	13.5	32.0	90.0	1.5	1.5	49.0	161
1210	0.4	18.4	49.1	120	2.6	2.8	87.0	301
1610	1.0	23.6	73.8	151	4.3	4.4	144	477
2010	1.6	27.1	91.5	173	6.0	6.3	232	666
2410	2.1	29.3	106	186	7.9	8.0	383	831
2820	2.8	31.2	115	198	9.1	9.2	405	948
3220	2.1	33.8	120	213	10.2	10.3	413	1050
3620	2.2	35.8	123	225	11.2	11.2	422	1160
4020	2.2	36.1	124	227	11.7	11.8	427	1192
5230	2.2	36.3	124	228	13.1	13.2	449	1312
6840	2.3	36.4	125	229	14.9	15.9	630	1540

TABLE 7.6. TRAP-MELT PREDICTIONS OF PRIMARY SYSTEM RETENTION FACTORS (RF) AND VOLUME SPECIFIC RETENTION FACTORS AS A FUNCTION OF TIME FOR THE TQUV SEQUENCE FOR THE GRAND GULF PLANT

(Times Measured from Start of Core Melting)

Time (s)	CsI		CsOH			Te		Aerosol			
	RF	Upper Annulus	RF	Steam Sep	Steam Dryers	RF	Steam Separators	RF	Core	Steam Sep	Steam Dryers
400	.01	.01	.30	.04	.25	.96	.79	.32	.31	-	-
800	.01	.01	.36	.05	.29	.96	.83	.30	.30	-	-
1210	.02	.02	.41	.07	.32	.95	.85	.29	.27	-	-
1610	.04	.04	.49	.09	.36	.97	.89	.30	.23	-	.03
2010	.06	.05	.53	.11	.37	.95	.81	.35	.18	.04	.08
2410	.07	.06	.57	.13	.39	.99	.93	.46	.16	.13	.12
2820	.09	.06	.58	.13	.40	1.00	.93	.43	.14	.11	.11
3220	.06	.06	.56	.12	.39	1.00	.92	.39	.13	.10	.10
3620	.06	.06	.55	.12	.38	1.00	.90	.37	.13	.09	.09
4020	.06	.06	.55	.12	.38	1.00	.90	.36	.13	.09	.09
5230	.06	.06	.54	.11	.38	.99	.89	.34	.13	.08	.08
6840	.06	.06	.54	.12	.38	.94	.85	.41	.21	.08	.08

reaction with RCS surfaces. Only a very small portion of the CsI and CsOH are predicted to condense on the surfaces since the system temperatures are significantly hotter than for the two sequences discussed above. This is illustrated in Figures 7.9 and 7.10. The Te retention shown in Figure 7.11 is also due to surface reactions. The reduction in aerosol retention depicted in Figure 7.12 for this sequence, relative to that observed in the TC case, is somewhat surprising, especially when the efficiency of the vapor-surface interaction is noted for the present case. The cause of the difference between the 74 percent retention exhibited in the TC sequence and the 41 given here is not apparent in the gross differences in the flow rates for these two sequences.

7.2.4 RCS Transport and Deposition for Sequence S_2E

The time interval between the start of core melting and the bottom head failure for the S_2E sequence is similar to that for the TQUV and TC sequences. This sequence is characterized by intermediate RCS pressures and by higher gas mass flow rates through the RCS than were predicted for the TQUV sequence.

Because of the high surface temperatures experienced in this sequence and the high flow rates, the RCS retention of CsI and CsOH is not great. The retention of these species throughout the RCS and in specific regions within the RCS are shown in Tables 7.7 and 7.8. The difference in the mass flow rates through the system between this sequence and TQUV is responsible for the much lower retention of CsOH seen here. Of the CsOH retained, just over half is retained due to the chemical reaction of this species with the system surfaces. With longer residence times, the amount of vapor retained via this mechanism would increase. Figures 7.13 and 7.14 illustrate the release of some of the condensed vapor due to an increasing surface temperature, especially in control volume 3 around 1500 s. These surface temperatures decrease after t = 1900 and thereby prevent much further reevaporation.

The Te retention in the RCS is in excess of 90 percent for this sequence and is illustrated in Figure 7.15. Most of the retention occurs on the top guide structure and stand pipes due to their high surface areas.

The aerosol retention in the RCS for S_2E is lower than for any other sequence analyzed for this plant due to the higher gas flow rates which are

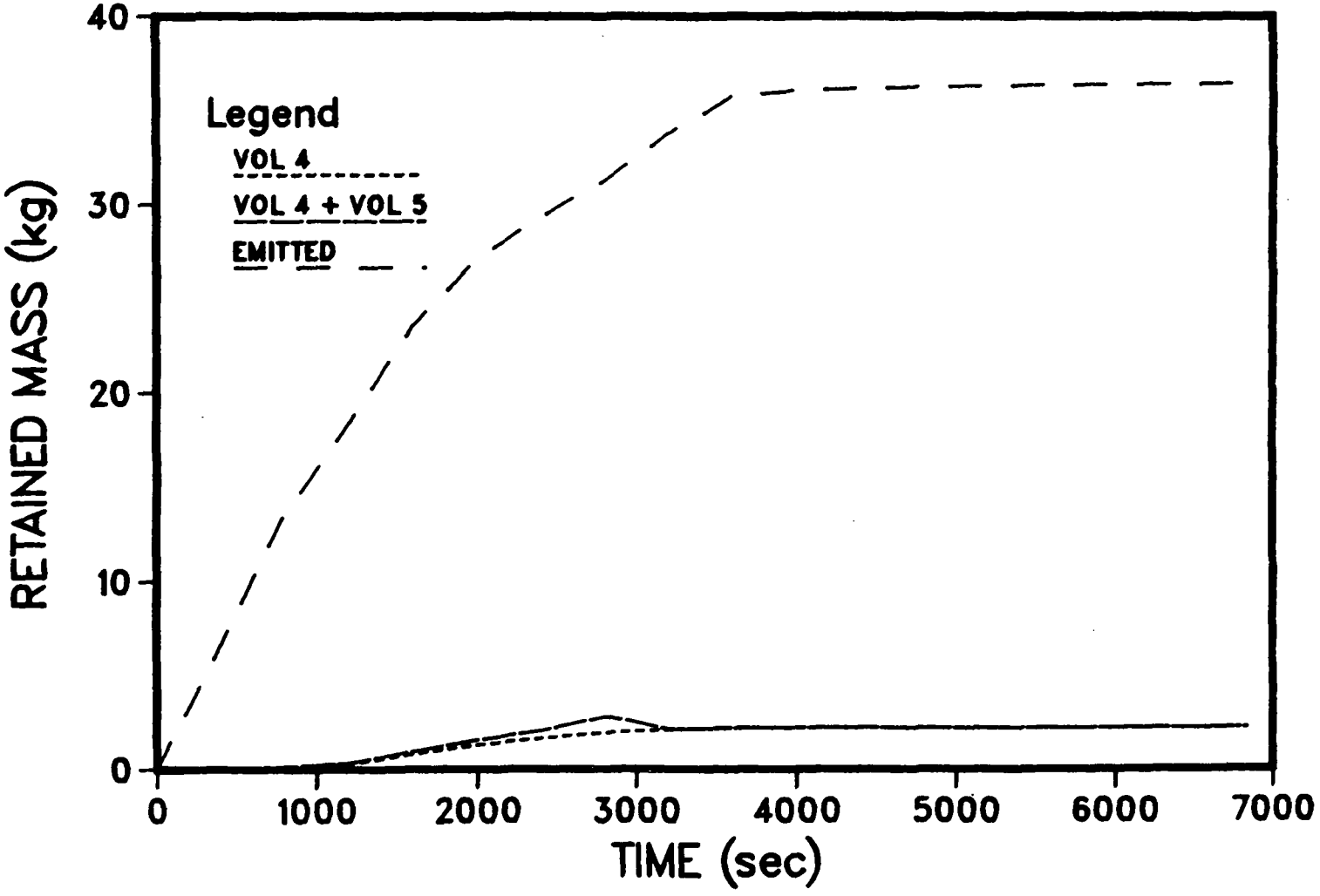

FIGURE 7.9. MASSES OF CsI EMITTED FROM CORE AND RETAINED IN THE RCS CONTROL VOLUMES AS FUNCTIONS OF TIME FOR THE TQUV SEQUENCE (Vol 1 = Core, Vol 2 = Steam Separators, Vol 3 = Steam Dryers, Vol 4 = Upper Annulus, Vol 5 = Relief Lines). Times Measured from Start of Core Melting.

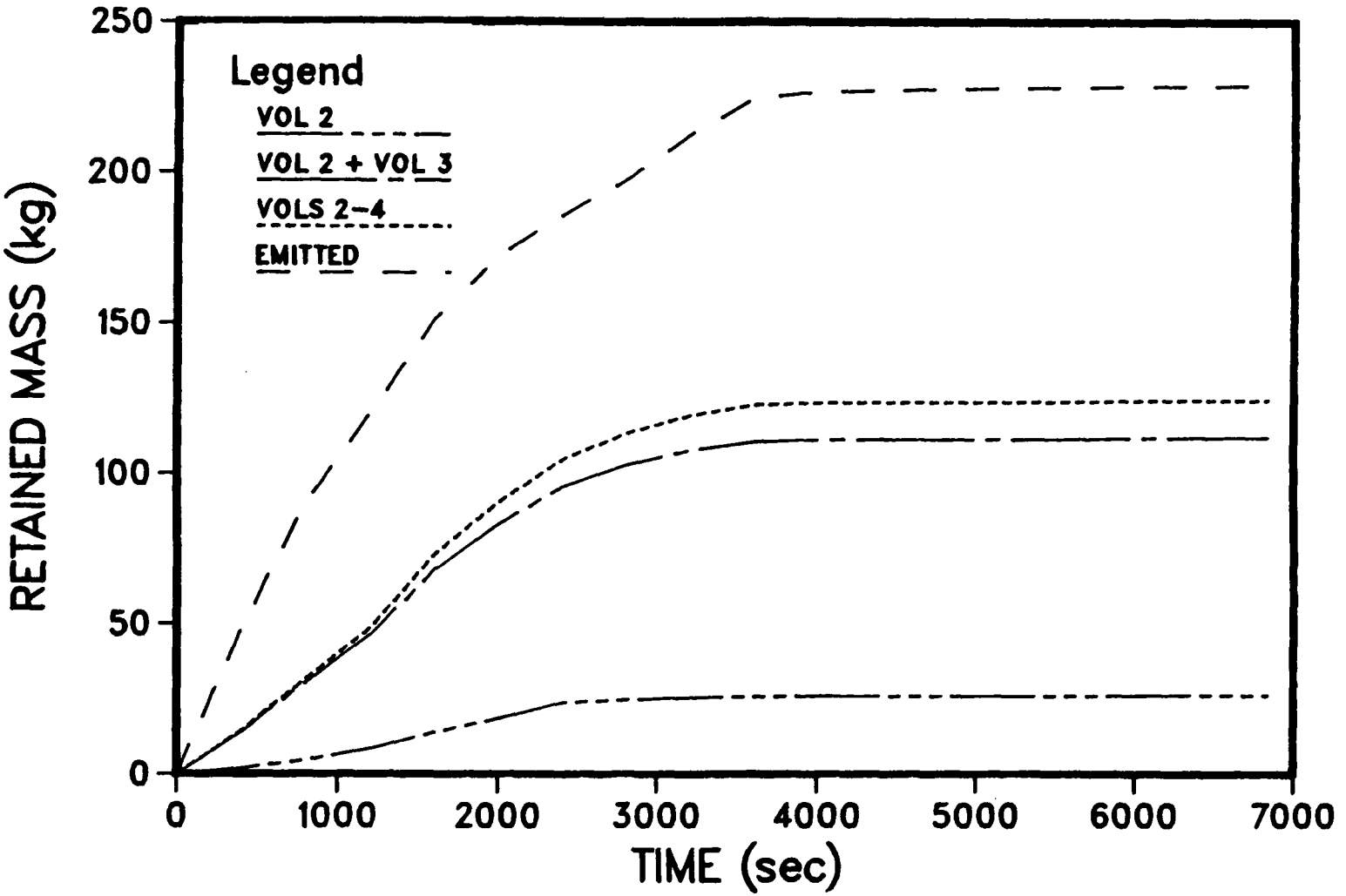

FIGURE 7.10. MASSES OF CsOH EMITTED FROM CORE AND RETAINED IN THE RCS CONTROL VOLUMES AS FUNCTIONS OF TIME FOR THE TQUV SEQUENCE (Vol 1 = Core, Vol 2 = Steam Separators, Vol 3 = Steam Dryers, Vol 4 = Upper Annulus, Vol 5 = Relief Lines). Times Measured from Start of Core Melting.

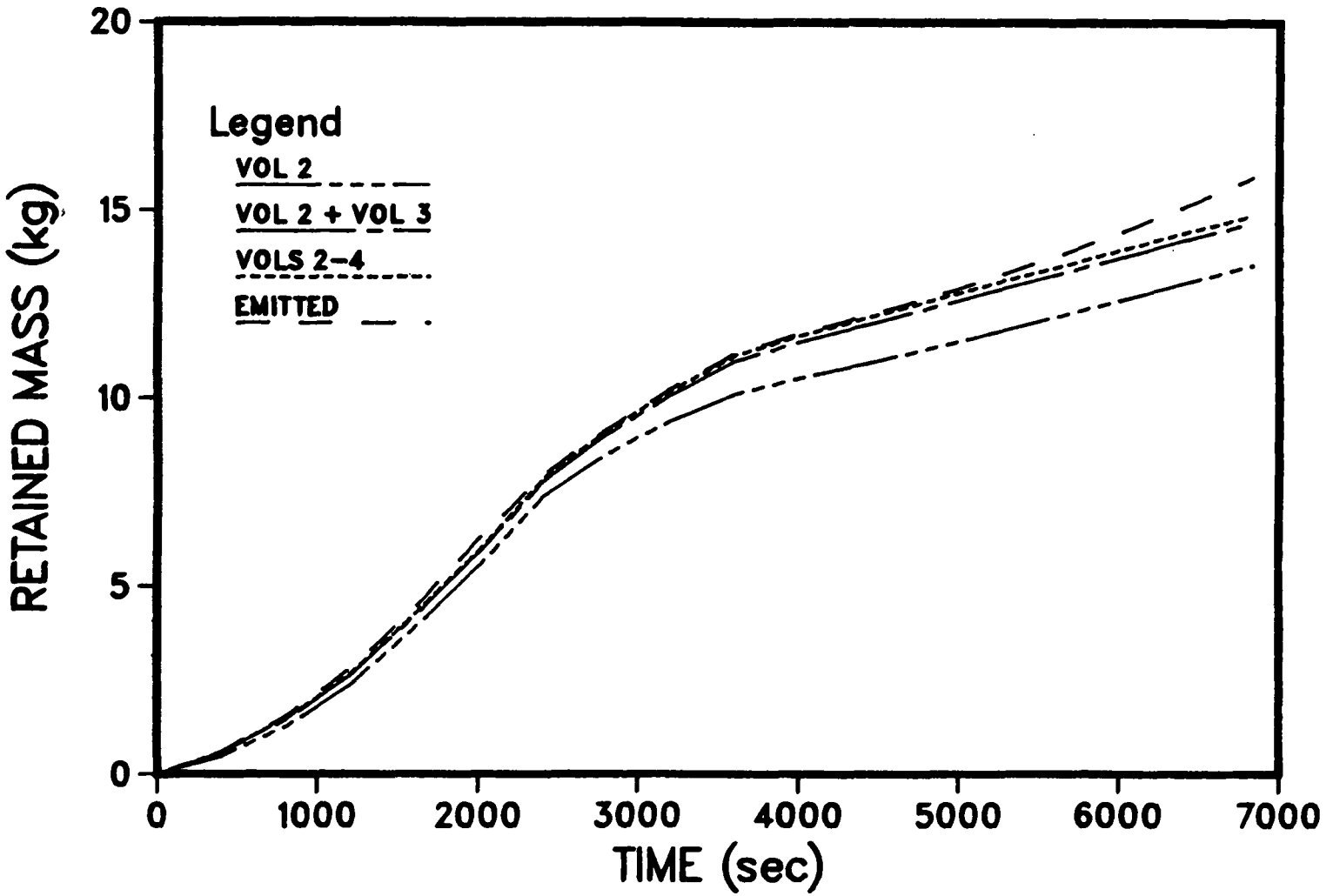

FIGURE 7.11. MASSES OF Te EMITTED FROM CORE AND RETAINED IN THE RCS CONTROL VOLUMES AS FUNCTIONS OF TIME FOR THE TQUV SEQUENCE (Vol 1 = Core, Vol 2 = Steam Separators, Vol 3 = Steam Dryers, Vol 4 = Upper Annulus, Vol 5 = Relief Lines). Times Measured from Start of Core Melting.

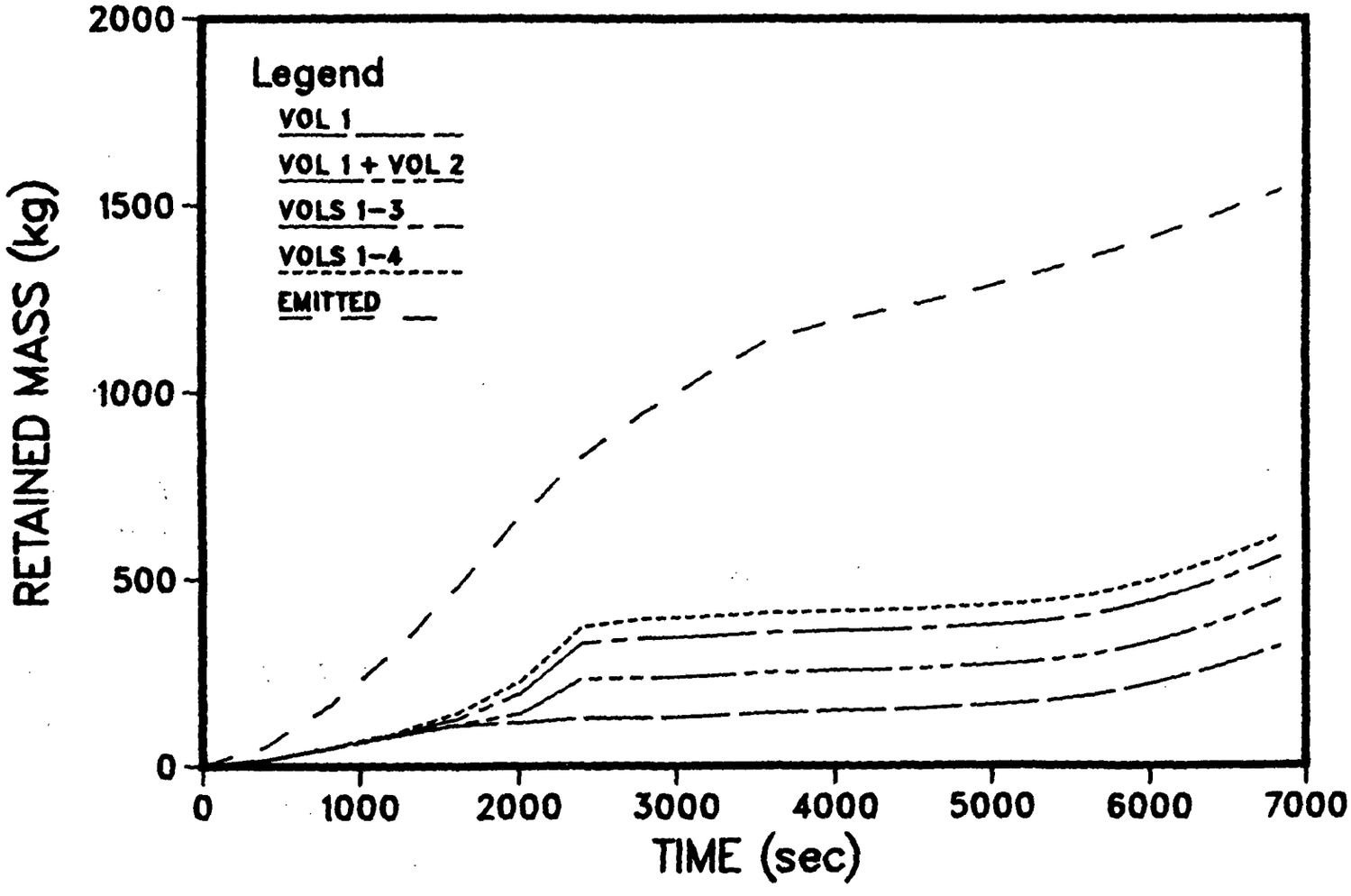

FIGURE 7.12. MASSES OF AEROSOL EMITTED FROM CORE AND RETAINED IN THE RCS CONTROL VOLUMES AS FUNCTIONS OF TIME FOR THE TQUV SEQUENCE (Vol 1 = Core, Vol 2 = Steam Separators, Vol 3 = Steam Dryers, Vol 4 = Upper Annulus, Vol 5 = Relief Lines). Times Measured from Start of Core Melting.

TABLE 7.7. CORSOR PREDICTIONS OF MASSES OF SPECIES RELEASED FROM THE CORE (TOT) AND TRAP-MELT PREDICTIONS OF MASSES RETAINED IN THE RCS (RET) DURING THE S_2E SEQUENCE FOR THE GRAND GULF PLANT

(Times Measured from Start of Core Melting)

Time (s)	CsI		CsOH		Te		Aerosol	
	Ret (kg)	Tot (kg)	Ret (kg)	Tot (kg)	Ret (kg)	Tot (kg)	Ret (kg)	Tot (kg)
290	-	0.9	1.0	12.4	-	-	0.2	3.8
880	0.6	11.7	8.7	78.1	0.5	0.6	3.3	91.1
1470	4.3	24.8	37.1	158	1.9	1.9	47.8	329
2050	3.5	30.6	35.8	193	3.1	3.2	68.0	531
2640	3.3	35.4	36.5	226	4.5	4.7	76.4	754
3230	3.2	36.2	36.3	227	5.6	5.7	80.4	866
3810	3.3	36.4	36.4	228	6.3	6.5	82.9	938
4400	3.3	36.4	36.4	229	7.3	8.5	97.4	1090
4990	3.3	36.4	36.4	229	8.3	8.6	125	1150
5870	3.3	36.4	36.4	229	9.5	10.3	266	1304

TABLE 7.8. TRAP-MELT PREDICTIONS OF PRIMARY SYSTEM RETENTION FACTORS (RF) AND VOLUME SPECIFIC RETENTION FACTORS AS A FUNCTION OF TIME FOR THE S_2E SEQUENCE FOR THE GRAND GULF PLANT

(Times Measured from Start of Core Melting)

Time (s)	CsI			CsOH				Te			Aerosol		
	RF	Stand Pipes	Lower Outer Annulus	RF	Top Guide	Stand Pipes	Lower Outer Annulus	RF	Top Guide	Stand Pipes	RF	Core	Lower Outer Annulus
290	.03	.01	.01	.08	.04	.01	.01	.90	.75	.10	.04	.02	-
880	.05	.02	.01	.11	.05	.02	.01	.94	.81	.10	.04	-	.01
1470	.17	.07	.06	.23	.06	.07	.05	.98	.82	.11	.15	.04	.05
2050	.11	.04	.08	.19	.05	.04	.08	.98	.77	.13	.13	.06	.04
2640	.10	.02	.07	.16	.05	.03	.07	.97	.70	.17	.10	.05	.03
3230	.09	.02	.07	.16	.05	.03	.07	.97	.66	.19	.09	.05	.02
3810	.09	.02	.07	.16	.05	.03	.07	.97	.66	.19	.09	.05	.02
4400	.09	.02	.07	.16	.05	.03	.07	.97	.66	.18	.08	.04	.02
4990	.09	.02	.07	.16	.05	.03	.07	.96	.67	.16	.11	.05	.02
5870	.09	.02	.07	.16	.05	.03	.07	.92	.67	.14	.20	.12	.03

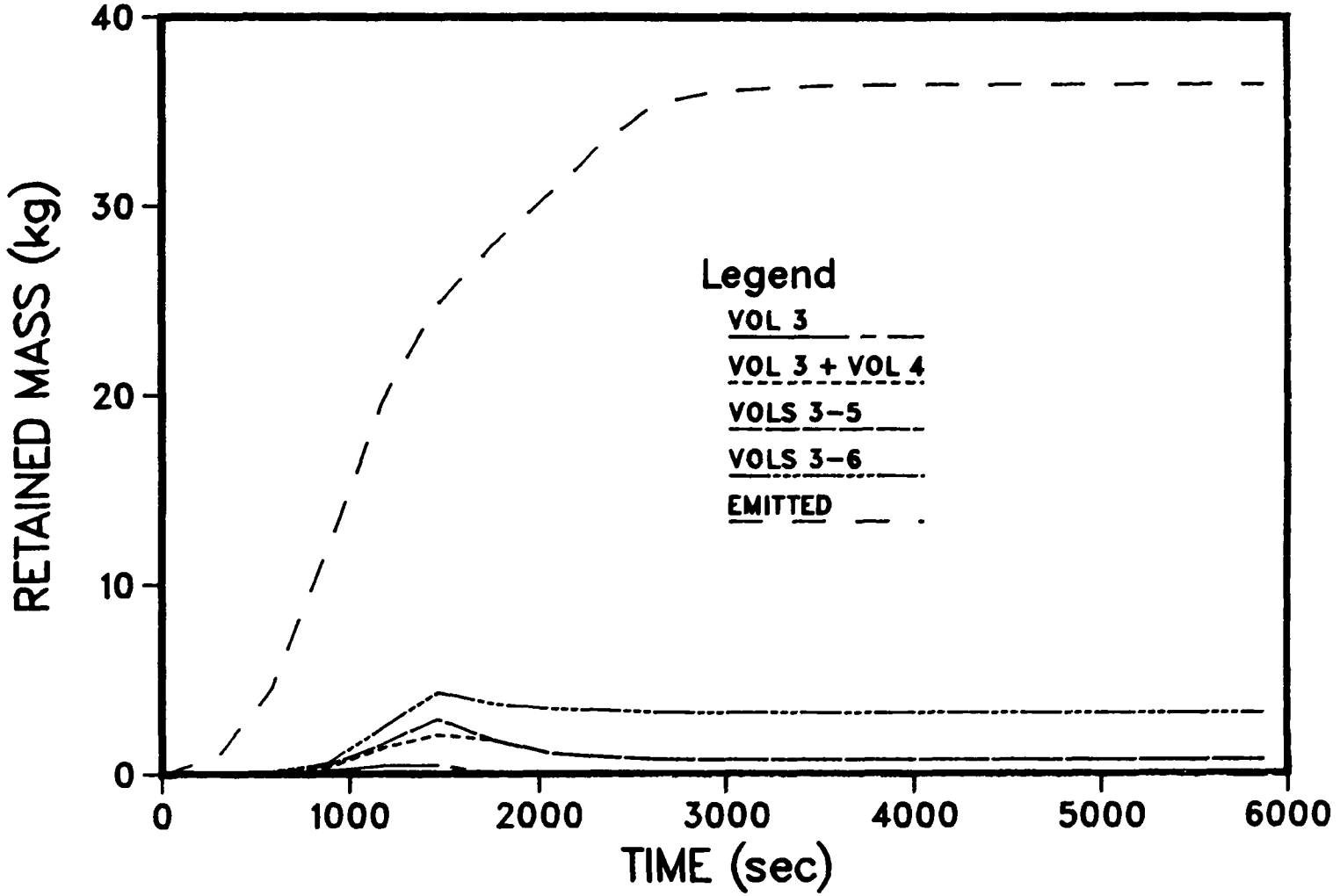

FIGURE 7.13. MASSES OF CsI EMITTED FROM CORE AND RETAINED IN THE RCS CONTROL VOLUMES AS FUNCTIONS OF TIME FOR THE S_2E SEQUENCE (Vol 1 = Core, Vol 2 = Top Guide, Vol 3 = Shroud Dome, Vol 4 = Stand Pipes, Vol 5 = Steam Separators, Vol 6 = Lower Outer Annulus). Times Measured from Start of Core Melting.

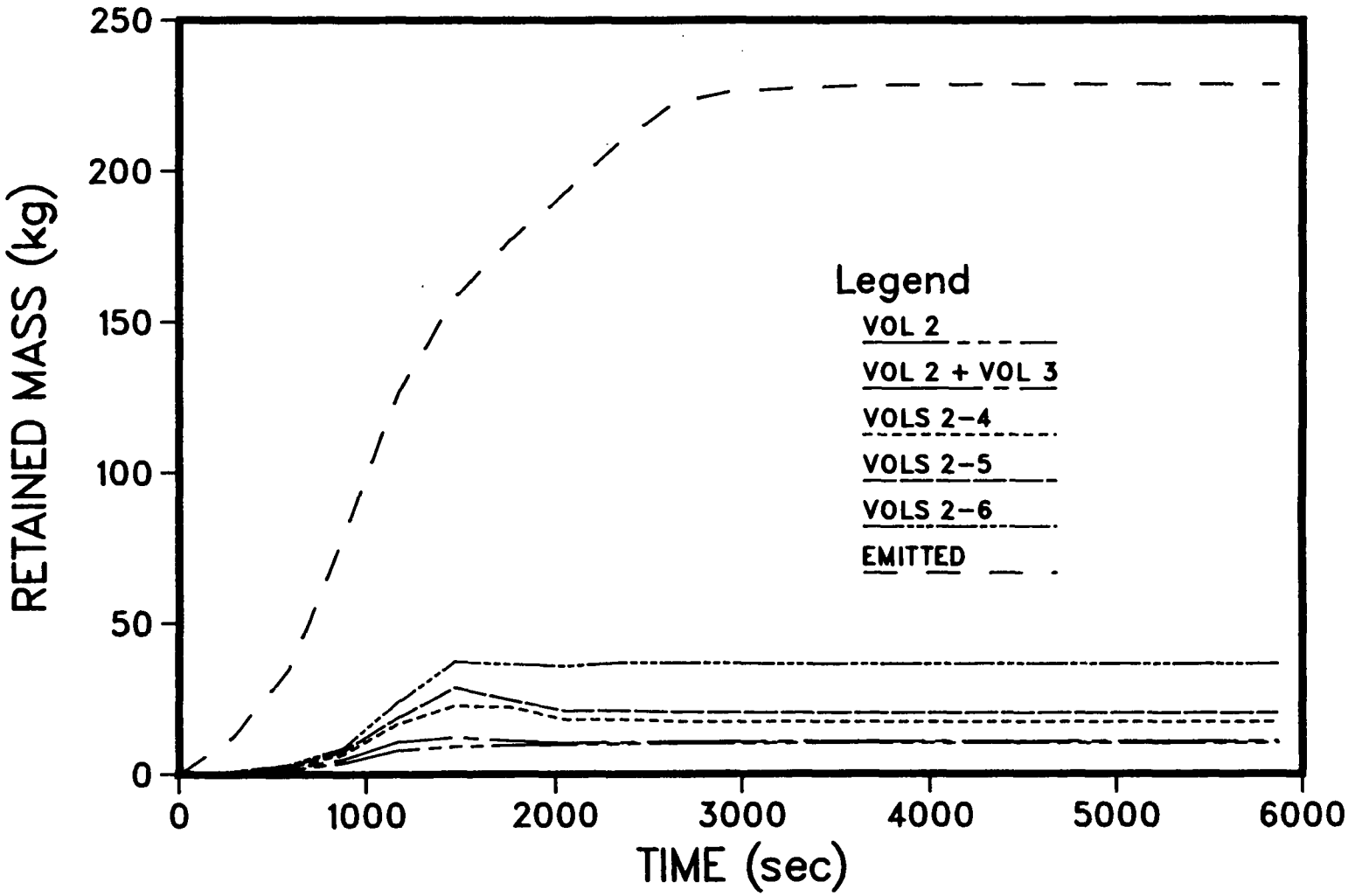

FIGURE 7.14. MASSES OF CsOH EMITTED FROM CORE AND RETAINED IN THE RCS CONTROL VOLUMES AS FUNCTIONS OF TIME FOR THE S_2E SEQUENCE (Vol 1 = Core, Vol 2 = Top Guide, Vol 3 = Shroud Dome, Vol 4 = Stand Pipes, Vol 5 = Steam Separators, Vol 6 = Lower Outer Annulus). Times Measured from Start of Core Melting.

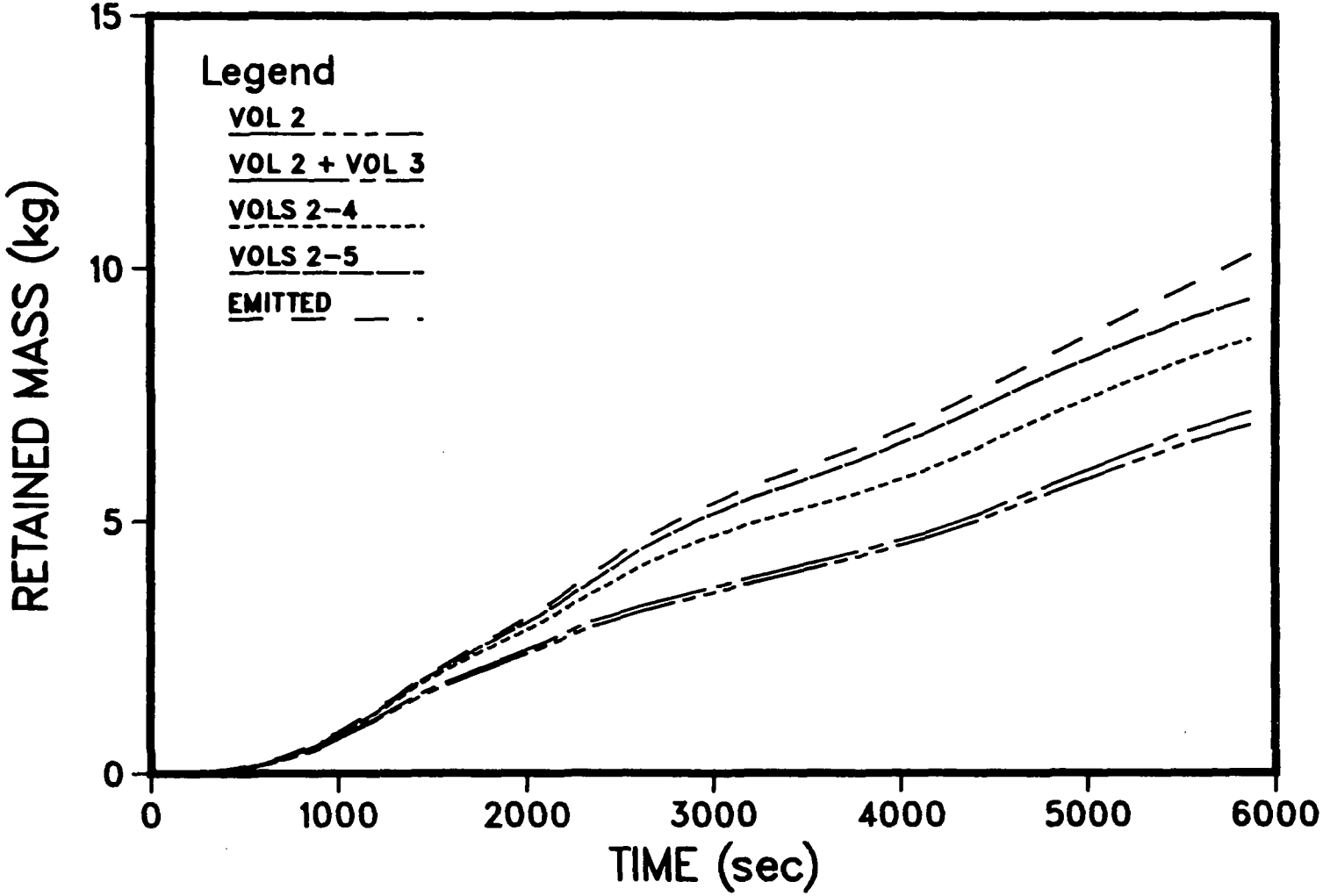

FIGURE 7.15. MASSES OF Te EMITTED FROM CORE AND RETAINED IN THE RCS CONTROL VOLUMES AS FUNCTIONS OF TIME FOR THE S_2E SEQUENCE (Vol 1 = Core, Vol 2 = Top Guide, Vol 3 = Shroud Dome, Vol 4 = Stand Pipes, Vol 5 = Steam Separators, Vol 6 = Lower Outer Annulus). Times Measured from Start of Core Melting.

predicted for this sequence. This causes lower residence times for the released aerosol in the RCS, and the smaller mass of aerosol results in lower concentrations also acts to lessen the extent of retention by reducing particle growth via agglomeration. In Figure 7.16, one can see the aerosol retention increasing after t = 5000 s due to the greatly reduced flow rate during this final period of the in-vessel portion of the accident.

7.3 Transport of Fission Products Through Containment

Results are presented in this section for analyses performed for the transport and retention of various fission products that leave the reactor coolant system. The various compartments of the reactor considered for these analyses include the suppression pool, the drywell, and the reactor containment building. The NAUA code that calculates transport of fission products in particulate form was utilized for the mentioned compartments except that the SPARC code was utilized for calculating the retention of fission products in the suppression pool.

In general, the containment codes used here need information on the thermal hydraulic conditions of an accident of interest. The conditions provided by the MARCH computer calculation were used. The typical required thermal hydraulic conditions are time-dependent containment temperature, pressure, and wall temperature, and the rates at which steam enters the containment, condenses on the containment structure, and leaks from the containment.

Perhaps the most important and critical input that containment codes also need is the fission product source term for both vapor and particulates. The source rates calculated as release from the primary system (TRAP-MELT code) and the VANESA code calculations for release during the core-concrete interaction were taken for the melt and vaporization releases, respectively. For the NAUA calculations, CsI, CsOH, and Te were distinguished and all the other species were treated as one group. All these species were assumed to be in the particulate form in the containment atmosphere because the temperature and pressure under the containment conditions indicated that these species will remain as particulates for all practical circumstances. Although it was assumed in the calculation that individual species are distributed evenly over all sizes of particulates, differential amounts of these species at a given time

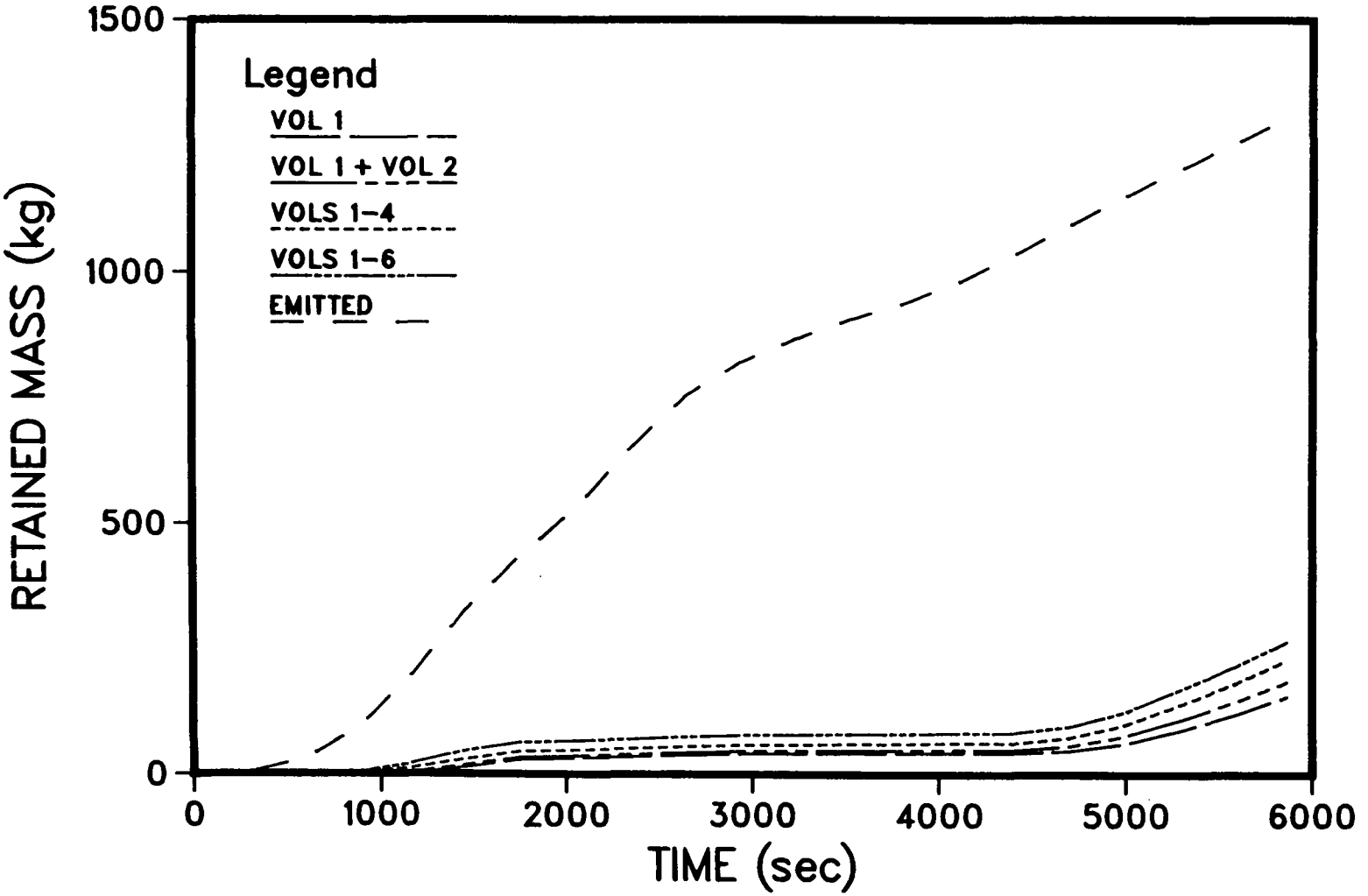

FIGURE 7.16. MASSES OF AEROSOL EMITTED FROM CORE AND RETAINED IN THE RCS CONTROL VOLUMES AS FUNCTIONS OF TIME FOR THE S_2E SEQUENCE (Vol 1 = Core, Vol 2 = Top Guide, Vol 3 = Shroud Dome, Vol 4 = Stand Pipes, Vol 5 = Steam Separators, Vol 6 = Lower Outer Annulus). Times Measured from Start of Core Melting.

due to different source timings were taken into consideration in the calculations.

Dimensions of the compartment volumes were based on geometric data provided in Chapter 4. The largest cross sectional area of a volume was used to estimate the floor area. This area directly affects the removal rate for particle sedimentation.

Four different accident sequences, TC, TPI, TQUV, and S_2E were considered in the present calculations. The S_2E sequence was analyzed assuming two different suppression pool bypass leak rates as described below.

7.3.1 TC Sequence

In this accident sequence heat and steam generated in the core are transmitted to the suppression pool causing the pool temperature and the containment pressure to rise to the containment failure level. Subsequently, the core starts melting and the fission products released from the RCS enter the containment. The flow path is such that the fission products released from the relief valve enter the suppression pool through the X quenchers and reach the containment before being released to the environment. As the reactor vessel fails, the fission products released from the core-concrete interaction enter directly into the drywell and are then passed through the suppression pool before being released to the failed containment. The sequential use of various computer codes for calculating the transport of fission products in this accident sequence is shown in Figure 7.17.

Since the first volume fission products encounter after being released from the RCS for the TC sequence is the suppression pool, the SPARC code was utilized to calculate the retention of fission products by the pool. The decontamination factors calculated are listed in Table 7.9. This table shows a particle size dependency that is similar to that shown previously for the TC sequence for the Peach Bottom reactor. Time variations of the calculated decontamination factor for 0.1 and 0.7 μm particles are, of course, due to the difference in the thermal hydraulic condition that prevails at the corresponding times. It should be noted that in this sequence the pool temperature is close to the boiling temperature during the period of interest and the decontamination factor is not very high.

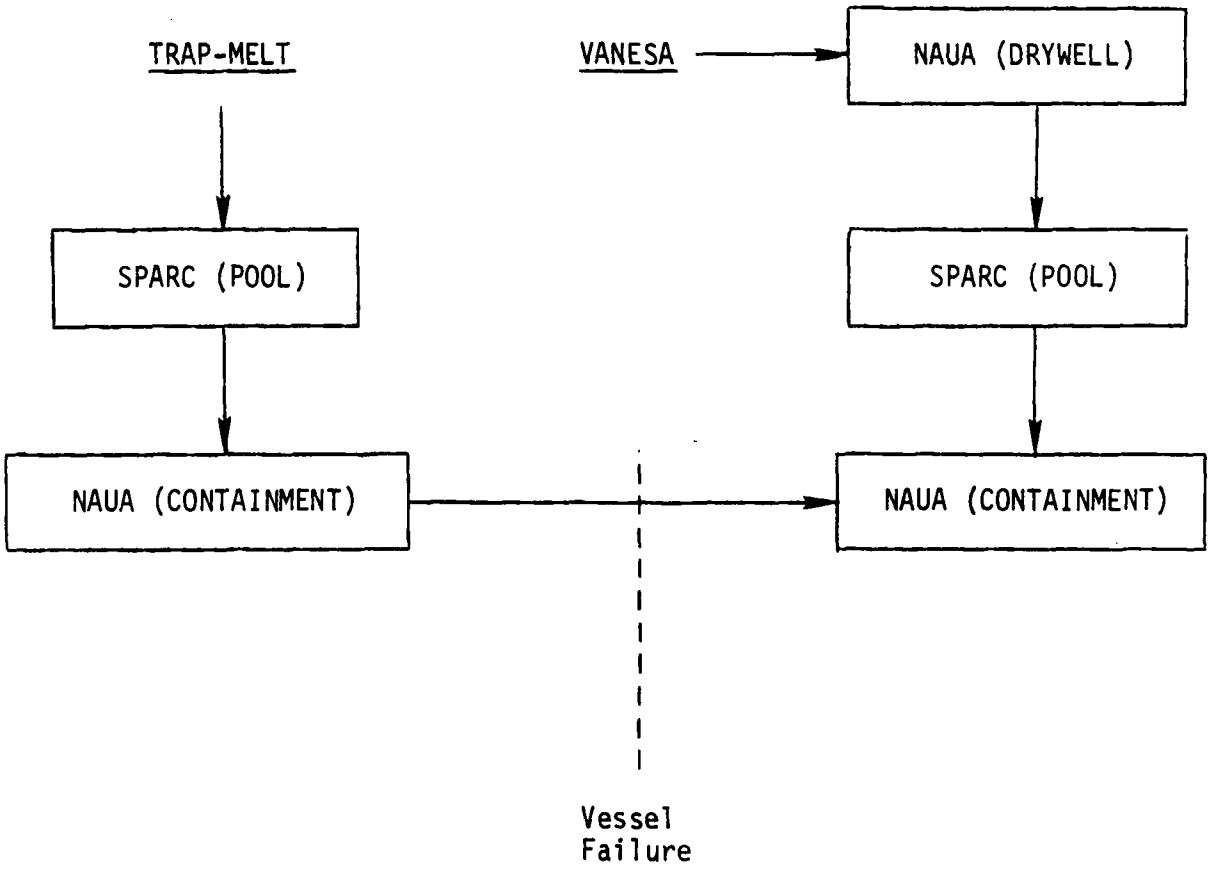

FIGURE 7.17. NAUA AND SPARC CALCULATION PATHS USED FOR PERFORMING ANALYSES OF TC AND TPI SEQUENCES

TABLE 7.9. DECONTAMINATION FACTORS CALCULATED AS A FUNCTION OF PARTICLE SIZE AND OF TIME FOR TC

Time (min)	Particle Diameter (μm) 0.1	0.7	1.2	5.1	8.4	DF Based on Total Mass
118	1.3	10^5(a)	10^5	10^5	10^5	1400
158	1.7	10^5	10^5	10^5	10^5	81500
207	6.9	10^5	10^5	10^5	10^5	47
258	1.02	8.6	1.63×10^3	10^5	10^5	43
300	1.04	10.6	2.35×10^3	10^5	10^5	59
400	1.1	17.3	3.95×10^3	10^5	10^5	60
618	1.15	23.3	5.86×10^3	10^5	10^5	27

(a) A decontamination factor larger than 10^5 is assumed to be 10^5.

Pool depth: 17' 10" (543 cm) up to vessel failure and 12' 10" (390 cm) thereafter.

Bubble diameter: 0.75 cm
Axes ratio: 1:3

Figure 7.18 is the suspended aerosol mass as a function of time for the containment. Sharp increases in the mass concentration as shown in Figure 7.18 represent the initial core melting time and the bottom head failure time, respectively. Figure 7.19 is the average radius of the aerosol mass suspended in the containment. It is interesting to note that due to the presence of the suppression pool, which removes predominantly large particles, the particle size in the containment is relatively small.

Table 7.10 is the calculated distribution of the CsI, CsOH, and Te that are located in the RCS, the suppression pool, the drywell, and the containment. The last column indicates that fractions of core inventory of these species between 3.5×10^{-4} to 8.8×10^{-3} are released to the environment. It is also noted that fractions of 0.77 for CsI, 0.49 for CsOH, and 0.45 for Te are captured in the suppression pool.

7.3.2 TPI Sequence

In this accident sequence a safety valve is stuck in the open position and suppression pool heat removal has failed; as in the TC sequence, the suppression pool temperature rises, causing the containment pressure subsequently to reach the failure point. For the purpose of performing calculations, this sequence is identical to that for the TC sequence in that the flow paths of fission products are the same and that the containment failure occurs before fission products are released from the RCS. However, the time scale for the present sequence is much more extended than that for the TC sequence. The key accident events and containment conditions used in the TPI analysis are given in Section 6.1.3.

Generally a calculation procedure similar to that adopted for the TC sequence was used. The sequential use of various computer codes depending upon the accident events is shown in Figure 7.17. The decontamination factors calculated by the SPARC code are listed in Table 7.11. It is shown in the table that the overall decontamination factor of the suppression pool ranges from 1.0 to 10^5. The calculated decontamination factor depends not only upon the thermal hydraulic conditions in the suppression pool but upon the particle size distribution of the aerosol entering the pool. For example, at 2100 minutes, the mass median particle size entering the suppression pool is found

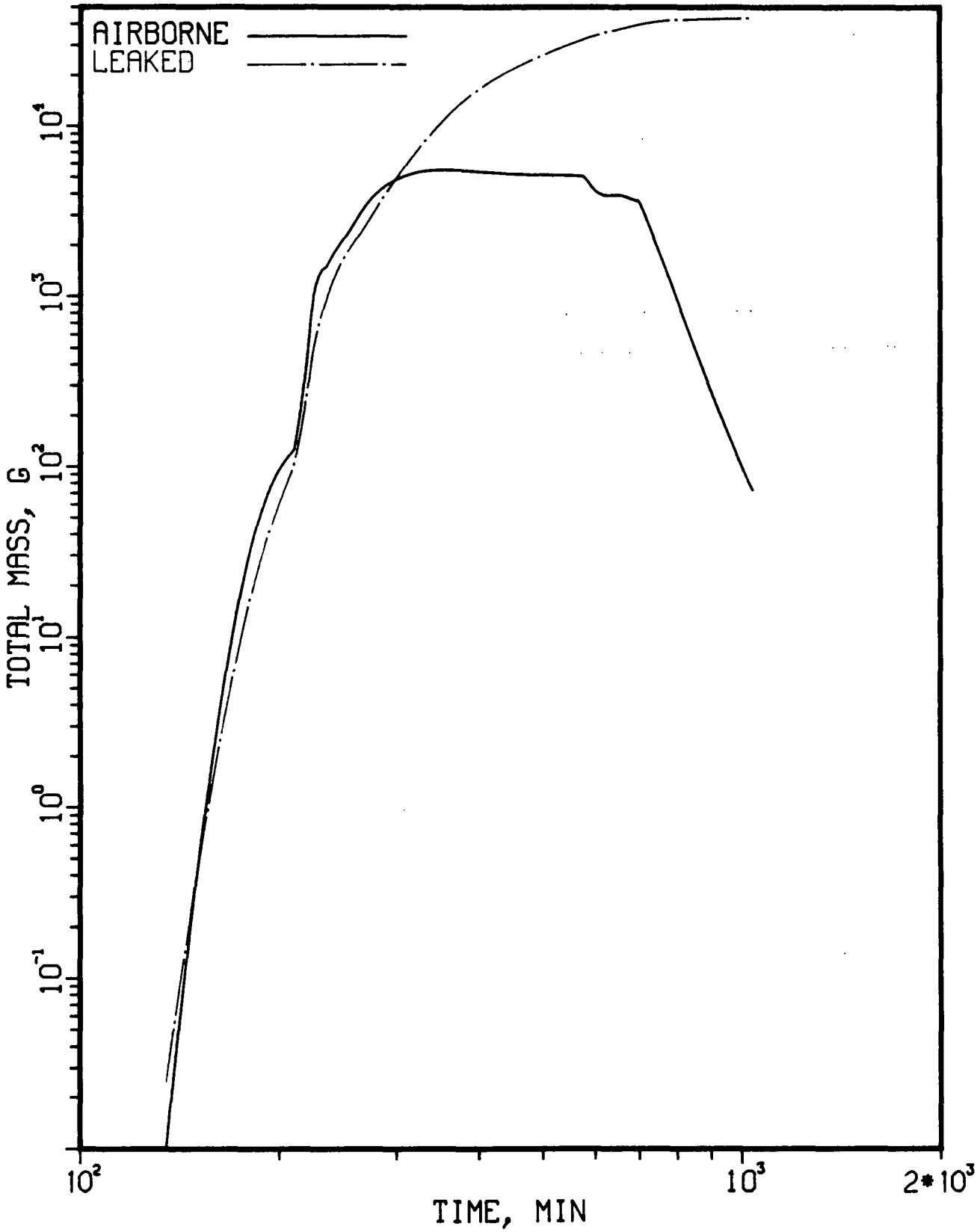

FIGURE 7.18. SUSPENDED AND LEAKED AEROSOL MASS IN THE CONTAINMENT (TC)

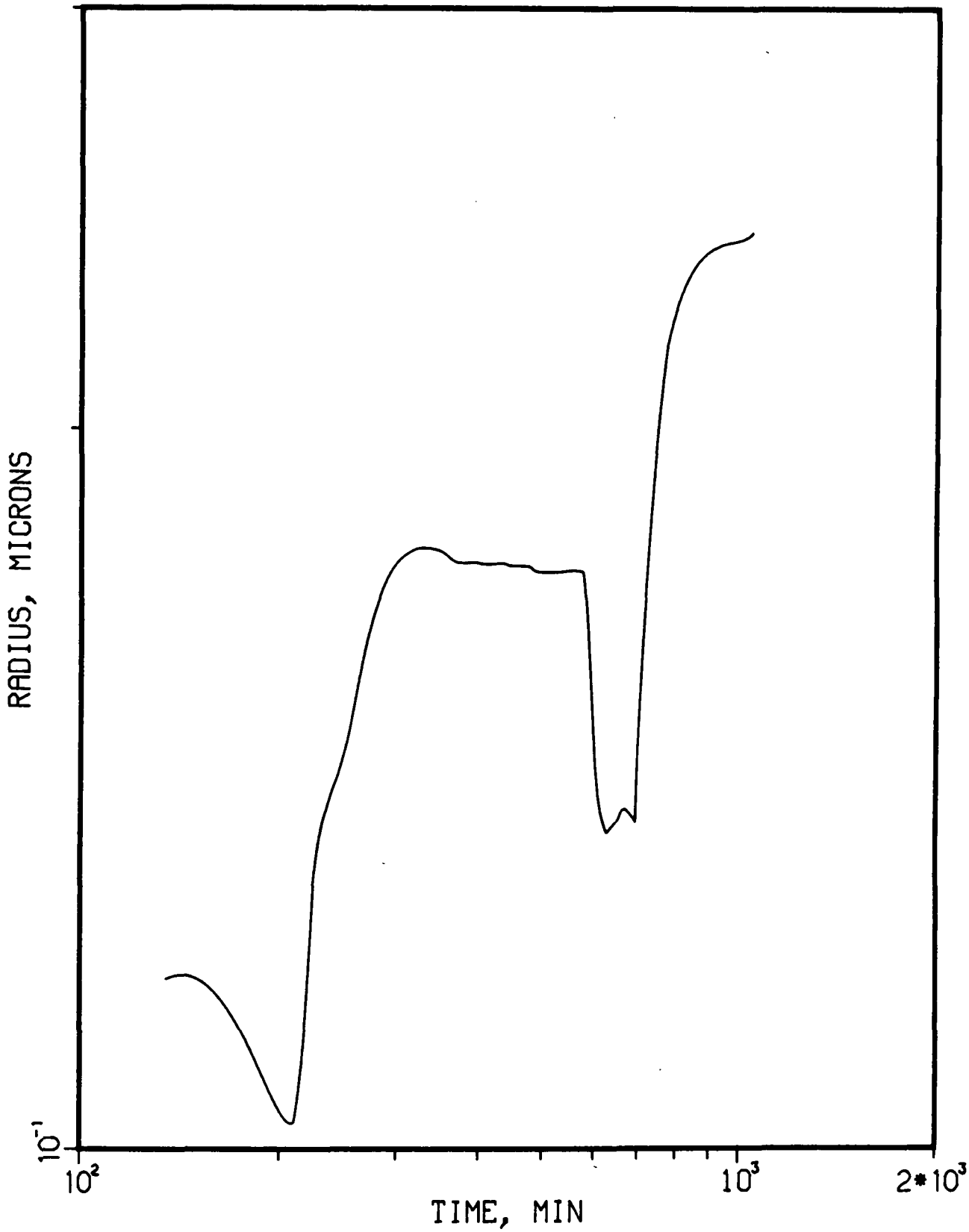

FIGURE 7.19. AVERAGE RADIUS OF AIRBORNE PARTICLES IN THE CONTAINMENT (TC)

TABLE 7.10. DISTRIBUTION OF SPECIES AT 25 HOURS AFTER ACCIDENT, TC

Species	Fraction of Core Inventory				
	RCS	Drywell	Pool	Containment	Environment
CsI	0.19	3.6×10^{-2}	0.77	1.9×10^{-4}	6.8×10^{-3}
CsOH	0.51	1.4×10^{-3}	0.49	9.2×10^{-6}	3.5×10^{-4}
Te	0.22	0.32[a]	0.45	4.3×10^{-4}	8.8×10^{-3}

(a) This number includes a fraction of 0.26 for Te not being released from the core-concrete interaction.

$3.5 \times 10^{-4} \times .9 =$

$+ 6.8 \times 10^{-3} \times .1 = 6.8 \times 10^{-4}$ $= 3.50 - 4$

$+ 6.8 - 4$

10.30×10^{-4}

TABLE 7.11. DECONTAMINATION FACTORS CALCULATED AS A FUNCTION OF PARTICLE SIZE AND OF TIME FOR TPI SEQUENCE

Time (min)	Particle Diameter (μm) 0.1	0.4	1.2	5.1	8.4	DF Based on Total Mass
1650	1.95	37.7	10^{5}(a)	10^{5}	10^{5}	23300
1750	11.2	6.69×10^{3}	10^{5}	10^{5}	10^{5}	14000
1850	34.5	141	10^{5}	10^{5}	10^{5}	8080
2004	7.3	15.8	10^{5}	10^{5}	10^{5}	284
2100	1.19	1.73	1.61×10^{3}	10^{5}	10^{5}	45.1
2200	1.08	1.66	1.82×10^{3}	10^{5}	10^{5}	77.4
2400	1.14	2.18	3.36×10^{3}	10^{5}	10^{5}	73.0

(a) A decontamination factor larger than 10^{5} is assumed to be 10^{5}.

Pool depth: 17' 10" (543 cm) up to vessel failure and 12' 10" (390 cm) thereafter.

Bubble diameter: 0.75 cm
Axes ratio: 1:3

to be about 1.0 μm causing the overall decontamination factor at that time to become as high as 45.1

Figure 7.20 is the calculated airborne mass as a function of time for the containment and Figure 7.21 is accumulated mass leaked out to the atmosphere. Table 7.12 is the locational distribution of various species as fraction of core inventory. It should be noted that a relatively small amount of core inventory fraction was found to be released. Compared to the TW sequence for the Peach Bottom reactor in which after the vessel failure the fission products bypass the suppression pool and are released directly to the atmosphere via the drywell, the flow paths in the present sequence are such that the released fission products enter the suppression pool regardless when they are released from the fuel. Since the suppression pool is a comparatively efficient means for scrubbing particulate matter, the overall fraction of the fission products that leave the reactor as shown in Table 7.12 is lower than that found for the Peach Bottom reactor.

7.3.3 TQUV Sequence

For analyzing this accident sequence three different flow paths were utilized depending upon the time to be examined compared to various prescribed accident events. Between the time of core melting and the head failure, the fission products enter the suppression pool via the safety valves and then reach the containment. Since it is predicted that the containment is intact during this period, the fission products transported into the containment are expected to undergo various aerosol behavior mechanisms, such as agglomeration and deposition. As the vessel fails, the fission products are released to the drywell and enter the suppression pool through the vents before reaching the containment. It should be mentioned that unlike in the TC and TPI sequences, the suppression pool here remains in a subcooled state over a long time period, thereby resulting in a comparatively high efficiency of retaining the fission products. After the containment fails due to the buildup of noncondensible gases, the fission products suspended in the containment as well as those still being transported to the containment through the suppression pool become released to the environment passing along the established leakage flows. It should be noted that sequential use of the NAUA and SPARC codes for the analyses for the TQUV sequence is essentially similar to that shown in Figure 7.17, if

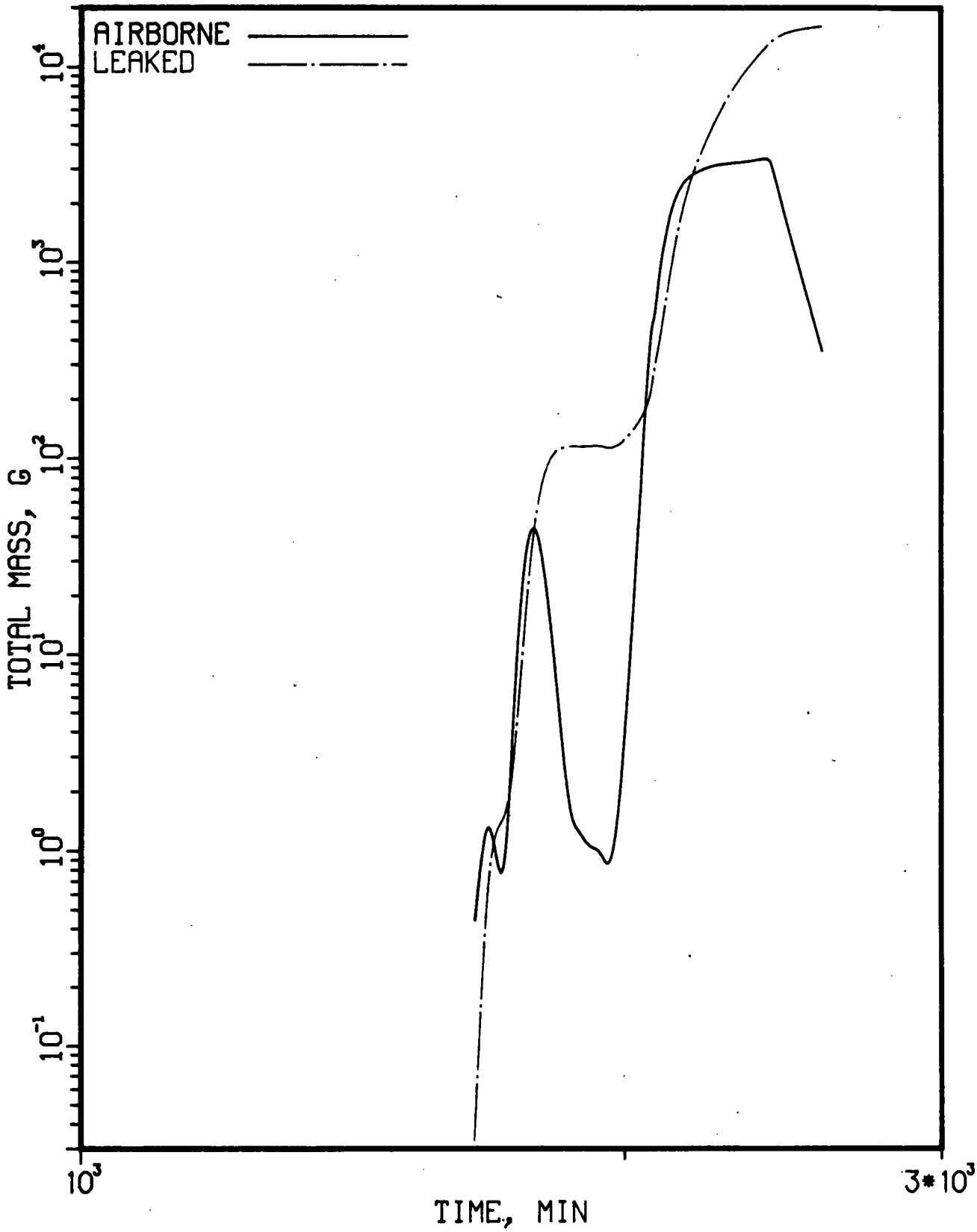

FIGURE 7.20. SUSPENDED AND LEAKED AEROSOL MASS IN THE CONTAINMENT (TPI)

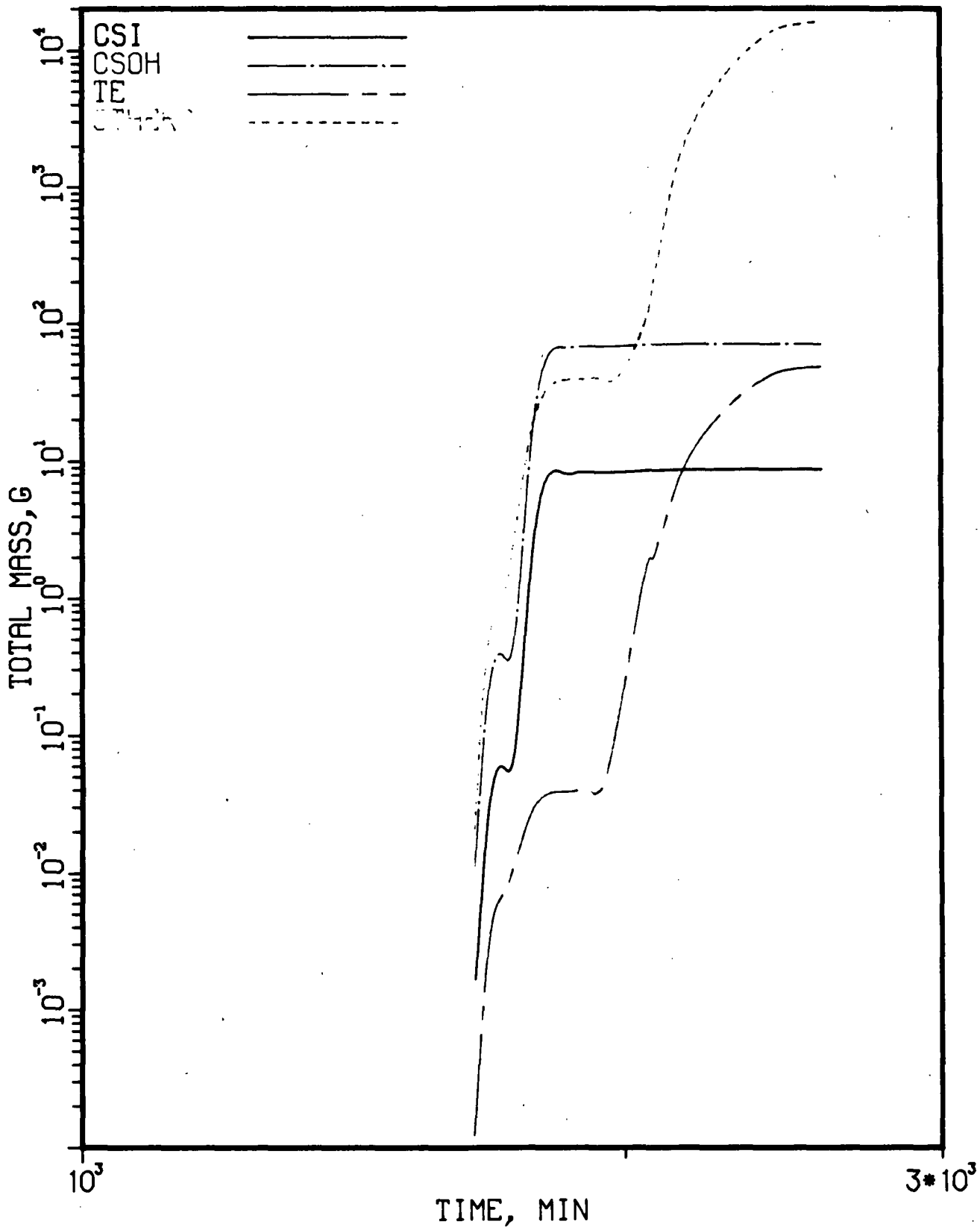

FIGURE 7.21. ACCUMULATED MASS LEAKED OUT TO ENVIRONMENT (TPI)

TABLE 7.12. DISTRIBUTION OF SPECIES AT 50 HOURS AFTER ACCIDENT, TPI

Species	Fraction of Core Inventory				
	RCS	Drywell	Pool	Containment	Environment
CsI	8.4×10^{-2}	3.9×10^{-3}	0.91	7.5×10^{-7}	2.4×10^{-4}
CsOH	0.24	3.7×10^{-3}	0.76	9.0×10^{-7}	3.1×10^{-4}
Te	0.45	0.41[(a)]	0.14	1.4×10^{-5}	1.3×10^{-3}

(a) This number includes a fraction of 0.35 for Te not being released from the core-concrete interaction.

the containment failure time and the corresponding leakage flow rate are properly reflected in the code input.

Figure 7.22 shows the suspended mass concentration of particulates in the containment. It is seen that the amount of the suspended particulates increases as the core starts melting at 118 minutes and the highest concentration results at a time of 550 minutes. It should be realized that during this time period, a considerable amount of particulate enters the suppression pool and is captured.

The particle size distribution of aerosol suspended in the containment at selected times is shown in Figure 7.23. It is noted that the mass median particle size of the aerosol ranges from 0.2 to 1 μm in diameter before the containment fails. As was discussed previously, scrubbing of particulates by the suppression pool depends substantially on the size of particles that enter the pool and the pool temperature. With a particle size of about 2 μm, aerosols were found to be removed rather effectively by the suppression pool. The pool depth utilized for this sequence was 13.5' (411 cm) until the vessel fails and 8.5' (260 cm) thereafter.

As mentioned before, the release timing of individual fission product species may be different from that for the total particulate and the time-dependent amounts of CsI, CsOH, and Te were distinguished in the present calculation. Table 7.13 shows the calculated fractions of the core inventory of each species found to reach various locations at the end of the accident. It is interesting to see that significant fractions of CsI and CsOH are captured by the suppression pool. As a result, about 0.1 percent is seen to escape the containment to reach the environment.

7.3.4 S_2 E Sequences

Unlike the previous three sequences, the S_2E accident sequence is caused by a small break in the primary coolant system accompanied by the failure of the emergency core cooling systems. The fission products released from the RCS are emitted to the drywell before flowing into the suppression pool and the containment. After bottom head failure, the vapor released from core-concrete interaction also passes through the drywell. Figure 7.24 shows the flow paths for the fission products in the calculation of the S_2E sequences. As depicted in Figure 7.24, some direct leakage from the drywell to the

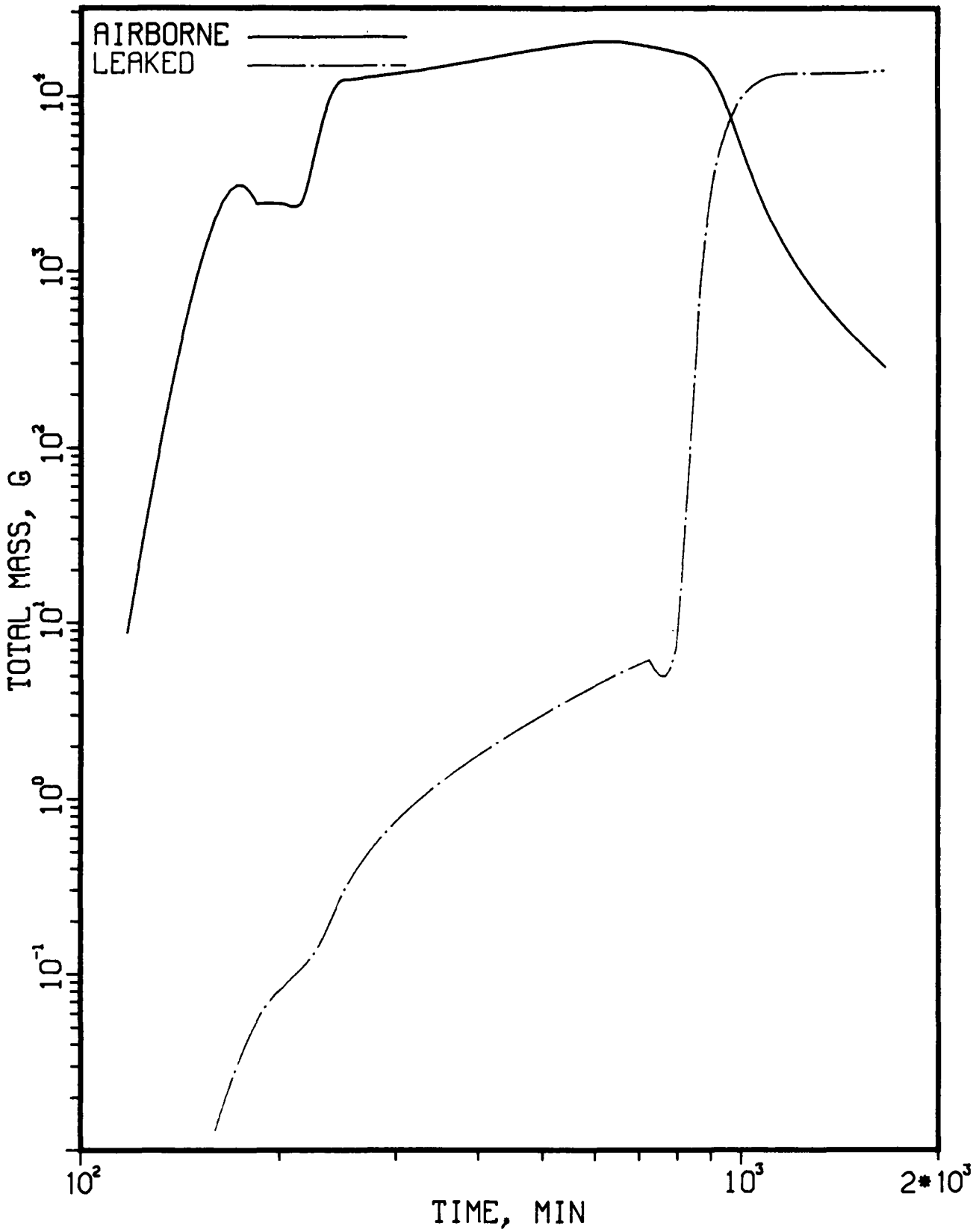

TABLE 7.22. SUSPENDED AND LEAKED MASS IN THE CONTAINMENT (TQUV)

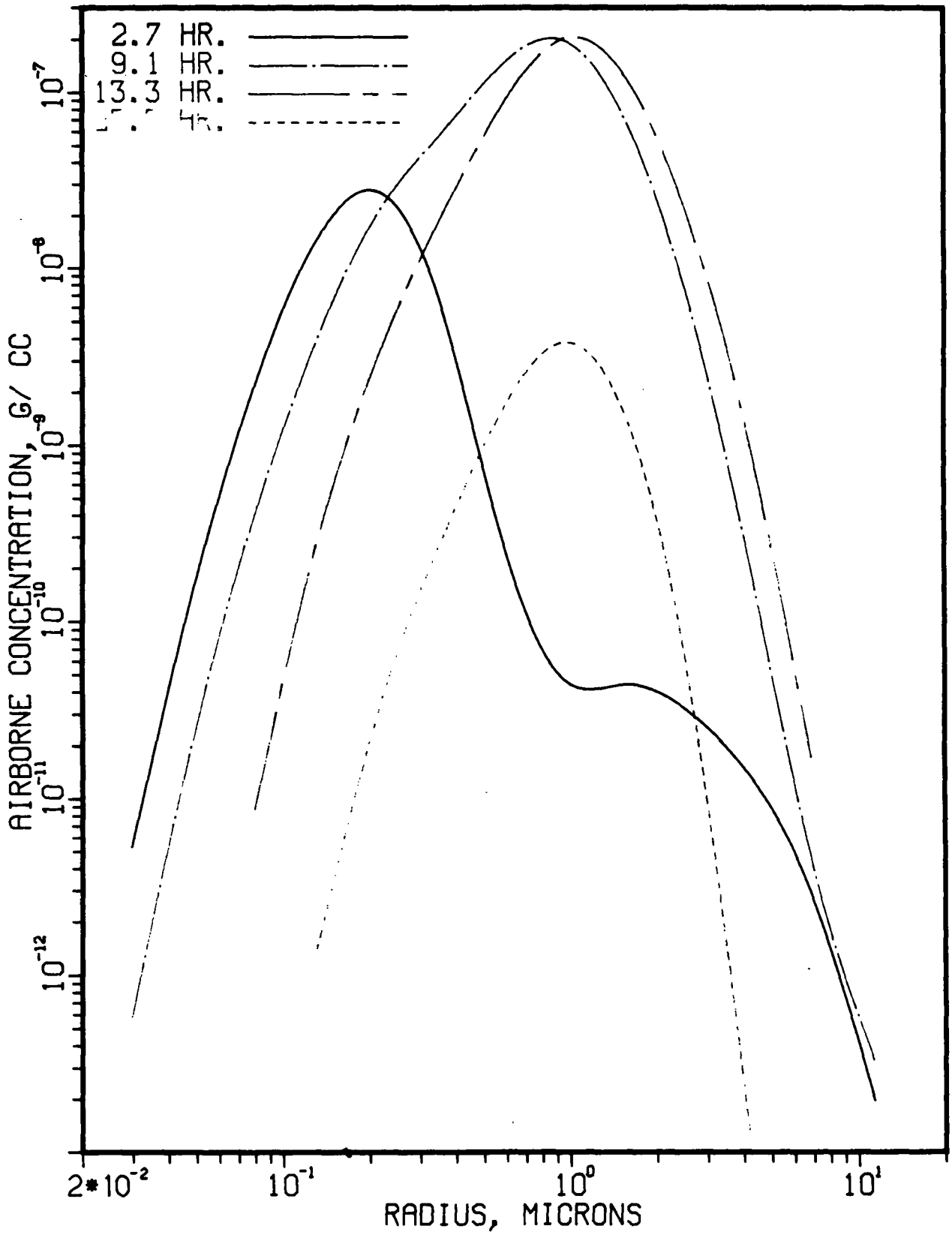

FIGURE 7.23. PARTICLE SIZE DISTRIBUTION OF AEROSOLS SUSPENDED IN THE CONTAINMENT (TQUV)

TABLE 7.13. DISTRIBUTION OF SPECIES AT 30 HOURS AFTER ACCIDENT, TQUV

Species	Fraction of Core Inventory				
	RCS	Drywell	Pool	Containment	Environment
CsI	6.3×10^{-2}	3.8×10^{-6}	0.94	6.8×10^{-4}	8.4×10^{-4}
CsOH	0.54	2.8×10^{-6}	0.46	3.5×10^{-4}	4.4×10^{-4}
Te	0.40	0.38[a]	0.21	1.6×10^{-3}	2.1×10^{-3}

(a) This number includes a fraction of 0.30 for Te not being released from the core-concrete interaction.

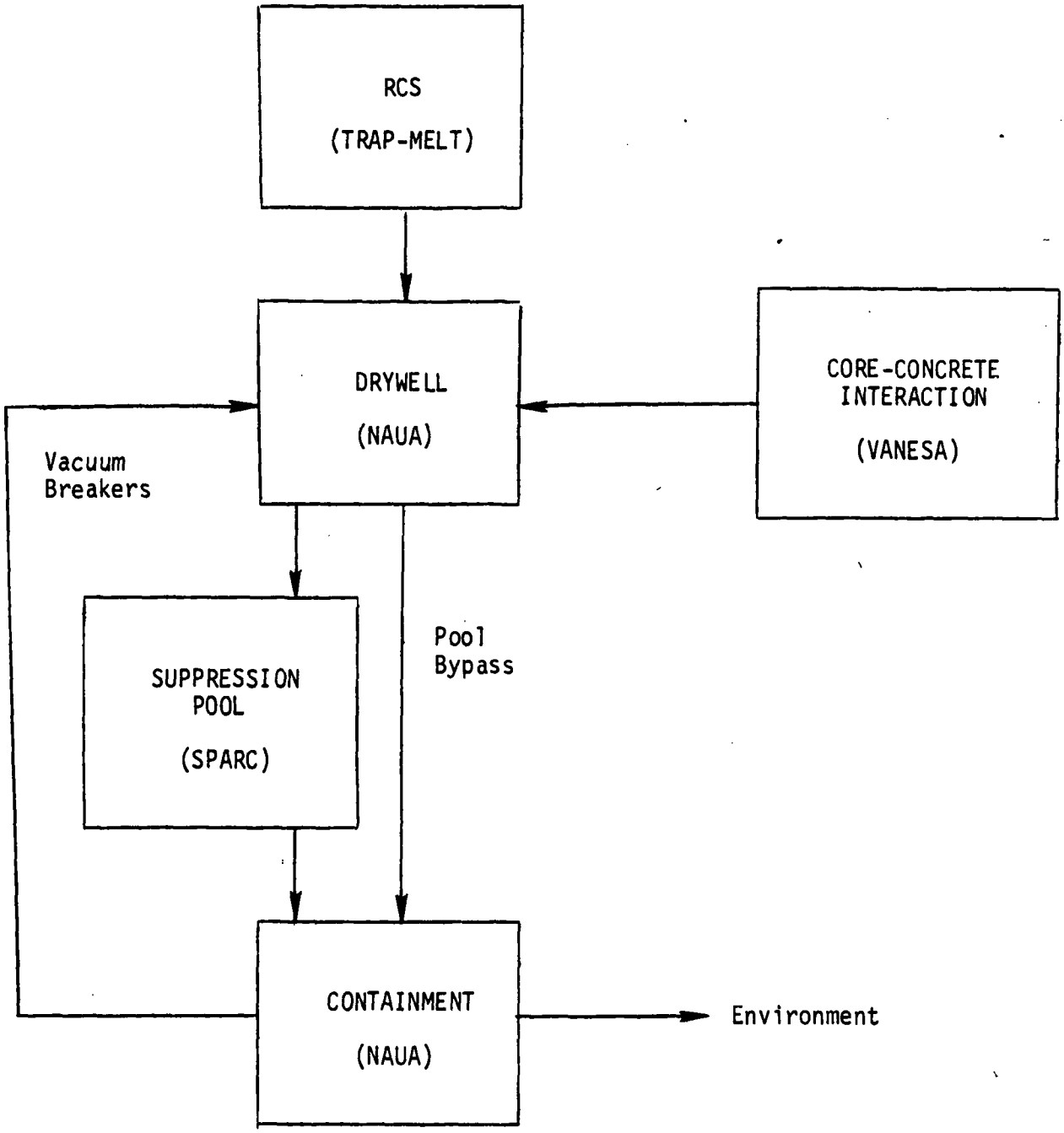

FIGURE 7.24. FISSION PRODUCTS FLOW PATHS AND CONTAINMENT CODES CALCULATION SEQUENCES (S_2E)

containment with suppression pool bypass occurs as well as the return of fission products from the containment to the drywell through the vacuum breakers. The vacuum breakers open when the pressure in the containment is higher than in the drywell, as may occur for hydrogen burns in the containment, for example. The suppression pool remained subcooled in this sequence, therefore, it is very effective in the removal of fission products. Table 7.14 shows the decontamination factor for the S_2E sequence with a pool bypass flow rate of 873 ft^3/min (nominal bypass rate).

The melts release starts at about 27 minutes after the initiation of the accident. The containment does not fail until 54 minutes when the second hydrogen burn occurs. Figure 7.25 shows the mass of each species leaked with time. Most of the CsI and CsOH are released during the early stages of the accident, in which the high decontamination factors prevail. This results in very little leakage into the environment for these two species. Later in the accident, the leakage of Te increased with time reflecting the relatively low DF during that time period. Nevertheless, due to suppression pool bypass, the leak fraction of CsI is of the same level as in the TC sequence. The higher level of the leak fraction for CsOH compared to the TC sequence is partially caused by the lower retention of CsOH in the primary system. Particle size distributions of aerosols in the containment are shown in Figure 7.26. The mass median particle radii are about 1 μm at the times shown. Figure 7.27 shows the airborne concentration and the accumulated mass leaked to the environment. The curve of leaked mass represents the sum of both that leaked out to the environment and to the drywell. The difference between Figures 7.25 and 7.27 is the aerosol mass returned to the drywell. Table 7.15 illustrates the locational distribution at the end of the calculation.

Another calculation for the S_2E sequence investigated the effect of a different bypass leak rate based on a stuck open vacuum breaker. In this variation, the bypass flow rate was 8730 ft^3/min, which is about 10 times of the nominal leak rate used in the previous case. A straightforward prediction leads to a higher leak fraction for Te. However, this is not true for CsI and CsOH (see Table 7.16). Due to the predicted cessation of bypass flow in two periods of time when hydrogen burning raises the pressure in the containment (27.8 min to 60.8 min and 63.0 min to 63.1 min), all the fission products leaking into the containment must then pass through the pool. There is only about one-half of the CsI and CsOH leaked out to the environment as was found for

not comparable to MARCH calculation for S2E w/o bypass.

TABLE 7.14. DECONTAMINATION FACTOR CALCULATED AS A FUNCTION OF PARTICLE SIZE AND OF TIME FOR S_2E

Time (min)	Particle Diameter (μm)					DF Based on Total Mass
	0.1	0.4	1.2	5.1	8.4	
28	75	$10^{5(a)}$	10^5	10^5	10^5	82700
39	7.8	10^5	10^5	10^5	10^5	90000
45.8	2.3	36	10^5	10^5	10^5	4250
54.4	1.4	14.5	10^5	10^5	10^5	1650
58.6	2.1	23	10^5	10^5	10^5	1300
59.5	2.5	30	10^5	10^5	10^5	1100
59.63	1.4	11	10^5	10^5	10^5	1060
80.7	8.8×10^3	7.8×10^4	10^5	10^5	10^5	99300
112.3	1.6	4.3	6.3×10^3	10^5	10^5	99800
119.2	24	90	10^5	10^5	10^5	3700
125.6	1.6	4.3	7.8×10^3	10^5	10^5	93
172.5	17	52	10^5	10^5	10^5	115
208.5	19	58	10^5	10^5	10^5	150
245.6	1.5	3.7	2.8×10^3	10^5	10^5	180
333	1.4	4.1	8.3×10^3	10^5	10^5	135
585	1.4	3.9	7.6×10^3	10^5	10^5	16
719	1.4	3.6	5.2×10^3	10^5	10^5	15

(a) A decontamination factor larger than 10^5 is assumed to be 10^5.

Pool depth: 13.5 ft

Bubble diameter: 0.75 cm
Aspect ratio: 1:3

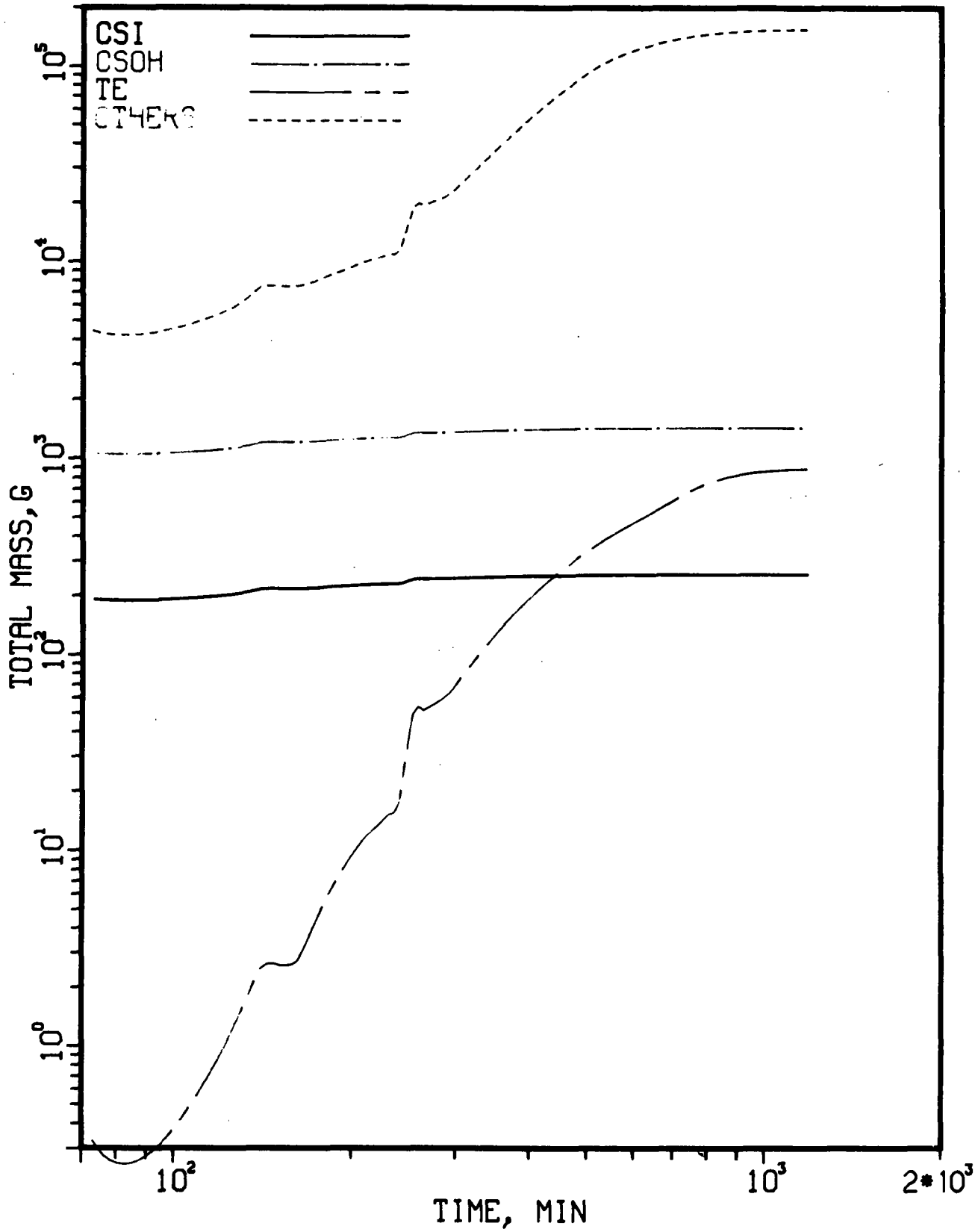

FIGURE 7.25. ACCUMULATED MASS LEAKED OUT TO ENVIRONMENT (S_2E)

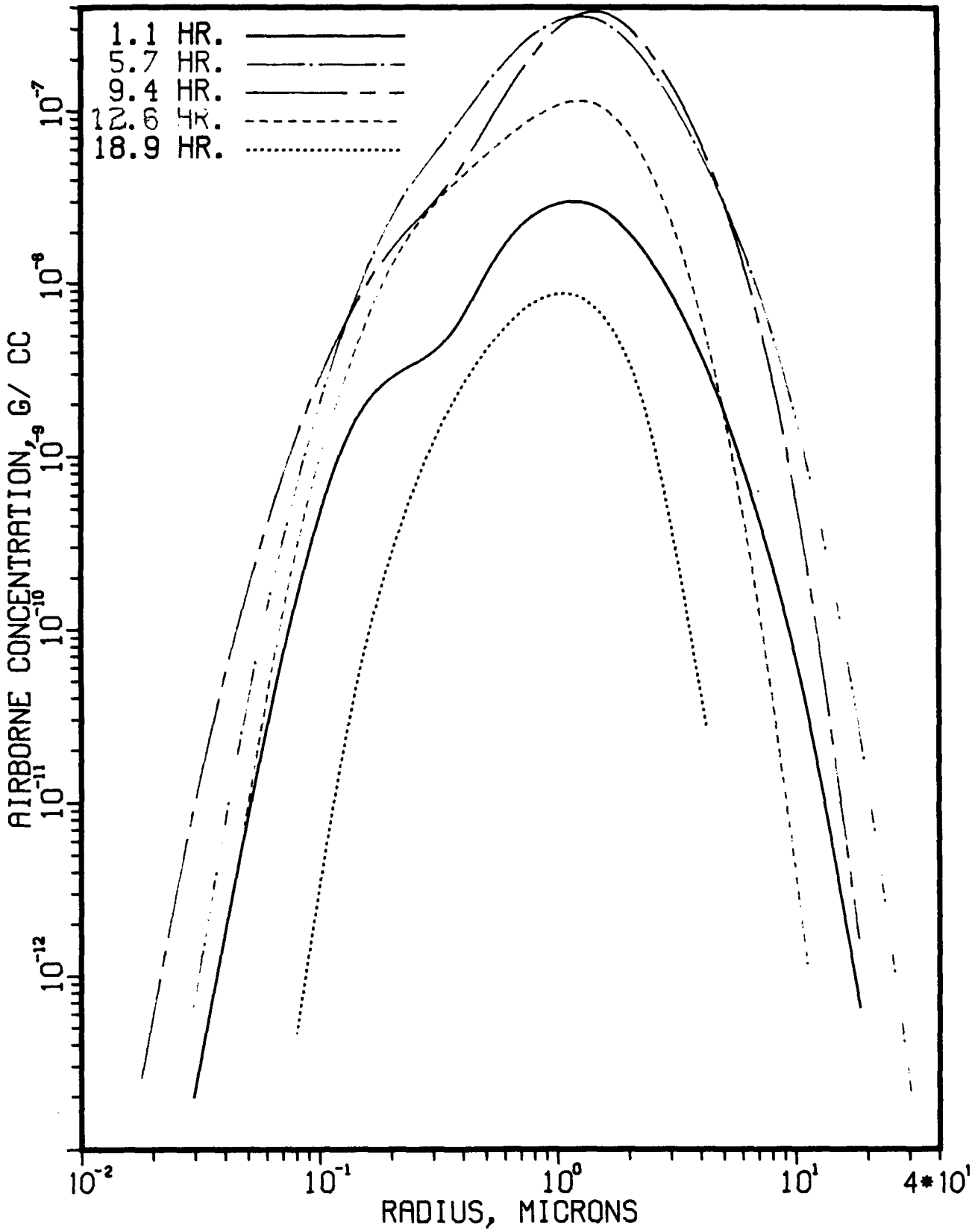

FIGURE 7.26. PARTICLE SIZE DISTRIBUTION OF AEROSOLS SUSPENDED IN THE CONTAINMENT (S_2E)

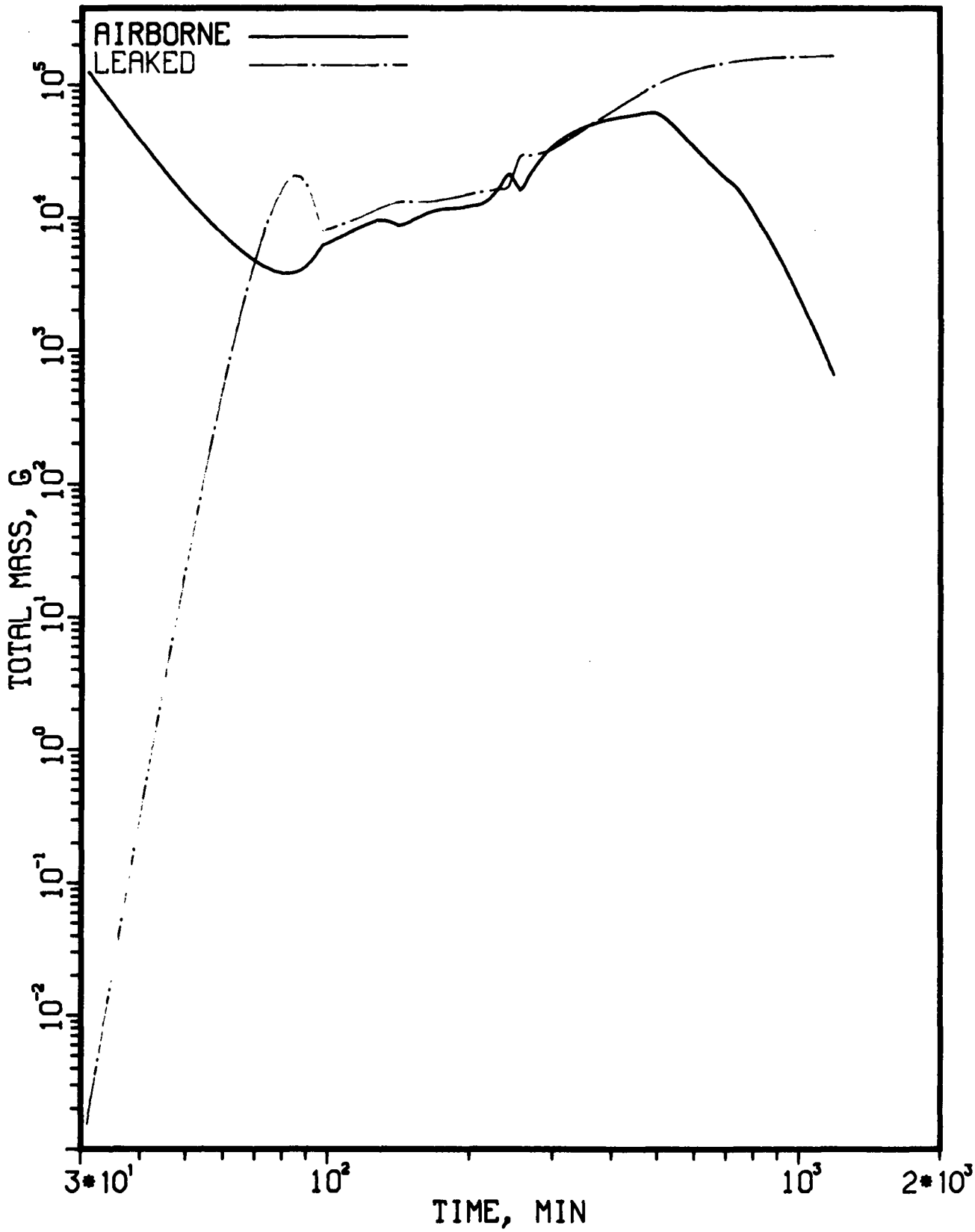

FIGURE 7.27. SUSPENDED AND LEAKED AEROSOL MASS IN THE CONTAINMENT (S_2E)

TABLE 7.15. DISTRIBUTION OF SPECIES AT 20 HOURS AFTER ACCIDENT, S_2E WITH NOMINAL POOL BYPASS

Species	Fraction of Core Inventory				
	RCS	Drywell	Pool	Containment	Environment
CsI	9.1×10^{-2}	1.4×10^{-2}	0.89	9.6×10^{-4}	7.0×10^{-3}
CsOH	0.16	1.3×10^{-2}	0.82	8.6×10^{-4}	6.3×10^{-3}
Te	0.26	0.39[a]	0.32	6.5×10^{-3}	2.4×10^{-2}

(a) This number includes a fraction of 0.355 for Te not being released from the core-concrete interaction.

TABLE 7.16. DISTRIBUTION OF SPECIES AT 24 HOURS AFTER ACCIDENT, S_2E WITH STUCK OPEN VACUUM BREAKER

Species	Fraction of Core Inventory				
	RCS	Drywell	Pool	Containment	Environment
CsI	9.1×10^{-2}	1.2×10^{-2}	0.89	2.0×10^{-3}	~~3.3×10^{-3}~~ 4.2×10^{-2}
CsOH	0.16	1.1×10^{-2}	0.82	1.9×10^{-3}	~~3.2×10^{-3}~~ 3.8×10^{-2}
Te	0.26	0.39[a]	0.11	0.10	0.14

(a) This number includes a fraction of 0.355 for Te not being released from the core-concrete interaction.

the S_2E case with nominal pool bypass. Figure 7.28 shows the accumulated leak masses of different species for the S_2E5 calculation.

7.3.5 Results for Fission Product Groups of Reactor Safety Study

As discussed, the results of calculations presented so far distinguished CsI, CsOH, and Te. In general, one can keep track of an increased number of species in the calculation. In order to demonstrate this capability, an additional NAUA calculation was performed for the TC sequence. The groups and the corresponding species considered in this additional calculation were already discussed in Section 6.2.1. Since the VANESA calculations for the release during the core-concrete interaction did not include all the species to be tracked, it was assumed that the species in a group not included in the original VANESA calculation are released at a rate identical to that for the species in the same group. For example, the release rate for Tc, Rh, and Pd in Group 6 was assumed to be the same as that for Ru and Mo combined after accounting for their core inventories. It should also be noted that Group 1 was not included in the NAUA calculation since Kr and Xe are in the gaseous form. Table 7.17 lists the calculated fraction of core inventory released to the environment as a function of both time and group for the TC sequence.

7.3.6 Summary

From the analyses discussed in this section, several interesting points can be noted. As in the results of the accident analyses considered in previous reports, most important factors that directly influence the amount of fission products released to the environment are the timing of source materials being released and the time of containment failure.

The role played by the suppression pool in the design considered here is much more important than that for the Peach Bottom reactor because in the Grand Gulf reactor the released fission products are passed through the suppression pool regardless of the source timing, except for the S_2E sequence which addressed the effect of pool bypass. It should be noted that the present analyses represent a first attempt to incorporate an analytic model predicting mechanistically the removal of particulates by the pool. While uncertainties

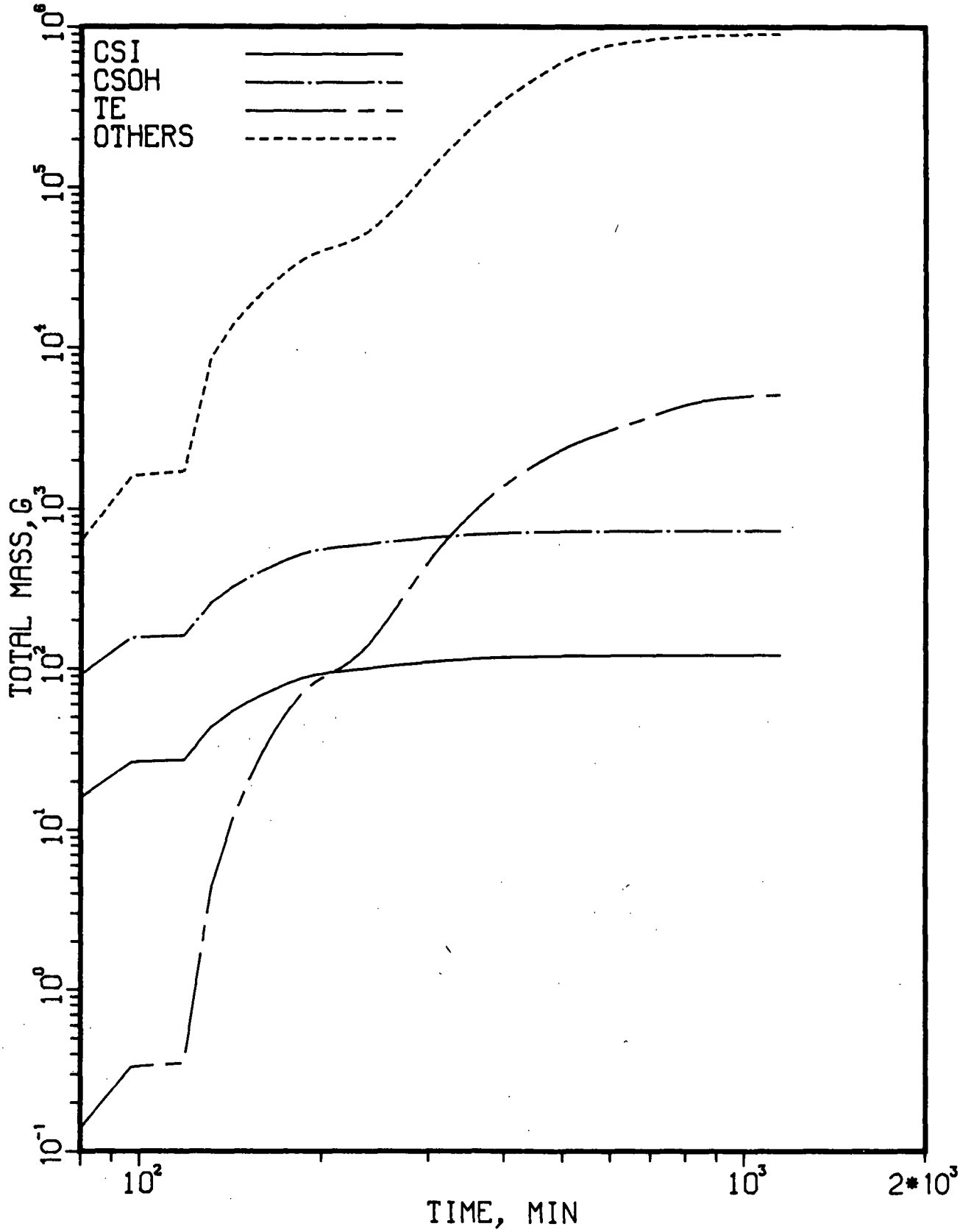

FIGURE 7.28. ACCUMULATED MASS LEAKED OUT TO ENVIRONMENT (S_2E5)

TABLE 7.17. FRACTION OF CORE INVENTORY RELEASED TO THE ATMOSPHERE FOR GROUPS OF REACTOR SAFETY STUDY (TC)

Time (hr)	I Group 2*	Cs Group 3	Te Group 4	Sr Group 5	Ru Group 6	La Group 7
1.5	0	0	0	0	0	0
2	4.4×10^{-8}	6.3×10^{-8}	4.2×10^{-14}	8.1×10^{-10}	2.8×10^{-10}	1.0×10^{-12}
4	1.5×10^{-3}	2.5×10^{-4}	3.0×10^{-4}	5.6×10^{-4}	3.8×10^{-5}	8.3×10^{-5}
7	6.6×10^{-3}	8.1×10^{-4}	3.5×10^{-3}	9.4×10^{-3}	7.6×10^{-5}	1.8×10^{-3}
10	6.8×10^{-3}	8.3×10^{-4}	5.5×10^{-3}	1.2×10^{-2}	7.7×10^{-5}	2.3×10^{-3}
15	6.8×10^{-3}	8.3×10^{-4}	8.6×10^{-3}	1.3×10^{-2}	7.7×10^{-5}	2.4×10^{-3}
20	6.8×10^{-3}	8.3×10^{-4}	8.8×10^{-3}	1.3×10^{-2}	7.7×10^{-5}	2.4×10^{-3}

* The release of volatile iodides is not included in these release fractions.

of the model's ability to accurately predict the behavior of the suppression pool are large and there are many calculational features that can be further improved in the future, these uncertainties and deficiencies are probably well within those involved in the current state of knowledge to predict the source term, various accident events, thermal hydraulic conditions, and other fission product behavior mechanism.

7.4 Discussion

The type of plant used to characterize BWR behavior in Volume II of this report was a Mark I design, the Peach Bottom 2 plant. Significant differences exist in the layout of the Mark III design considered here that affect the consequences of severe accident sequences to the extent that it is not truly appropriate to compare results for Mark III sequences with WASH 1400 release categories. Other differences between the Peach Bottom 2 and Grand Gulf plants exist in the reactor coolant system design as well as in the containment configuration. The BWR 4 nuclear steam supply system in Peach Bottom 2 and the BWR 6 system in Grand Gulf are sufficiently similar, however, that the results of systems analyses lead to quite similar dominant accident sequences. The results of the Accident Sequence Evaluation Program identify the sequences TC, TW, and TQUV as dominating the predicted risk for this type of design largely on the basis of sequence probability. As for the Peach Bottom 2 design, pipe break accidents do not appear as dominant risk contributors because of the diversity of makeup water supplies available. In this study of the Mark III design, Sequences TC, TQUV, and TPI were emphasized. The S_2E sequence was included in the analyses in order to investigate the effect on the predicted consequences of possible bypass of the suppression pool by the released fission products.

The time-integrated release fractions for the four core meltdown categories used to describe consequences for the BWR plant in WASH 1400 are shown in Table 7.18. All of the in-vessel steam explosion failure sequences, α, were assigned to the BWR 1 category. The comparatively large release of ruthenium in this WASH 1400 category is assumed to result from fuel fragmentation, dispersal, and air oxidation following the steam explosion. Containment overpressure failure modes were in general assigned to Categories 2 or 3, depending on the assumed location of primary containment failure and the

TABLE 7.18. WASH-1400 RELEASE CATEGORIES

Release Category	Fraction of Core Inventory Released						
	Xe-Kr	I	Cs-Rb	Te-Sb	Ba-Sr	Ru	La
BWR 1	1.0	0.4	0.4	0.7	0.05	0.5	5×10^{-3}
BWR 2	1.0	0.9	0.5	0.3	0.1	0.03	4×10^{-3}
BWR 3	1.0	0.1	0.1	0.3	0.01	0.02	3×10^{-3}
BWR 4	0.6	8×10^{-4}	5×10^{-3}	4×10^{-3}	6×10^{-4}	6×10^{-4}	1×10^{-4}

associated pathway to the environment. The γ' failure mode, which involved a direct release to the environment, was usually assigned to Category 2 and the γ failure mode, which involved release to the reactor building, was assigned to Category 3 for each sequence. The final core melt release category, Category 4, has significantly smaller release fraction than the other three categories. The principal sequences in this category involved isolation failures in which the small leakage rate from the primary containment could be treated by the Standby Gas Treatment System prior to release to the environment.

The predicted modes of containment failure and pathways to the environment for the Mark III design differ from those in the Mark I design. The expected location of failure of the primary containment is in the upper region of the outer containment volume. This location would be analogous to a failure in the vapor space of the wetwell in the Mark I design. In the analyses performed for WASH 1400 it was assumed that failure would occur in the wetwell region. It was also assumed, however, that failure in this region would result in loss of suppression pool water. In many important accident sequences this assumption resulted in little or no attenuation of the source term by the suppression pool. In contrast, the likely failure location in the Mark III design is sufficiently remote from the pool that it is unlikely to be affected by the failure. In each of the transient sequences analyzed for the Mark III design, all components of the fission product release passed through the pool prior to release to the environment. In the S_2E sequence, potential pool bypass by the fission products was explicitly considered. In Volume II of this report failure of the containment was assumed to occur in the drywell region of the Mark I design, again leading to bypass of the suppression pool during some portions of the sequences considered. Drywell failure is unlikely to occur in the Mark III design and the drywell is surrounded by the outer containment. In two of the sequences analyzed in the Mark III design, the pool water would be saturated (or boiling). The results of the analyses are therefore quite sensitive to the magnitude of fission product retention predicted for saturated pools. In the WASH-1400 analyses, no fission product attenuation by saturated pools was considered.

In the analyses performed for the Mark I design in Volume 2, consideration was given to the response of the reactor building following failure of the primary containment. It was recognized that a significant potential existed for retention in the reactor building, depending on the conditions in the

building and the availability and effectiveness of the Standby Gas Treatment System. The limited strength of the shield building surrounding the Grand Gulf containment and the lower capacity of the SGTS indicate that the likelihood of obtaining significant retention in this region prior to release is minimal for this design.

In this study the only containment failure mode that has been investigated involves overpressure failure, as the result of steam production prior to core melting as in TC and TPI, due to the buildup of noncondensible gases during core meltdown as in TQUV, or due to hydrogen burning in sequence S_2E. Consideration was also given to failure by hydrogen combustion in the TQUV sequence but the analyses indicated that the performance of the igniters should be adequate to prevent failure.

A steam explosion failure mode was not analyzed. It was recognized that this mode of failure could result in a large source term to the environment but the likelihood of this event based on research performed subsequent to WASH 1400 is low. The results of a steam explosion can also be inferred from the results of the sequences analyzed. After the time of the explosion and associated failure of containment, little additional retention would be expected for fission products subsequently released from the fuel.

Table 7.19 shows the release fractions for the volatile fission products for the four sequences analyzed. By comparison with Table 7.18 it can be seen that the predicted release fractions for the sequences considered are roughly comparable to those in Category 4 in WASH-1400. Thus, despite the assumed direct pathway to the environment from the containment after containment failure, the estimated consequences in terms of release fractions for the TC and TPI sequences are approximately two orders of magnitude less in these analyses than those for the similar scenario, TW$_Y$, in WASH 1400 as represented by Category 2. Much of the additional retention in the present analyses is the result of retention in the RCS and in the suppression pool. It will be recalled that no credit for retention by saturated pools was taken in WASH-1400.

The predicted effectiveness of the subcooled suppression pool in the removal of fission products in the TQUV and S_2E sequences is quite large and dominates the results for the sequence. At this level of decontamination the noble gas release begins to dominate the public health consequences from the accident and the sensitivity of risk to additional decontamination is small.

As discussed in the earlier volumes of this report, it is important that the reader recognize that although single value "best estimate" results have been reported, the results may be very sensitive to modeling assumptions and limitations in the capabilities of the computer codes used. The results of the Mark III analyses are not as sensitive to the predicted timing and mode of failure of the containment as the results of the Mark I analyses, assuming that our current understanding of the failure mode of the Mark III design is correct. The results are very sensitive to the modeling of fission product retention in saturated (or boiling) suppression pools. Clearly this is an area requiring further research. The amount of ultimate retention to be expected in the reactor coolant system is also an area of large uncertainty that could have a effect on source term magnitudes, though the sensitivity for the Mark III design is again not as great for the Mark I design.

*U.S. GOVERNMENT P RINTING OFFICE : 1984 0-421-297/4049

120555066637 1 1R3
US NRC
RES-DIV OF ENGINEERING TECH
BRANCH CHIEF
CHEMICAL ENGR BR
SS-1130
WASHINGTON DC 20555